INSTITUTE OF AGEING AND CHRONIC DISEASE

SUPEROXIDE IN SKELETAL MUSCLE; SITES THAT REGULATE INTRACELLULAR CHANGES DURING CONTRACTIONS AND ROLE IN AGE RELATED DEGENERATION

George Konstantinos Sakellariou

Thesis submitted in accordance with the requirements of the University of Liverpool for the degree of Doctor in Philosophy

Liverpool, October 2013

ABSTRACT

Ageing is defined as an age-related increase in susceptibility to diseases and death and is a complex process that affects every major system at the molecular, cellular and organ level. Although the exact cause of ageing is unknown, there is significant evidence that oxidative stress plays a major role in the ageing process.

Skeletal muscle produces oxidants from a variety of different sources with nitric oxide and superoxide being the primary radical species. Nitric oxide is regulated by the activity of nitric oxide synthases, however the sites that modulate changes in superoxide remain unclear. Skeletal muscle ageing is associated with a reduction in muscle mass and strength and leads to a significant vulnerability that opposes healthy ageing. Reports have indicated a positive correlation between tissue concentrations of oxidised macromolecules in skeletal muscle of old individuals, which implies the possible involvement of reactive species in the processes of skeletal muscle ageing. The role of oxidants in skeletal muscle ageing has also been extensively examined in different model organisms, which have undergone genetic manipulations and reports have shown that absence of Cu, Zn superoxide dismutase (SOD1) in homozygotic SOD1 knockout mice, induces an acceleration of skeletal muscle ageing phenotypic changes which further provides support for the implication of radical species in the processes of muscle ageing.

The overall aim of the work carried out in this thesis was; i) to develop specific techniques to determine changes in superoxide within the cytosolic and mitochondrial compartment of skeletal muscle, ii) to identify the major sites for superoxide generation in skeletal muscle and iii) to identify the reactive species that are involved in the accelerated loss of muscle mass in the homozygotic SOD1 knockout mouse model and to characterize the changes in redox status and adaptive responses that occur in muscles from the SOD1 knockout mice.

The results of carried out in this thesis indicated that the superoxide sensitive fluorescent probes dihydroethidium and MitoSOX Red were capable of selectively detecting changes in superoxide within the cytosolic and mitochondrial matrix of skeletal muscle, respectively. Specific pathway inhibitors and immunolocalisation techniques showed that the major sub-cellular sites contributing to cytosolic superoxide changes in skeletal muscle both at rest and during contractions were the NAD(P)H oxidases. Finally with the use of single isolated muscle fibres from the flexor digitorum brevis muscle, it was concluded that formation of peroxynitrite in muscle fibres was a major effect of lack of SOD1 in SOD1 null mice, which may contribute to fibre loss in this model.

Techniques developed in this study to monitor real-time changes in superoxide in the mitochondrial and cytosolic compartment of muscle fibres provided a useful tool to i) examine the sub-cellular pathways that are involved in the regulation of superoxide at rest and during contractile activity in skeletal muscle and to ii) determine the role of superoxide in skeletal muscle degeneration observed in SOD1 knockout mice. These results may have widespread implications for the understanding of diverse scientific areas, including the responses of muscle to exercise training, age-related loss of muscle mass and function, as well as inflammatory or degenerative muscle diseases, such as the muscular dystrophies that are associated with increased levels of oxidative damage.

Doctor of Philosophy Declaration

I hereby declare that this dissertation is a record of work carried out in the Institute of Ageing and Chronic Disease at the University of Liverpool during the period from January 2010 to June 2013. The dissertation is original in content except where otherwise indicated.

October 2013

.....

(George K. Sakellariou)

ACKNOWLEDGEMENTS

This dissertation has been the most significant academic challenge I have ever had to face. I sincerely express my gratitude and appreciation to everyone whose contribution either directly or indirectly has helped in the eventual realisation of this work.

I am extremely grateful to Prof. Malcolm Jackson and Prof. Anne McArdle who have been my academic supervisors since 2008 when I joined the group. Their significant help during my MPhil and PhD degrees, constructive criticism and valuable comments made this work a reality. Their knowledge and commitment to high standards inspired and motivated me. I would like to express my gratitude to all the members of the Musculoskeletal Biology group for their assistance during my PhD degree. Of those members special thanks go to Tim Pearson, my friend Adam Lightfoot as well as past members of the group including Jesus Palomero, Graeme Close, Lea Zibrik and Liliana Shalamanova. I would also like to thank Aphrodite Vasilaki who I consider as my sister, she has always supported me throughout my career in the lab and has been a source of encouragement.

I would like to use this opportunity to thank the Institute of Ageing and Chronic Disease, the Biomedical Services Unit and the University of Liverpool for providing all the necessary equipment and support in order for this project to be completed and the National Institutes of Health, US (NIH) for their generous financial support.

I would like to extend my gratitude to Prof. Arlan Richardson and Prof. Holly Van Remmen (University of Texas Health Science Center, San Antonio, Texas, USA) for the provision of the SOD1 knockout and nNOS transgenic mice as well as Prof. Mike B Reid (University of Kentucky Center for Muscle Biology) for the kind gift of the SS-31 peptide.

I would also like to use this opportunity to thank Mr Athanasios Koutromanos, who has always given me a helping hand when needed and whose opinion I have always greatly valued. Special thanks also go to the first person that introduced me to the world of science, Associate Prof. Thanasis Jamurtas, (University of Thessaly, Greece) who was also my undergraduate and MSc academic supervisor. Finally I would like to express my deepest gratitude to my family, friends and my partner Ritika Kumar who played an indispensible part in the successful completion of this project, for their encouragement, motivation, love and profound understanding.

Dedication

To my uncle Vasilis Sakellariou who recently passed away but also my parents Pamela and Kostas who have always supported me throughout my life.

LIST OF ABBREVIATIONS

2-OH-E^+	2-hydroxyethidium
3-NT	3-nitrotyrosine
4-HNE	4-hydroxynonenal
4Cl-DZ	4'-Chlorodiazepam
α_{1s} DHPR	α_{1s} subunit of dihydropyridine receptor
ANT	Adenine-nucleotide translocator
Ant A	Antimycin A
APO	Apocynin
AT	Anterior tibialis
Bax CB	Bax channel blocker
BCA	Bicinchoninic acid
BEL	Bromoenol lactone
CAIII	Carbonic anhydrase III
CAT	Catalase
CM-DCFH DA	5-(and 6-) chloromethyl-2',7'- dichlorodihydrofluorescein diacetate
CoQ	Coenzyme Q
CoQ_{10}	Coenzyme Q_{10}
CsA	Cyclosporin A
CuZnSOD	Copper-zinc superoxide dismutase
Cyclo D	Cyclophilin D
DAF-FM DA	4-amino-5-methylamino-2', 7'-difluorofluorescein diacetate
DAPI	4',6-diamidino-2-phenylindole dihydrochloride
DCFH	2', 7'- Dichlorodihydrofluorescin:
DHE	Dihydroethidium
DIDS	4,4'-diisothiocyano-2,2'-disulfonic acid stilbene
DPI	Diphenyleneiodonium chloride
DS	Dextran sulphate
DUOX	Dual oxidase
E^+	Ethidium
ecSOD	Extracellular superoxide dismutase
EDL	Extensor digitorum longus

eNOS	Endothelium nitric oxide synthase
ETC	Electron transport chain
F-actin	Fibrous actin
FAD	Flavin adenine dinucleotide
FBS	Foetal bovine serum
FDB	Flexor digitorum brevis
FMN	Flavin mononucleotide
G-actin	Globular actin
GPX	Glutathione peroxidase
GRX	Glutaredoxin
GSH	Reduced glutathione
GSSG	Glutathione disulfide
GTN	Gastrocnemius
H_2O_2	Hydrogen peroxide
$HOO^{\cdot}$	Hydroperoxyl radical
HSP	Heat Shock Protein
iMAC	Inner membrane anion channel
IMM	Inner mitochondrial membrane
iNOS	Inducible nitric oxide synthase
$iPLA_2$	Calcium-independent phospholipase A_2
MDA	Malondialdehyde
MEM	Minimum essential medium eagle
Mgreen	Manders's co-localization coefficient for channel 2
MIS	Mitochondrial intermembrane space
$mitoK_{ATP}$	Mitochondrial ATP-dependent K^+ channel
MnSOD	Manganese superoxide dismutase
MPO	Myeloperoxidase
mPTP	Mitochondrial permeability transition pore
Mred	Manders's co-localization coefficient for channel 1
NADH	Nicotinamide adenine dinucleotide
NADPH	Nicotinamide adenine dinucleotide phosphate
nNOS	Neuronal nitric oxide synthase
nNOSTg	nNOS transgenic
NO	Nitric oxide

NOC-7	3-(2-hydroxy-1-methyl-2-nitrosohydrazino)-N-methyl-1-propanamine
NOS	Nitric oxide synthase
NOX	Nicotinamide adenine dinucleotide phosphate oxidase
$O_2^{\cdot-}$	Superoxide
$^{\cdot}OH$	Hydroxyl radical
OGG1	8-Oxoguanine glycosylase
OMM	Outer mitochondrial membrane
$ONOO^-$	Peroxynitrite
PRX	Peroxiredoxin
R	Mander's overlap
RNS	Reactive nitrogen species
ROH	Alcohol
RONS	Reactive oxygen and nitrogen species
ROOH	Hydroperoxide
ROS	Reactive oxygen species
Rot	Rotenone
Rr	Pearson's correlation
RyR1	Ryanodine receptor-Ca^{2+} release channel
SN	Sciatic nerve
SOD	Superoxide dismutase
SOL	Soleus
SR	Sarcoplasmic reticulum
T-Tubule	Transverse Tubule
Tn	Troponin
TOM	Translocase of outer membrane
TRX	Thioredoxin
TRXR	Thioredoxin reductase
UA	Uric acid
VDACs	Voltage dependent anion channels
XO	Xanthine oxidase

PUBLISHED ARTICLES

Results from this study were published in:

1) Antioxidants and Redox Signaling "Studies of mitochondrial and nonmitochondrial sources implicate nicotinamide adenine dinucleotide phosphate oxidase(s) in the increased skeletal muscle superoxide generation that occurs during contractile activity, (Sakellariou et al., 2013a)". A selection of confocal images was used for the front cover of the journal (volume 18, Issue 6, January 2013).

2) Free Radical Research "Redefining the major contributors to superoxide production in contracting skeletal muscle. The role of NAD(P)H oxidases." (Sakellariou at al., 2013b) [Epub ahead of print].

3) Aging Cell "Role of superoxide–nitric oxide interactions in the accelerated age-related loss of muscle mass in mice lacking Cu,Zn superoxide dismutase, (Sakellariou et al., 2011)". A selection of confocal images was used for the front cover of the journal (volume 10, Issue 5, October 2011).

This work was also presented at the following scientific meetings:

1) Experimental Biology Conference; San Diego, California, USA, 2012 under the title "Studies of mitochondrial and non-mitochondrial sources implicate NADPH oxidase(s) in the increased skeletal muscle superoxide generation that occurs during contractile activity".

2) SFRR-Europe 2011 Meeting; Istanbul, Turkey under the title "NADPH oxidase is a major contributor of superoxide production at rest and during contractile activity in skeletal muscle".

3) SFRR-Europe Summer school; Protein maintenance and turnover in ageing & diseases; Spetses, Greece, 2010 under the title "Effect of increasing frequency of contractions on ROS production from different sites during contractile activity in skeletal muscle fibres".

4) 7th International Medical Postgraduate Conference; Hradec Kralove, Czech Republic, 2010 under the title "Investigating the mechanisms underlying the pathogenesis of age-related loss of muscle mass and function in skeletal muscles lacking SOD1".

5) Main Meeting of The Physiological Society; Manchester, UK, 2010 under the title "Intracellular interactions of superoxide and nitric oxide in skeletal muscle".

6) Experimental Biology Conference; Anaheim, California, USA, 2010 under the title "The effect of nNOS overexpression on intracellular ROS activities in skeletal muscle fibres at rest and following a period of contractile activity".

7) Main Meeting of The Physiological Society; Dublin, Ireland, 2009 under the title "Real-time measurement of intracellular reactive oxygen and nitrogen species in single isolated mature skeletal muscle fibres in mice overexpressing nNOS".

TABLE OF CONTENTS

LIST OF FIGURES

LIST OF TABLES

LIST OF SCHEMES

CHAPTER 1

INTRODUCTION

Skeletal muscle is the largest pool of proteins in humans and exhibits a complex structure and architecture. Skeletal muscle ageing is associated with a reduction in muscle mass and strength and is a contributor to frailty and loss of independence in the elderly. The problem is universal and leads to a significant vulnerability that opposes healthy ageing, but the mechanisms underlying the muscle loss during ageing remain to be defined. Skeletal muscle produces oxidants from a variety of different sources and oxidative damage has been suggested to be among the factors contributing to the initiation and progression of muscle atrophy that occurs during ageing. The overall aim of the work carried out in this thesis was to identify the major sources of reactive oxygen species in skeletal muscle and to investigate their effect in skeletal muscle age-related degeneration.

This introductory chapter details the features of skeletal muscle, the sources and reactive species produced by skeletal muscle as well as the role that oxidants have been reported to play in skeletal muscle metabolism.

1.1. FEATURES OF SKELETAL MUSCLE

1.1.1 Skeletal muscle

Skeletal muscle, also known as striated muscle is one of three major muscle types in the human body, the others being cardiac (heart) muscle and smooth muscle (Martini, 2005). Skeletal muscle is considered an organ of the muscular system, is the largest protein store and is under the control of the peripheral nervous system. There are 640 individually named skeletal muscles and they comprise 42% of total body mass in an average adult male and 36% in an adult female (Marieb and Hoehn, 2010). Skeletal muscle, as its name implies, is attached to the skeleton by bundles of collagen fibres

known as tendons (Figure 1.1), which function to transmit forces, thus effecting skeletal movement such as locomotion and maintaining posture. Although the basis for motion mediated by all three types of muscle cells is the conversion of chemical energy into mechanical energy, skeletal muscle exhibits a complex structure and architecture, which is essential and directly related to its primary function, contraction.

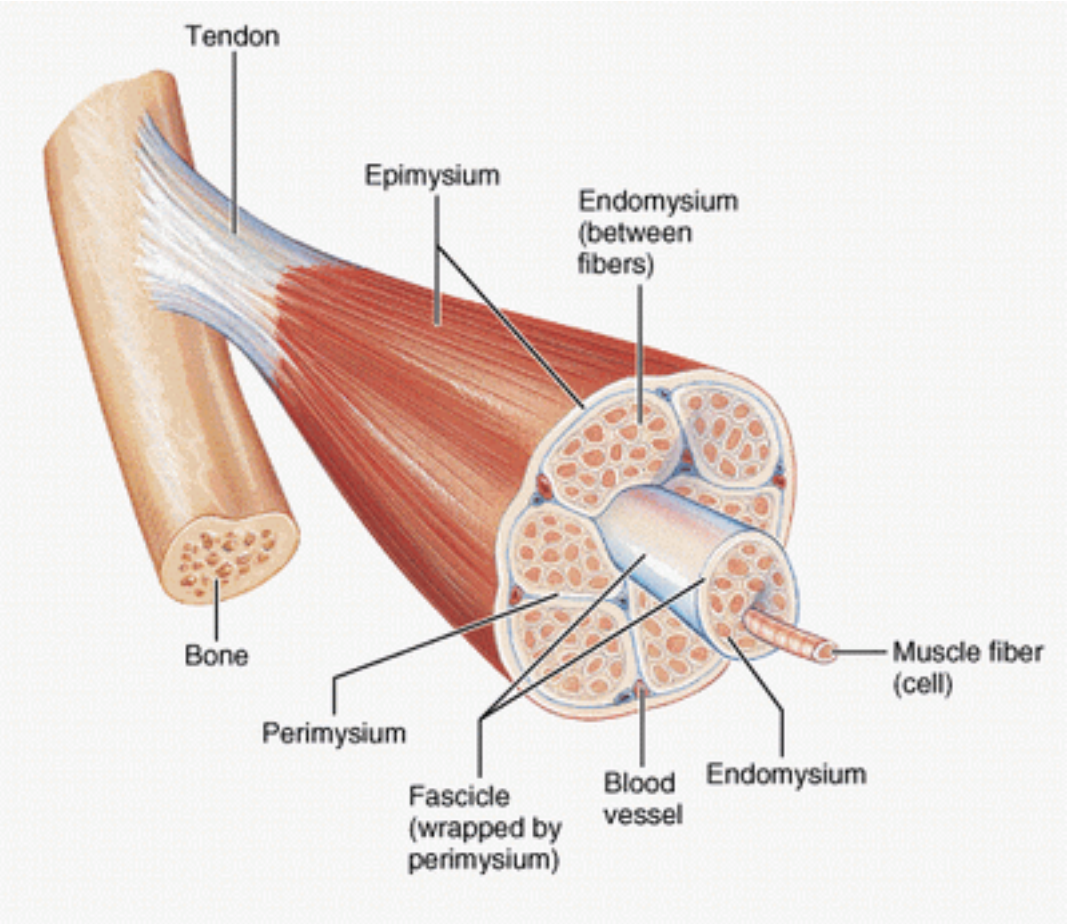

Figure 1.1 Schematic representation of skeletal muscle structure (from Hemmings and Hopkins, 2005).

1.1.2 Skeletal muscle structure

Skeletal muscles vary considerably in size and shape, are extremely specialized and exhibit unique structural features. Starting with the largest structure of skeletal

muscle, the epimysium, a layer of connective tissue that sheaths the entire muscle (Figure 1.1). Connective tissue from the epimysium extends into the muscle, dividing the tissue into compartments, the fascicles. Individual fascicles are also surrounded by a layer of connective tissue, the perimysium and contain bundles of individual muscle fibres (muscle cells) (Figure 1.1). Finally a delicated network of loose connective tissue, the endomysium, is found between the muscle fibres of a fascicle. This sheath is very important in the physiology of muscle contraction because it electrically insulates the individual muscle cells from each other (Mougios, 2006).

1.1.3 Structural features of muscle fibres

Skeletal muscles consist of hundreds, or possibly thousands of individual muscle fibres (Marieb and Hoehn, 2010; Martini, 2005). Skeletal muscle fibres are long, cylindrical cells which present densely packed striations, perpendicular to their longitudinal axis. An example of a single isolated muscle fibre is presented in figure 1.2. The striations consist of alternative dark and light areas. Every dark area is called A band and every light area the I band. More about the alternations of A and I band will be discussed in Sections 1.1.4 and 1.1.5 of this chapter.

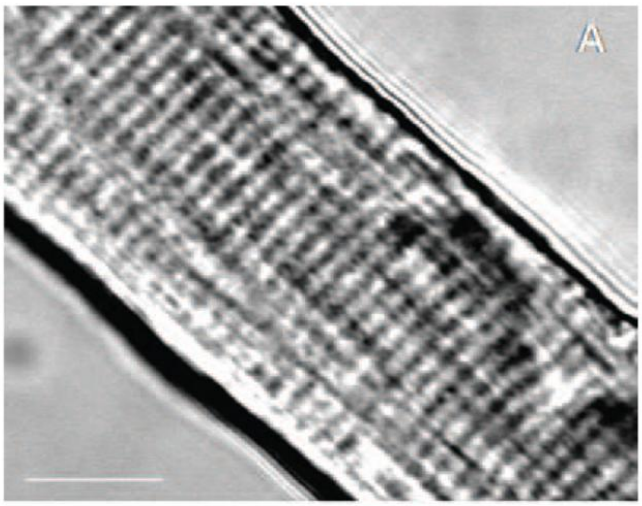

Figure 1.2 Single isolated skeletal muscle fibre presents intense transverse stripes under a light microscope. Dark stripes are called A bands and light stripes I bands. 63X original magnification, scale bar = 30 μm (picture from Palomero *et al*, 2008).

Muscle fibres are multinucleated cells (Figure 1.3) that are bound by a plasma membrane, the sarcolemma (Figure 1.4) and an overlying basal lamina (Marieb and Hoehn, 2010; Martini, 2005). There are specialized invaginations of the sarcolemma that run transversely across the cell (Figure 1.4). These invaginations are known as transverse tubules (T-tubules) and are essential for carrying the depolarisation brought to the cell by a motor nerve impulse (Figure 1.5) into the muscle cell (Mougios, 2006).

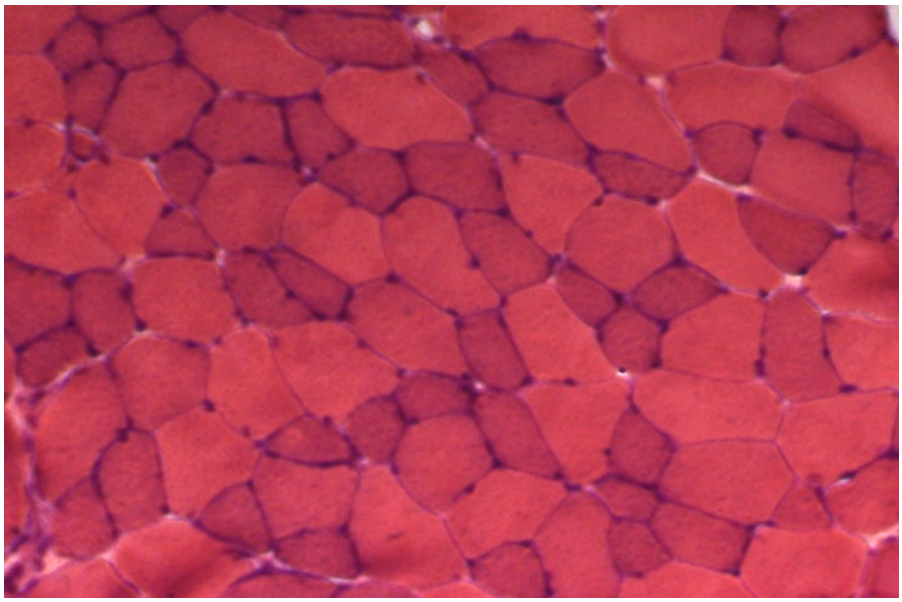

Figure 1.3 Cross section of an EDL skeletal muscle showing individual fibres along with the nuclei (image provided by Dr A. Vasilaki)

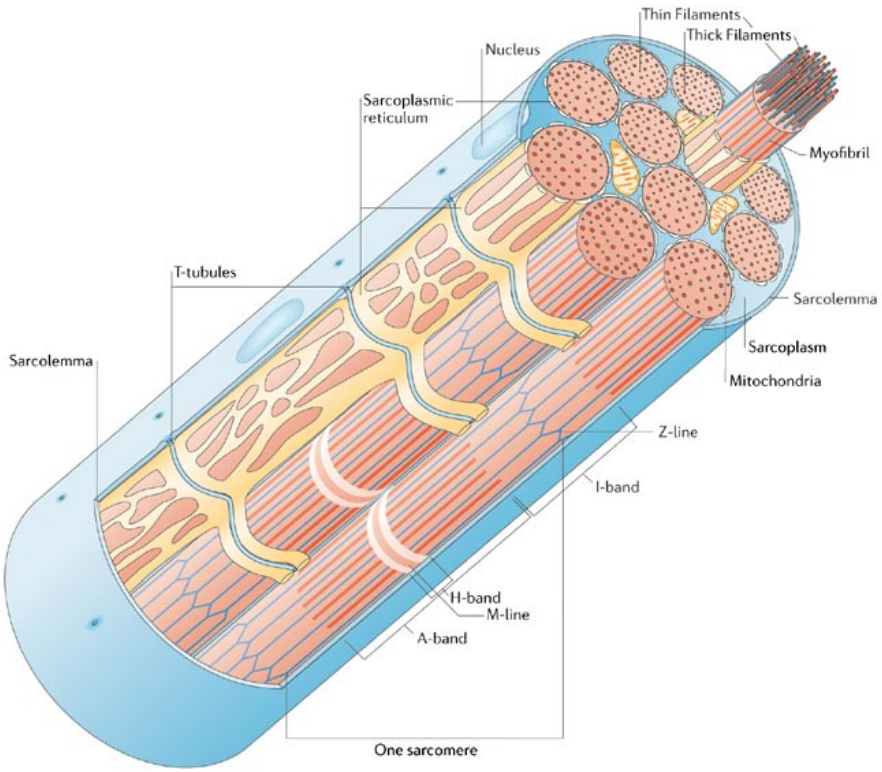

Figure 1.4 Schematic representation of the structure of a skeletal muscle fibre (from Davies and Nowak, 2006).

Skeletal muscles must have neuronal innervation to function and a microscopy image of the synapse (neuromuscular junction) between the end of the axon (a long slender projection of the neuron that conducts electrical impulses away from the neuron cell body) and the plasma membrane of a muscle cell is shown in Figure 1.5 (Ruff, 2011). The motor end plate represents the final synapse in the motor pathway, between a nerve cell and the individual fibre it controls. Each skeletal muscle fibre irrespective of its size has only one neuromuscular junction (Ruff, 2011) and evidence has shown that if the axons to a myofibre fail to develop, or are damaged, the muscle cells will wither in the process known as neurogenic atrophy (Wong and Martin, 2010).

The sarcoplasm is the specialised cytoplasm of a muscle cell that surrounds organelles and other insoluble cytoplasmic components including the Golgi apparatus, the sarcoplasmic reticulum (a network which acts as a calcium (Ca^{2+}) storage site), mitochondria, myoglobin (a 17kDa protein which receives oxygen from the blood, stores it and transports it inside the muscle cells) the endoplasmic reticulum and abundant myofibrils (Mougios, 2006).

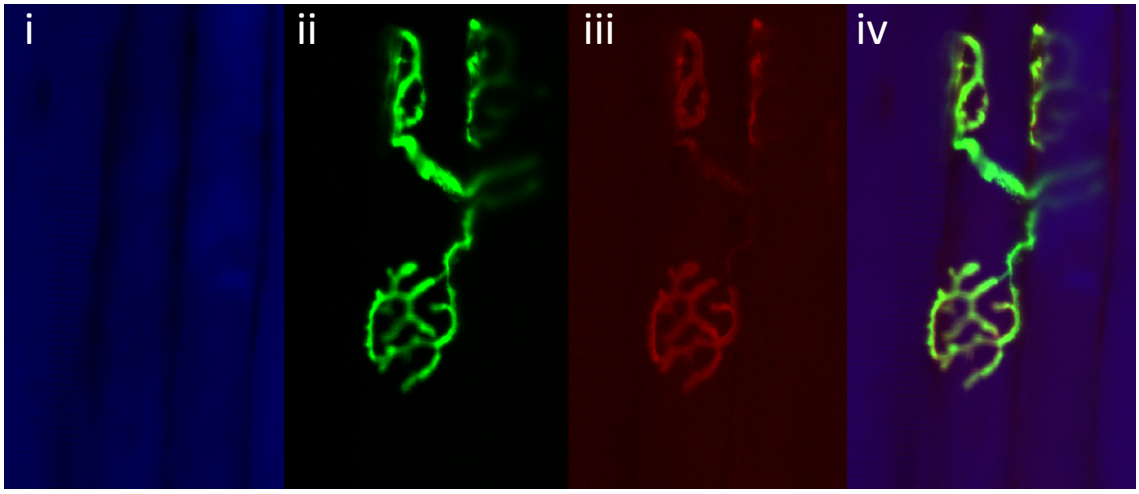

Figure 1.5 Confocal images showing the synapse (neuromuscular junction) between the axons and a group of motor endplates in skeletal muscle. (i) Fibres were stained with phalloidin (blue), (ii) Axons from mice overexpressing YFP in the nerve (green), (iii) Motor endplate stained with bungarotoxin (red), (iv) merged image of i-ii-iii (image provided by Dr A. Vasilaki)

1.1.4 Myofibril structure

Skeletal muscle fibres consist of parallel myofibrils, which are embedded in the sarcoplasm of the cell and comprise the basic unit of the muscle (Figure 1.6). The alternation of A and I bands mentioned in Section 1.1.3 persist in every myofibril and the striations on skeletal muscle fibres are due to the alignment of A bands in adjacent myofibrils (Martini, 2005; Mougios, 2006).

A and I bands are not uniform. The A band has a stripe in the middle, the H zone which is less dense than the rest of the band (Figures 1.6 and 1.7). In the middle of the H zone, the dense line is called the M line. The I band also has a dense line in the middle called the Z line or Z disc (Figures 1.6 and 1.7). This symmetrical pattern is

repeated along the entire myofibril and permits the definition of a minimal complete functional unit, the sarcomere, which is defined as the segment of a myofibril between two Z lines (Figures 1.6 and 1.7) (Martini, 2005; Mougios, 2006).

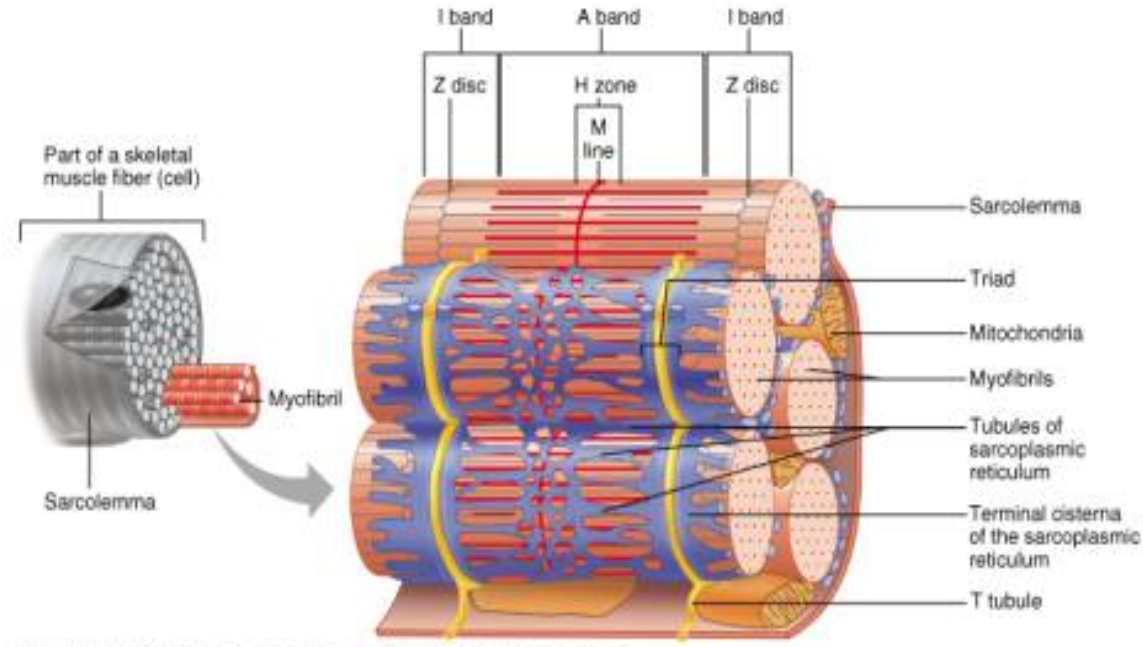

Figure 1.6 Schematic representation of myofibril structure (from Marieb, 2001).

1.1.5 Sarcomere architecture

The sarcomere has a filamentous appearance and is approximately 2.3um long in the myofibrils of fibres under resting conditions. Electron micrographs of cross sections of myofibrils have revealed that sarcomeres consist of two kinds of filaments, the thick filaments with a diameter of 15nm and the thin filaments with a diameter of 9nm (Figure 1.7), (Mougios, 2006). The I band consists of thin filaments while the A band presents a mixed make up of both thin and thick filaments. The H zone consists of thick filaments and the rest of the band by both kinds of filaments in a symmetrical arrangement (Figure 1.7).

Thick filaments are composed mainly of myosin while the thin filaments of actin, tropomyosin and troponin proteins. The data in figure 1.7 show that thick and thin filaments interdigitate at the two ends of the A bands which interact through cross bridges. The cross bridges are part of the myosin molecules and protrude from the surface of each thick filament and point toward the surrounding thin filaments (Harrington and Rodgers, 1984). It is essential to mention that the interaction of the myosin cross-bridges with actin is what generates the force for contractions and further details on sarcomere contraction will be mentioned in the following Section (1.1.6) of this chapter.

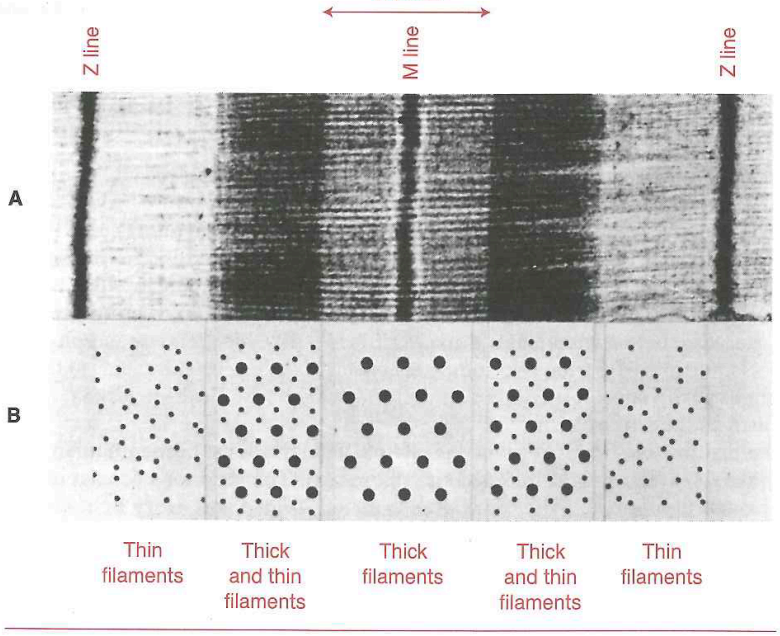

Figure 1.7 Electron micrograph of a sarcomere. (A) A longitudinal section of a myofibril presents repetitive symmetrical pattern. The part between two Z lines shown here is called a sarcomere. (B) Cross sections at different points along the sarcomere reveals its structural details (from Mougios, 2006).

1.1.6 The mechanism of muscle contraction

Sarcomeres are the fundamental contractile units of skeletal muscle, which shorten in proportion to the whole muscle. Studies on the mechanism of muscle contraction have shown that there is no proportional shortening in the parts of the sarcomere and examination by electron microscopy revealed that the I band and H zone shorten, whereas the A band does not change. This observation has made it clear that the lengths of both the thin and thick filaments are constant during contraction but their overlap increases, which suggests that sarcomere contraction is caused by the active sliding of thick and thin filaments past each other. This has been proposed as the sliding-filament model that is widely accepted as the theory for muscle contraction (Huxley and Niedergerke, 1954).

The major proteins involved in force generation are myosin and actin. As mentioned in previous Section (1.1.5), thick filaments consist of myosin, the most abundant protein of muscle tissue which accounts half of its protein mass. On the other hand, thin filaments consist mainly of actin, tropomyosin and troponin. Actin is the main component of the thin filaments and it exists in two forms, globular actin (G-actin) and fibrous actin (F-actin) (Mougios, 2006). F-actin forms the trunk to which tropomyosin and troponin attach in the thin filaments. Tropomyosin consists of two similar stringlike subunits in an α-helical conformation. Molecules of tropomyosin join in a row to form fibres which run along each thin filament while following the twisting of the actin monomers (Figure 1.8). Troponin is a complex of three different subunits (TnC, TnI, TnT) and is attached to tropomyosin. TnT subunit binds to tropomyosin, TnI to actin and TnC to Ca^{2+}.

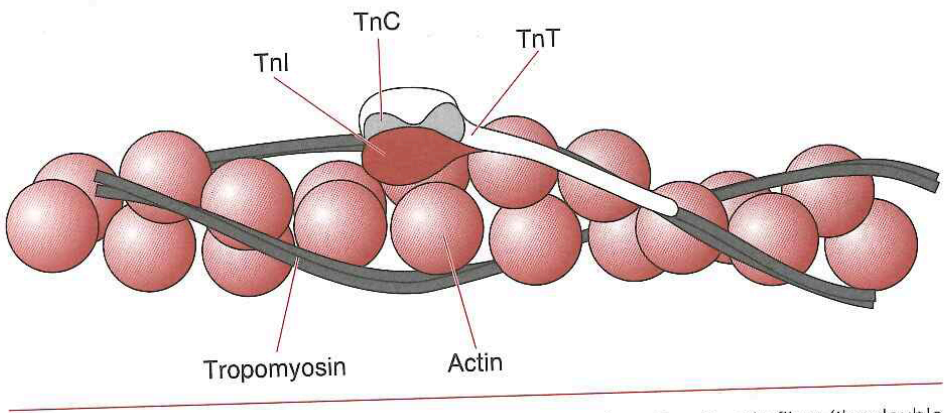

Figure 1.8 Thin-filament proteins. A thin filament consists of an F-actin fibre, two tropomyosin molecules, and troponin (Tn) complexes places at regular intervals. Every troponin complex consists of TnC, TnI and TnT (from Mougios, 2006).

The interaction of the myosin cross-bridges with actin is what generates the force for contractions. Under resting conditions (when a muscle is at rest), the interaction among actin-tnI-TnT-tropomyosin hold tropomyosin close to the actin monomers where the myosin heads bind, thus tropomyosin hinders the interaction on thin and thick filaments (Harrington and Rodgers, 1984). However, under contracting conditions, muscle excitation by the nervous system results in the release of Ca^{2+} from the sarcoplasmic reticulum to the sarcoplasm of myofibres. The increased Ca^{2+} ions bind on the TnC subunit and elicit a change in its conformation. As a result, TnC detaches TnI from actin, moving tropomyosin away from the binding sites of myosin on actin (Harrington and Rodgers, 1984). Cross-bridges of myosin bind to actin and the muscle contracts. Contractile activity will seize when the Ca^{2+} ions are sequestered in the sarcoplasmic reticulum by the calcium ATPases (calcium pumps that transfer cytosolic Ca^{2+} into the sarcoplasmic reticulum during muscle relaxation) and the actin-TnI-TnT-tropomyosin interaction is then restored (Mougios, 2006).

1.2. REACTIVE OXYGEN AND NITROGEN SPECIES PRODUCED BY SKELETAL MUSCLE

1.2.1 Skeletal muscle produces reactive species

Molecular oxygen is one of the most abundant elements in the atmosphere (nearly 21% by volume), and its ability to accept electrons makes it vital for a variety of physiological processes. Aerobic organisms including humans have adapted well to the atmosphere, using atmospheric oxygen by respiration and to obtain energy efficiency. Resting and contracting skeletal muscles require energy and in biological systems, the energy is accumulated as ATP and released by its hydrolysis (Marieb and Hoehn, 2010; Martini, 2005). Skeletal muscle mitochondria are implicated in the processes of ATP production via the mitochondrial oxidative phosphorylation, a metabolic pathway that takes place in the inner mitochondrial membrane and results in the production of ATP by reducing molecular oxygen to water (Scheffler, 1999; Kemp, 2004). Although oxidative phosphorylation is a vital part of metabolism, it produces reactive oxygen intermediates, which can lead to the propagation of free radicals, molecules that contain one unpaired electron and are capable of independent existence (Radak, 2000). Other metabolic pathways unrelated to mitochondrial oxidative phosphorylation are also implicated in the production of reactive species and a detailed description of the main sources of reactive molecules are discussed in Section 1.2.3.

More than 50 years ago, reports showed that oxygen toxicity caused cellular damage by the generation of reactive oxygen species (Fenn et al., 1957; Gerschman et al., 1954) and the first studies to report that reactive species are produced in skeletal muscle appeared in the 1980s (Davies et al., 1982b; Dillard et al., 1978; Jackson et al., 1985). It is now widely accepted that resting and contracting skeletal muscles produce reactive oxygen and nitrogen species (RONS). Reactive oxygen species (ROS) is a

general term that refers to molecular oxygen-derived molecules that are reactive species including oxygen-centered radicals but also non-radical species which are reactive derivatives of oxygen (Halliwell and Gutteridge, 2007). Similarly, the term reactive nitrogen species (RNS) refers to both nitrogen radicals along with other reactive molecules where the reactive centre is nitrogen (Jackson, 2008; Jackson, 2009; Palomero and Jackson, 2010).

RONS are constantly produced by skeletal muscle in both humans and animals and their generation is augmented during contractile activity (Close et al., 2005; Palomero et al., 2008). The first studies identified an increase in end-point indicators of the reactions of oxidants in tissues during and following exercise and claimed that the increase in reactive species appeared to be in major part due to generation by contracting skeletal muscle (Davies et al., 1982b; Dillard et al., 1978; Jackson et al., 1985). Now, the field of redox biology has advanced significantly and with the development of analytical approaches, researchers have been able to confirm previous reports by detecting real time changes in RONS generation during and following contractile activity (Palomero et al., 2008; Pye et al., 2007; Vasilaki et al., 2010).

Free radical generation by skeletal muscle has been detected and quantified by a wide array of methods including spectrophotometry, fluorescence, chemiluminescence and spin traps (Balon and Nadler, 1994; Close et al., 2007; Diaz et al., 1993; Jackson et al., 1985; Palomero et al., 2008; Pattwell et al., 2003; Phung et al., 1994; Pye et al., 2007; Reid et al., 1992) and it is widely accepted that the primary radical species generated by skeletal muscle include nitric oxide (NO) and superoxide (McArdle and Jackson, 2000; Jackson and McArdle, 2011; Palomero and Jackson, 2010). Both NO and superoxide are reactive and can readily react to form a series of other RONS. Details on the chemistry of the main radical species (NO and superoxide) as well as the

sources that are produced from in skeletal muscle are presented in detail in the following two Sections (1.2.2 and 1.2.3, respectively).

1.2.2 Chemistry of reactive oxygen and nitrogen species

Skeletal muscles produce reactive species including radical species but also non-radical species, which are reactive derivatives of oxygen and nitrogen. The main reactive molecules produced in biological species are presented in table 1.1.

Reactive oxygen species	Molecular formula	Formation
Free radical species		
Superoxide radical	O_2^-	One-electron reduction of ground state molecular oxygen
Hydroperoxyl radical	HOO•	Protonation of the superoxide radical
Hydroxyl radical	HO•	One-electron reduction of hydrogen peroxide and three-electron reduction of ground state molecular oxygen
Nitrogen monoxide	NO	One-electron reduction of nitrite
Alkoxyl radical	RO•	One-electron reduction of hydroperoxide
Peroxyl radical	ROO•	One-electron oxidation of hydroperoxide
Nonradical species		
Singlet oxygen	$^1\Delta_g O_2$ ($^1O_2$)	Excitation of ground state molecular oxygen
Hydrogen peroxide	H_2O_2	Two-electron reduction of ground state molecular oxygen, followed by protonation, and protonation of the peroxide ion
Peroxynitrite	$ONOO^-$	Reaction of nitrogen monoxide with the superoxide radical
Hydroperoxide	ROOH	Autoxidation and singlet oxygen oxygenation of unsaturated compounds
Ozone	O_3	Oxidation of ground state molecular oxygen with atomic oxygen formed by photolysis of ground state molecular oxygen
Hypochlorous acid	HC1O	Hydrolysis of molecular chlorine
Excited carbonyl	RR′CO*	Cleavage of dioxetane and self-decomposition of peroxyl radicals

Table 1.1 Reactive oxygen and nitrogen species relevant to biological species (from Radak, 2000).

1.2.2.1 Superoxide radical

Superoxide anion, is considered a primary radical (i.e the first radical to be produced) and arises either through incomplete reduction of oxygen in electron transport systems or as a specific product of enzymatic systems (Powers and Jackson, 2008). It is produced from one electron reduction of oxygen and has a negative charge. Due to its negative charge, superoxide is an anion radical and can pass through biomembranes only through an anion channel (Lynch and Fridovich, 1978). Superoxide has a relatively long half life and does not react directly with polypeptides, sugars, or nucleic acids but can further interact with other molecules to generate secondary ROS, either directly or prevalently through enzyme or metal-catalyzed processes (Fridovich, 1986). In aqueous solutions, superoxide can be protonated to produce hydroperoxyl radical ($HOO^{\cdot}$) or depleted undergoing a dismutation reaction to produce hydrogen peroxide (H_2O_2); ($2O_2^{\cdot-} + 2H^+ \rightarrow H_2O_2 + O_2$) (Valko et al., 2007). However, this dismutation is considered to be very slow because superoxide radicals electrostatically repel each other and the rate constant of the dismutation of superoxide to H_2O_2 is approximately $2 \times 10^9\ M^{-1}\ s^{-1}$ (Beckman and Koppenol, 1996).

1.2.2.2 Nitric oxide radical

Nitric oxide (NO) also known as nitrogen monoxide is considered a primary radical species and arises through the conversion of arginine to citrulline by the nitric oxide synthases, utilising nicotinamide adenine dinucleotide phosphate (NADPH) as a cofactor (Moncada et al., 1991; Szabo et al., 2007). NO is a weak reducing agent, reacts with oxygen to form nitric dioxide (NO_2), and reacts very rapidly with superoxide to produce peroxynitrite ($ONOO^-$) and subsequently other RNS (Droge, 2002). NO is a small reactive molecule, containing one unpaired electron and its half-life *in vivo* is

thought to be less than 10 seconds (Chiueh, 1999; Moncada et al., 1991). Although it reacts rapidly with many radicals, NO is generally unreactive and does not react rapidly with most biomolecules (Radak, 2000). NO stability is greater in an environment with a lower oxygen concentration (halflife > 15 seconds) and is soluble in both aqueous and lipid media. NO readily diffuses through the cytoplasm and plasma membranes and in the extracellular milieu, it reacts with oxygen and water to form nitrate and nitrite anions (Halliwell and Gutteridge, 2007; Powers and Jackson, 2008). In addition, NO reacts with free and bound transition metal ions such as the ferrous ion in guanyl cyclase thus activating this enzyme and resulting in the formation of cGMP, a second messenger for relaxing blood vessels (Valko et al., 2006; Wink et al., 1996). Due to this property, NO released from the endothelium is called the endothelium-derived relaxing factor (EDRF) (Stamler and Meissner, 2001). Heme proteins are intimately associated with the biological action of NO and binding of NO to Fe^{2+} plays a major role in its inactivation and removal through binding to the iron (Fe) in hemoglobin (Powers and Jackson, 2008). The toxicity of NO is linked to its ability to generate highly reactive species when combined with other reactive species such as superoxide anions.

1.2.2.3 Hydrogen peroxide

Hydrogen peroxide (H_2O_2) belongs to the family of ROS, has no unpaired electrons, thus it is a non-radical molecule. H_2O_2 is a relatively stable compound, it is not very reactive and acts as either a mild oxidising or weak reducing agent. H_2O_2 is permeable to membranes and has a relatively long half-life (Powers and Jackson, 2008; Radak, 2000). In addition to formation by dismutation of superoxide, a number of enzyme systems also generate H_2O_2 including urate, amino acid oxidases and nicotinamide adenine dinucleotide phosphate oxidases (Valko et al., 2006; von

Lohneysen et al., 2008). H_2O_2 is unable to oxidise DNA or lipids directly but can inactivate some enzymes by oxidation of essential thiol groups, compounds that contain the functional group composed of sulphur-hydrogen (S-H) (Halliwell and Gutteridge, 2007; Brodie and Reed, 1987). For instance, evidence has shown that high concentrations of H_2O_2 can inactivate glyceraldehyde-3-phosphate dehydrogenase, thus inhibit glycolysis (Brodie and Reed, 1987). The generation of various free radicals is closely linked with the participation of redox-active metals and the cytotoxicity of H_2O_2 occurs through its ability to generate highly reactive species such as the hydroxyl radical through metal-catalyzed reactions (Valko et al., 2006; Jackson, 2011).

1.2.2.4 Hydroxyl radical

Hydroxyl radicals are the most highly reactive radical species present in biological systems and are generated from the reductive decomposition of H_2O_2 with reduced transition metal ions, Fe or copper (Cu); ($H_2O_2 + Fe^{2+} \rightarrow Fe^{3+} + {}^{\cdot}OH + {}^{-}OH$) and ($H_2O_2 + Cu^{1+} \rightarrow Cu^{2+} + {}^{\cdot}OH + {}^{-}OH$) a reaction called the Fenton reaction (Powers and Jackson, 2008; Halliwell and Gutteridge, 2007). There is controversy about whether Fenton reactions can occur *in vivo* due to a) its small rate constant and b) from the fact that the concentration of Fenton reaction reactive transition metal ions is very low (Radak, 2000). It has been suggested that Fe regulation ensures that there is no free intracellular Fe, but it has been shown that a rapid increase in superoxide production can oxidise Fe cluster-containing enzymes (Fe-containing molecules) thus releasing "free iron" which facilitates hydroxyl radical production from H_2O_2 (Valko et al., 2006). Superoxide radical can also participate in the Haber-Weiss reaction, where Fe or Cu is maintained in a reduced form by superoxide; ($O_2^{\cdot-} + Fe^{3+} \rightarrow Fe^{2+} + O_2$) and ($O_2^{\cdot-} + Cu^{2+} \rightarrow Cu^{1+} + O_2$) and hence capable of catalyzing the formation of the hydroxyl radical

from H_2O_2; ($O_2^{\cdot-} + H_2O_2 \rightarrow {}^{\cdot}OH + {}^{-}OH + O_2$) (Valko et al., 2007). Hydroxyl ions have a strong oxidizing potential with a half-life in aqueous solution of less than 1ns (Valko et al., 2006) and react rapidly with almost any biomolecule that is near its formation site (Powers and Jackson, 2008). Thus, the oxidative damage will depend on its formation site, for example generation of hydroxyl ions close to DNA could modify the DNA bases or cause strand breakage (Mello Filho et al., 1984). Hydroxyl radicals are membrane impermeant and can initiate lipid peroxidation through hydrogen abstraction and to produce peroxyl radicals, which derive from the one electron oxidation of hydroperoxides (Radak, 2000).

1.2.2.5 Peroxynitrite

Peroxynitrite is an oxidatively active molecule and is formed through the reaction of superoxide with NO thus reducing their bioavailability; ($O_2^{\cdot-} + NO \rightarrow ONOO^-$), (Jackson et al., 2007; Szabo et al., 2007; Trujillo et al., 2008). This reaction has received considerable attention as a potentially deleterious reaction or as a detoxification mechanism for ROS. This reaction occurs approximately three times faster than the dismutation of superoxide and even faster than the reaction of NO with heme proteins (Powers and Jackson, 2008) and has one of the highest rate constants known for reactions of NO, 7.0×10^9 M^{-1} s^{-1} (Valko et al., 2006; Beckman and Koppenol, 1996). Peroxynitrite anion is a relatively long-lived toxic compound and it reacts with thiol compounds forming disulfides (Radi et al., 1991). Peroxynitrite and its protonated form, peroxynitrous acid (ONOOH); ($ONOO^- + H^+ \rightarrow ONOOH$) can oxidise various biological molecules including, nucleic acids, proteins and phospholipids (Powers and Jackson, 2008; Valko et al., 2006). Another potentially important reaction of peroxynitrite is nitration of tyrosine residues in the presence of transition metal ions

(Ischiropoulos et al., 1992). This reaction is a prerequisite for the cyclic interconvertion between the phosphorylated and the unphosphorylated forms of tyrosine (Hunter, 1995), which is crucial for signal transduction in the cell. However overproduction of peroxynitrite can cause oxidative damage to molecular components of the cell, alter the structure of proteins and inhibit their normal function (Valko et al., 2007; Szabo et al., 2007).

1.2.3 Sources of RONS in skeletal muscle

Since the initial observations that skeletal muscle produces RONS (Davies et al., 1982b; Jackson et al., 1983), a great deal of research has been undertaken to identify the sources that contribute to RONS production. It has been shown that resting and contracting skeletal muscles produce oxidants from a variety of cellular locations and Figure 1.9 shows an updated schematic representation from a recent report of the various sites and mechanisms that have been proposed for RONS generation (intracellular and extracellular) in skeletal muscle (Jackson, 2011).

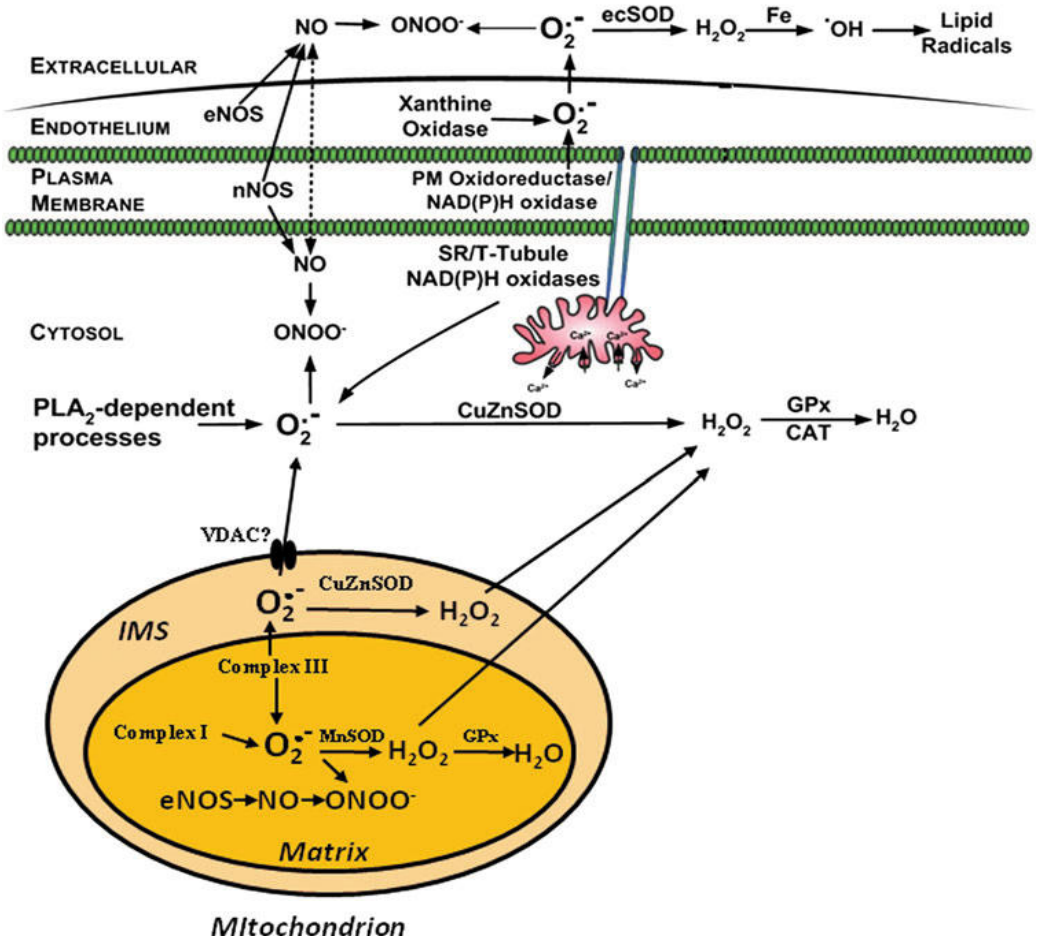

Figure 1.9 Schematic representation of the sites and mechanisms proposed for RONS generation in skeletal muscle fibres (from Jackson, 2011).

1.2.3.1 Sources of NO in skeletal muscle

The production of NO is mediated by a series of specific enzymes, the nitric oxide synthases (NOS) which are regulated by calcium and calmodulin (a calcium-binding messenger protein) (Davidson and Duchen, 2006) and catalyse the production of NO from the amino acid L-arginine by utilizing NADPH (Jackson, 2008; Palomero and Jackson, 2010). There are three different isoforms of NOS; the neuronal (type I or nNOS), the endothelial (type III or eNOS) and the inducible isoform of NOS (type III or iNOS) (Kobzik et al., 1994; Silvagno et al., 1996; Thompson et al., 1996), (Table 1.2).

Studies have shown that skeletal muscles express nNOS, which was originally found in neural tissue but is also present in most cell types. Neuronal nNOS is expressed along the sarcolemma of skeletal muscle fibres together with the dystrophin–glycoprotein complex via a linkage to α1-syntrophin (Brenman et al., 1996; Brenman et al., 1995). Type III isoenzyme (eNOS) was originally described in endothelial cells but also localised to the muscle mitochondria (Stamler and Meissner, 2001; Kobzik et al., 1994) (see figure 1.9). The third isoform of NOS (iNOS) is involved in the immune response, and is also expressed in skeletal muscle in response to a septic challenge or inflammatory conditions (Powers and Jackson, 2008), and evidence has shown that expression of NO from iNOS has been implicated in skeletal muscle dysfunction (Gath et al., 1996; Krause et al., 1998). From the three NOS isoenzymes, nNOS has been reported to be the prime source of the NO release from skeletal muscle and is strongly expressed in fast twitch muscle fibres (Hirschfield et al., 2000). NO can diffuse through the plasma membrane, thus the intracellular sources of NO may play a role in the extracellular release.

Autoregulation of blood flow refers to the continuous adjustment in blood supply to various organs that is individualized in relation to metabolic demand and NO has been implicated in the microvascular response to muscle contractions (Stamler and Meissner, 2001). Studies in rat and human skeletal muscles have addressed the question of "NO involvement" by infusion of NOS inhibitors and it is believed that NO or nitrosothiol derived from microvascular endothelial cells factors importantly in control of skeletal muscle blood flow (Hickner et al., 1997; Thomas and Victor, 1998). In relations to this, increased blood flow during contractile activity is critical in providing L-arginine to skeletal muscle, the substrate of NOS isoenzymes (Stamler and Meissner, 2001).

NOS ISOFORMS	SUBCELLULAR LOCATION	CHARACTERISTICS	REFERENCES
nNOS	Plasma membrane	i) interacts with α_1-syntrophin in the membrane cytoskeleton-dystrophin complex of skeletal muscle, ii) has been reported to be the major site of NO release from skeletal muscle.	(Brenman et al., 1996; Brenman et al., 1995; Powers and Jackson, 2008)
eNOS	Mitochondria	Activated through association with the 90-kDa heat shock protein.	(Garcia-Cardena et al., 1998; Stamler and Meissner, 2001)
iNOS	Extracellular space	i) expressed in skeletal muscle under inflammatory conditions, ii) activity is directly coupled to O_2 concentration.	(Powers and Jackson, 2008) (Dweik et al., 1998)

Table 1.2 Characteristics of nitric oxide synthase (NOS) isoforms expressed in skeletal muscle.

1.2.3.2 Sources of superoxide in skeletal muscle

Superoxide anion is generated through either incomplete reduction of oxygen in electron transport systems or as a specific product of enzymatic systems. A variety of different potential sources of superoxide in skeletal muscle have been recognized such as generation by the mitochondria (Davies et al., 1982b; Halliwell and Gutteridge, 2007; Murphy, 2009; Loschen et al., 1974), the nicotinamide adenine dinucleotide phosphate (NADPH) oxidase enzymes (Xia et al., 2003; Hidalgo et al., 2006; Mofarrahi et al., 2008; Whitehead et al., 2010), enzymes of the phospholipase A_2 family (PLA_2) (Gong et al., 2006; Nethery et al., 1999) and xanthine oxidase (Gomez-Cabrera et al., 2010; Gomez-Cabrera et al., 2003), (see figure 1.9).

1.2.3.2.1 Mitochondrial sources

Skeletal muscle consists of oxidative (type I), fast oxidative (Type IIα) and fast glycolytic (IIβ and IIx) muscle fibers of which slow type I myofibers are rich in mitochondria. Mitochondria have generally been cited as the major source of ROS in muscle cells (Davies et al., 1982a; Davies et al., 1982b; Kanter, 1994; Urso and Clarkson, 2003) and the mechanisms of mitochondrial superoxide formation within skeletal muscle have been extensively studied for over 30 years. The mitochondrial electron transport chain is the main source of ATP in the mammalian cell (Mougios, 2006; Scheffler, 1999; Kemp, 2004) and during energy transduction, 2-5% of the oxygen (the final electron acceptor of the electron transport chain) consumed by mitochondria may undergo one electron reduction, forming superoxide (Boveris and Chance, 1973; Loschen et al., 1974). Studies investigating mitochondria at the ultrastructural level have reported that the main sites of mitochondrial superoxide generation are complexes I (NADH dehydrogenase) and III (cytochrome bc1) of the electron transport chain (Barja, 1999; Muller et al., 2004). The mechanism of complex I dependent superoxide release involves a high $NADH/NAD^+$ ratio in the mitochondrial matrix leading to increased superoxide production from the flavin mononucleotide (FMN) cofactor in complex I (Murphy, 2009). FMN cofactor accepts electrons from the NADH and passes them through the iron-sulfur clusters chain to the Coenzyme Q (CoQ) reduction site and the proportion of the FMN that is fully reduced is thought to be set by the $NADH/NAD^+$ ratio (Kussmaul and Hirst, 2006; Murphy, 2009). Mitochondrial complex III has also shown to produce superoxide (Cadenas et al., 1977) and catalyzes the transfer of electrons from reduced CoQ to cytochrome c, with a concomitant translocation of protons across the inner mitochondrial membrane (Baum et al., 1967). Studies using the complex III inhibitor antimycin A have shown this

compound to enhance superoxide production in skeletal muscle mitochondria (Muller et al., 2004) which derives from the reaction of O_2 with a ubisemiquinone bound to the Qo site (Turrens et al., 1985; Murphy, 2009).

Superoxide anion is a membrane impermeant radical thus it is highly compartmentalized and research has been undertaken to identify the side of the inner mitochondrial membrane (those being the mitochondrial intermembrane space and the mitochondrial matrix), to which complex I and III release superoxide. With the development of analytical approaches, studies have delineated the x-ray structure of both complexes I and III and have concluded that complex I derived superoxide is exclusively released into the mitochondrial matrix whereas complex III dependent superoxide is released to both the mitochondrial matrix and the mitochondrial intermembrane space (Muller et al., 2004). The mitochondrial electron transport chain was the first source of superoxide to be suggested in skeletal muscle (Davies et al., 1982a; Davies et al., 1982b), however other metabolic pathways have also been identified and contribute to the intracellular/extracellular generation of superoxide. These are described in detail in the following Sections of this chapter.

1.2.3.2.2 Nicotinamide adenine dinucleotide phosphate oxidase enzymes

Nicotinamide adenine dinucleotide phosphate (NADPH) oxidase (NOX) was fist discovered in phagocytes (Babior, 1978) and is considered a multi-component enzyme system that functions to generate superoxide. During the respiratory burst of phagocytic cells (neutrophils, macrophages and lymphocytes), NADPH oxidase catalyses the reduction of oxygen to superoxide by utilizing NADH and/or NADPH as a substrate (Babior, 1995; Bedard and Krause, 2007). NADPH oxidase localizes on the

plasma membrane of phagocytic cells and is a major component in immune defence since NOX-dependent superoxide production is used for the bactericidal action of these cells (Babior, 1995; Vazquez-Torres et al., 2000). The multicomponent enzyme system consists of catalytic and regulatory subunits which have distinct roles to initiate assembly and activation of the enzyme system (Bedard and Krause, 2007). There are five catalytic/membrane NOX isoforms (NOX1, NOX2, NOX3, NOX4 and NOX5) and two dual oxidase enzymes (DUOX1 and DUOX2), a small membrane-bound integral subunit ($p22^{phox}$) localized to the membrane and three regulatory/cytosolic subunits; $p40^{phox}$, $p47^{phox}$ and $p67^{phox}$ (Bedard and Krause, 2007; Lambeth et al., 2007), (Figure 1.10). In addition, phagocyte NOX has been suggested to require the participation of a small GTP binding protein Rac (Rac1 and Rac2), for enzyme activation (Takeya and Sumimoto, 2003; Groemping and Rittinger, 2005), Rac has been shown to regulate a number of cell signaling pathways (Groemping and Rittinger, 2005). Under non-activating conditions (resting phagocytes), $p47^{phox}$, $p67^{phox}$ and $p40^{phox}$ proteins form a complex within the cytosolic compartment of phagocytic cells in which $p67^{phox}$ tethers $p47^{phox}$ to $p40^{phox}$ (Kuribayashi et al., 2002). However, upon cell stimulation, the cytosolic complex $p47^{phox}$-$p67^{phox}$-$p40^{phox}$ translocates to the membrane and rapidly assembles with the membrane bound NOX2/$p22^{phox}$ complex to form the active NOX2 enzyme complex (Robinson, 2008; Robinson, 2009). This interaction occurs due to a conformational change of $p47^{phox}$ during cell activation, which renders $p47^{phox}$ capable of binding on $p22^{phox}$ (Kuribayashi et al., 2002). NOX2 contains binding sites for the co-enzymes flavin adenine dinucleotide (FAD) and NADPH and following assembly, electrons from NADPH are transferred across the membrane with the use of two haem groups and accepted by molecular O_2 to generate superoxide, which is released on the outer side of the phagocytic membrane (Lambeth, 2004).

NADPH oxidases have recently been shown to be more widespread and studies have identified NADPH oxidase expression in skeletal muscle (Hidalgo et al., 2006; Javesghani et al., 2002; Xia et al., 2003; Espinosa et al., 2006; Mofarrahi et al., 2008; Whitehead et al., 2010). Although little information is available regarding the role and regulation of this complex in generation of superoxide in skeletal muscle, evidence suggests that skeletal muscle cells contain NADPH oxidase enzymes on the muscle fibre plasma membrane (Whitehead et al., 2010; Javesghani et al., 2002), the sarcoplasmic reticulum (SR) (Sun et al., 2011; Xia et al., 2003) and transverse tubules (T-Tubules) (Hidalgo et al., 2006). Pharmacological studies have indicated that skeletal muscle NADPH oxidase can alter the intracellular (Whitehead et al., 2010) and extracellular (Pattwell et al., 2004) content of superoxide. NOX expression on the SR and T tubules seems unlikely to contribute to the extracellular release since superoxide is a membrane impermeable anion. Recent reports have shown that skeletal muscle membrane depolarization may increase the activity of the complex and can influence calcium release by the SR through oxidation of the ryanodine receptor (Cherednichenko et al., 2004; Hidalgo et al., 2006). In addition, NADPH oxidases can also be stimulated by the activation of the phospholipase A_2 enzymes (Zhao et al., 2002).

NADPH oxidases are also expressed in endosomes and studies have shown that NOX-dependent superoxide production is important in the redox-dependent activation of NF-κB transcription factor (Mumbengegwi et al., 2008; Oakley et al., 2009) (see Section 1.7). Reports have examined how superoxide produced within the endosomes can facilitate redox-dependent signaling events in the cytoplasm and have provided evidence that the chloride channels located on the endosomal surface mediate the release of superoxide from the endosomes to the cytosolic compartment of epithelial (Mumbengegwi et al., 2008) and vascular smooth muscle cells (Lassegue, 2007).

Research in skeletal muscle has shown that recycling of endosomes is important for trafficking and maintenance of proteins at the neuromuscular junction and recent reports have shown that endocytic recycling regulators localise to the primary synaptic clefts of the neuromuscular junction (Mate et al., 2012). However, to my knowledge there is no evidence in the literature to suggest that endosomes are expressed in the intracellular compartment of skeletal muscle and contribute to superoxide changes.

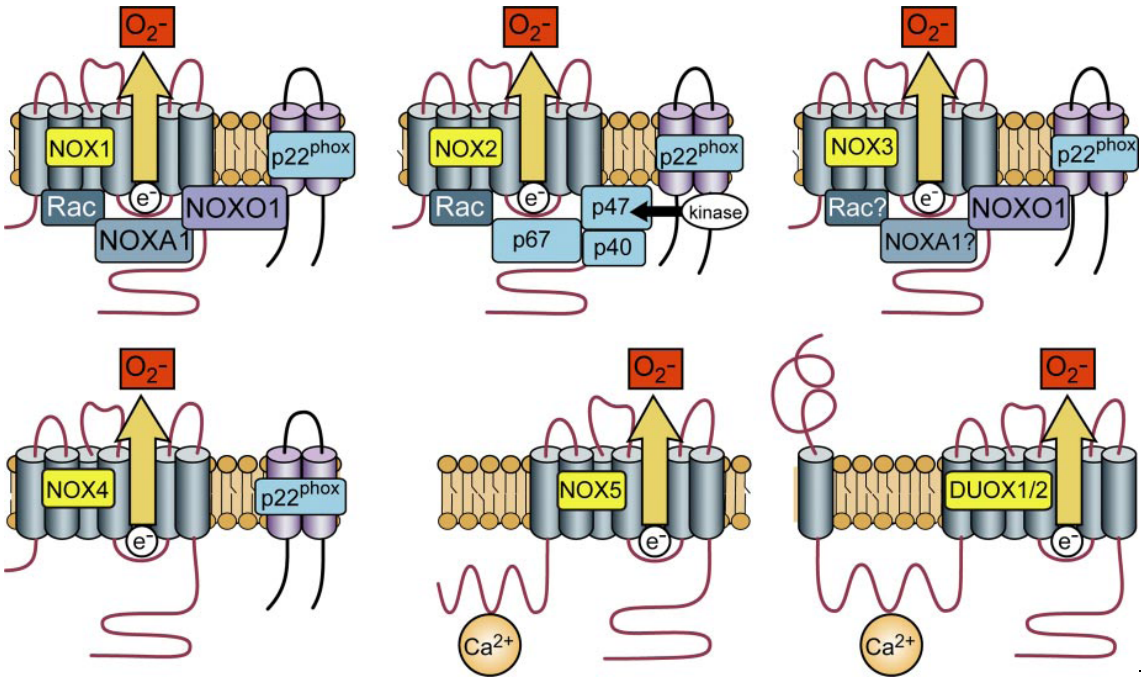

Figure 1.10 Schematic representation of the NADPH oxidase isoforms. Despite their similar structure and enzymatic function, NOX family enzymes differ in their mechanism of activation. NOX1 activity requires $p22^{phox}$, NOXO1 (or possibly p47phox in some cases) and NOXA1, and the small GTPase Rac. NOX2 requires $p22^{phox}$, $p40^{phox}$, $p47^{phox}$, $p67^{phox}$, and Rac. NOX3 requires $p22^{phox}$ and NOXO1. NOX4 requires $p22^{phox}$, but in reconstitute systems it is constitutively active without the requirement for other subunits. NOX5, DUOX1, and DUOX2 are activated by Ca^{2+} and do not appear to require subunits (from Bedard and Krause, 2011).

1.2.3.2.3 Phospholipase A_2 enzymes

Phospholipase A_2 enzymes (PLA_2) is a family of enzymes that cleave membrane phospholipids to release arachidonic acid, which also acts as a substrate for ROS-generating enzyme systems such as the lipoxygenases (Zuo et al., 2004). There are two forms of PLA_2 enzymes present in skeletal muscle, the calcium-dependent ($sPLA_2$) isoform which is located within the mitochondria and has been reported to stimulate the intracellular ROS generation during contractile activity (Nethery et al., 1999) and the calcium-independent form ($iPLA_2$) which is expressed in the cytosolic compartment of skeletal muscle cells and has been shown to modulate cytosolic oxidant changes in skeletal muscle (Gong et al., 2006). In addition, the cytosolic isoform ($cPLA_2$), which is not expressed in muscle cells is activated by micromolar concentrations of calcium and has also been claimed to stimulate ROS generation (Muralikrishna Adibhatla and Hatcher, 2006; Powers and Jackson, 2008). Although the contribution of PLA_2 enzymes to superoxide production has not been extensively studied in skeletal muscle, other studies suggest that this family of enzymes might not directly produce superoxide but that it can regulate the activity of the lipoxygenases by modulating the release of arachidonic acid (Zuo et al., 2004).

1.2.3.2.4 Xanthine oxidase

Xanthine oxidase (XO) has been identified as a source for superoxide generation based on the effects of XO inhibitors (allopurinol or oxypurinol) (Gomez-Cabrera et al., 2003; Heunks et al., 2001). XO catalyzes the oxidation of hypoxanthine to xanthine and can further catalyze the oxidation of xanthine to uric acid. It is highly expressed in endothelial cells (Friedl et al., 1990; Cross and Jones, 1991) and recent

studies in skeletal muscle have show that XO activity may contribute to the increased extracellular superoxide release observed during contractile activity (Gomez-Cabrera et al., 2010).

1.2.4 Which is the major intracellular source for superoxide in skeletal muscle?

Considerable research has been undertaken to identify the major sites that contribute to superoxide production in skeletal muscle both at rest and during contractile activity. As mentioned earlier (Section 1.2.3.2), superoxide anion is generated through either incomplete reduction of oxygen in electron transport systems or as a specific product of enzymatic systems. Although there is little consensus on the prime intracellular sources for superoxide production in muscle, early studies suggested that the mitochondrial respiratory chain was the predominant source during contractile activity (Davies et al., 1982a; Koren et al., 1983). These studies supported early reports published in the 1970's which suggested that 2–5% of the total oxygen consumed by mitochondria may undergo one-electron reduction with the generation of superoxide (Boveris and Chance, 1973; Loschen et al., 1974) and based on this observation, a large number of publications relate the increase in superoxide to the elevated oxygen consumption that occurs with increased mitochondrial activity, implying potentially a 50–100 fold increase in superoxide generation in skeletal muscles subjected to aerobic contractions.

However, recent studies examining the major contributors to superoxide production in skeletal muscle have produced inconsistent findings. Reports from this group have shown that the intracellular ROS changes in skeletal muscle increased by only 2 to 4-fold during contractile activity (McArdle et al., 2005; Palomero et al., 2008;

Pye et al., 2007; Vasilaki et al., 2010). Further studies investigating mitochondrial superoxide production failed to observe changes in MitoSOX Red fluorescence (a mitochondrial superoxide sensitive fluorescent probe) upon tetanic stimulation of single muscle fibres suggesting that superoxide production was not altered with increased contractile activity (Aydin et al., 2009). In relation to this, recent assessments of the rate of superoxide production by mitochondria indicate that only ~0.15% of the total oxygen consumed by mitochondria is reduced to superoxide (St-Pierre et al., 2002), a value that is an order of magnitude lower than the original estimates of 2-5%. Moreover, recent reports have demonstrated that mitochondrial ROS generation is higher during the basal respiration state (state 4) compared with state 3 (maximal ADP-stimulated respiration) (Adhihetty et al., 2005; Kozlov et al., 2005), which further limits the mitochondrial generation of ROS during contractions since skeletal muscle mitochondria during aerobic contractions are predominantly in State 3.

Collectively, these findings imply that mitochondria might not generate superoxide to the extent that was previously estimated. The possibility that other sources unrelated to mitochondria might contribute to superoxide in skeletal muscles has not been examined extensively although non-mitochondrial sites for superoxide production including NADPH oxidases and PLA_2 enzymatic systems have been identified (Section 1.2.3.2). Hence, additional research is required to determine the sites that contribute to superoxide in skeletal muscle both at rest and during contractile activity.

1.3. THE REGULATION OF RONS IN SKELETAL MUSCLE

Skeletal muscle has a well-developed system to regulate the cellular production of RONS and protect the myocytes from oxidative injury (the term oxidative stress and the effect of reactive species in inducing oxidative damage has been described in detail in Section 1.3). The antioxidant network (the system that functions to prevent oxidative injury) consists of enzymatic and non-enzymatic antioxidants that work in a coordinated fashion to resist redox disturbances in the muscle cell.

1.3.1 Enzymatic systems

The main antioxidant enzymes include the superoxide dismutases, glutathione peroxidases, and catalase. There are however additional enzymes such as peroxiredoxins, glutaredoxins, and thioredoxin reductases, which also contribute significantly to preventing RONS toxicity in muscle fibres. In addition, a number of enzymes are involved in the supply of substrates for primary antioxidant enzymes such as glutathione reductase and glucose-6-phosphate dehydrogenase but they do not directly scavenge oxidants.

1.3.1.1 Superoxide dismutase

Superoxide dismutase (SOD) was discovered in 1969 (McCord and Fridovich, 1969) and represents a family of metalloenzymes that catalyze the one electron dismutation of superoxide radical to H_2O_2 and oxygen (Jackson and McArdle, 2011; Palomero and Jackson, 2010). This reaction is considered to be very slow since superoxide radicals electrostatically repel each other (see Section 1.2.2.1). SOD metalloenzymes require a redox active transition metal bound to its active site to

accomplish the catalytic dismutation of superoxide anion (Culotta et al., 2006), which activity is also pH dependent (Radak, 2000). There are three SOD isoenzymes depending on the metal ion in the active site. Skeletal muscle expresses copper-zinc SOD (CuZnSOD or SOD1), which is a highly stable enzyme located within the cytosol and the mitochondrial intermembrane space, and manganese SOD (MnSOD or SOD2), which is not as stable as SOD1 and is found in the mitochondrial matrix (Powers and Jackson, 2008; Radak, 2000). There is however an additional isoform of SOD, the extracellular SOD isoenzyme (ecSOD or SOD3) which is present in the interstitial spaces of tissues and extracellular fluids of many cell types and tissues (Zelko et al., 2002; Culotta et al., 2006), thus SOD3 accounts for the majority of the SOD activity in plasma, lymph and synovial fluid (Mates and Sanchez-Jimenez, 1999). Reports have also shown that SOD3 can be bound to heparin and its primary function is to reduce superoxide that is formed outside cell membranes due to inflammation and ischemia-reperfusion (Fridovich, 1995). SOD provides the first line of enzymatic defence against superoxide and studies have shown that exercise can induce an increase in both SOD1 and SOD2 activities (Leeuwenburgh et al., 1997; Oh-ishi et al., 1997). SOD1 protein has a half-life of 6 to 10 min whereas SOD2 5 to 6 hours (Gorecki et al., 1991) and table 1.3 shows the antioxidant enzyme activity of SOD1 and SOD2 in a variety of tissues including fast and slow skeletal muscles. Oxidative muscle fibres have shown to have a higher mRNA and protein expression of SOD1 and SOD2 compared with fast glycolytic fibres (Radak, 2000). In skeletal muscle, 15-35% of the total SOD activity is in the mitochondria with the SOD2 isoenzyme accounting for 15-20% (Leeuwenburgh et al., 1997) and the remaining 65-85% is in the cytosol (Powers et al., 1994; Ji et al., 1988). Although superoxide is not considered a highly reactive molecule, the importance of SOD as an important cellular redox system regulator is best illustrated in

studies using homozygotic SOD1 knockout mice, which will be described in detail in Section 1.5.

	SOD			GPX				
Tissues	Cu/Zn (unit/mg)	Mn (unit/mg)	Total (unit/g ww)	Cyto (unit/mg)	Mito (unit/mg)	Total (unit/g ww)	CAT (unit/g ww)	GR (unit/g ww)
Liver	500	50	14,400	550	430	85	670	40
Heart	65	21	2610	150	70	17	84	1.3
Soleus	48	7	1300	n.d.	n.d.	13	61	0.8
DVL	21	8	1360	23	17	2	18	0.4
SVL	21	5	887	n.d.	n.d.	0.9	15	0.3
Erythrocytes	n.a.	n.a.	8.8	n.a.	n.a.	25	10	35

Table 1.3 Antioxidant enzyme activity of superoxide dismutase (SOD), glutathione peroxidase (GPX), catalase (CAT) and glutathione reductase (GR) in various rat tissues including the liver, heart, soleus, deep vastus lateralis (DVL), superficial vastus lateralis (SVL) and erythrocytes; n.d., not determined (from Radak, 2000).

1.3.1.2 Glutathione peroxidase

Glutathione peroxidase (GPX) is a homotetramer with each 22kDa subunit containing a selenium atom in the form of a selenocysteine and catalyzes the reduction of H_2O_2 to H_2O or organic hydroperoxide (ROOH) to alcohol (ROH) by using reduced glutathione (GSH) or in some cases thioredoxin (TRX) or glutaredoxin (GRX) as the electron donor (Bjornstedt et al., 1994; Holmgren et al., 2005). In addition, recent reports also suggest that GPX is also implicated in the reduction of hydroxyl radical activity by elimination of H_2O_2 (Landis and Tower, 2005). When GSH provides the electrons to GPX to catalyse the reduction of ROS, GSH is oxidised to glutathione disulfide (GSSG) and further details regarding the regulation of GSH-GSSG are discussed in Section 1.3.2.1.1. GPX is highly specific for its hydrogen donor GSH and

its kinetic characteristics make it a versatile hydroperoxide remover in the cell thus inhibiting lipid peroxidation, DNA and RNA damage (Radak, 2000). Mammalian cells express five isoforms of GPX (GPX1-GPX5), which differ in substrate specificity and cellular localization (Brigelius-Flohe, 1999) with GPX1 as the cytosolic form (Frey et al., 2009) and GPX4 as the most widely expressed. GPX2 and GPX3 are rarely detectable in most tissues and GPX5 is the least described isoenzyme (Mates and Sanchez-Jimenez, 1999). The expression of the GPX genes is controlled by different mechanisms including oxygen tension, metabolic rate (Radak, 2000), toxins and xenobiotics (Halliwell and Gutteridge, 2007) as well as growth and development (Moscow et al., 1992). Similarly to SOD, type I muscle fibres express higher amounts of GPX compared with type IIb fibres (Powers et al., 1994) and its expression and activity increases with endurance exercise (Sen et al., 1992; Leeuwenburgh et al., 1997; Leeuwenburgh et al., 1994). Exercise-induced increase in GPX depends on both the duration and the intensity of the training regime, with moderate and high intensity exercise producing the largest increase in GPX activity (Powers et al., 1994). Table 1.3 shows the antioxidant enzyme activity of GPX in a variety of tissues including fast and slow skeletal muscles.

1.3.1.3 Catalase

Catalase (CAT) is a homotetramer with a molecular mass of 240kDa and its antioxidant property is to catalyze the breakdown of H_2O_2 into H_2O and O_2 (Jackson, 2008; Jackson, 2009). CAT requires heme (Fe^{3+}) as a cofactor, bound at the enzyme's active site for its catalytic function (Zamocky and Koller, 1999). As mentioned earlier, GPX is also a H_2O_2 regulator, and has a much higher affinity for H_2O_2 at low

concentrations (K_m = 1μM) compared with CAT (K_m = 1mM) (Powers and Jackson, 2008). However, under conditions where H_2O_2 is significantly increased, CAT becomes more significant in protecting biological systems and its catalytic function prevails since it cannot be saturated under any H_2O_2 concentration since there is no apparent Vmax (Mates and Sanchez-Jimenez, 1999). In addition, CAT does not require reducing equivalents to function as a H_2O_2 reducer and is therefore considered an energy efficient antioxidant (Vetrano et al., 2005). The cellular location of CAT is different in comparison with GPX as it is mainly found in the cytosolic compartment of the muscle fibres. CAT activity increases with increased H_2O_2 and reports have shown that similarly to SOD and GPX, CAT protein expression and enzymatic activity is higher in highly oxidative fibres (Laughlin et al., 1990; Leeuwenburgh et al., 1994).

1.3.1.4 Additional RONS regulatory enzymes

In addition to SODs, GPXs and CAT, skeletal muscles express additional enzymes such as peroxiredoxins, thioredoxin reductases and glutaredoxins which have significant antioxidant defense properties and can further contribute to maintain the redox homeostasis in skeletal muscle cells.

1.3.1.4.1 Thioredoxin system

The thioredoxin (TRX) system consists of thioredoxins (TRXs) and thioredoxin reductases (TRXRs) (Dimauro et al., 2012). TRXs are a class of small multifunctional proteins that are present in all eukaryotic and prokaryotic organisms and are susceptible to oxidation/reduction in the presence of oxidants (Powis and Montfort,

2001). TRXs are present in various cellular compartments; Trx1 isoform is found in the nucleus and cytosol (Trx1 can be imported into the nucleus from the cytoplasm during various forms of oxidative stress (Wei et al., 2000)) and TRX2 is localized in the mitochondria (Spyrou et al., 1997). The oxidised form of TRXs is reduced by TRXRs, by utilizing electrons from NADPH (Holmgren, 1985). Similarly to the TRXs there are two isoforms of TRXRs; the cytosolic and nuclear isoform (TRXR1) and the mitochondrial isoform (TRXR2) (Dimauro et al., 2012). TRXs are key intracellular regulators of redox signaling and evidence has shown that the TRX system is responsible for maintaining proteins in their reduced state and the control of apoptosis (Arner and Holmgren, 2000).

1.3.1.4.2 Glutaredoxins

Glutaredoxins (GRXs) share many of the functions of TRXs but are reduced by GSH rather than a specific reductase (Berndt et al., 2007). GRXs are small redox enzymes that exist in either a reduced or oxidised form and are involved in the protection and repair of protein and non-protein thiols during periods of oxidative stress (Berndt et al., 2007). Human cells express three types of GRX; GRX1 is found in the cytosol, GRX2 and GRX5 are located in the mitochondria (Powers and Jackson, 2008). GRXs show overlapping functions with the TRX system and have been reported to inhibit apoptosis and reduce protein disulfides at the expense of GSH (Enoksson et al., 2005).

1.3.1.4.3 Peroxiredoxins

Peroxiredoxins (PRXs) were discovered in the late 80's (Kim et al., 1988; Kim et al., 1985) and have recently received much attention. PRXs, initially know as thiol-specific antioxidants (Chae et al., 1993) are a family of cysteine-dependent thioredoxin peroxidases (Wood et al., 2003). PRXs are considered important antioxidant enzymes, which are capable of reducing both hydroperoxides and H_2O_2 (Rhee et al., 2005b; Rhee et al., 2005c) with the use of electrons provided by TRXs (Rhee et al., 2005a). Following detoxification of H_2O_2, the oxidised form of PRX is inactive, requiring the donation of electrons from reduced TRX to restore its catalytic activity (Pillay et al., 2009). Skeletal muscles express six isoforms of PRX, which are present in the cytosol (PRX I, II, VI), the mitochondrion (PRX III) and the extracellular space (PRX IV) (Powers and Jackson, 2008). An additional isoform of PRX, (PRXV) is expressed in the cytosol, mitochondria, nuclei and perixosomes (Rhee et al., 2005a) and is considered a peroxynitrite reductase (Dubuisson et al., 2004; Trujillo et al., 2008).

1.3.2 Non-Enzymatic systems

In addition to the antioxidant enzyme defence network, skeletal muscle also contains non-enzymatic systems, which regulate reactive species and protect muscle cells from oxidative injury. These are water soluble and fat soluble (Halliwell and Gutteridge, 2007) and are classified into two categories: i) the endogenously produced and ii) dietary antioxidants which cannot be synthesized or induced and must be taken from the diet.

1.3.2.1 Endogenous non-enzymatic antioxidants

The most important non-enzymatic endogenously produced antioxidants are glutathione, uric acid, bilirubin and coenzyme Q_{10}.

1.3.2.1.1 Glutathione

Reduced glutathione (GSH) is the most abundant endogenous antioxidant in eukaryotic cells and is a major player in the regulation of the cellular redox state (Kim and Vaziri, 2010). GSH a tripeptide and is synthesized in the liver, by GSH synthetase (Radak, 2000). The release of GSH from the liver is stimulated by catecholamines, glycagon and vasopressin and is transported to tissues via the circulation (Lu et al., 1992; Sies and Graf, 1985). GSH is the most abundant non-protein thiol in cells and plays an important role in converting disulfides to thiols as well as maintaining substrate levels for GPX to eliminate H_2O_2 and hydroperoxides (Meister and Anderson, 1983). Glutamate cysteine ligase (GCL) catalyzes the rate-limiting step in the formation of GSH (Krejsa et al., 2010). The GCL holoenzyme consists of two separately coded proteins, a catalytic subunit (GCLC) and a modifier subunit (GCLM). Both GCLC and GLCM are controlled transcriptionally by a variety of cellular stimuli, including oxidative stress (Krejsa et al., 2010). Expression of GCL is regulated by the redox-sensitive transcription factor Nrf2 (Kim and Vaziri, 2010) (see Section 1.7) and experimental evidence undertaken in Nrf2-null mice has shown that regulation of GSH in cardiomyocytes is linked to the Nrf2 regulated pathway (Brewer et al., 2011). By donating a pair of hydrogen ions, GSH is oxidised to glutathione disulfide (GSSG) (Powers and Jackson, 2008). Although GSSG levels in most tissues are very low (de la Asuncion et al., 1996), the reduction of GSSG is catalyzed by glutathione reductase

(GR), a flavin containing enzyme, where NADPH is used as the reducing agent (Halliwell and Gutteridge, 2007; Radak, 2000). In many tissues, NADPH is produced by glucose-6-phosphate dehydrogenase, however studies in skeletal muscle have identified that NADPH is primarily supplied by isocitrate dehydrogenase (Vetrano et al., 2005). GSH can react directly with a variety of radicals by donating a hydrogen atom (Yu, 1994) and has been shown to reduce vitamin C and E radicals derived in chain breaking reactions with alkoxyl or lipid peroxyl radicals (Powers and Jackson, 2008; Radak, 2000). The GSH concentration varies from tissue to tissue and studies in skeletal muscle have shown that type I muscle fibres contain a higher GSH content than type IIb although the ratio GSH/GSSG (an additional indicator of redox status) appears to be consistent across various fibre types (Ji, 1995). Intracellular GSH levels are regulated by GSH utilization and GSH synthesis and due to the large muscle mass of the body, the relatively high concentration of GSH in skeletal muscle can influence plasma GSH levels (Kretzschmar et al., 1992; Sen et al., 1992). High intracellular levels of GSSG have shown to inactivate enzymes and cause damage to the cell (Halliwell and Gutteridge, 2007), however skeletal muscle fibres are capable of exporting GSSG to maintain the GSH/GSSG ratio (Meister and Anderson, 1983).

1.3.2.1.2 Uric acid

Uric acid (UA) may also function to protect muscle fibres against oxidative injury and is a strong reducing agent by acting as an electron donor (Halliwell and Gutteridge, 2007). UA is a by-product of purine metabolism and has shown properties in scavenging peroxyl and hydroxyl radicals as well as singlet oxygen (Davies et al., 1986; Sevanian et al., 1985). In humans, over half of the antioxidant capacity of blood

plasma derives from UA (Maxwell et al., 1997). Contractile activity of high intensity has shown to increase plasma UA levels due to increased release of hypoxanthine and xanthine from the muscle into the circulation and the subsequent convertion of these products to UA by xanthine oxidase, which is present in endothelial cells of blood vessels (Samra et al., 1991). At physiological pH, uric acid exists mainly as urate (Powers and Jackson, 2008), which has also been shown to protect against oxidative damage by acting as an electron donor (Halliwell and Gutteridge, 2007). Urate is also capable of preventing hydroxyl radical formation by hindering the Fenton reaction as it is considered a metal ion chelator (Halliwell and Gutteridge, 2007).

1.3.2.1.3 Bilirubin and Coenzyme Q_{10}

Bilirubin is the final product of hemoprotein catabolism, and similarly to UA it possesses antioxidant properties against peroxyl radicals and lipid peroxidation (Stocker et al., 1987a; Stocker et al., 1987b). Contractile activity has shown to increase blood levels of bilirubin and evidence suggests that is can protect cells from the toxic levels of H_2O_2 (Baranano et al., 2002). Upon oxidation, bilirubin is converted to biliverdin and then recycled back to bilirubin, a reaction catalysed by biliverdin reductase (Liu et al., 2006; Baranano et al., 2002). Coenzyme Q_{10} (CoQ_{10}) also known as ubiquinone contributes to peroxyl radical scavenging and inhibits lipid peroxidation (Sena et al., 2008). CoQ_{10} is abundant on the inner mitochondrial membrane and plays an essential role in mitochondrial electron transport as an electron carrier (Halliwell and Gutteridge, 2007). Although few data are available regarding the role of CoQ_{10} as an antioxidant *in vivo*, evidence has shown that exercise can increase the CoQ_{10} content in skeletal muscle (Gohil et al., 1987).

1.3.2.2 Dietary antioxidants

Nutrition significantly impacts the cellular antioxidant system and research has identified that dietary antioxidants such as vitamin C, vitamin E and carotenoids also exert defensive properties and protect muscle cells from RONS toxicity. Vitamin E is a lipid-soluble antioxidant and possesses strong membrane-stabilizing effects, thus it protects cells from lipid peroxidation (Dillard et al., 1978; Jackson et al., 2007). Intervention studies have shown that vitamin E deficiency can disturb cell membrane fluidity (Dillard et al., 1978), alter GSH/GSSG (Anzueto et al., 1993) and exacerbate mitochondrial dysfunction and lipid peroxidation in skeletal muscle (Davies et al., 1982b). Carotenoids which are also located in the membranes of tissues show significant antioxidant defence properties by protecting myocytes from lipid peroxidation (Krinsky, 1998). Due to their structural arrangement, carotenoids are efficient biological antioxidants and can scavenge superoxide and peroxyl radicals (Krinsky, 1998). In contrast, vitamin C is a hydrophilic vitamin and therefore functions in a aqueous environment, the cytosolic cellular compartment and extracellular fluid (Beyer, 1994). Vitamin C scavenges superoxide, hydroxyl radical, and lipid hydroperoxide radicals (Carr and Frei, 1999) and can additionally play an important role in the recycling of vitamin E (Packer et al., 1979). Most mammalian species synthesize vitamin C. High doses can have a prooxidant effect (Yu, 1994) and induce hydroxyl radical formation due to reaction with transition metal ions (Halliwell and Gutteridge, 2007).

1.4. RONS METABOLISM IN GLYCOLYTIC AND OXIDATIVE SKELETAL MUSCLE FIBRES

Reports have demonstrated the existence of differences between glycolytic and oxidative skeletal muscle fibres in RONS metabolism (Picard et al., 2012). Experimental evidence in both permeabilised fibres and in isolated mitochondria have shown that H_2O_2 release was two - to threefold higher from mitochondria in white gastrocnemius (fast glycolytic) compared with the soleus muscle (oxidative) under basal state 2 respiration in the presence of complex I or complex II substrates (Picard et al., 2011; Anderson and Neufer, 2006). As a consequence, superoxide leak expressed as a percentage of total electron flux through the respiratory chain was 3.5-fold greater in mitochondria from the white gastrocnemius compared with that of the soleus muscle (Picard et al., 2008). Although the mechanisms underlying this substantial difference in H_2O_2 release are not fully understood, there is evidence of fibre type differences in the subcellular H_2O_2 scavenging systems (Treberg et al., 2010). Direct measurements in muscle fibres have shown that the capacity of mitochondria from fast-glycolytic fibres to scavenge an exogenous H_2O_2 load is approximately 40–50% lower compared with mitochondria from slow-oxidative fibres (Anderson and Neufer, 2006). This can be attributed to the activities of important antioxidant enzymes, which are significantly lower in glycolytic muscle compared with oxidative muscle. Reports have shown that glutathione peroxidase and catalase, the main H_2O_2 reducing systems are on average 88% lower in glycolytic compared with oxidative muscles (Picard et al., 2012). Overall, current evidence suggests that oxidative muscle fibres, fibres which contain a large mitochondrial biomass are more protected against ROS toxicity whereas fast glycolytic muscles exhibit a greater ROS production. In relation to this, it has been suggested that the higher intracellular ROS content in fast-twitch muscles may be required to maintain

redox-dependent signaling pathways such as the control of redox-sensitive transcription factors (see Section 1.7).

1.5. RONS INDUCE OXIDATIVE DAMAGE TO SKELETAL MUSCLE CELLS

Oxidative stress is defined as an imbalance between oxidants and antioxidants (Sohal and Weindruch, 1996) and early studies that examined the effect of oxidant production during contractile activity suggested that these species were inevitably damaging to muscle cells (Davies et al., 1982b). The first evidence that contracting skeletal muscles produce free radicals appeared in the early 80's and it was suggested that oxidants are essentially by-products of metabolism and deleterious to cells and tissues (Davies et al., 1982b). Excess RONS production and accumulation can induce severe cellular damage, leading to physiological dysfunction and cell death, contributing to chronic disease development (Zelko et al., 2002) and it is clear that oxidants can act as mediators of contraction-induced damage to skeletal muscle (Jackson et al., 1985; Reid et al., 1992) in situations where RONS are excessively augmented or when antioxidant defenses are compromised (Jackson et al., 2007; McArdle et al., 1999; Powers and Jackson, 2008). Elevated oxidants can result in oxidative damage to virtually all macromolecules including proteins, carbohydrates, lipids and nucleic acids (mitochondrial and nuclear) leading to mutagenesis and loss of function (Pulliam et al., 2012). The sensitivity of a particular target is defined by the local redox state and the intrinsic sensitivity of the molecule to oxidation-reduction (Halliwell and Gutteridge, 2007; Radak, 2000) and studies in skeletal muscle have identified that oxidants can induce oxidative damage to redox sensitive contractile

proteins such as myosin heavy chain proteins (Coirault et al., 2007; Yamada et al., 2006) and troponin C (Kaneko et al., 1992; Plant et al., 2000), see Sections 1.1.5 and 1.1.6 for a detailed description of muscle contractile proteins. In particular, *in vitro* experiments have shown that peroxynitrite can mediate the oxidation of myosin heavy chains as shown by the increase in protein carbonylation in purified myosin fractions (Coirault et al., 2007). Further reports have also examined the functional consequences of myosin oxidation on motor function and have reported that the velocity of actin sliding over myosin is significantly reduced following myosin heavy chain oxidation indicating that oxidative modification of myosin may impair actin-myosin binding (Coirault et al., 2007; Yamada et al., 2006). Skeletal muscle mitochondria were suggested to be the major sources of oxidative damage in skeletal muscle but it is now clear that there are endogenous sources of reactive species other than mitochondria (see Section 1.2.3.2). Inflammatory and degenerative muscle diseases, such as muscular dystrophies (Whitehead et al., 2010) or immobilization of skeletal muscle (Kondo et al., 1991; Kondo et al., 1993) are associated with increased levels of oxidative damage and muscle weakness. Oxidative stress can contribute to the rate of muscle atrophy by promoting the activation of calpain (Kondo et al., 1992; Powers et al., 2007) and/or capsase-3 (Du et al., 2004; McClung et al., 2007) and the magnitude of the change in redox state determines the biological effect.

1.6. RONS ARE IMPLICATED IN THE PROCESSES OF SKELETAL MUSCLE AGEING

Ageing is defined as an age-related increase in susceptibility to diseases and death (Maynard Smith, 1962). Ageing is a complex process that affects every major

system at the molecular, cellular and organ levels and although the exact cause of ageing is unknown, there is significant evidence that oxidative stress plays a major role in the ageing process. As early as 1956, Denham Harman suggested that free radicals are likely to be involved in ageing and proposed the free radical theory of ageing (Harman, 1956). This theory has gained considerable momentum in recent years due to the ability of reactive species to modulate a variety of intracellular signal transduction processes that are linked to widespread biological processes. The basis of the oxidative stress hypothesis is that ageing occurs as a result of an imbalance between oxidants and antioxidants, which leads to the accrual of damaged proteins, lipids and DNA macromolecules with age (Harman, 1956)**,** resulting in a progressive loss in the functional efficiency of various cellular processes (Muller et al., 2007).

Studies in the 70's suggested that mitochondrial organelles could generate a disproportionately large amount of reactive oxygen species (Boveris and Chance, 1973). Based on this finding, Harman proposed a modification of the free radical theory (Harman, 1956) and described the mitochondrial theory of ageing (Harman, 1972) giving a central role to mitochondria. Over the last 4 decades, there has been an enormous increase in information concerning the effect of oxidants with age and although there is evidence in support of the oxidative stress theory of ageing, there are also studies that do not directly support this theory (Muller et al., 2007; Perez et al., 2009a; Perez et al., 2009b; Sohal and Orr, 2012).

The causes of ageing can be divided into exogenous/extrinsic (including environmental stresses such as pollution, exercise and nutrition) and endogenous/intrinsic (including genetically associated processes and passive random biochemical processes which may involve reactive species associated damage) (Radak, 2000). The extrinsic factors can influence intrinsic causes and reactive species reactions

can affect ageing extrinsically and intrinsically, in active and passive ways (Radak, 2000). Many studies have indicated a positive correlation between tissue concentration of oxidised macromolecules and life span including an increase in DNA damage (Wang et al., 2010; Mecocci et al., 1999), accumulation of oxidised proteins (Mecocci et al., 1999; Goto et al., 1995) and increased levels of lipid peroxidation (Reckelhoff et al., 1998; Miro et al., 2000) with age. Increased DNA damage has been shown to alter genetic stability and may induce the expression of genes that regulate cell proliferation and/or block the expression of certain genes, thus permit damage with increasing age (Simic, 1992). RONS induced DNA sequence changes or mutations have been suggested to affect the cellular state of differentiation (Cutler, 1991; Halliwell and Gutteridge, 2007) and in relation to the mitochondrial theory of ageing (Harman, 1972), the accumulation of mitochondrial DNA damage (Wang et al., 2010) has been proposed to prevent the rejuvenation of the mitochondrial population and lead to bionergetic decline and cellular death (Miquel et al., 1998). The accumulation of altered/oxidised proteins in aged tissues further implies the possible involvement of RONS in the processes of ageing (Goto et al., 1995; Simic, 1992). Aged tissues show an accumulation of catalytically inactive or less active forms of enzymes and the observed age-related changes in catalytic activity have been suggested to occur due to oxidative modifications induced by reactive species (Goto et al., 1995; Simic, 1992). Age-related changes in lipid peroxidation have also been observed with tissues from aged rodents showing higher levels of lipid peroxidation and intervention studies have shown that vitamin E supplementation can reduce lipid peroxidation and LDL oxidation in tissues from aged rodents (Yu et al., 1998; Reckelhoff et al., 1998)

The role of oxidants in ageing has also been extensively examined in different model organisms, which have undergone genetic manipulations with inconsistent

findings (Muller et al., 2006; Vasilaki et al., 2010; Jakupoglu et al., 2005; Conrad et al., 2004; Ran et al., 2007). Transgenic and knockout mouse studies have provided insight into the function of RONS regulatory enzymes in ageing and it has been shown that homozygotic mice lacking SOD2 (Li et al., 1995), TRX1 (Matsui et al., 1996), TRX2 (Nonn et al., 2003), TRXR1 (Jakupoglu et al., 2005) and TRXR2 (Conrad et al., 2004) are embryonically lethal, suggesting that these enzymes are required for embryonic development. Mouse models with a shorten lifespan include $PRX1^{-/-}$ (Neumann et al., 2003), $PRX2^{-/-}$ (Lee et al., 2003) and $SOD1^{-/-}$ mice (Muller et al., 2006; Vasilaki et al., 2010) whereas $GPX1^{-/-}$ (Perez et al., 2009a; Perez et al., 2009b) and $SOD3^{-/-}$ (Carlsson et al., 1995; Sentman et al., 2006) knockout mouse studies showed not effect on lifespan. In contrast, transgenic mouse studies which included overexpression of RONS protective enzymes have failed to provide evidence of increased lifespan with the exception of mitochondrial catalase overexpressing mice which showed a 21% increase in lifespan (Schriner et al., 2005). As mentioned earlier (Section 1.3.1.3), catalase is not expressed in mitochondria and the effect on lifespan is likely to be related to a reduction in H_2O_2.

The reduction in lifespan shown in $PRX1^{-/-}$ and $PRX2^{-/-}$ mice is much more pronounced in $SOD1^{-/-}$ mice (30% reduction) and provides support for the oxidative theory of ageing. In addition, homozygotic SOD1 knockout mice show an accelerated, age-related loss of skeletal muscle mass, which mimics the loss that occurs in wild type control mice past median lifespan and in older humans (Larkin et al., 2011; Jang et al., 2010). Studies in humans have shown that by the age of 70, the cross-sectional area of skeletal muscle is reduced by 25–30%, and muscle strength is reduced by 30–40% (Porter et al., 1995). Oxidative damage has been claimed to be involved in the loss of tissue function that occurs during ageing, and skeletal muscle of old rodents has been

reported to contain increased amounts of the products of oxidative damage to biomolecules such as lipid, DNA, and proteins in comparison with young or adult rodents (Broome et al., 2006; Sastre et al., 2003; Vasilaki et al., 2007). Elevated oxidative stress has also been observed in skeletal muscles from SOD1 knockout mice, thus this mouse model may potentially provide a useful model to study the role of a chronic oxidative stress in loss of skeletal muscle and to uncover potential targets for intervention for preventing sarcopenia in humans.

As mentioned earlier in Section 1.3.1.1, SOD1 is present in the cytosol and mitochondrial intermembrane space and catalyzes the autocatalytic oxidation and reduction of superoxide to molecular oxygen and H_2O_2. Hence, the skeletal muscle ageing phenotypic changes seen in SOD1 knockout mouse model are hypothesised to be related to elevated superoxide content. However, superoxide can react rapidly with NO to form peroxynitrite (see Section 1.2.2.5), thus alternative species might play a key role in the observed muscle atrophy. Hence, to identify the reactive species that are implicated in skeletal muscle degeneration it is essential to monitor specific radical species and further research is warranted to assess the changes in RONS and adaptive responses that occur in skeletal muscles from SOD1 knockout mice.

1.7. RONS ARE IMPORTANT REGULATORY MOLECULES IN SKELETAL MUSCLE

Although high levels of reactive species can induce cellular oxidative damage (see Sections 1.3 and 1.4), recent data indicate that RONS play multiple regulatory roles and influence the biology of skeletal muscles by fulfilling important cellular functions (Droge, 2002; Jackson et al., 2007; Powers and Jackson, 2008; Reid et al., 1993;

Jackson et al., 2002; Go and Jones, 2010; Gong et al., 2006). The concept that oxidants are essential in the physiology of skeletal muscles contrasts starkly with previous evidence that RONS were inevitably damaging to cellular components of muscle cells. Due to recent advances in the field of muscle redox status there is evidence that the cellular redox balance can be harnessed and changed to better suit specific metabolic needs, and that it can be considered as a dynamic condition, fluctuating from a relatively reduced state to relative oxidation, depending on functional requirements (Hwang et al., 1992; Ziegler, 1985). Indeed, for some cellular processes, a particular redox state "optimal redox state" is required for optimal function and changes to the oxidised or reduced state might be detrimental (Andrade et al., 1998; Aghdasi et al., 1997; Radak, 2000).

1.7.1 RONS regulate Ca^{2+} release from the sarcoplasmic reticulum

Recent reports have shown that oxidants control Ca^{2+} release in skeletal muscle by controlling the opening of calcium release channels (ryanodine receptor) in the sarcoplasmic reticulum (Hidalgo et al., 2006; Sun et al., 2011). This has been suggested to occur via oxidative modification of the ryanodine receptor in which, critical thiol groups are oxidised (Abramson and Salama, 1989; Hidalgo et al., 2006). This implies the existence of an optimal redox state for ryanodine receptor in which the state of the redox sensitive thiol groups modulates the channel activity. In relation to this, sarcoplasmic Ca^{2+} ATPases are also redox sensitive and exposure to oxidants has shown to inhibit the enzymatic activity of these proteins (Andrade et al., 1998).

1.7.2 RONS regulate the activation of enzymes and protein kinases

Oxidants and reductants have shown to modulate the activity of a variety of enzymes including enzymes involved in glycolysis, tricarboxylic acid cycle and oxidative phosphorylation (Stamler and Meissner, 2001; Ziegler, 1985; Gardner et al., 1995). Nitric oxide increases during periods of contractile activity (Pye et al., 2007) and it has shown to increase the supply of glucose to the exercised muscles by dilating the arterioles and by inhibiting the enzymatic activity of creatine phosphokinase, glyceraldehyde-3-phosphate dehydrogenase, cytochrome c oxidase and aconitase (Balon and Nadler, 1994; Stamler and Meissner, 2001). As mentioned earlier in Section 1.2.2.2, NO can stimulate guanylyl cyclases thus increase the cGMP content which can in turn activate a number of protein kinases, phosphodiesterases and ion channels (Stamler and Meissner, 2001; Schmidt et al., 1993; Lucas et al., 2000).

1.7.3 RONS regulate redox-sensitive transcription factors

Recent reports also suggest that reactive species are important signaling molecules as they can initiate and mediate signal transduction pathways (Droge, 2002; Jackson, 2008; Powers and Jackson, 2008). Studies in skeletal muscle have shown that changes in cell signaling following contractile activity are likely to be mediated by the increased RONS production observed during contractions (Vasilaki et al., 2006; McArdle et al., 2001). Studies from this group have showed that the exercise dependent increase in Heat Shock Protein (HSP) 60 and 70 (proteins that are associated with significant protection against subsequent cellular damage) as well as SOD and CAT activity (McArdle et al., 2001) was attenuated following pre-supplementation with antioxidant vitamin C, supporting the possibility that these responses were regulated by reactive species (Jackson et al., 2004; Khassaf et al., 2003). One mechanism by which

cells respond to RONS is through activation of redox sensitive transcription factors (Jackson et al., 2002; Go and Jones, 2010; Mann et al., 2007a) which are involved in the upregulation of antioxidant enzymes such as nuclear factor erythroid 2-related factor (Nrf2), Nuclear Factor κB (NFκB) and Activator Protein -1 (AP-1) (Jackson et al., 2002; Powers and Jackson, 2008; Mann et al., 2007a; Mann et al., 2007b; Pamplona and Costantini, 2011; Kim and Vaziri, 2010), HSPs are primarily regulated by the transcription factor Heat Shock Factor (HSF1) (Cotto and Morimoto, 1999). Additional studies from this group have confirmed that an isometric protocol that increased oxidants generation in mouse skeletal muscle, activated the transcription factors NFκB, AP-1 and HSF1 which resulted in increased content of SOD, CAT and HSPs (Vasilaki et al., 2006).

The ability of cells and tissues from old mammals to respond to a variety of stresses by an increased content of HSPs and RONS protective enzymes is severely attenuated (Demirel et al., 2003; Hall et al., 2000). Reports in skeletal muscle have shown that the increase in the protein expression of antioxidant enzymes and HSPs that is evident in muscles of adult rodents following isometric contractions was abolished in muscles of old rodents and this inability to adapt was due to the lack of complete activation of the appropriate transcription factors (Vasilaki et al., 2006). Recent experimental evidence suggest a molecular cross-talk between Nrf2 and NFκB signaling pathways (Stepkowski and Kruszewski, 2011) and studies have demonstrated that the age-related inability to activate the redox-sensitive transcription factors including Nrf2, NFκB, AP-1 and HSF1 and the subsequent failure of HSP and antioxidant protective enzyme upregulation plays a critical role in the development of functional deficits that occur with ageing in skeletal muscle (Vasilaki et al., 2010; Steinbaugh et al., 2012;

Safdar et al., 2010). Transgenic studies have shown that overexpression of HSP70 in mouse skeletal muscle provided protection against the fall in specific force associated with ageing and facilitated rapid and successful regeneration following contraction-induced damage in muscles of old HSP70 overexpressor mice compared with the impaired regeneration and recovery normally observed in old WT mice (McArdle et al., 2004). This protection was associated with prevention of oxidative damage and importantly, maintenance of the ability of muscles of old HSP70 overexpressor mice to activate NFκB following contractions (Broome et al., 2006) indicating a close relationship between retention of the ability of muscle from old mice to regenerate and the ability of those muscles to activate transcription factors (Safdar et al., 2010). A schematic figure of how reactive species can activate the Nrf2 pathway and subsequently the expression of RONS protective enzymes is shown in figure 1.11.

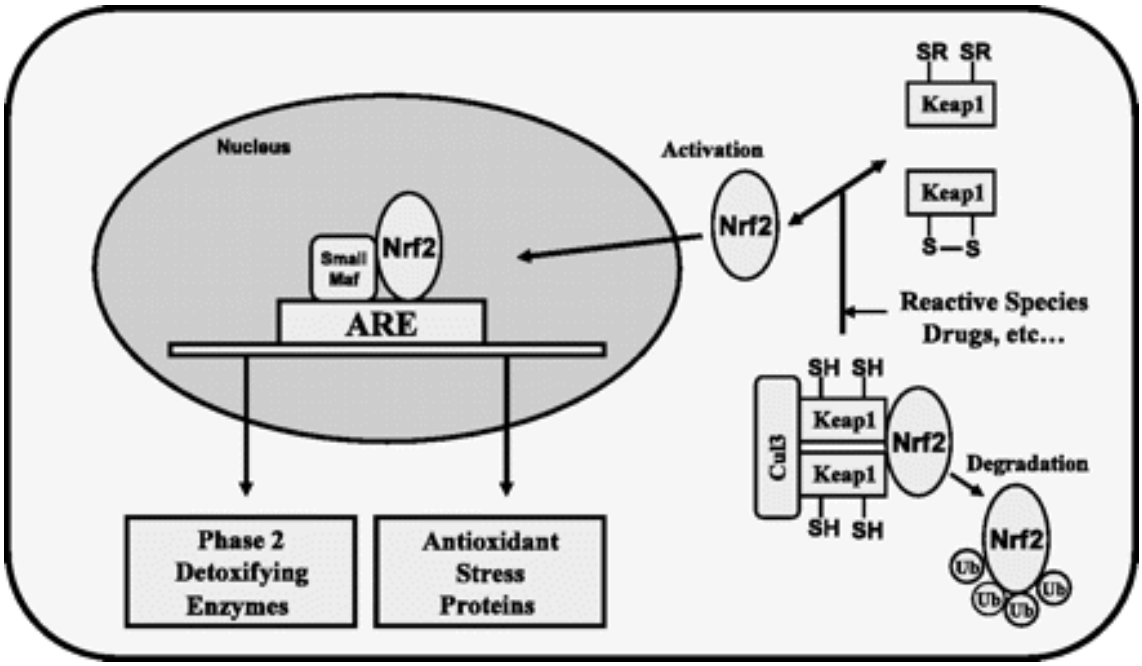

Figure 1.11 Schematic representation of Nrf2 activation by reactive species. Under normal conditions, Nrf2 is sequestered in the cytoplasm via binding to its repressor molecule, Keap1. Oxidants cause dissociation of Nrf2-Keap1 complex, which culminates in ubiquitination of Keap1 and nuclear translocation of Nrf2. After heterodimerization with other transcription factors such as small Maf, within the nucleus, Nrf2 promotes transcriptional activation of antioxidant and detoxifying enzymes by binding to the antioxidant responsive elements (ARE) in the promoter regions of the target genes (from Ramplona and Costantini, 2011).

1.7.4 RONS regulate skeletal muscle force production

The physiological importance of oxidants as regulators of skeletal muscle metabolism is further implied from the strong relationship between reactive species and skeletal muscle force production. Studies have identified that muscle redox status has an important influence on force production in unfatigued skeletal muscle. It has been shown that a modest increase in oxidants in skeletal muscle fibres resulted in an increase in force production (Reid et al., 1993) whereas muscles exposed to higher or

lower ROS concentrations, the force production was lower, indicating that skeletal muscle force production is likely mediated by reactive species production (Reid and Moody, 1994). A potential pathway that might be involved in modification of skeletal muscle force production is the effect of oxidants on the calcium sensitivity of myofilaments (Smith and Reid, 2006).

1.8. SUMMARY

In summary, RONS are constantly produced by resting and contracting skeletal muscle fibres from a variety of cellular locations. The generation of oxidants is augmented during contractile activity and this increase may induce oxidative damage to muscle cells when antioxidant defenses are compromised or when RONS production is grossly excessive. Although the field of muscle redox biology has advanced rapidly and many sources have been identified to contribute to this apparent increase, there is still however considerable debate regarding the major sites that contribute to the increased rate of muscle superoxide generation during contractile activity (see Section 1.2.4). Recent advances in redox biology have shown that reactive species production under physiological conditions plays important roles in the physiological adaptations of muscle to contractions. It has become clear that low-to-moderate levels of oxidants are essential in the physiology of skeletal muscle as they are implicated in the control of gene expression, regulation of cell signaling pathways, and modulation-optimization of skeletal muscle force production. In contrast, excess RONS production can induce severe cellular damage, leading to physiological dysfunction and cell death. In addition, oxidative stress is implicated in the processes of skeletal muscle ageing and genetic interventions ($SOD1^{-/-}$ mice) have provided evidence that increased levels of oxidative

damage contribute to the rate of muscle atrophy, though the specific oxidants that play a key role in skeletal muscle ageing are yet to be examined.

1.9. AIMS

Hence, the main aims of this thesis were:

- Develop specific techniques to examine cytosolic and mitochondrial superoxide in single isolated mature skeletal muscle fibres.
- Identify the major sites that regulate cytosolic superoxide in both resting and contracting isolated fibres.
- Identify the reactive species that are involved in the accelerated loss of muscle mass in the homozygotic SOD1 knockout mouse model and to characterize the changes in redox status and adaptive responses that occur in muscles from the SOD1 knockout mice.

CHAPTER 2

EXPERIMENTAL METHODS

2 EXPERIMENTAL METHODS

2.1 CHEMICALS AND REAGENTS

Unless stated otherwise, all chemicals used in this study were obtained from Sigma Chemical Company, Dorset, UK.

2.2 ISOLATION OF SINGLE MATURE SKELETAL MUSCLE FIBRES

Single muscle fibres were isolated from the *FDB* muscles of mice as previously described (Palomero et al., 2008; Pye et al., 2007). *FDB* is a small and thin muscle located in the midline of the sole of the foot and in the presence of collagenase, single viable intact myofibres are dissociated from the muscle. Mice (males and females) were killed by cervical dislocation and the flexor digitorum brevis (FDB) muscles were dissected. The selection of gender of mice for each study was based entirely on the available mice at that time. Studies have shown that on average, the skeletal muscle of women typically has 60–80% of the strength, muscle fibre cross sectional area and whole muscle anatomical cross-sectional area of men (Folland and Williams, 2007). However, there is no evidence in the literature to suggest that skeletal muscles from female mice show a different pattern in RONS activation in comparison to skeletal muscles from male mice hence it was assumed that single muscle fibres from male and female mice would respond in the same way.

Single muscle fibres were isolated from the *FDB* muscles of mice according to the method of Shefer & Yablonka-Reuveni (Shefer and Yablonka-Reuveni, 2005). *FDB* muscles were incubated for 1.5 h at 37^{o}C in 0.4% (w/v) sterile Type I collagenase in minimum essential medium eagle (MEM) which contained all 21 amino acids, ribonucleosides, deoxyribonucleosides, sodium bicarbonate and was additionally

supplemented with 2mM glutamine, 50 i.u. penicillin, 50μg ml^{-1} streptomycin and 10% foetal bovine serum (FBS) (Invitrogen Ltd, Paisley, UK). Muscles were agitated every 20 min to improve digestion of the connective tissue. Single myofibres were released by gentle trituration with a wide-bore pipette and were washed three times in MEM containing 10% FBS. Free single muscle fibres were separated from damaged fibres and contaminating cells by centrifugation at low speed (600 g for 30 s at 25°C). Single fibres were plated onto pre-cooled 35 mm cell culture dishes pre-coated with Matrigel (BD Biosciences, Oxford, UK) and were allowed to attach for 45 min before adding 2 ml of MEM containing 10% FBS. Pre-cooling was necessary to prevent premature solidification of the collagen before fibre attachment. Fibres were incubated for 16 h at 37^{o}C, 21% O_2 in 5% CO_2 tissue culture incubator. It has recently been shown that fibres prepared and cultured in this manner are viable for up to 6 days in culture (Palomero et al., 2008), but they have routinely been used at 16 h following isolation. Experiments were only performed on fibres that displayed excellent morphology and exhibited intense transverse striations along the sarcolemma. All experiments were undertaken in the presence of 21% O_2 environment.

2.3 USE OF ROS SENSITIVE FLUORESCENT DYES TO STUDY INTRACELLULAR CHANGES IN ROS IN SINGLE SKELETAL MUSCLE FIBRES

2.3.1 Use of CM-DCFH DA to monitor changes in ROS production in single isolated fibres

To monitor changes in ROS production, single *FDB* muscle fibres were loaded with CM-DCFH DA as previously described (Palomero et al., 2008). Fibres were loaded by incubation in 2ml Dulbecco's phosphate-buffered saline (D-PBS) containing

10μM 5- (and 6-) chloromethyl-2',7'-dichlorodihydrofluorescein diacetate (CM-DCFH DA) (Molecular Probes, OR, USA) for 30 min at 37°C. Cells were washed twice with D-PBS and were maintained in MEM without Phenol Red containing 10% FBS during the experimental period. MEM contained 19 amino acids; the essential amino acids and the non-essential amino acids including L-ala, L-asn, L-asp, L-glu, L-gly, L-pro and L-ser. CM-DCFH DA readily diffuses into cells and within the cytoplasm the acetate group is cleaved by cytosolic esterases to yield CM-DCFH, a hydrophilic non-fluorescent molecule that is retained by the cell. Intracellular ROS, particularly hydrogen peroxide, convert CM-DCFH to its fluorescent derivate, CM-DCF.

2.3.2 Use of DAF-FM DA to monitor intracellular NO activity in isolated fibres

The method used was described in detail in a previous study by Pye *et al*. (2007). Fibres were loaded by incubation in 2ml Dulbecco's phosphate-buffered saline (D-PBS) containing 10μM 4-amino-5-methylamino-2′,7′-difluorofluorescein diacetate (DAF-FM DA) (Molecular Probes, OR) for 30 min at 37°C. Cells were then washed twice with D-PBS and were maintained in MEM containing 10% FBS without Phenol Red during the experimental period. MEM contained 19 amino acids; the essential amino acids and the non-essential amino acids including L-ala, L-asn, L-asp, L-glu, L-gly, L-pro and L-ser. DAF-FM DA readily diffuses into cells and within the cytoplasm releases DAF-FM by the action of intracellular esterases. DAF-FM is essentially non-fluorescent until it is nitrosylated by products of oxidation of NO, resulting in DAF-FM triazole which exhibits about a 160-fold greater fluorescence quantum efficiency (Kojima et al., 1999).

2.3.3 Use of dihydroethidium (DHE) to monitor cytosolic superoxide changes in isolated fibres

For the detection of cytosolic superoxide, fibres were loaded with 5μM dihydroethidium (DHE) (Molecular Probes, OR), in a similar manner to CM-DCFH DA and DAF-FM DA. DHE is a non charged fluorescent probe specifically sensitive to superoxide (Bindokas et al., 1996; Zuo et al., 2004) and displays "blue" fluorescence" (Zielonka and Kalyanaraman, 2010) in the cytoplasm of single muscle fibres. Upon oxidation, the oxidised form of DHE becomes positively charged, contributing to its tendency to accumulate in the nucleus and intercalate with the negatively charged DNA phosphate backbone, producing Ethidium (E^+) and 2-hydroxyethidium (2-OH-E^+) fluorescence (Zielonka and Kalyanaraman, 2010). DHE is not targeted to mitochondria and its oxidation is likely to be influenced by cytosolic sources of superoxide production (Johnson-Cadwell et al., 2007; Gao and Wolin, 2008). Application of the technique to the study of single isolated mature skeletal muscle fibres is examined in detail in Chapter 3.

2.3.4 Use of MitoSOX Red to monitor mitochondrial superoxide changes in isolated fibres

Fibres were loaded with 250nM MitoSOX Red (Invitrogen), using the same protocol as for CM-DCFH DA, DAF-FM DA and DHE. MitoSOX Red is a derivative of DHE designed for highly selective detection of superoxide in mitochondria and exhibits fluorescence (MitoSOX Red fluorescence) on oxidation and subsequent binding to mitochondrial DNA (Robinson et al., 2006).

2.4 MICROSCOPY AND FLUORESCENT IMAGING

The imaging system consisted of a Zeiss Axiovert 200M epifluorescence microscope equipped with X10 and X20 objectives. Different excitation/ emission filters were used according to the fluorescent probe:

A 500/20 nm excitation, 535/30 nm emission filter set was used for DAF-FM fluorescence, a 510–560 nm excitation/590 nm emission filter set was used for E^+ and MitoSOX Red fluorescence and a 450–490 nm excitation/515–565 nm emission filter set was used for the detection of CM-DCF fluorescence.

Using a ×20 objective and exposures as indicated for individual experiments, fluorescence images were captured with a computer-controlled Zeiss MRm charged-coupled device (CCD) camera (Carl Zeiss GmbH) and analysed with Axiovision 4.0 image capture and analysis software (Carl Zeiss Vision, GmbH). All experiments were carried out at 25°C.

Exposure of fibres loaded with DAF-FM to ultraviolet (UV) light was minimised by use of a 200 ms exposure time. In DHE and CM-DCFH loaded fibres, the image capture was limited to 50 and 100 ms, respectively.

CM-DCF, DAF-FM, E^+ and MitoSOX Red fluorescence was determined from user-defined segments of single muscle fibres and the background fluorescence (from areas of the field containing no fibres) was subtracted from fibre measurements. Data were recorded in grayscale units.

2.5 CONTRACTILE ACTIVITY INDUCED BY ELECTRICAL STIMULATION

Using established techniques (Palomero et al., 2008; Pye et al., 2007), contractile activity of single isolated muscle fibres was induced by electrical field stimulation in 35mm dishes using platinum electrodes (Harvard Apparatus, Kent, UK). Following 10 min at rest, fibres were electrically stimulated with trains of bipolar square wave pulses of 2ms in duration for 0.5 of a sec every 5 sec at 50 Hz and 30 V/well. A schematic illustration of the standard contractile activity protocol is shown below (Figure 2.1). The total stimulation time was 10 min and the stimulation period commenced at 10 min following the beginning of the experiment and it was followed by a further 10 min period at rest.

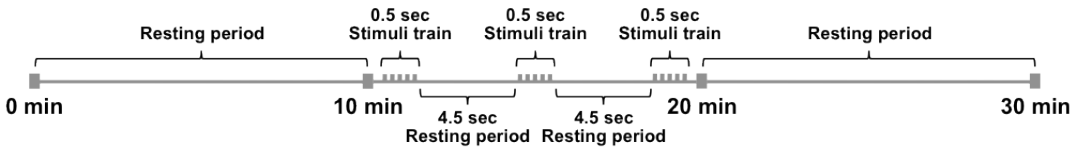

Scheme 2.1 Schematic illustration of the contractile activity protocol.

2.6 SAMPLE PREPARATION FOR THE QUANTIFICATION OF MUSCLE PROTEINS

Prior to analysis, tissues (muscles and organs) from the mice were ground under liquid nitrogen and the resulting powder was homogenised (Sartorius BBI Systems, Model POTTER S, Germany) in 800µl of 1% sodium dodecyl sulphate (SDS) containing protease inhibitors (1mM iodoacetimide, 1mM benzithonium chloride, 5.7mM Phenylmethylsulphonyl fluoride). Samples were then centrifuged at 10,000 g

for 10 min at 4°C (Eppendorf Centrifuge 5402, London, U.K.) and the supernatants were stored at –80°C until analysis.

2.7 BICINCHONINIC ACID (BCA) ASSAY

Total protein content was quantified for each sample using a BCA assay according to the manufacturer's protocol.

Reagents

Reagent A: Bicinchoninic acid (BCA) solution comprised of 160mM $NaCO_3.H_2O$, 25mM BCA-Na, 7mM Na_2 tartrate & 0.95% $NaHCO_3$. Reagent B: 160mM $CuSO_4.5H_2O$, c) Bovine serum albumin (BSA) 1mg/ml. Reagent C prepared by adding 12.5ml of Reagent A to 250µl of Reagent B.

Samples were analysed against a range of standards 50-500 µg/ml from a 1mg/ml stock solution of BSA. Samples and standards were added to a 96-well microplate at a volume of 20 µl. Reagent C was added to each well (180µL) and the microplate was incubated at 50°C for 30 minutes. The absorbance of both the samples and standards was then read using a microplate reader at 570nm and the protein content was determined by using the standard curve.

2.8 WESTERN BLOTTING OF MUSCLE PROTEINS

For assessment of specific proteins in muscle, 30-100µg of total protein was combined with equal volumes of protein loading buffer (National Diagnostics) and boiled for 5 min. Samples were allowed to cool for 15 min and then applied to a 8-15% polyacrylamide gel via a 4% stacking gel. Proteins were separated by electrophoresis at

a constant current of 40 mA. Once separated, the proteins were transferred to a nitrocellulose membrane by a Multiphore continuous blotting system (Pharmacia, Uppsala, Sweden). Over approximately a 90 min period a constant current over 0.8 mA cm^{-2} was applied to the gel to allow the successful transfer of proteins. Ponceau S solution was used to determine whether proteins had been transferred successfully on the nitrocellulose membrane. Membranes were blocked for 2h in a 3% milk solution at room temperature and probed overnight using antibodies against the proteins of interest as previously described (McArdle et al., 2001). Glyceraldehyde 3-phosphate dehydrogenase (GAPDH) protein content was also determined and served the control-loading sample. Though GAPDH is one of the most commonly used loading controls in skeletal muscle, recent reports suggest that the use of GAPDH as a "housekeeping protein" must be carefully evaluated (Gilda and Gomes, 2013). For such reason, all blots were ponceau S stained following transfer to evaluate equivalent loading of the samples. Horseradish peroxidase conjugated anti-mouse IgG, anti-rabbit IgG (Cell Signaling, Hitchin, UK), anti-goat IgG, or anti-chicken IgY (Thermo Scientific, Loughborough, UK) were used as the secondary antibody. Peroxidase activity was detected using an ECL kit (Amersham International Cardiff, UK), and band intensities were analysed using Quantity One Software (Biorad, US). The specificity of the bands were identified in comparison with a sample that had not been exposed to the primary antibody and the molecular weight was determined by using rainbow coloured protein markers (Amersham International).

Details regarding the antibodies used in the present study are shown in the results chapters (Chapters 3,4 and 5) "Experimental Procedures".

2.9 SUBCELLULAR FRACTIONATION

Mitochondrial and cytosolic fractions from *GTN* skeletal muscle were isolated as described recently by Dimauro *et al*. 2012 (Dimauro et al., 2012). Fresh *GTN* muscles were washed with cold PBS, and placed in a pre-chilled glass Petri dish and minced on ice using sharp scissors. The PBS was aspirated and samples were resuspended in 300-500µl of STM buffer (comprising: 250mM sucrose, 50mM Tris-HCl pH 7.4, 5mM MgCl2), protease and phosphatase inhibitor cocktails and homogenized for 1 minute on ice using a tight-fitting Teflon pestle attached to a Potter S homogeniser (set to 600-1,000 rpm) by slowly stroking the pestle up and down. Thereafter, the homogenate was decanted into a centrifuge tube and maintained on ice for 30 minutes, vortexed at maximum speed for 15 seconds and then centrifuged at 800*g* for 15 minutes at 4°C. The pellet (labeled as P1) was discarded and the supernatant was kept (labeled as S1) and used for subsequent isolation of mitochondrial and cytosolic fractions.

Cytosolic and mitochondrial fractions were extracted from S1 by centrifugation at 800*g* for 10 minutes. The supernatant (S2) was saved and the pellet (P2) was discarded. S2 was then centrifuged at 11,000*g* for 10 minutes 4°C and the supernatant (S3) was precipitated in cold 100% acetone at -20°C for at least 1 hour followed by centrifugation at 12,000*g* for 5 minutes, the pellet (P3) was then resuspended in 100-300 μL STM buffer and labelled as "cytosolic fraction". Pellet P3 was resuspended in 50-100 μL SOL buffer (comprising: 50mM Tris HCl pH 6.8, 1mM EDTA, 0.5% Triton-X-100, protease and phosphatase inhibitors) by sonication on ice at high setting for 5-10 seconds with 30 seconds pauses and labelled as "mitochondrial fraction". The purity of the different sample fractions, representing the cytoplasmic, and mitochondrial

compartments was validated by western blot analysis of "house-keeper" marker proteins that are specific for each cellular compartment.

2.10 RNA EXTRACTION, DNase TREATMENT AND cDNA SYNTHESIS

2.10.1 RNA isolation

RNA from single muscle cells and tissues was extracted using Tri Reagent (Qiagen, Sussex, UK). Muscles were ground and placed into Tri Reagent (1ml per 50-100mg of tissue) and centrifuged at 12,000g for 10mins at 4^{o}C to remove insoluble material. Samples were then allowed to stand for 5mins at room temperature. Chloroform (200μL) was then added to the supernatants, samples were shaken vigorously for 15sec and allowed to stand for 15mins at room temperature. Samples were then centrifuged at 12,000g for 15mins at 4^{o}C. Centrifugation separated the mixtures into 3 phases: a red organic phase (containing protein), an interphase (containing DNA) and a colourless upper aqueous phase (containing RNA).

The aqueous phase was transferred to a fresh tube and 0.5ml of isopropanol was added to each sample. The samples were allowed to stand for 5-10mins at room temperature and centrifuged at 12,000g for 10mins at 4^{o}C. The supernatants were then discarded and the RNA pellets were washed by adding 1mL of 75% ethanol. Samples were then centrifuged at 7,500g for 5mins at 4^{o}C. Following centrifugation, the RNA pellets were briefly dried for 5-10mins by air-drying and 100μL of RNase-free H_2O was added to each RNA pellet. The samples were then mixed by repeated pipetting.

2.10.2 Purification and DNase treatment of total RNA

All RNA samples were DNase-treated and purified using the RNeasy MinElute cleanup-kit (Qiagen) as described below.

Reagents

- Buffer RLT
- Buffer RPE
- RNase- Free water
- RNeasy MinElute Spin Columns
- Collection tubes (1.5 & 2ml)

RNA samples were adjusted to a volume of 100µl with RNase-free water. RTL buffer (350uL) was added, followed by 250µL Ethanol (100%) and mixed well by pipetting. Samples were transferred to an RNeasy MinELute Spin column, placed in a 2mL collection tube. Samples were centrifuged for 15sec at 8,000g and the flow-through was discarded. RNeasy MinELute Spin column were placed in a new 2ml collection tube and RPE buffer (500µl) was added to the spin columns and centrifuged for 15sec at 8,000g to wash the spin column membrane. The flow-through was discarded as previously. Addition of 80% Ethanol (500µL) to the RNeasy MinELute Spin column followed and samples were centrifuged for 2min at 8,000g to wash the spin column membrane. The flow-through and collection tube were discarded. RNeasy MinELute Spin columns were placed in a new collection tube (2mL) and centrifuged at full speed (20,800g) for 5 min. The flow-though and collection tubes were discarded. Finally, the spin column was placed in a new collection tube (1.5mL) and 14µL of

RNase-free water was added directly to the centre of the spin column membrane. Columns were centrifuged for 1min at full speed (20,800g) to elute the RNA.

A schematic illustration of the steps described above is shown below (Figure 2.1).

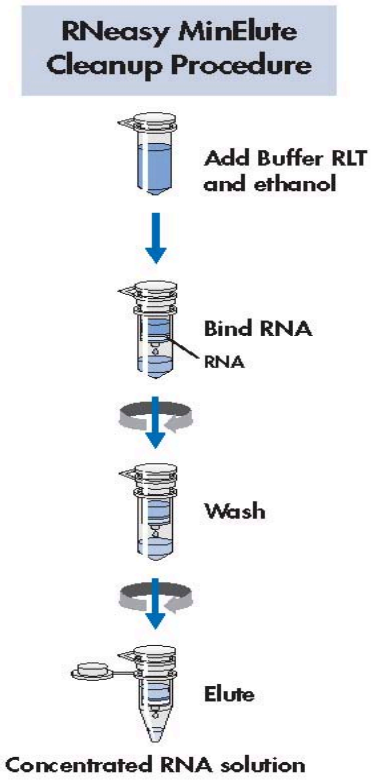

Figure 2.1 RNeasy MinElute Cleanup Procedure used to DNAse and purify RNA samples (from the product specification sheet provided by the company).

2.10.3 RNA content of samples using the RiboGreen RNA quantitation assay

The RNA content of the samples was measured using the RiboGreen RNA quantitation assay kit (Molecular probes, Leiden, The Netherlands).

Reagents

- RiboGreen RNA quantitation reagent (Component A).
- 20X TE (Component B), 25ml of 200mM Tris-HCl, 20mM EDTA, pH 7.5 (20X TE) in DEPC-treated water.
- Ribosomal RNA standard (Component C), 100μg/ml in TE.

A range of standards between 0-1μg/ml was prepared from a stock solution of 100μg/ml Component C in 1X TE solution. 100μL from the standard, blank or sample and 100μl of Component A were placed in a 96 well plate. Samples were then incubated at room temperature for 2-5mins. The fluorescence of standards and samples was measured (excitation 480nm, emission 520nm) using a fluorescence microplate reader (Fluostar optima, BMG, Germany). The RNA content of each sample was calculated from the standard curve.

2.10.4 Generation of first-strand cDNA

Purified RNA was utilised to generate first-strand cDNA using the iScript cDNA Synthesis kit (Bio-Rad, Hertfordshire, UK).

Reagents

- 5 x iScript reaction mix
- iScript reverse transcriptase
- Nuclease-free water

Purified RNA (1ug/sample) was added in DNAse-RNAse free eppendorfs along with 5μL of master mix, which consisted of 4μL of 5 x iScript reaction mix and 1μL of iScript reverse transcriptase. To reach a final volume of 20μL, Nuclease-free water was added in each sample. To confirm the absence of genomic DNA, additional samples were prepared in which iScript reverse transcriptase was not added. For cDNA synthesis, the complete reaction mix was incubated in a PCR thermal cycler (Bio Gene Rapid cycler, Idaho Technology, Idaho Falls, USA) using the protocol:
5 minutes at 25 ^{o}C, 30 minutes at 42 ^{o}C, 5 minutes at 85 ^{o}C, 5 minutes at 4 ^{o}C.

Following first strand synthesis, cDNA was transferred into new DNAse-RNAse free eppendorfs and stored in -20 ^{o}C until further analysis.

2.10.5 Assessing the optimal annealing temperature for each primer set

Primers for real-time PCR analyses were designed (primer sets are described in "Experimental procedures" of the results chapters) and the optimal annealing temperature for each primer set was determined by using an annealing temperature gradient between 55 and 62°C. An example is shown in figure 2.3. Real-time PCR reactions were performed on an iCycler Detection System using iQ SYBR Green Supermix (Bio-Rad, Hertfordshire, UK) and the specificity of the PCR products was determined by melt curve analysis and agarose gel electrophoresis.

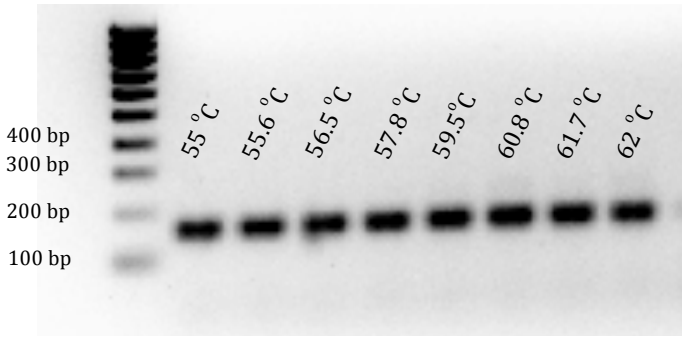

Figure 2.2 Experimental determination of optimal annealing temperature for $p67^{phox}$ (protein of the NADPH oxidase complex) transcript in *GTN* skeletal muscle. The PCR product corresponds to the amplicon size shown in table 2.1 below.

Primer Name (ID)	Forward Primer Sequence	Reverse Primer Sequence	Amplicon Size (bp)
$p67^{phox}$	gaccttaaagaggccttgacg	atgccaactgctcttctgct	160

Table 2.1 Sequences of the specific primers used for RT-PCR amplification of $p67^{phox}$ in *GTN* skeletal muscle.

2.11 ASSESSING CHANGES IN REDOX STATUS OF TISSUES

2.11.1 Assessing changes in the 3-nitrotyrosine (3-NT) content of proteins

Peroxynitrite was assessed via changes in the level of nitration of tyrosine residues of proteins in muscle. Previous studies have indicated that the 3-nitrotyrosine (3-NT) content of the major muscle protein, carbonic anhydrase III (CAIII), is a relatively sensitive marker of muscle oxidative stress (Vasilaki et al., 2007), and this

was examined using the techniques described by Vasilaki *et al.* (2007). Skeletal muscles were ground under liquid nitrogen as described in section 2.6 and total cellular protein (50 μg) was separated on 1D SDS-PAGE followed by western blotting as described in section 2.8. The content of 3-NT was analyzed by using a mouse monoclonal antibody (Cayman Chemical Co., Ann Arbor, Michigan, USA), and the bands were visualized using a Biorad Chemi-Doc System (Biorad Laboratories Ltd, Hemel Hempstead, UK). Densitometric quantification of the CAIII band was undertaken, and the protein content was normalized to the GAPDH content of the same sample. Comparisons were made between samples on the same gel/western blot.

2.11.2 Assessing changes in protein oxidation

Protein oxidation was assessed via changes in protein carbonyls. Cellular proteins (50 μg) were separated on 1D SDS-PAGE and transferred on a PVDF membrane as per the manufacturer's instructions.

Derivatization

1. Following the electroblotting step, PVDF membranes were immersed in 100% methanol for 15 seconds, and then allowed to dry at room temperature for 5 minutes.
2. Membranes were equilibrated in TBS containing 20% Methanol for 5 minutes and were washed in 2N HCl for 5 minutes.
3. Membranes were incubated with 1X DNPH solution (a solution used to derivatize the carbonyl groups) for exactly 5 minutes and were washed three times in 2N HCl, 5 minutes each time, followed by five minute washes in 100% methanol, 5 minutes each time.

Immunoblotting

Membranes were blocked and probed for 2h using a freshly diluted 1:1000 Rabbit Anti-DNP Antibody (Cell Biolabs, San Diego, CA, USA). Secondary HRP conjugated antibody was applied as described in paragraph 2.8.

2.11.3 Assessing changes in lipid peroxidation

Lipid peroxides are unstable indicators of oxidative stress that decompose to form more complex and reactive compounds such as Malondialdehyde (MDA) and 4-hydroxynonenal (4-HNE), natural bi-products of lipid peroxidation. Lipid peroxidation was assessed via changes in 4-HNE protein conjugates and MDA - protein adducts. Both markers were assessed using the same protocol as for 3-NT (section 2.11.1). Rabbit Anti-MDA primary antibodies (Cell Biolabs, San Diego, CA, USA) and rabbit anti 4-HNE (Abcam, Cambridge, UK) were used.

2.12 HISTOLOGICAL ANALYSIS OF SKELETAL MUSCLE

2.12.1 Preparation of muscle blocks

Anterior tibialis (AT) and GTN skeletal muscles were fixed as described below.

Reagents

All reagents were purchased from Merck Ltd. (Dorset, U.K)

- O.C.T. mounting compound
- Iso-pentane

AT and *GTN* muscles were orientated with fibres running transversely on cork discs, surrounded by O.C.T. mounting compound and frozen in iso-pentane pre-cooled in liquid nitrogen. Blocks were stored at –70^{o}C prior to histological analysis. Sections (10μm) from the centre of the muscles were taken onto glass cover slips using a cryostat (Bright Instrument Co., Huntingdon, UK) and stained with haematoxylin and eosin.

2.12.2 Haematoxylin and eosin (H&E) staining

Reagents

All reagents were purchased from (Merck Ltd., Dorset, U.K)

- Harris' Haematoxylin: 5% solution
- Eosin: 1% solution
- DPX mountant

Sections were placed in Harris' Haematoxylin for 3-5 min, rinsed in distilled H_2O and counterstained in eosin for 30 sec. Sections were then dehydrated in 3x Absolute alcohol and cleaned in xylene. Cover slips were mounted onto microscope slides using DPX mountant. Sections were analysed with the use of an inverted miscroscope (Zeiss Axiovert 200M microscope).

2.13 STATISTICAL ANALYSES

Data are presented as mean ± SEM for each experiment. For each experiment, n number of fibres (minimum 6-7 fibres) were taken from a minimum of 4 different mice. When more than 1 fibre studies were undertaken from the same mouse, the mean value of the fibres studied/mouse was considered for the statistical analyses. For multiple comparisons at any time point, analysis was by one-way ANOVA followed by the post hoc LSD test. Single comparisons between two experimental conditions at a time point were undertaken using the unpaired Student's t test. Comparisons between data from individual fibres at different time points were undertaken using Student's paired t test. Data were analysed using SPSS 18 and p values of less than 0.05 were considered statistically significant.

CHAPTER 3

DEVELOPMENT OF TECHNIQUES TO EXAMINE CYTOSOLIC AND MITOCHONDRIAL SUPEROXIDE IN SINGLE ISOLATED MATURE SKELETAL MUSCLE FIBRES

3.1 INTRODUCTION

Skeletal muscle produces reactive oxygen and nitrogen species (RONS) from a variety of cellular locations and it is widely accepted that nitric oxide (NO) and superoxide are the primary radical species (Jackson, 2011). Superoxide and NO are the precursors for the generation of a number of secondary species (Chapter 1, Section 1.2.2) and their production is augmented during periods of contractile activity (Close et al., 2005; Palomero et al., 2008).

Monitoring specific radical species in sub-cellular compartments may have widespread implication for the understanding of diverse scientific areas, including the responses of muscle to exercise training (Vasilaki et al., 2006), age-related loss of muscle mass and function (Vasilaki et al., 2010), as well as inflammatory or degenerative muscle diseases, such as the muscular dystrophies that are associated with increased levels of oxidative damage and muscle weakness (Wallace and McNally, 2009). However, direct measurement of radical species in living cells is inherently difficult because of the short half-life and the labile and reactive nature of these species.

Early studies examining changes in RONS production in skeletal muscle, assessed changes in end-point indicators of the reactions of oxidants in tissues (Davies et al., 1982; Dillard et al., 1978; Jackson et al., 1985) and although assessment of oxidatively modified molecules might provide a useful tool to assess changes in muscle redox status, this approach however is not suitable to determine real-time changes in RONS at discrete subcellular sites.

Studies from this group have established techniques to examine intracellular NO changes in single muscle fibres (Pye et al., 2007), but no technique for direct real-time monitoring of superoxide formation in muscle cells is available.

3.2 AIMS

The aim of the current chapter was to develop reliable techniques to assess mitochondrial and cytosolic changes in superoxide in single isolated mature skeletal muscle fibres.

3.3 EXPERIMENTAL PROCEDURES

3.3.1 Mice

Female C57Bl/6 mice, 4-8 months old were used in this study. All experiments were performed in accordance with UK Home Office guidelines under the UK Animals (Scientific Procedures) Act 1986. Mice were killed by cervical dislocation and the *flexor digitorum brevis* (*FDB*) muscles were rapidly removed for isolation of single muscle fibres.

3.3.2 Chemicals and Reagents

Unless stated otherwise, all chemicals used in this study were obtained from Sigma Chemical Company, Dorset, UK.

3.3.3 Isolation of single mature skeletal muscle fibres

Single muscle fibres were isolated from the *FDB* muscles of mice as described in Section 2.2. Briefly, *FDB* muscles were dissected and incubated for 1.5 h in collagenase to digest the connective tissue. Muscles were agitated every 30 min during the digestion period and single myofibres were released by gentle trituration with a wide-bore pipette. Fibres were washed three times in MEM containing 10% FBS and were plated onto precooled culture dishes precoated with Matrigel (BD Biosciences) and were allowed to attach for 45 min before adding 1 mL MEM containing 10% FBS. Analyses were only performed on fibres that displayed good morphology and prominent cross-striations.

3.3.4 Use of dihydroethidium (DHE) and MitoSOX Red to monitor cytosolic and mitochondrial changes in superoxide in isolated fibres

A detailed description of the ROS sensitive dyes used in this study is presented in Section 2.3. Briefly, single isolated mature fibres were loaded by incubation in 2mL Dulbecco's phosphate-buffered saline (D-PBS) containing 5μM dihydroethidium (DHE) or 250nM MitoSOX Red (Invitrogen) for 30 min at 37^{o}C. Cells were then washed twice with D-PBS and the fibres were maintained in MEM without Phenol Red during the experimental protocol.

3.3.5 Use of 4-Amino-5-Methylamino-2', 7'-Difluorofluorescein Diacetate (DAF-FM DA) and 5- (and 6-) chloromethyl-2',7'-dichlorodihydrofluorescein diacetate (CM-DCFH DA) to monitor NO and H_2O_2 changes in isolated fibres

A detailed description of DAF-FM DA and CM-DCFH DA dyes used in this study is presented in Section 2.3. Briefly, single isolated mature fibres were loaded by incubation in 2mL Dulbecco's phosphate-buffered saline (D-PBS) containing 10μM 4-amino-5-methylamino-2′,7′-difluorofluorescein diacetate (DAF-FM DA) or 10μM 5-(and 6-) chloromethyl-2',7'-dichlorodihydrofluorescein diacetate (CM-DCFH DA) (Molecular Probes, OR, USA) for 30 min at 37^{o}C. Cells were then washed twice with D-PBS and the fibres were maintained in MEM without Phenol Red during the experimental protocol.

3.3.6 Microscopy and fluorescent imaging

For details see Section 2.4. Briefly, the image capture system consisted of a Zeiss Axiovert 200M microscope equipped with 500/20 nm excitation, 535/30 nm

emission filter set for DAF-FM fluorescence, a 510–560 nm excitation/590 nm emission filter set for ethidium (E^+) and MitoSOX Red fluorescence and a 450–490 nm excitation/515–565 nm emission filter set for the detection of CM-DCF fluorescence. Using a X20 objective, fluorescence images were captured with a computer-controlled Zeiss MRm charged-coupled device (CCD) camera (Carl Zeiss GmbH) and analyzed with Axiovision 4.0 image capture and analysis software (Carl Zeiss Vision GmbH).

3.3.7 Contractile activity induced by electrical stimulation

Contractions in single isolated muscle fibres were induced by electrical field stimulation using established techniques (Palomero et al., 2008; Pye et al., 2007). Following loading, fibres remained at rest for 10 min and were then exposed to trains of bipolar square wave pulses of 2 ms in duration for 0.5 sec at 50 Hz and 30 V/well. The contraction protocol has been used in previous studies and shown to increase ROS activities in single isolated muscle fibres (Palomero et al., 2008; Pye et al., 2007). A video of contracting *FDB* fibres was presented in previous work by Palomero *et al* (Palomero et al., 2008). For details see Section 2.5.

3.3.8 Use of pharmacological agents

Increased superoxide generation was induced by menadione (5μM). Incubation of fibres with the superoxide scavengers; 4, 5-dihydroxy-1, 3-benzenedisulphonic acid (Tiron, 1mM), or 4-hydroxy-2, 2, 6, 6- tetramethylpiperidine 1-oxyl (Tempol, 100μM) was commenced at 1h prior to loading the fibres with DHE. Hydrogen peroxide (H_2O_2) was used at a concentration of 2μM. Generation of NO was induced by the NO donor 3-(2-hydroxy-1-methyl-2-nitrosohydrazino)-N-methyl-1-propanamine (NOC-7, 125μM). Mitochondrial superoxide production was induced by treatment of fibres with Rotenone

(Rot; 250nM) or Antimycin A (Ant A; 10μM). The mitochondria-targeted SS-31 peptide (10μM) was obtained from W.M. Keck Fdn. Biotechnology Resource Laboratory at Yale, 77 University, New Haven, CT, USA. SS-31 (D-Arg-Dmt-Lys-Phe-NH_2) has a positive charge of 3+ at physiological pH which makes it targeted to mitochondria (inner mitochondrial membrane) and its antioxidant property is due to incorporation of a dimethyl tyrosine (Dmt) residue (Szeto, 2006a; Szeto, 2006b). Incubation of fibres with SS-31 peptide commenced at 4h prior to the start of fluorescence measurements. All reagents were maintained in the incubation medium during the loading and experimental periods. Most of the pharmacological agents have previously been used in skeletal muscle studies (Nethery et al., 2000; Nethery et al., 1999; Whitehead et al., 2010; Pye et al., 2007) at similar concentrations to the ones used in this study. The final drug concentrations were defined following preliminary studies in which cell viability was determined by assessment of propidium iodide exclusion and control experiments were undertaken to examine any potential effects of the drugs on muscle contractions.

3.4 RESULTS

3.4.1 Development of a technique to examine cytosolic changes in superoxide

3.4.1.1 *Representative images of DHE loaded fibres*

Figures 3.1 A (i) and B (i) show bright-field images of single muscle fibres displaying good morphology and well-defined striations along the sarcolemma. The unreacted form of DHE "blue fluorescence" appeared to accumulate in the cytosol (Figure 3.1 A ii & iii) but upon reaction with superoxide, the oxidised form of DHE indicated by ethidium (E^+) fluorescence was predominantly localized to nuclei, shown by the co-localization of DAPI with E^+ fluorescence (Figure 3.1 B iv).

(A)

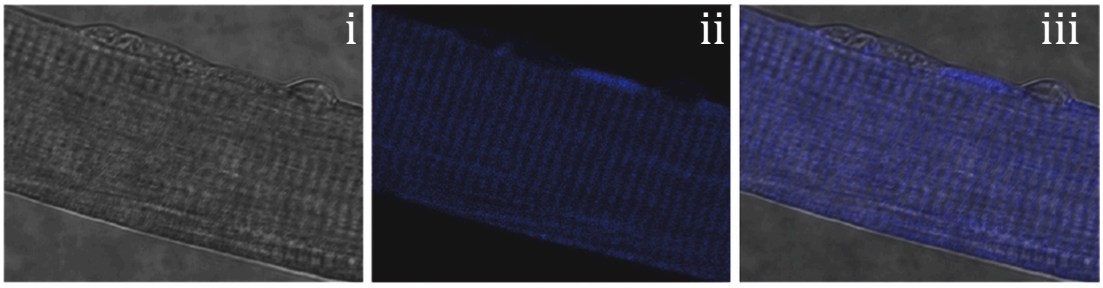

(B)

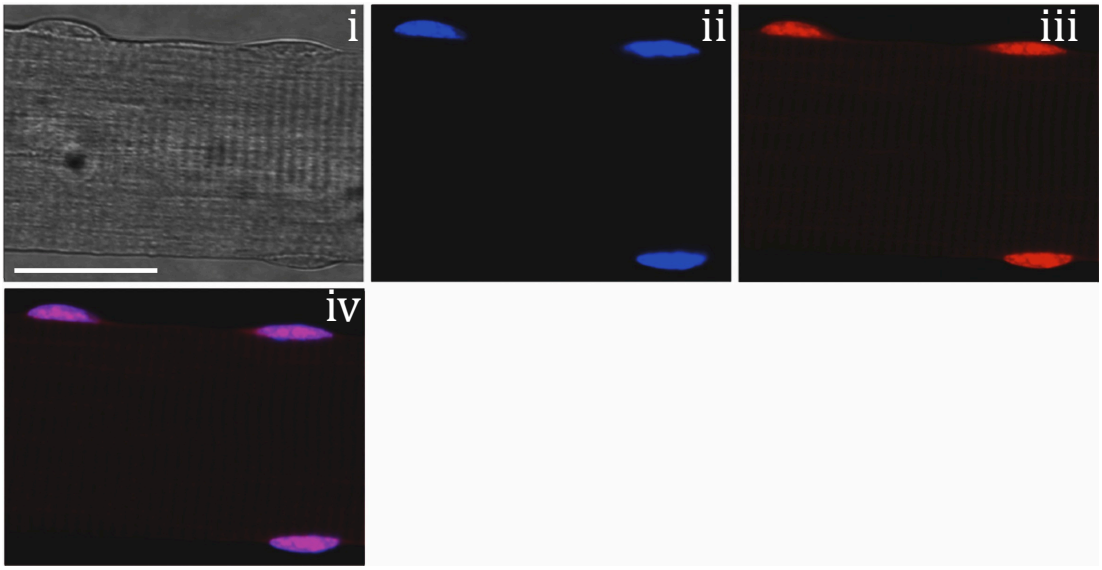

Figure 3.1 (A) Confocal images of a single isolated fibre from the *FDB* muscle after 16 hours in culture. Bright field (i), fluorescent image showing blue fluorescence from non-oxidized DHE (ii), merged image of i and ii (iii). **(B)** Confocal images of a single isolated fibre under bright field (i), fluorescent image showing 4',6-diamidino-2-phenylindole dihydrochloride (DAPI) staining (ii), fluorescent image showing ethidium (E^+), the oxidized form of DHE (iii) and a merged image of ii and iii (iv). 60x original magnification (bar = 30 μm).

3.4.1.2 *Effect of menadione, a superoxide anion generator on DHE oxidation*

Menadione, a redox cycling agent mediates the transfer of electrons from NADPH or NADH to 0_2 generating a flux of superoxide in a process called redox cycling (Greenberg et al., 1990). Figure 3.2 shows the effect of addition of menadione on resting *FDB* muscle fibres at 30 min of the experimental period (Figure 3.2). Menadione caused an increase in the rate of change in DHE oxidation that was significantly higher than in untreated fibres within 20 min following exposure (Figure 3.2). No changes in fibre viability were observed following addition of menadione.

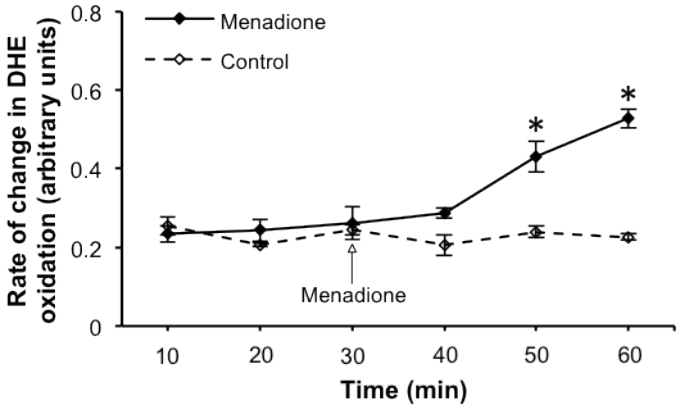

Figure 3.2 Rate of change in DHE oxidation from DMSO treated fibres (control group) and fibres treated with menadione (5μM) at 30 minutes. *P<0.05 compared with values from control non-treated fibres at the same time point. Data are presented as mean (±SEM), n = 5–7 fibres in each group (from 5-6 mice).

3.4.1.3 *Effect of superoxide scavengers (Tiron/Tempol) on DHE oxidation following contractile activity*

To further assess the specificity of DHE oxidation to monitor changes in superoxide in muscle in response to a physiological stimulus such as contractile activity, fibres were incubated with the superoxide scavengers Tiron or Tempol, and were subjected to a 10 min period of contractile activity (Figure 3.3). Emission fluorescence significantly increased by the contraction protocol, but this increase was abolished in the presence of either compound (Figure 3.3).

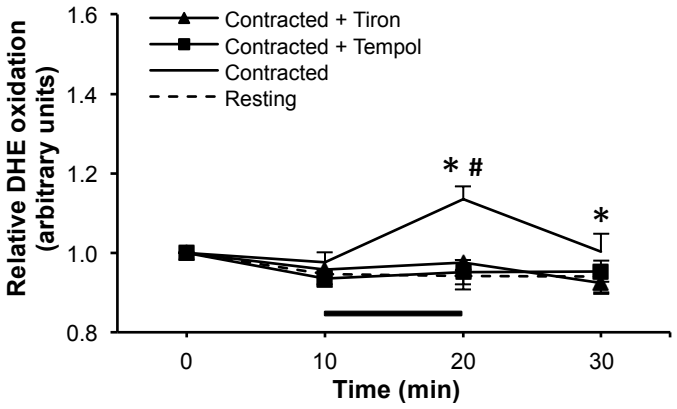

Figure 3.3 Relative change in DHE oxidation from *FDB* fibres over 30 minutes at rest, following 10 minutes of contractile activity without treatment, and from fibres subjected to contractions following pre-treatment with the superoxide scavengers Tiron (1mM) or Tempol (100μM). *P<0.05 compared with values from previous time point from fibres of the same group; $^{\#}$P<0.05 compared with resting non-contracted fibres and fibres subjected to contractile activity in the presence of Tiron or Tempol. Data are presented as mean (±SEM), for 7 fibres in each group (from 5-6 mice). Black bar indicates the contractile activity period.

3.4.1.4 *Effect of hydrogen peroxide (H_2O_2) and NO on DHE oxidation*

Further experiments were undertaken to examine the specificity of DHE towards superoxide, by examining the capacity of H_2O_2 and NO to oxidize DHE in muscle fibre. DHE oxidation was unaffected following exposure of fibres to H_2O_2 or the NO donor 3-(2-hydroxy-1-methyl-2-nitrosohydrazino)-N-methyl-1-propanamine (NOC-7) at 10 min of the experimental period (Figures 3.4 and 3.5).

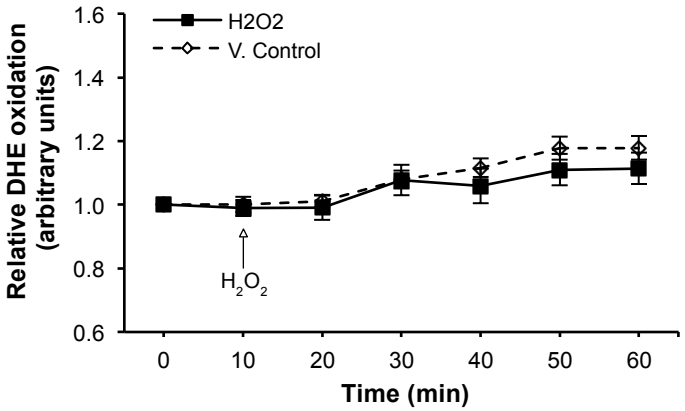

Figure 3.4 Relative change in DHE oxidation from PBS vehicle-treated fibres (V control) and fibres treated with H_2O_2 (2μM) at 10 min. Data are presented as mean (±SEM), n = 4-5 fibres in each group (from 4 mice).

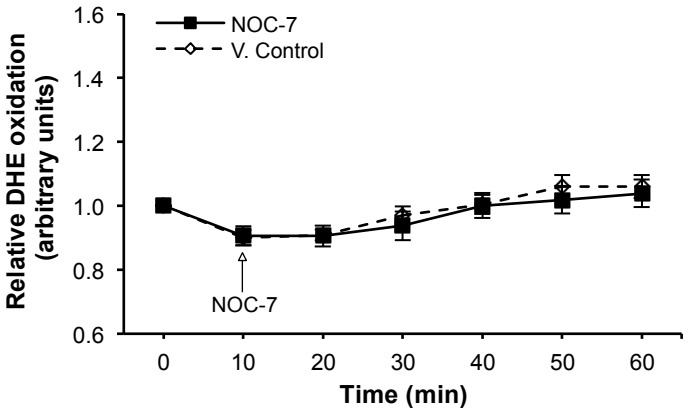

Figure 3.5 Relative change in DHE oxidation from PBS vehicle-treated fibres (V control) and fibres treated with the NO donor 3-(2-hydroxy-1-methyl-2-nitrosohydrazino)-N-methyl-1-propanamine (NOC-7, 125μM) at 10 min. Data are presented as mean (±SEM), n = 4-5 fibres in each group (from 4 mice).

In contrast, positive control experiments using 5- (and 6-) chloromethyl-2',7'-dichlorodihydrofluorescein diacetate (CM-DCFH DA) and 4-amino-5-methylamino-2',7'-difluorofluorescein diacetate (DAF-FM DA) loaded fibres showed a marked increase in DCF fluorescence following addition of H_2O_2 or DAF-FM fluorescence following NOC-7 indicating an intracellular increase in H_2O_2 and NO (Figures 3.6 and 3.7, respectively). CM-DCFH DA fluorescent probe has been used as a general indicator of ROS changes and H_2O_2 has been reported to induce CM DCFH oxidation in single muscle fibres (Palomero et al., 2008). DAF-FM DA is a relatively specific probe which reacts with NO and application of the technique to the study of NO changes in single isolated mature skeletal muscle fibres has been reported in previous work from Pye *et al.* (2007).

Overall, these data imply that the technique based on monitoring DHE oxidation from single muscle cells, is capable of detecting changes in superoxide at rest but also in response to a physiological stimulus such as contractile activity.

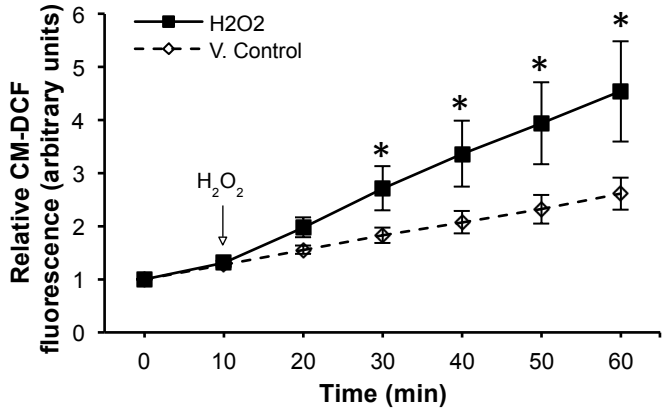

Figure 3.6 Relative change in CM-DCF fluorescence from CM-DCFH DA loaded *FDB* fibres either PBS treated (V control) or treated with H_2O_2 (2μM) at 10 min. *P<0.05 compared with values from the control vehicle-treated fibres at the corresponding time points. Data are presented as mean (±SEM), n = 5-6 fibres in each group.

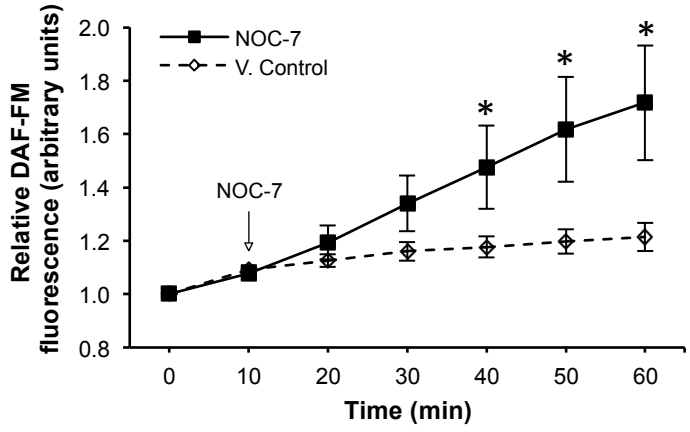

Figure 3.7 Relative change in DAF-FM fluorescence from DAF-FM DA loaded *FDB* fibres either PBS treated (V control) or treated with NOC-7 (125μM) at 10 min. *P<0.05 compared with values from the control vehicle-treated fibres at the corresponding time points. Data are presented as mean (±SEM), n = 4-5 fibres in each group.

3.4.2 Development of a technique to examine mitochondrial changes in superoxide

MitoSOX Red is a fluorescent probe, commonly used to assess changes in mitochondrial superoxide. The difference between DHE and MitoSOX Red is that MitoSOX Red has a triphenylphosphonium cation that facilitates its preferential accumulation and retention within mitochondria (Robinson et al., 2006), which after oxidation interacts with mitochondrial DNA\RNA enhancing its fluorescence to enable the detection of superoxide.

3.4.2.1 *Representative images of MitoSOX Red loaded fibres*

MitoSOX Red selectively accumulated in the mitochondria of single muscle fibres as shown by the co-localization of MitoTracker Green FM with MitoSOX Red fluorescence (Figure 3.8 v), co-localization coefficients; Pearson's correlation (Rr)=0.51, Mander's overlap (R)=0.78, Manders's co-localization coefficient for channel1 (Mred)=0.91, Manders's co-localization coefficient for channel2 (Mgreen)=0.99. MitoSOX Red fluorescence was not detectable in the nuclei of MitoSOX Red loaded muscle fibres (Figure 3.8 v).

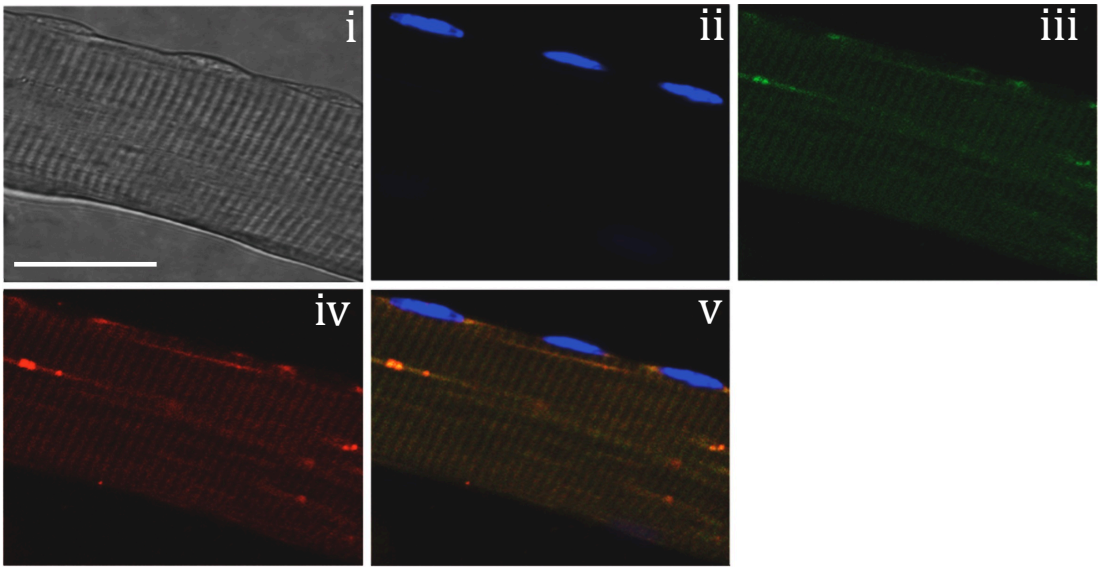

Figure 3.8 Confocal images of a single isolated fibre under bright field (i), fluorescent image following loading with DAPI (ii), fluorescence image following loading with MitoTracker Green FM (15nM) (iii), fluorescent image from MitoSOX Red (iv) and a merged image of ii, iii and iv (v). 60x original magnification. (bar = 30 μm).

3.4.2.2 *Effect of the mitochondrial electron transport chain inhibitors Antimycin A (Ant A) and Rotenone (Rot) on MitoSOX Red fluorescence*

Previous studies have shown that skeletal muscle mitochondria produce superoxide from both complexes I and III of the electron transport chain (Muller et al., 2004). Superoxide generated at complex I appears to be released into the mitochondrial matrix, but complex III releases superoxide to both sides of the inner mitochondrial membrane; the matrix and the MIS (Muller et al., 2004).

Figures 3.9 and 3.10 show the effect of Ant A and Rot electron transport chain inhibitors on MitoSOX Red fluorescence of resting *FDB* muscle fibres. Treatment of fibres with either compound at 30 min induced a significant increase in fluorescence indicating an increase in superoxide within the mitochondrial matrix of the muscle fibres.

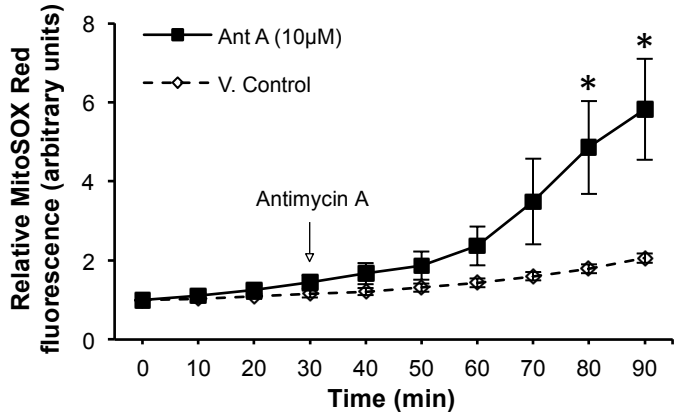

Figure 3.9 Relative change in MitoSOX Red fluorescence from ethanol vehicle-treated fibres (V control) and fibres treated with Ant A (10μM) at 30 min. *P<0.05 compared with values from the control vehicle-treated fibres at the same time point (n = 6-8 fibres in each group).

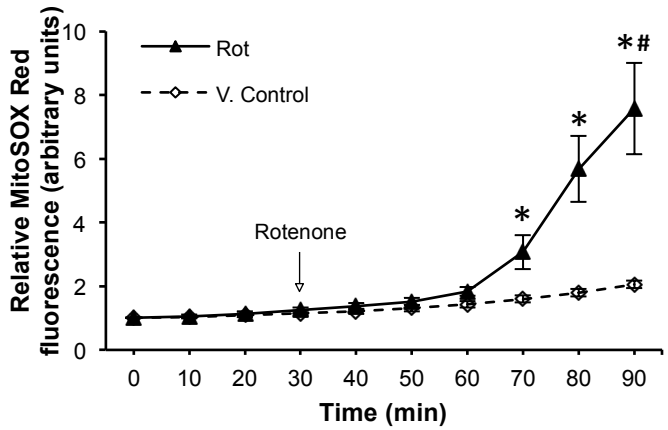

Figure 3.10 Relative change in MitoSOX Red fluorescence from DMSO vehicle-treated fibres (V control) and fibres treated with Rot (250nM) at 30 min. *P<0.05 compared with values from control vehicle-treated fibres at the same time point. (n = 6-9 fibres in each group).

3.4.2.3 *Effect of SS-31 peptide, a mitochondrial targeted antioxidant peptide on MitoSOX Red fluorescence following addition of Rot*

To further assess the specificity of MitoSOX Red to monitor mitochondrial changes in superoxide in muscle, fibres were pretreated with the SS-31 peptide, a mitochondrial targeted antioxidant peptide that accumulates on the inner mitochondrial membrane (IMM) and can scavenge superoxide to form tyrosine hydroperoxide (Dai et al., 2011; Maack and Bohm, 2011). SS-31 attenuated the anticipated increase in MitoSOX Red fluorescence following addition of Rot in single muscle fibres (Figure 3.11).

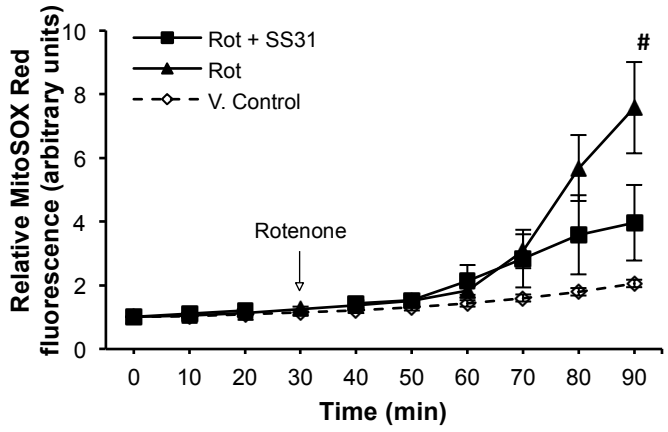

Figure 3.11 Relative change in MitoSOX Red fluorescence from DMSO vehicle-treated fibres (V control) and fibres treated with Rot at 30 min. A group of Rot-treated fibres was also pre-treated with SS-31 peptide (10μM). $^{\#}P<0.05$ compared with values from rotenone-treated fibres incubated in the presence of SS-31 peptide at the corresponding time point (n = 6-9 fibres in each group).

3.4.2.4 *Effect of H_2O_2 and NO on MitoSOX Red fluorescence*

Further experiments were undertaken to examine the specificity of MitoSOX Red towards superoxide, by examining the ability of H_2O_2 and NO to oxidise MitoSOX Red in fibres. Both H_2O_2 and the NO donor 3-(2-hydroxy-1-methyl-2-nitrosohydrazino)-N-methyl-1-propanamine (NOC-7) failed to oxidise the probe (Figures 3.12 and 3.13, respectively).

These data imply that the technique based on monitoring MitoSOX Red from single muscle cells, is capable of selectively detecting changes in superoxide within the mitochondrial matrix of muscle fibres.

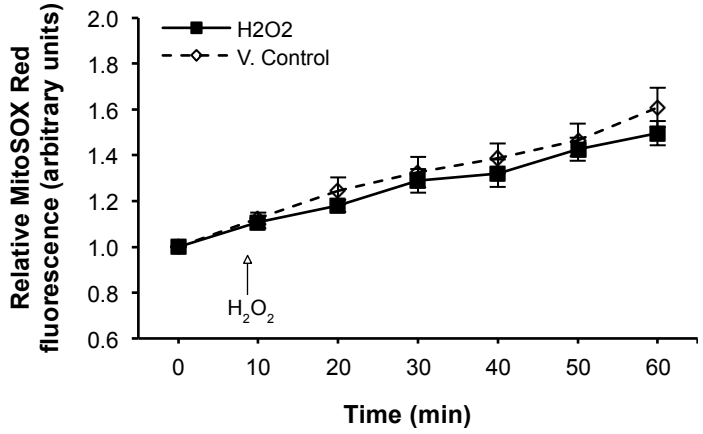

Figure 3.12 Relative change in MitoSOX Red fluorescence from PBS vehicle-treated fibres (V Control) and fibres treated with H_2O_2 (2μM) at 10 min (n = 4-6 fibres in each group).

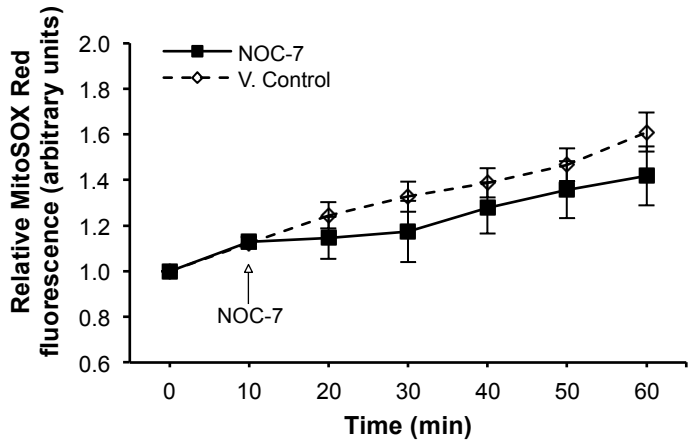

Figure 3.13 Relative change in MitoSOX Red fluorescence from PBS vehicle-treated fibres (V Control) and fibres treated with NOC-7 (125μM) at 10 min (n = 4-6 fibres in each group).

3.5 DISCUSSION

The work described in this chapter has examined the use of DHE and MitoSOX Red superoxide sensitive florescent dyes to determine changes in superoxide within the cytosolic and mitochondrial compartment of mature single muscle fibres. Oxidation of dihydroethidium (DHE) and MitoSOX Red fluorescence has been used as a means of monitoring cytosolic and mitochondrial changes in superoxide by following ethidium (E^+) and 2-hydroxyethidium (2-OH-E^+) formation (Zielonka and Kalyanaraman, 2010). This technique has only been rarely used to examine skeletal muscle (Zuo et al., 2000; Zuo and Clanton, 2002), and hence the objectives of the current study were to examine the reliability of this approach as a means of monitoring intracellular cytosolic and mitochondrial superoxide changes in muscle fibres.

3.5.1 Methodological considerations

Multiple approaches including electron-spin resonance spectroscopy (Pattwell et al., 2003), fluorescence-based microscopic assays (Palomero et al., 2008; Pye et al., 2007), microdialysis (Close et al., 2007) and HPLC techniques (Pattwell et al., 2003) have been used to assess intracellular and extracellular changes in RONS produced by skeletal muscle. In the current study, the aim was to develop a technique with the use of fluorescence imaging microscopy, which would enable monitoring of real-time changes in superoxide in single isolated muscle fibres both at rest and during contractile activity.

For the purposes of this study we utilized an *ex vivo* single muscle fibre approach in which we isolated single skeletal muscle fibres from the flexor digitorum brevis muscle. The merit of this approach is that it enables the analysis of superoxide in the absence of non-myogenic cells such as lymphocytes, endothelial cells and fibroblasts. The single muscle fibres used in this study were isolated from adult muscle and hence more closely reflect the situation in muscle *in vivo* in comparison with immature skeletal myotubes in culture.

3.5.2 DHE and MitoSOX Red oxidation by single muscle fibres

The assessment of E^+ fluorescence following MitoSOX Red and DHE loading as a measure of superoxide anion radical in cellular compartments has been criticised and recent studies have identified 2-hydroxyethidium (2-OH-E^+) as a specific product of the reaction of DHE with superoxide (Zielonka and Kalyanaraman, 2010). In the present study the use of DHE oxidation to assess cytosolic superoxide changes by monitoring changes in E^+ fluorescence was evaluated in single skeletal muscle fibres. To assess the specificity of this method, DHE loaded fibres were initially exposed to menadione, a

known inducer of intracellular superoxide generation, which caused an increase in E^+ fluorescence. To further assess the specificity of E^+ fluorescence to monitor changes in superoxide in muscle in response to contractile activity, fibres were incubated with the superoxide scavengers Tiron or Tempol, and the anticipated increase in fluorescence following contractions was completely abolished with either compound. Similarly, MitoSOX Red loaded fibres showed an increase in the emission florescence following addition of Rot and Ant A indicating an increase in superoxide within the mitochondrial matrix. The anticipated increase in Rot-induced MitoSOX Red fluorescence was inhibited in fibres pretreated with the mitochondrial targeted antioxidant SS31 peptide further implying that MitoSOX Red selectively reacts with ROS generated within the mitochondrial matrix. Finally, the specificity of DHE and MitoSOX Red towards superoxide, was examined by treatment of fibres with exogenous H_2O_2 and NO and examining whether this oxidized the superoxide sensitive fluorescent probes. Both compounds failed to oxidise the probes. These data imply that the technique developed in this study based on monitoring E^+ fluorescence from single muscle cells following loading with DHE and MitoSOX Red, is capable of detecting changes in superoxide production at rest but also in response to a physiological stimulus such as contractile activity.

3.5.3 Physiological implications

The production of reactive oxygen and nitrogen species by skeletal muscle is important as it underlies oxidative damage in many degenerative muscle diseases and plays multiple regulatory roles by fulfilling important cellular functions (Section 1.6). With the development of techniques to assess real-time changes in superoxide within the mitochondrial and cytosolic sites of single muscle fibres, this would provide a useful

tool to examine potential sub-cellular pathways that are involved in the regulation of cytosolic and mitochondrial superoxide content at rest and during contractile activity. Techniques established in this study might also be utilized as an approach to determine the sub-cellular superoxide producing sources that might be implicated in pathological muscle diseases such as the muscular dystrophies.

3.6 CONCLUSION

In conclusion, these data imply that techniques based on use of single mature skeletal muscle fibres loaded with DHE and MitoSOX Red are capable of detecting cellular changes in superoxide within the cytosolic and mitochondrial compartment that occur in response to a pharmacological stimulant or in response to a physiological stimulus such as contractile activity.

CHAPTER 4

IDENTIFYING THE SUB-CELLULAR SITES THAT REGULATE CYTOSOLIC SUPEROXIDE IN SKELETAL MUSCLE AT REST AND DURING CONTRACTILE ACTIVITY

4.1 INTRODUCTION

Since the initial observations that skeletal muscles produce free radicals (Davies et al., 1982; Jackson et al., 1983), a great deal of research has been undertaken to identify the sources that are responsible for the increased generation of RONS during contractions. As mentioned in the introduction (Section 1.2), it is now clear that superoxide and NO are the primary reactive oxygen and nitrogen species generated within skeletal muscle both at rest and during contractile activity. Although the production of NO by the nitric oxide synthases has been well described (Stamler and Meissner, 2001; Palomero and Jackson, 2010), there is still considerable debate over the prime cytosolic source(s) of superoxide in skeletal muscle.

Early studies suggested that the mitochondrial respiratory chain was the predominant source that accounted for the increased superoxide production following contractions (Boveris and Chance, 1973; Loschen et al., 1974; Davies et al., 1982), but recent data from our group (McArdle et al., 2005; Palomero et al., 2008) and others (Michaelson et al., 2010; St-Pierre et al., 2002; Di Meo and Venditti, 2001; Herrero and Barja, 1997; Aydin et al., 2009) have cast considerable doubt on this theory. Reassessment of the rate of oxidant production by mitochondria has shown that only 0.15% of the total amount of oxygen is reduced with the production of superoxide (St-Pierre et al., 2002), a value that is an order of magnitude lower than the original estimate of 2-3% (Chance et al., 1979; Naqui et al., 1986). In addition, growing evidence indicates that mitochondrial superoxide generation is higher during state 4 respiration compared with state 3 (Di Meo and Venditti, 2001; Herrero and Barja, 1997), implying that skeletal muscle mitochondria are not the major sources of oxidant production during contractions.

Work presented in my MPhil thesis "Factors influencing the intracellular generation of ROS by skeletal muscle fibres, 2009", showed that contractile activity induced a significant increase in dihydroethidium (DHE) oxidation, indicating an increase in superoxide within the cytoplasmic compartment of the muscle cells (I have described these findings in more detail in the results section of this chapter, Section 4.4). In contrast, other studies investigating mitochondrial superoxide production failed to observe changes in MitoSOX Red fluorescence upon tetanic stimulation of single *FDB* muscle fibres suggesting that mitochondrial superoxide production was not increased with increased contractile activity (Aydin et al., 2009). Recent findings have supported this proposal by showing no changes in the mitochondrial redox potential from single muscle fibres subjected to a tetanic stimulation protocol (Michaelson et al., 2010). Taken together, these data argue against major formation of ROS within skeletal muscle mitochondria during increased contractile activity.

Skeletal muscle mitochondria produce superoxide from both complexes I and III of the electron transport chain (Muller et al., 2004). While complex I-generated superoxide is exclusively released into the matrix, complex III can release superoxide to both sides of the inner mitochondrial membrane; the mitochondrial matrix and the mitochondrial intermembrane space (MIS) (Muller et al., 2004). Studies investigating mitochondrial superoxide formation or mitochondrial changes in redox potential commonly use MitoSOX Red and mito-roGFP constructs. However, due to their chemical structure, these probes preferentially accumulate in the mitochondrial matrix, thus they do not reflect changes in superoxide within the MIS. Although superoxide is a relatively membrane impermeant anion (Powers and Jackson, 2008), studies using isolated mitochondria have provided evidence that channels of the outer mitochondrial

membrane (OMM) can permit diffusion of superoxide from the MIS to the cytosol (Han et al., 2003; Budzinska et al., 2009). Thus the increase in cytoplasmic superoxide observed during contractile activity might be related to superoxide released into the cytosol across the OMM. However, the role of the OMM in mediating the diffusion of superoxide from the intermembrane space to the cytosol of skeletal muscle has not been studied.

Additional extramitochondrial sites for superoxide production within skeletal muscle have been identified including the nicotinamide adenine dinucleotide phosphate (NADPH) oxidase enzymes (Espinosa et al., 2006; Hidalgo et al., 2006; Mofarrahi et al., 2008; Xia et al., 2003), enzymes of the phospholipase A_2 family (Gong et al., 2006; Nethery et al., 1999), and xanthine oxidase (Gomez-Cabrera et al., 2010) but their contribution to the cytosolic production of superoxide in skeletal muscle has not been evaluated.

4.2 AIMS

The aim of this chapter was to identify, by using a variety of different approaches, the potential pathways that are involved in the regulation of cytosolic superoxide both at rest and during contractile activity in single isolated mature skeletal muscle fibres.

4.3 EXPERIMENTAL PROCEDURES

4.3.1 Mice

Female C57Bl/6 mice, 4-8 months old were used in this study. All experiments were performed in accordance with UK Home Office guidelines under the UK Animals (Scientific Procedures) Act 1986. Mice were killed by cervical dislocation and the *flexor digitorum brevis* (*FDB*) muscles were rapidly removed for isolation of single muscle fibres. Other muscles and tissues were harvested and stored at -70^{o}C until analysis.

4.3.2 Chemicals and Reagents

Unless stated otherwise, all chemicals used in this study were obtained from Sigma Chemical Company, Dorset, UK.

4.3.3 Isolation of single mature skeletal muscle fibres

Single muscle fibres were isolated from the *FDB* muscles of mice as described in Section 2.2. Briefly, *FDB* muscles were dissected and incubated for 1.5 h in collagenase to digest the connective tissue. Muscles were agitated every 30 min during the digestion period and single myofibres were released by gentle trituration with a wide-bore pipette. Fibres were washed three times in MEM containing 10% FBS and were plated onto precooled culture dishes precoated with Matrigel (BD Biosciences) and were allowed to attach for 45 min before adding 1 mL MEM containing 10% FBS. Analyses were only performed on fibres that displayed good morphology and prominent cross-striations.

4.3.4 Use of dihydroethidium (DHE) and MitoSOX Red to monitor cytosolic and mitochondrial changes in superoxide in isolated fibres

A detailed description of the ROS sensitive dyes used in this study is presented in Section 2.3. Briefly, single isolated mature fibres were loaded by incubation in 2mL Dulbecco's phosphate-buffered saline (D-PBS) containing 5μM dihydroethidium (DHE) or 250nM MitoSOX Red (Invitrogen) for 30 min at 37^{o}C. Cells were then washed twice with D-PBS and the fibres were maintained in MEM without Phenol Red during the experimental protocol.

4.3.5 Microscopy and fluorescent imaging

For details see Section 2.4. Briefly, the image capture system consisted of a Zeiss Axiovert 200M microscope equipped with a 510–560 nm excitation/590 nm emission filter set for the detection of ethidium (E^{+}) and MitoSOX Red fluorescence. Using a X20 objective, fluorescence images were captured with a computer-controlled Zeiss MRm charged-coupled device (CCD) camera (Carl Zeiss GmbH) and analyzed with Axiovision 4.0 image capture and analysis software (Carl Zeiss Vision GmbH).

4.3.6 Contractile activity protocols

Contractions in single isolated muscle fibres were induced by electrical field stimulation using established techniques (Palomero et al., 2008; Pye et al., 2007). Following loading, fibres remained at rest for 10 min and were then exposed to trains of bipolar square wave pulses of 2 ms in duration for 0.5 sec at 50 Hz and 30 V/well. The duty cycle, (i.e. proportion of time that the fibre was stimulated) was varied to modify the intensity of the contraction protocol. Contractile activity protocols are shown schematically below (Scheme 4.1). The High contraction protocol consisted of a 2.5 sec

stimulation cycle (20% duty cycle), the Moderate a 5 sec stimulation cycle (10% duty cycle) and the Low protocol a 10 sec stimulation cycle (5% duty cycle). The Moderate intensity protocol has been used in previous studies and shown to increase ROS activities in single isolated muscle fibres (Palomero et al., 2008; Pye et al., 2007). A video of contracting *FDB* fibres was presented in previous work by Palomero *et al* (Palomero et al., 2008).

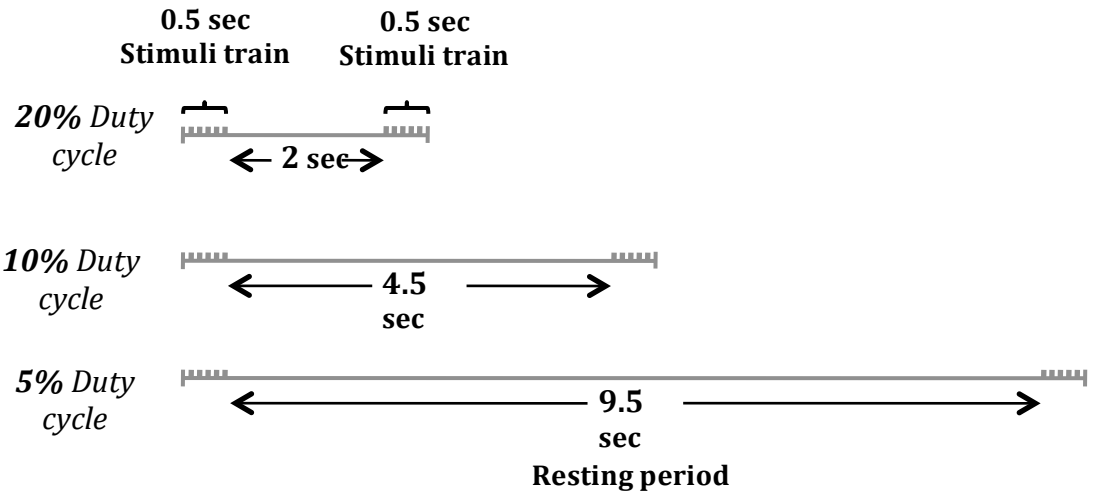

Scheme 4.1 Schematic illustration of the protocols for electrical stimulations at different intensities. The stimuli train was constant in all contraction protocols. The time at rest between repetitions varied according to the intensity of each protocol.

4.3.7 Use of pharmacological agents to identify sources of superoxide

Mitochondrial superoxide production was induced by treatment of fibres with Rotenone (Rot; 250nM) or Antimycin A (Ant A; 5 or 10μM). The mitochondria-targeted SS-31 peptide (10 or 100μM) was obtained from W.M. Keck Fdn. Biotechnology Resource Laboratory at Yale, 77 University, New Haven, CT, USA.

Cyclosporin A (CsA; 0.5μM), 4'-Chlorodiazepam (4Cl-DZP; 12μM), Dextran sulphate Mr 6,500 - 10,000 (DS; 0.1mM) and the BAX channel blocker (Bax CB; (±)-1-(3,6-dibromocarbazol-9-yl)-3-piper azin-1-yl-propan-2-ol; 5μM; Merck Chemicals Ltd, Nottingham, UK) were used to assess the role of specific pathways in superoxide release from mitochondria. The contribution of NADPH oxidase enzymes was assessed using the NADPH oxidase inhibitors; Apocynin (APO; 0.5mM), Diphenyleneiodonium chloride (DPI; 10μM; Enzo Life Sciences, Exeter, UK), gp91ds-tat and the control peptide scrambled-tat (5μM; Anaspec, Fremont, USA). The calcium-independent phospholipase A_2 enzyme ($iPLA_2$) was blocked by the selective inhibitor bromoenol lactone (BEL; 0.6μM; Enzo Life Sciences). Incubation of fibres with inhibitors was commenced at 30 min prior to the start of fluorescence measurements, with the exception of the SS-31 peptide, which was added 4 h prior to measurements. Most of the pharmacological agents have previously been used in skeletal muscle studies (Nethery et al., 2000; Nethery et al., 1999; Whitehead et al., 2010; Pye et al., 2007) at similar concentrations to the ones used in this study. Cell viability following treatments was determined by assessment of propidium iodide exclusion and control experiments were undertaken to examine any potential effects of the drugs on muscle contractions. Contractile activity was monitored and fibres that did not visibly contract during the entire contractile activity period were excluded.

4.3.8 RNA isolation and RT-PCR analysis

For details see Section 2.10. Briefly, RNA from single muscle cells was extracted using Tri Reagent (Qiagen, Sussex, UK). All RNA samples were DNase-treated and purified using the RNeasy MinElute cleanup-kit (Qiagen). Purified RNA was utilized to generate first-strand cDNA using the iScript cDNA synthesis kit (Bio-

Rad, Hertfordshire, UK). The primers for real-time PCR analyses used in this study are shown below in Table 4.1. GAPDH was used as the only reference gene, this might be a limitation since evidence has shown that contractile activity but also RONS can alter GAPDH mRNA expression in skeletal muscle (Brownson et al., 1988).

Primer Name (ID)	Forward Primer Sequence	Reverse Primer Sequence	Amplicon Size (bp)
NOX2	cctgaatttcaactgtatgctga	cctgaatttcaactgtatgctga	151
NOX4	ggatttgctactgcctccat	agtgactccaatgcctccag	163
Rac 1	gccaatgttatggtagatggaaa	tttcaaatgatgcaggactca	151
$p67^{phox}$	gaccttaaagaggccttgacg	atgccaactgctcttctgct	160
$p47^{phox}$	gtccctgcatcctatctgga	atgacctcaatggcttcacc	155
$p22^{phox}$	gccattgccagtgtgatcta	tggtaggtggttgcttgatg	118
$p40^{phox}$	tgacttcactgggaacagca	tagccagttggtggtgtcct	184
GAPDH	ccgtagacaaaatggtgaagg	tcgttgatggcaacaatctc	109

Table 4.1 Sequences of the specific primers used for RT-PCR amplification of NADPH oxidase subunits in isolated fibres from the *FDB* muscle.

4.3.9 Western blotting of muscle proteins

For details see Section 2.8. Briefly, 30-100μg of total protein was applied to a 8-15% polyacrylamide gel with a 4% stacking gel. Proteins were separated by electrophoresis and were transferred to a nitrocellulose membrane by a Multiphore continuous blotting system (Pharmacia, Uppsala, Sweden). Membranes were blocked for 2h in a 3% milk solution at room temperature and probed overnight using antibodies shown in Table 4.2. Glyceraldehyde 3-phosphate dehydrogenase (GAPDH) protein content was also determined and served the control-loading sample. Horseradish peroxidase conjugated anti-mouse IgG, anti-rabbit IgG (Cell Signaling, Hitchin, UK), anti-goat IgG, or anti-chicken IgY (Thermo Scientific, Loughborough, UK) were used

as the secondary antibody. Peroxidase activity was detected using an ECL kit (Amersham International Cardiff, UK), and band intensities were analysed using Quantity One Software (Biorad, US). The specificity of the bands were identified in comparison with a sample that had not been exposed to the primary antibody and the molecular weight was determined by using rainbow coloured protein markers (Amersham International).

Antibody	Company	Catalogue No	Species	Dilution
GAPDH	Abcam	Ab8245-100	Mouse	1:5000
COXIV	Abcam	Ab59426	Mouse	1:4000
VDAC1	Abcam	Ab40747	Rabbit	1:3000
VDAC2	Abcam	Ab37985	Goat	1:500
VDAC3	Thermo Scientific	PA1-959	Chicken	1:500
BAX	Santa Cruz	Sc-493	Rabbit	1:500
$iPLA_2$	Cayman	160507	Rabbit	1:500
NOX2	Abcam	Ab80508	Rabbit	1:1000
NOX4	Abcam	Ab61248	Rabbit	1:1000
Rac1	Cytoskeleton	ARC03	Mouse	1:500
P67phox	BD Transduction	610913	Mouse	1:1000
P47phox	Santa Cruz	Sc-14015	Rabbit	1:500
P22phox	Abcam	Ab75941	Rabbit	1:1000
P40phox	Santa Cruz	Sc-30087	Rabbit	1:500
MPO	Abcam	Ab45977	Rabbit	1:1000

Table 4.2 Antibodies used for western blotting.

4.3.10 Subcellular fractionation

Mitochondrial and cytosolic fractions from *GTN* skeletal muscle were isolated as described in Section 2.9. Briefly, *GTN* muscles were dissected and minced on ice and homogenized in STM buffer (comprising: 250mM sucrose, 50mM Tris-HCl pH 7.4, 5mM MgCl2), protease and phosphatase inhibitor cocktails. The homogenate was decanted into a centrifuge tube and maintained on ice for 30 minutes and then centrifuged at 800*g* for 15 minutes at 4°C. The supernatant was kept (labeled as S1) and centrifuged at 800*g* for 10 minutes at 4°C for subsequent isolation of mitochondrial and cytosolic fractions. The supernatant (S2) was then centrifuged at 11,000*g* for 10 minutes at 4°C. The resulting pellet following S2 centrifugation was resuspended in 50-100 μ L SOL buffer (comprising: 50mM Tris HCl pH 6.8, 1mM EDTA, 0.5% Triton-X-100, protease and phosphatase inhibitors) by sonication on ice and labelled as "mitochondrial fraction" whereas the supernatant (S3) was precipitated in cold 100% acetone at -20°C for 1 hour followed by centrifugation at 12,000*g* for 5 minutes, the pellet was then resuspended in 100-300 μ L STM buffer and labelled as "cytosolic fraction".

4.3.11 Immunoprecipitation of p40^{phox}

Single isolated muscle fibres from the *FDB* muscle, powdered frozen muscle tissue from *GTN*, and liver tissue were homogenised and lysed in CelLytic-M Mammalian Cell Lysis/Extraction Reagent. Protein extracts (~1mg protein/sample) were incubated with 2µg of anti-p40^{phox} antibody (Santa Cruz Biotechnology, Middlesex, UK) overnight at 4°C. The mixture was added to 30µL of protein G-Sepharose beads and was further incubated for 2 h at 4°C. Beads were centrifuged and washed five times with immunoprecipitation buffer and bound proteins were eluted by

boiling in loading buffer (National Diagnostics, Hessle, UK) before being resolved by electrophoresis and identified by western blotting.

4.3.12 Immunocytochemistry of NADPH oxidase subunits in single isolated muscle fibres

Single skeletal muscle fibres from the *FDB* muscle were isolated and plated on culture dishes. Cells were rinsed with warm PBS and immediately fixed in 4% paraformaldehyde for 20 min at room temperature. After three washes with PBS, fibres were permeabilised and blocked in PBS containing 0.1% Triton X-100 and 1% bovine serum albumin (BSA). After 10 h incubation, fibres were washed with PBS and incubated overnight at 4^{o}C with primary antibodies (see Table 4.3) diluted in PBS and 1% BSA. Fibres were washed with PBS plus 1% BSA three times for 5 min, followed by incubation with appropriate secondary antibodies (Alexa Fluor 488 and 532; Invitrogen, diluted 1:800) for 1.5 h at room temperature.

Fluorescence images were obtained using a C1 confocal laser-scanning microscope (Nikon Instruments Europe BV, Surrey, UK) equipped with a 405nm excitation diode laser, a 488nm excitation argon laser and a 543nm excitation helium-neon laser. Emission fluorescence was detected through a set of 450/35, 515/30 and 605/15-emission filters. Using a ×60 objective, fluorescence images were captured and analysed with the EZC1 V.3.9 (12bit) acquisition software. To quantify sub-cellular (cytosolic and membrane) fluorescent distribution and the degree of co-localization of proteins and fluorescent probes in muscle fibres, NIH Image J software was used. Co-localization coefficients: Pearson's correlation (Rr) coefficient (correlation of intensity distribution between channels), Mander's overlap (R) coefficient and Manders's co-

localization coefficient for each image (proportion of one channel signal coincident with the signal in other channel); channel 1 (Mred) and channel 2 (Mgreen) were calculated over the entire confocal image.

Antibody	Company	Catalogue No	Species	Dilution
Rac1	Cytoskeleton	ARC03	Mouse	1:40
P40phox	Santa Cruz	Sc-30087	Rabbit	1:50
P47phox	Santa Cruz	Sc-14015	Rabbit	1:20
P67phox	BD Transduction	610913	Mouse	1:50
NOX2	Abcam	Ab80508	Rabbit	1:50
NOX4	Abcam	Ab61248	Rabbit	1:50
P22phox	Abcam	Ab75941	Rabbit	1:30
α_{1s} DHPR	Thermo Scientific	MA3-920	Mouse	1:50
Caveolin-3	Santa Cruz	Sc-55518	Mouse	1:50

Table 4.3 Antibodies used to immunostain single *FDB* muscle fibres.

4.4 RESULTS

To define the sources that modulate cytosolic changes in superoxide at rest and during contractile activity, single muscle fibres were loaded with the superoxide sensitive fluorescent probes DHE and MitoSOX Red as previously described (Section 2.3). The experiments presented in chapter 3 indicated that techniques based on use of single mature skeletal muscle fibres loaded with DHE and MitoSOX Red appeared capable of detecting cellular changes in superoxide that occur in response to drug-stimulants or in response to the physiological stimulus such as contractile activity. In the present study, specific inhibitors of potential pathways and immunolocalization techniques were also used to identify sub-cellular sites contributing to cytosolic superoxide.

Previous work from my MPhil thesis "Factors influencing the intracellular generation of ROS by skeletal muscle fibres" showed that DHE oxidation in fibres increased in an intensity dependent manner following muscle contractions (Sakellariou, 2009). The contractile activity protocols used in that study are shown in Scheme 4.1 (Section 4.3.6), with fibres subjected to the High, Moderate and Low contracted groups showing a 5.8, 4.1 and 2.8 fold increase following contractions compared with resting fibres (Figure 4.1, data taken from MPhil). The experiments undertaken at that time implied that contractile activity increased in an intensity dependent manner the cytosolic superoxide content of single muscle fibres since DHE oxidation reflects changes in superoxide within the cytoplasmic compartment of the muscle fibres. These data are reproduced here for completeness. The following new data focus on identifying the sites that contribute to cytosolic superoxide changes both at rest and following contractile activity.

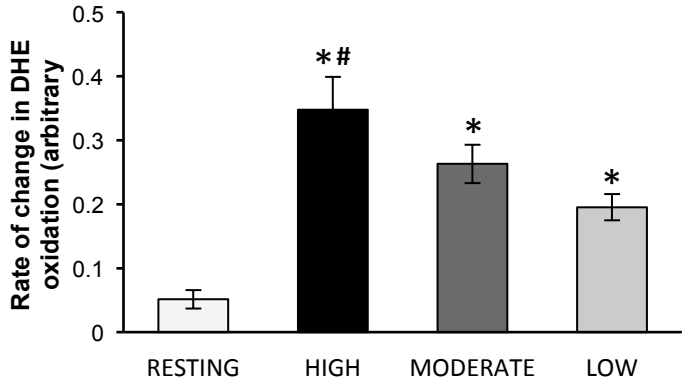

Figure 4.1 Rate of change in DHE oxidation from resting *FDB* fibres and fibres subjected to a 10 min period of contractile activity with different intensities. *P<0.05 compared with fibres from the resting group. #P<0.05 compared with fibres subjected to the Low contractile activity protocol (n = 7-8 fibres in each group), (Figure taken from MPhil; Sakellariou, 2009).

Intracellular sources of superoxide production that have been proposed include mitochondria, NADPH oxidase enzymes (Hidalgo et al., 2006; Mofarrahi et al., 2008), and enzymes of the phospholipase A_2 family (Gong et al., 2006; Nethery et al., 1999), but their contribution to cytosolic changes in superoxide in skeletal muscle during contractions has not been fully evaluated. The results of this chapter aim to evaluate the contribution of these sources to superoxide production both at rest and during contractile activity in skeletal muscle.

4.4.1 Contribution of mitochondria to cytosolic superoxide in single skeletal muscle fibres at rest and during contractile activity

Changes in superoxide within the mitochondrial matrix were monitored with MitoSOX Red. As shown in previous chapter (Figure 3.8), MitoSOX Red selectively accumulates in the mitochondria of single muscle fibres and can react with superoxide,

formed within the mitochondrial matrix as indicated by the increase in MitoSOX Red fluorescence following addition of Rot and Ant A (Figures 3.9 and 3.10).

4.4.1.1 Skeletal muscle mitochondria release superoxide to the cytosol of fibres following treatment with Antimycin A

To examine mitochondria as a potential source of superoxide detected in the cytosol, DHE loaded fibres were treated with 5 or 10 μM Ant A at 30 min. Treatment of fibres with Ant A induced a dose dependent increase in DHE oxidation compared with control untreated fibres, indicating extramitochondrial superoxide release (Figure 4.2).

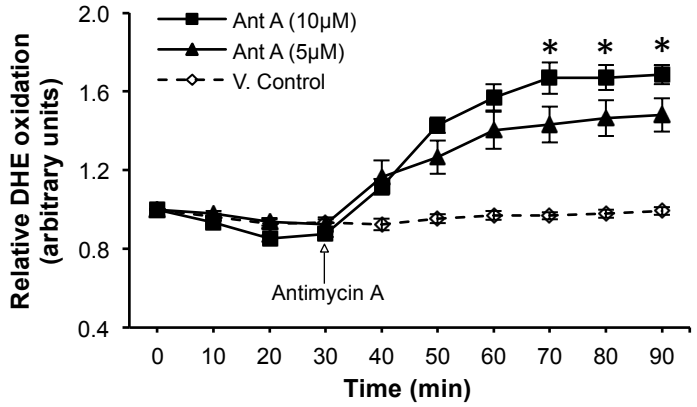

Figure 4.2 Relative change in DHE oxidation from ethanol vehicle-treated fibres (V control) and fibres treated with Ant A (5 or 10μM) at 30 min. *P<0.05 compared with values from fibres treated with 5μM Ant A or control vehicle-treated fibres at the same time point (n = 7-8 fibres in each group).

4.4.1.2 Release of superoxide from mitochondria following treatment with Ant A does not occur through the mitochondrial permeability transition pore (mPTP) or the inner membrane anion channel (iMAC)

4.4.1.2.1 *The effect of Ant A on DHE oxidation in SS31 loaded fibres*

Treatment of isolated skeletal muscle mitochondria with Ant A increases superoxide on both sides of the inner mitochondrial membrane; the MIS and mitochondrial matrix (Muller et al., 2004). It has previously been reported that both of these compartments can release superoxide into the cytosol through the mitochondrial permiablility transition pore (mPTP) - that spans the inner (IMM) and outer (OMM) mitochondrial membrane (Gomez-Cabrera et al., 2010), the inner membrane anion channel (iMAC) (Maack and Bohm, 2011; Pouvreau, 2010) or through channels located on the OMM which allow the passage of solutes and proteins between the MIS and cytosplasm (Budzinska et al., 2009; Han et al., 2003).To identify if either the mPTP or iMAC contributed to the extramitochondrial superoxide release seen following treatment with Ant A, fibres were pretreated with the SS-31 peptide, the mitochondrial targeted antioxidant peptide which was shown in previous chapter to scavenge superoxide within the mitochondrial matrix (Figure 3.11) .

Treatment of fibres with SS-31 at either 10 or 100μM had no effect on DHE oxidation with the treated fibres showing a similar increase in fluorescence compared with vehicle-control fibres following addition of Ant A (Figure 4.3) suggesting that the extramitochondrial superoxide release seen following treatment with Ant A was not derived from the matrix through the mPTP or the iMAC.

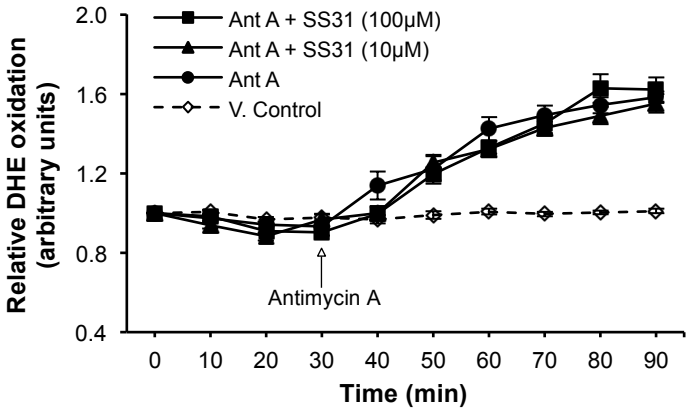

Figure 4.3 Relative change in DHE oxidation from ethanol vehicle-treated fibres (V control) and fibres loaded with Ant A (5μM) at 30 min. Two groups of Ant A-treated fibres were also pre-treated with the mitochondrial targeted SS-31 peptide (dissolved in PBS) at 10 or 100μM (n = 6 fibres in each group).

4.4.1.2.2 *The effect of iMAC and mPTP inhibitors on DHE oxidation following treatment with Ant A*

The potential role of the mPTP and iMAC in release of superoxide was further examined using the mPTP - cyclosporin A (CsA) and iMAC - 4 chlorodiazepam (4Cl-DZP) inhibitors. Neither CsA or 4CL-DZP was found to affect DHE oxidation in Ant A-treated fibres (Figure 4.4) providing further evidence that superoxide formed within the mitochondrial matrix does not diffuse to the cytosplasm of single muscle fibres.

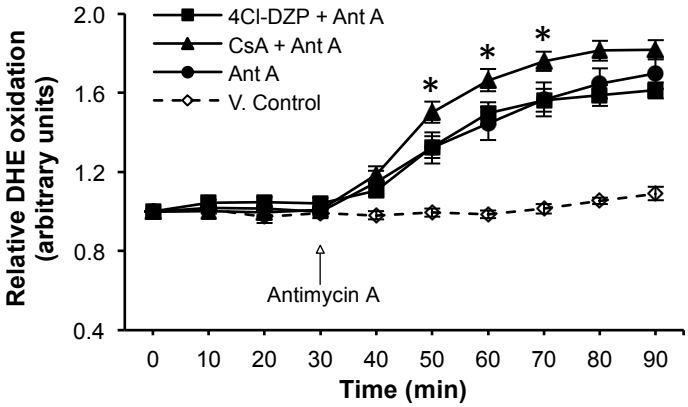

Figure 4.4 Relative change in DHE oxidation from ethanol vehicle-treated fibres (V control) and fibres loaded with Ant A (5μM) at 30 min. Two groups of Ant A-treated fibres were also pre-treated with the mPTP (CsA, 0.5μM) or iMAC (4Cl-DZP, 12μM) inhibitors (both inhibitors were dissolved in ethanol). *P<0.05 compared with values from fibres in all other Ant A treated groups and control vehicle-treated fibres at the corresponding time points (n = 6-8 fibres in each group).

4.4.1.2.3 *The effect of rotenone on DHE oxidation*

The role of matrix superoxide was also examined by treatment of fibres with the complex I inhibitor, Rot. This was previously (Chapter 3) shown to increase MitoSOX Red oxidation (Figure 3.11), but no effect was seen on DHE oxidation (Figure 4.5) indicating that complex I-dependent superoxide is exclusively released into the matrix and does not release superoxide to the cytoplasm from intact mitochondria.

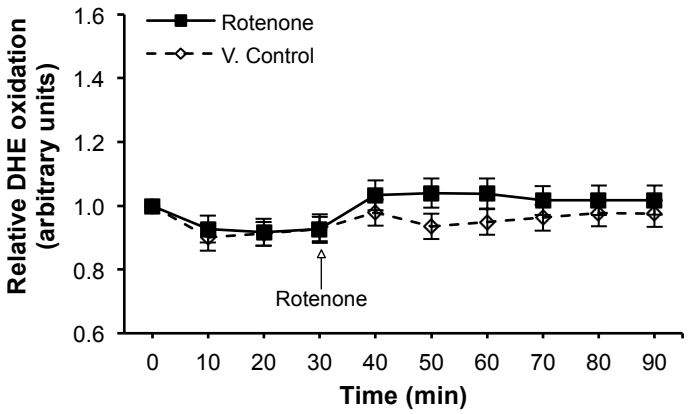

Figure 4.5 Relative change in DHE oxidation from control DMSO vehicle-treated fibres (V control) and fibres treated with rotenone at 30 min (n = 5-7 fibres in each group).

4.4.1.3 Channels of the outer mitochondrial membrane mediate the diffusion of superoxide from the MIS to the cytosol of skeletal muscle fibres

Taken together the data presented in Figures 4.3, 4.4 & 4.5 suggest that the diffusion of superoxide from the mitochondria to the cytosol of single muscle fibres following treatment with Ant A did not derive from the mitochondrial matrix but was likely to originate from the MIS.

4.4.1.3.1 *Purity of cytosolic and mitochondrial fractions*

In order to identify the channels that might play a role in the diffusion of superoxide from the MIS to the cytosol in single muscle fibres, mitochondrial and cytosolic fractions from *GTN* muscles were prepared. Figure 4.6 shows the relative purity of the mitochondrial and cytosolic fractions obtained. GAPDH was only present in the cytosolic fractions and COXIV in the mitochondrial fractions.

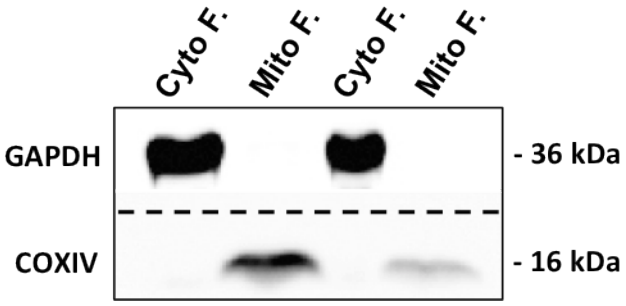

Figure 4.6 Example western blots for GAPDH and cytochrome oxidase IV (COXIV) to illustrate the purity of the extracted mitochondrial (Mito F) and cytosolic (Cyto F) fractions obtained from *GTN* muscle.

4.4.1.3.2 *Protein expression of VDAC isoforms in skeletal muscle*

Previous studies in isolated cardiac mitochondria have shown that the voltage dependent anion channels (VDACs) located on the OMM can mediate the release of superoxide from the MIS. We initially assessed the protein expression of all three isoforms of VDAC in cytosolic and mitochondrial fractions from *GTN* muscle and lysates from single skeletal muscle fibres (Figure 4.7). All three isoforms were highly expressed in the skeletal muscle mitochondrial fractions (Figure 4.7).

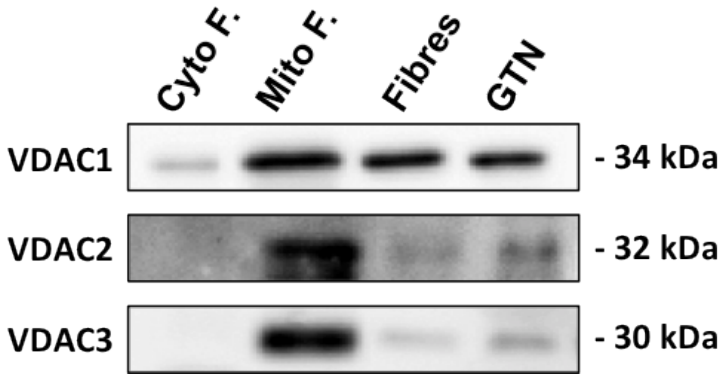

Figure 4.7 Representative western blots of VDAC1, VDAC2 and VDAC3 proteins in cytosolic (Cyto F) and mitochondrial (Mito F) fractions from *GTN* muscle, in lysate from single isolated fibres from the *FDB* muscle (fibres) and whole *GTN* muscle.

4.4.1.3.3 *Effect of VDAC inhibition by dextran sulfate (DS) at rest and following exposure to Ant A*

In the presence of dextran sulfate (DS), a VDAC inhibitor, the anticipated increase in DHE oxidation following treatment with Ant A at 30 min was partially inhibited over the first 20 minutes following addition of Ant A, but by the end of the experiment the level was comparable with those from fibres loaded with Ant A only (Figure 4.8). These data support the possibility that i) VDACs play a key role in mitochondrial superoxide release and ii) channels of the OMM other than VDACs might also mediate the diffusion of superoxide from the MIS to the cytosol of single muscle fibres. No effect on baseline DHE oxidation was observed following treatment of fibres with DS alone at 30 min (Figure 4.9) implying that intact skeletal muscle mitochondria do not release superoxide to the cytosol of resting muscle fibres.

Effects of inhibition of VDAC by 4,4'-diisothiocyano-2,2'-disulfonic acid stilbene (DIDS) inhibitor could not be assessed as this agent was found to affect fibre viability at IC_{50} values of 0.2mM.

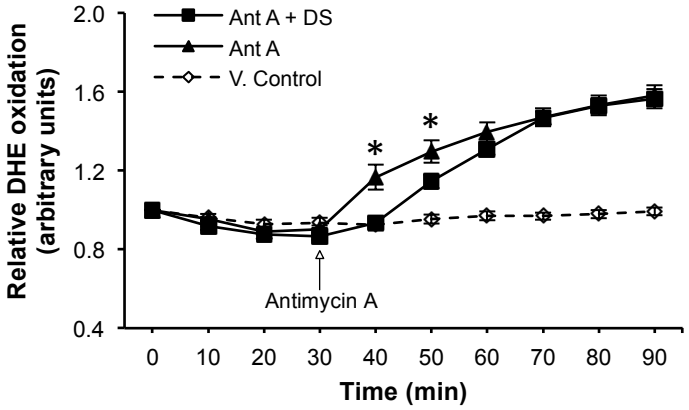

Figure 4.8 Relative change in DHE oxidation from ethanol vehicle-treated fibres (V control) and fibres loaded with Ant A (5μM) at 30 min. A group of Ant A-treated fibres was also pre-treated with DS (0.1mM). DS was dissolved in PBS. *P<0.05 compared with fibres treated with DS at the corresponding time point (n = 7 fibres in each group).

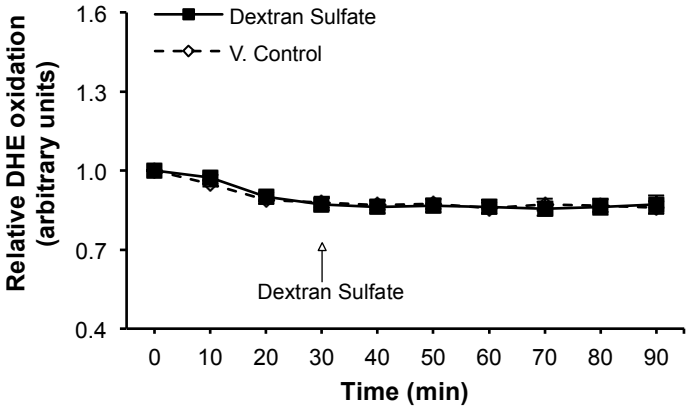

Figure 4.9 Relative change in DHE oxidation from PBS vehicle-treated fibres (V control) and fibres treated with DS (0.1mM) at 30 min (n = 7-8 fibres in each group).

4.4.1.3.4 *Effect of a Bax channel blocker and/or VDAC inhibitors following exposure to Ant A*

Further experiments were undertaken to identify whether the Bax channel, an additional channel located on the OMM (Martinou, 1999), would play a role in the release of superoxide following treatment of fibres with Ant A. The protein expression of the Bax channel in mitochondrial fractions and lysate from single muscle cells is shown in (Figure 4.10). Following inhibition of the Bax channel with the Bax channel blocker (Bax CB), fibres showed a reduction in DHE oxidation during the 40-50 minute period following addition of Ant A (Figure 4.11). Fibres pretreated with the Bax channel blocker and VDAC inhibitor together, showed a further reduction in fluorescence, with the relative change in DHE oxidation being statistically lower (~13%) during the 20-50 min period following Ant A treatment compared with fibres treated with Ant A only (Figure 4.11). The increase in DHE oxidation in the Bax CB and DS group was lower over the 30-90 min time course compared with the Ant A treated fibres (Figure 4.11) but this did not occur in fibres treated with DS only (Figure 4.8), suggesting that both channels play a synergistic role in mediating the diffusion of superoxide from the MIS across the OMM. Inhibition or blocking of these two OMM channels did not completely prevent extramitochondrial superoxide release following treatment of fibres with Ant A (Figure 4.11). To ensure that data were not influenced by any direct interactions between Ant A and DHE, that were unrelated to effects of Ant A on the electron transport chain, control experiments were conducted in a cell-free medium but these showed no effect of Ant A on DHE or MitoSOX Red oxidation.

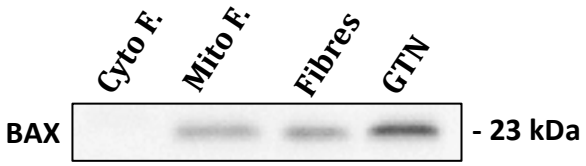

Figure 4.10 Representative western blot of Bax protein in cytosolic (Cyto F) and mitochondrial (Mito F) fractions from *GTN* muscle, in lysate from single isolated *FDB* muscle fibres and whole *GTN* muscle.

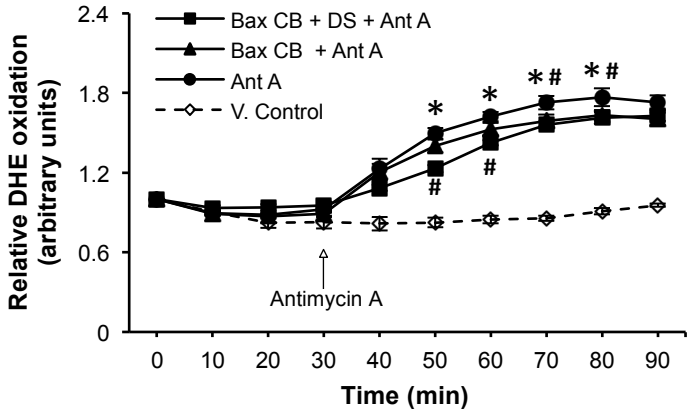

Figure 4.11 Relative change in DHE oxidation from ethanol vehicle-treated fibres (V control) and fibres loaded with Ant A (5μM) at 30 min. Two groups of Ant-A treated fibres were also pre-treated with Bax CB (5μM) or with Bax CB (5μM) and DS (0.1mM). *P<0.05 compared with values from Ant A treated fibres preincubated with Bax CB and DS at the same time point. #P<0.05 compared with values from fibres treated with Ant A in the presence of Bax CB at the same time point (n = 6-7 fibres in each group).

4.4.1.3.5 *Effect of a Bax channel blocker and/or VDAC inhibitors on DHE oxidation during contractile activity*

Data in Figures 4.8 and 4.11 suggest that mitochondria in single skeletal muscle fibres can release superoxide from the MIS to the sarcoplasm of muscle cells. To investigate the possibility that skeletal muscle mitochondria release superoxide from the MIS to the cytosol during contractions, muscle fibres were subjected to a 10 min contractile activity period following treatment with the Bax and VDAC inhibitors (Figure 4.12). Contractile activity induced a significant increase in DHE oxidation in the presence or absence of the inhibitors compared with values from fibres from the resting group (Figure 4.12). No differences in the rate of change in DHE oxidation were observed between untreated fibres and fibres treated with VDAC and/or Bax inhibitors following contractions (Figure 4.12) indicating that the increase in superoxide in response to contractions was unlikely to derive from the MIS and likely originated from non-mitochondrial sources.

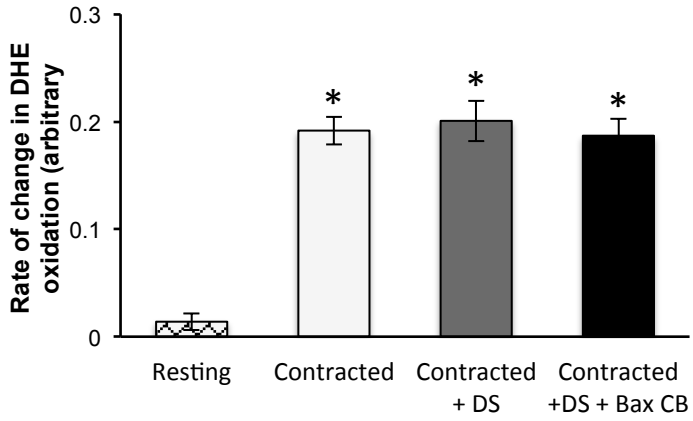

Figure 4.12 Rate of change in DHE oxidation from resting fibres and fibres subjected to the Moderate contraction protocol for a period of 10 min. Contracted fibres were either untreated, treated with DS or treated with DS and Bax CB. *P<0.05 compared with values from fibres at rest (n = 9-11 fibres in each group).

4.4.2 The contribution of iPLA$_2$ enzymes to cytosolic superoxide

4.4.2.1 *Expression of iPLA$_2$ in skeletal muscle*

Previous studies have reported that iPLA$_2$ enzymes can modulate the cytosolic oxidant activity in skeletal muscle cells indicated by a reduction in 2', 7'-dichlorodihydrofluorescin (DCFH) oxidation following inhibition of iPLA$_2$ (Gong et al., 2006). The present study initially assessed the expression of iPLA$_2$ and Figure 4.13 shows the presence of iPLA$_2$ in cytosolic fractions from *GTN* muscle and in lysate from single muscle fibres.

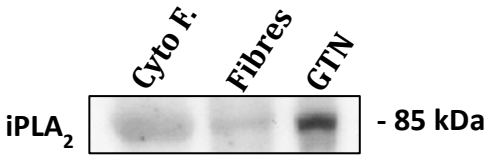

Figure 4.13 Representative western blot of iPLA$_2$ protein in cytosolic fraction (Cyto F) from *GTN* muscle, in lysate from single isolated *FDB* muscle fibres and whole *GTN* muscle.

4.4.2.2 *Effect of inhibition of iPLA$_2$ enzymes on cytosolic superoxide at rest and during contractile activity*

To identify the contribution of iPLA$_2$ enzymes to cytosolic superoxide production at rest, quiescent muscle fibres were treated with the selective iPLA$_2$ inhibitor Bromoenol lactone (BEL) at 30 min of the experimental period (Figure 4.14). No differences in the relative change in DHE oxidation were observed between the treated and non-treated groups of fibres (Figure 4.14). The same pattern was observed following a period of contractions, with fibres from all contracted groups showing a similar increase in DHE oxidation following contractions (Figure 4.15).

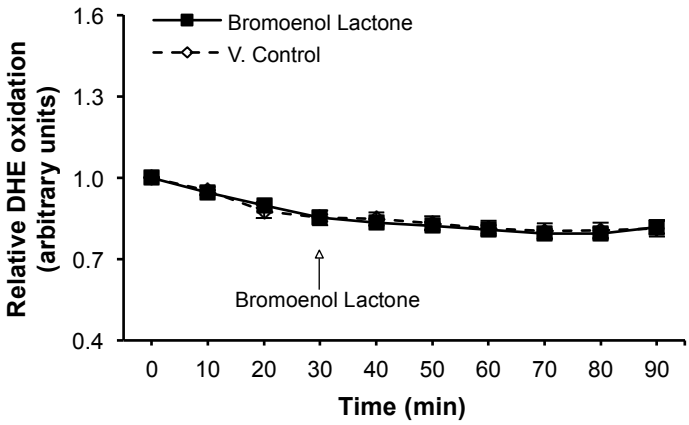

Figure 4.14 Relative change in DHE oxidation from DMSO vehicle-treated fibres (V control) and fibres treated with BEL (0.6μM) at 30 min (n = 7-10 fibres in each group).

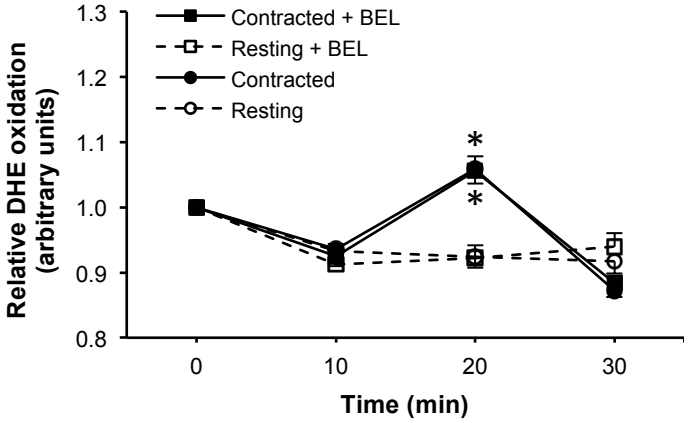

Figure 4.15 Relative change in DHE oxidation from resting *FDB* fibres and fibres subjected to the Moderate contraction protocol over the 10 - 20 min period. Fibres were either untreated or treated with BEL (0.6μM). *P<0.05 compared with values from fibres of the same group prior to contractions (n = 7-8 fibres in each group).

4.4.3 Contribution of NADPH oxidase(s) to cytosolic superoxide

Expression of NADPH oxidase(s) in skeletal muscle

4.4.3.1 *mRNA expression in single FDB muscle fibres*

There is evidence that skeletal muscles express NADPH oxidase(s) (Whitehead et al., 2010; Mofarrahi et al., 2008; Hidalgo et al., 2006; Espinosa et al., 2006), but little information is available regarding the role and regulation of this complex in generation of superoxide in skeletal muscles. As mentioned previously in Chapter 1 (Section 1.2), NADPH oxidases are a family of enzymes, which consist of both catalytic and regulatory subunits. Other studies have identified various NADPH oxidase subunits in mouse and rabbit skeletal muscles (Whitehead et al., 2010; Hidalgo et al., 2006), but to our knowledge no studies have examined the expression in pure skeletal muscle, devoid of all non-myogenic cells. To assess the expression of the NADPH oxidase components in a pure skeletal muscle preparation, RNA was extracted from single isolated *FDB* muscle fibres. The optimal annealing temperature for each primer set was determined as described in hapter 2 “Experimental Methods” and the primer sets used in this study are depicted in Table 1, Section 4.3.8. The mRNA expression of NOX2 and NOX4 catalytic subunits as well as Rac1, $p67^{phox}$, $p47^{phox}$, $p22^{phox}$, $p40^{phox}$ regulatory components is shown in Figure 4.16. GAPDH was used as the control.

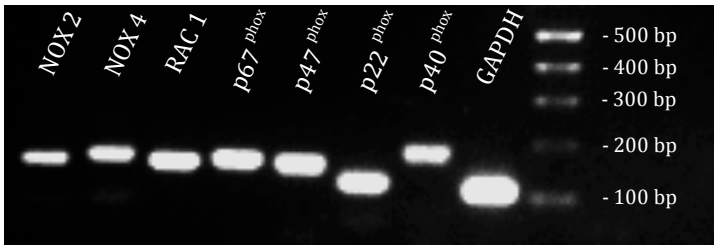

Figure 4.16 RT-PCR amplification of NOX2, NOX4, Rac1, $p67^{phox}$, $p47^{phox}$, $p22^{phox}$, $p40^{phox}$ and GAPDH transcripts in single isolated fibres from the *FDB* muscle. The PCR products correspond to the amplicon sizes shown in Table 4.1 in the Experimental procedures (Section 4.3.8).

4.4.3.2 *Protein expression in single FDB muscle fibres*

Further experiments were undertaken to determine the protein expression of the NADPH oxidase subunits in single *FDB* muscle fibres. Figure 4.17 shows the protein expression of NOX2, NOX4, Rac1, $p67^{phox}$, $p47^{phox}$, $p22^{phox}$ and $p40^{phox}$ in lysates from single muscle fibres and whole *GTN* skeletal muscles. $p40^{phox}$ was immunoprecipitated, for details see Section 4.3.11. Appropriate positive controls were included for each antibody.

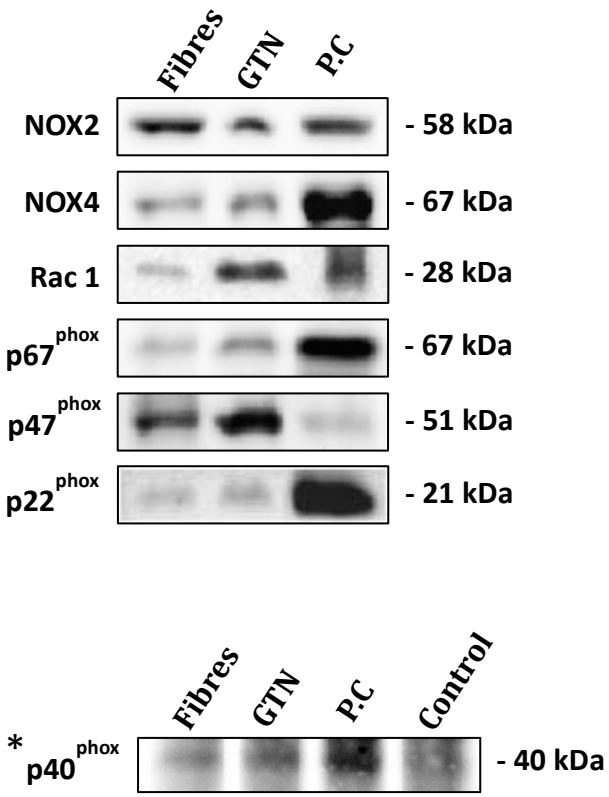

Figure 4.17 Representative western blots of NOX2, NOX4, Rac1, $p67^{phox}$, $p47^{phox}$, $p22^{phox}$ and $p40^{phox}$ proteins in lysate from single isolated *FDB* muscle fibres and whole *GTN* muscle. Appropriate positive controls (PC) are shown: lysate from mouse heart for NOX2, NOX4 and $p40^{phox}$; lysate from mouse liver for $p67^{phox}$ and $p22^{phox}$; Human platelet extract for Rac1 and Raw macrophage 264.7 whole cell lysate for $p47^{phox}$. *$p40^{phox}$ was immunoprecipitated, see Section 4.3.11 for details.

4.4.3.3 *Protein expression of NOX isoforms in mitochondrial fractions*

Recent evidence has shown that cardiac (Ago et al., 2010; Dai et al., 2011; Kuroda et al., 2010) and liver (Block et al., 2009) mitochondria express NOX4. To identify if either NOX2 or NOX4 oxidases are present in skeletal muscle mitochondria, further experiments were undertaken in mitochondrial fractions from *GTN* muscles and demonstrated the presence of NOX4 in this fraction (Figure 4.18).

(A)

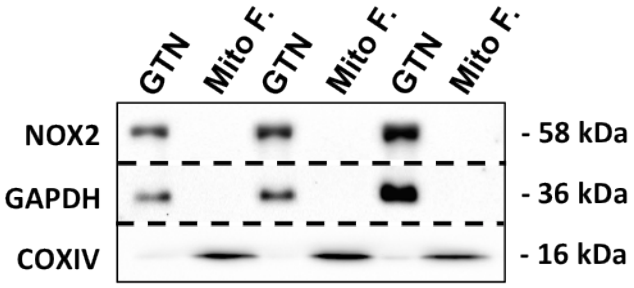

(B)

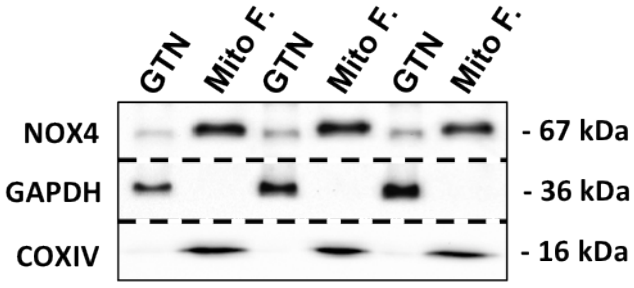

Figure 4.18 Representative western blots of NOX2 (A) and NOX4 (B) proteins in mitochondrial (Mito F) fractions from *GTN* muscle compared with lysate from whole *GTN* muscle.

Effect of inhibition of NADPH oxidase(s) on cytosolic superoxide at rest and during contractile activity

4.4.3.4 *Effect of diphenyleneiodonium chloride (DPI) inhibitor on DHE oxidation*

The role of NADPH oxidase complexes in producing superoxide under resting conditions was initially assessed by use of the non-specific inhibitor, Diphenyleneiodonium chloride (DPI) (Figure 4.19). Resting muscle fibres treated with DPI at 30 min of the experimental period showed an unexpected increase in DHE oxidation compared with control non-treated fibres (Figure 4.19). In addition, this flavoprotein inhibitor DPI also prevented the fibres from contracting. An alternative NADPH oxidase inhibitor, 4-(2-aminoethyl)-benzenesulfonyl fluoride (AEBSF) inhibitor also could not be assessed since this agent also influenced muscle contractions.

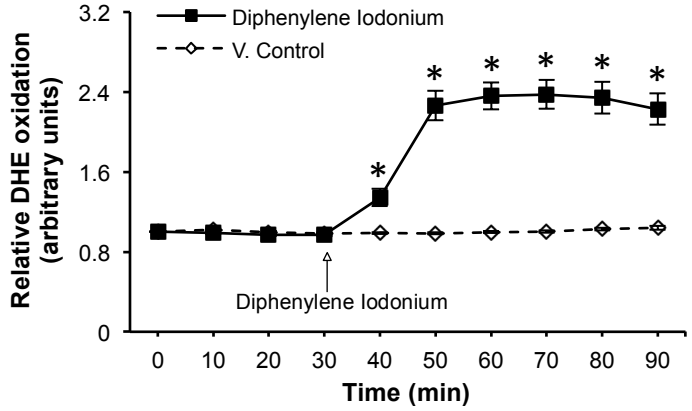

Figure 4.19 Relative change in DHE oxidation from DMSO vehicle-treated fibres (V control) and fibres treated with DPI (10μM) at 30 min. *P<0.05 compared with values from control vehicle-treated fibres at the same time points (n = 6-8 fibres in each group).

4.4.3.5 *Effect of apocynin (APO) inhibitor on DHE oxidation*

Fibres were incubated in the presence of apocynin (APO), a non-specific NADPH oxidase inhibitor, with the quiescent muscle fibres showing a reduction in fluorescence by a mean of 10% over the 50-90 min time course compared with vehicle-treated fibres (Figure 4.20). APO was also found to decrease DHE oxidation following a period of contractile activity. The contraction–induced increase in fluorescence was reduced by a mean of 70% compared with untreated fibres (Figures 4.21 and 4.22).

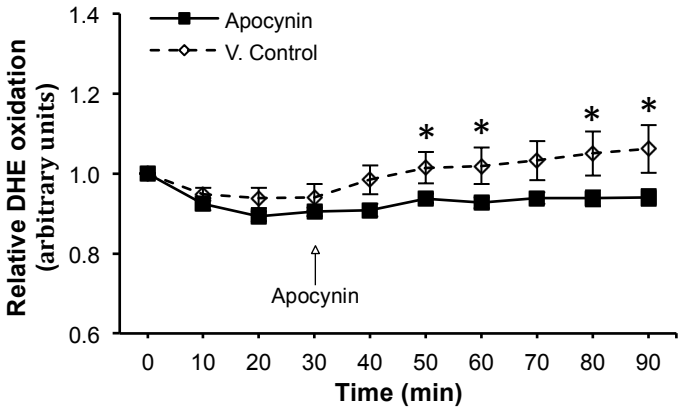

Figure 4.20 Relative change in DHE oxidation from PBS vehicle-treated fibres (V control) and fibres treated with APO (0.5mM) at 30 min. *P<0.05 compared with values from control vehicle-treated fibres at the same time points (n = 9 fibres in each group).

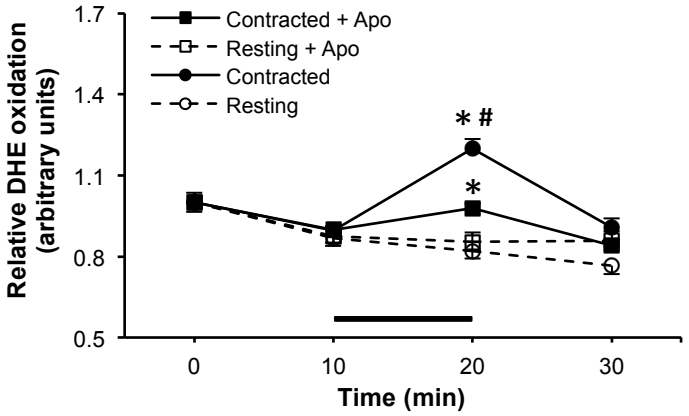

Figure 4.21 Relative change in DHE oxidation from resting *FDB* fibres and fibres subjected to the Moderate contraction protocol over the 10 - 20 min period. Fibres were either untreated or treated with APO (0.5mM). *P<0.05 compared with values from fibres of the same group prior to contractions. #P<0.05 compared with contracted fibres treated with APO at the corresponding time point (n = 14-17 fibres in each group).

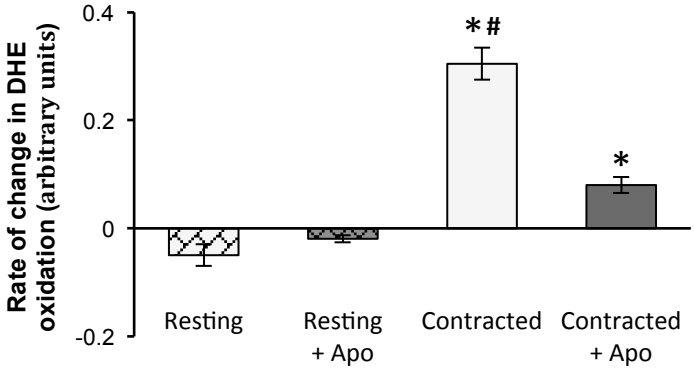

Figure 4.22 Rate of change (net change in fluorescence following the contractile activity period) in DHE oxidation from resting fibres and fibres subjected to a 10 min period of contractile activity. Fibres were either untreated or treated with APO (0.5mM). *P<0.05 compared with fibres from both resting groups. #P<0.05 compared with contracted fibres treated with APO (n = 14-17 fibres in each group).

Recent work suggests that APO may act as a scavenger for reaction products of H_2O_2, excluding superoxide, in vascular cells that lack myeloperoxidase (MPO) or produce low amounts of ROS (Heumuller et al., 2008). MPO is an enzyme that catalyses the production of hypochlorous acid (Spickett et al., 2000) and immunoblotting experiments failed to identify any MPO in skeletal muscle cells (Figure 4.23). Hence the potential inhibitory effect of gp91ds-tat, a specific peptide inhibitor of NADPH oxidases, was also examined.

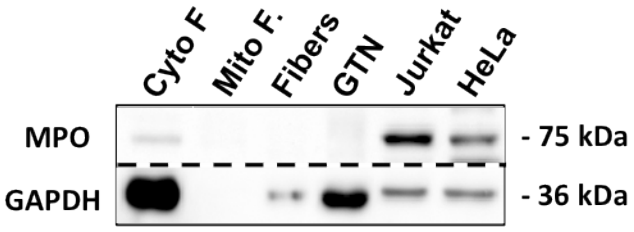

Figure 4.23 Representative western blot of myeloperoxidase (MPO) in cytosolic (Cyto F) and mitochondrial (Mito F) fractions from *GTN* muscle, in lysate from whole *GTN* muscle and single isolated *FDB* muscle fibres. Human Jurkat cells and HeLa cells were used as positive controls.

4.4.3.6 *Effect of gp91ds-tat inhibitor on DHE oxidation*

Resting fibres incubated in the presence of gp91ds-tat showed a decline in fluorescence by a mean of 18% compared with vehicle-treated fibres and fibres treated with the control peptide, scrambled-tat (Figure 4.24). Treatment of fibres with gp91ds-tat also prevented the increase in DHE oxidation in response to a 10 min period of contractions (Figure 4.25). DHE oxidation was significantly increased by contractions in both the vehicle control and scrambled-tat treated fibres, but the scrambled-tat treated fibres also showed a lower rate of increase in DHE oxidation than the vehicle-treated control group (Figure 4.25).

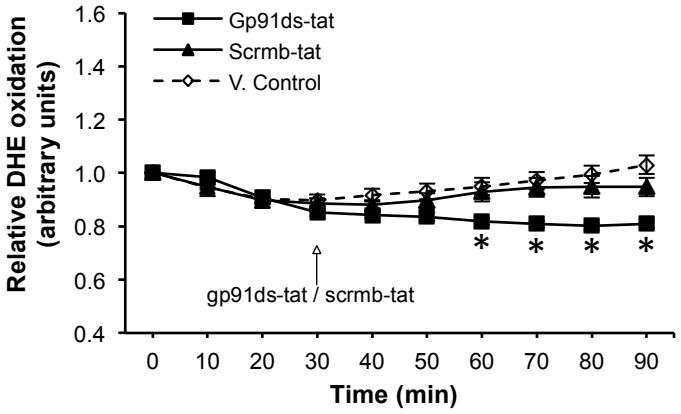

Figure 4.24 Relative change in DHE oxidation from PBS vehicle-treated (V control) fibres, gp91ds-tat (5μM) treated fibres and scrmb-tat (5μM) treated fibres at 30 min. *P<0.05 compared with values from control vehicle-treated fibres and fibres treated with scrmb-tat at the corresponding time points (n = 6-7 fibres in each group).

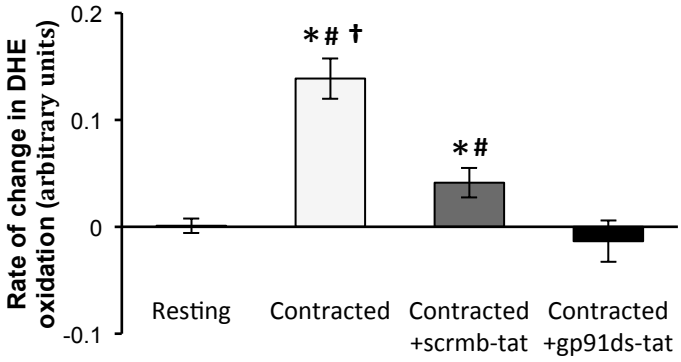

Figure 4.25 Rate of change in DHE oxidation from resting *FDB* fibres and fibres subjected to the Moderate contraction protocol for a period of 10 min. Contracted fibres were either untreated or treated with gp91ds-tat (5μM) or scrmb-tat (5μM). *P<0.05 compared with values from fibres of the resting group. $^{\#}$P<0.05 compared with contracted fibres treated with gp91ds-tat. †P<0.05 compared with values from contracted fibres treated with scrmb-tat (n = 7 fibres in each group).

Identifying the sub-cellular location of the NADPH oxidase components in single muscle fibres.

4.4.3.7 *Identifying the sub-cellular location of the regulatory NADPH oxidase components in single muscle fibres*

To determine the cellular location of NADPH oxidase subunits, immunocytochemistry of single isolated fibres from the *FDB* muscle was undertaken. Figure 4.26 shows the expression of the regulatory subunits ($p40^{phox}$, $p47^{phox}$, $p67^{phox}$ and Rac1) of the NADPH oxidase complex. These proteins were found to be localized on, or in close proximity to the sarcolemma, but immunofluorescence from $p40^{phox}$ and $p67^{phox}$ was also observed in the cytosolic compartment of the muscle fibres (Figure 4.26).

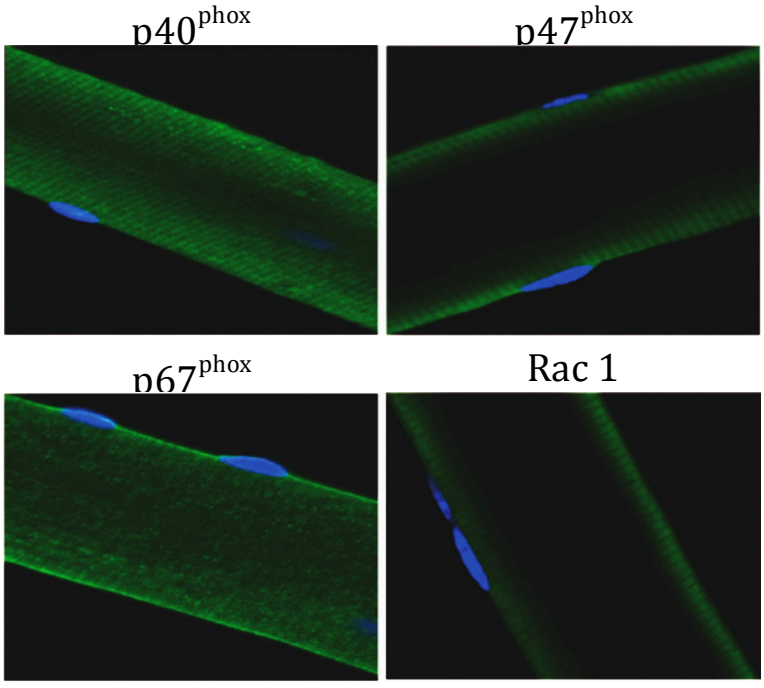

Figure 4.26 Immunocytochemistry of single isolated fibres from the *FDB* muscle showing the expression of $p40^{phox}$, $p47^{phox}$, $p67^{phox}$ and Rac1 subunits of the NADPH oxidase complex.

4.4.3.8 *Identifying the sub-cellular location of the catalytic NADPH oxidase components in single muscle fibres*

The catalytic subunits (NOX2 and NOX4) and the small membrane-bound integral subunit ($p22^{phox}$) were found to be localised on the plasma membrane of the muscle fibres, as indicated by co-localisation (yellow staining) with caveolin-3, the muscle-specific caveolin isoform, present in sarcolemmal caveolae (Whitehead et al., 2010), (Figure 4.27). A striated pattern of staining for all three subunits was also observed in close proximity to the sarcolemma, potentially due to expression in the T-tubules (Figure 4.27).

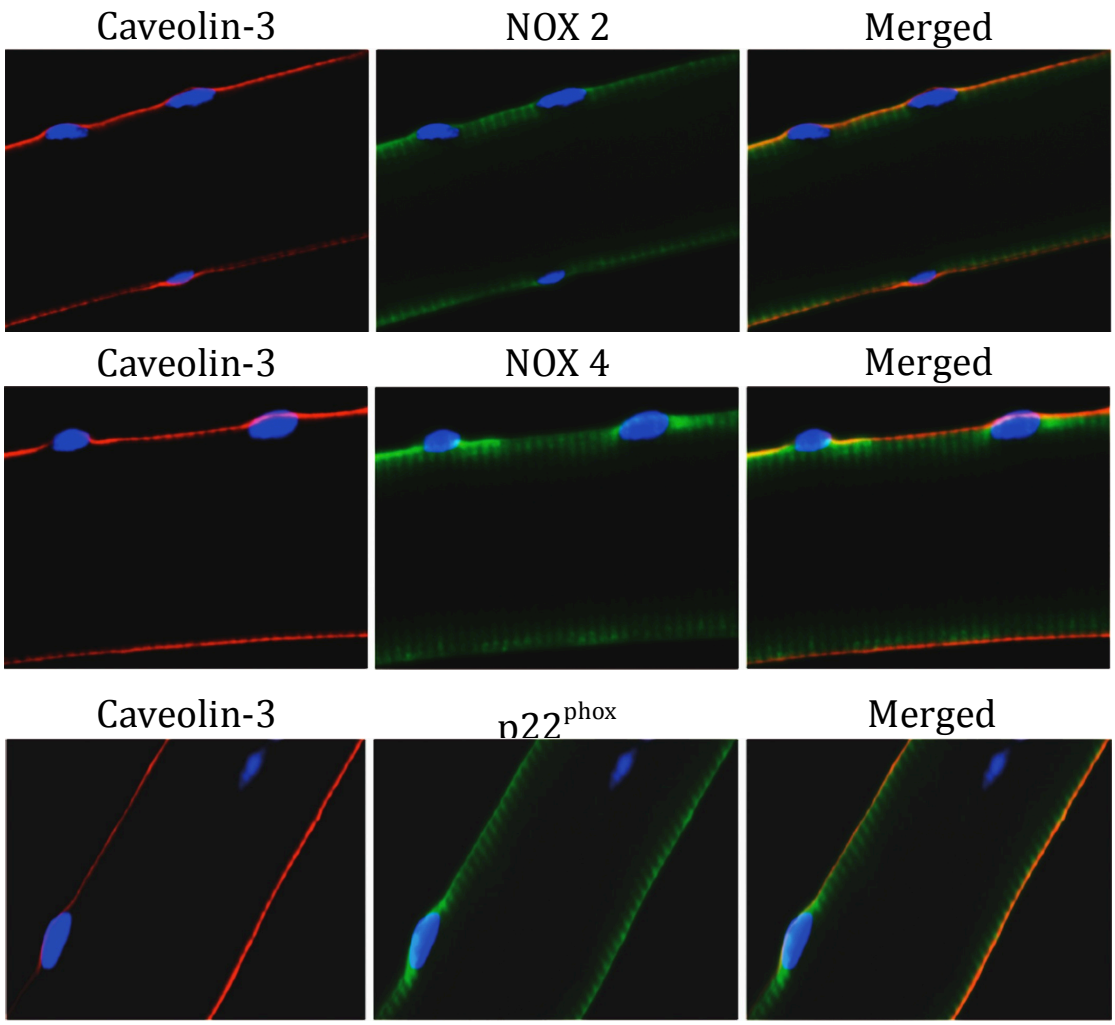

Figure 4.27 Immunocytochemistry for the NOX2, NOX4 and $p22^{phox}$ NADPH oxidase components. Fibres were co-immunostained with an antibody to Caveolin-3 (red staining) to demonstrate sarcolemmal co-localisation (yellow staining).

4.4.3.9 *Examining the T-Tubular expression of NOX2, NOX4 and p22phox in single muscle fibres*

To examine the possibility of at T-tubular NOX2, NOX4 and $p22^{phox}$ expression, the membrane bound subunits of the NADPH oxidase complex from single muscle fibres were co-immunostained with the α_{1s} subunit of the dihydropyridine receptor (α_{1s} DHPR), that is located on the T-tubule membrane (Hidalgo et al., 2006) (Figure 4.28). Confocal images showed a high degree of co-localization (yellow staining) strongly

suggesting that the NADPH oxidase components; NOX2 (Rr=0.60, R=0.67, Mred=0.85, Mgreen=0.96), NOX4 (Rr=0.98, R=0.98, Mred=0.98, Mgreen=1) and $p22^{phox}$ (Rr=0.92, R=0.97, Mred=1, Mgreen=0.92) were also expressed on the T-tubule membrane in skeletal muscle fibres (Figure 4.28).

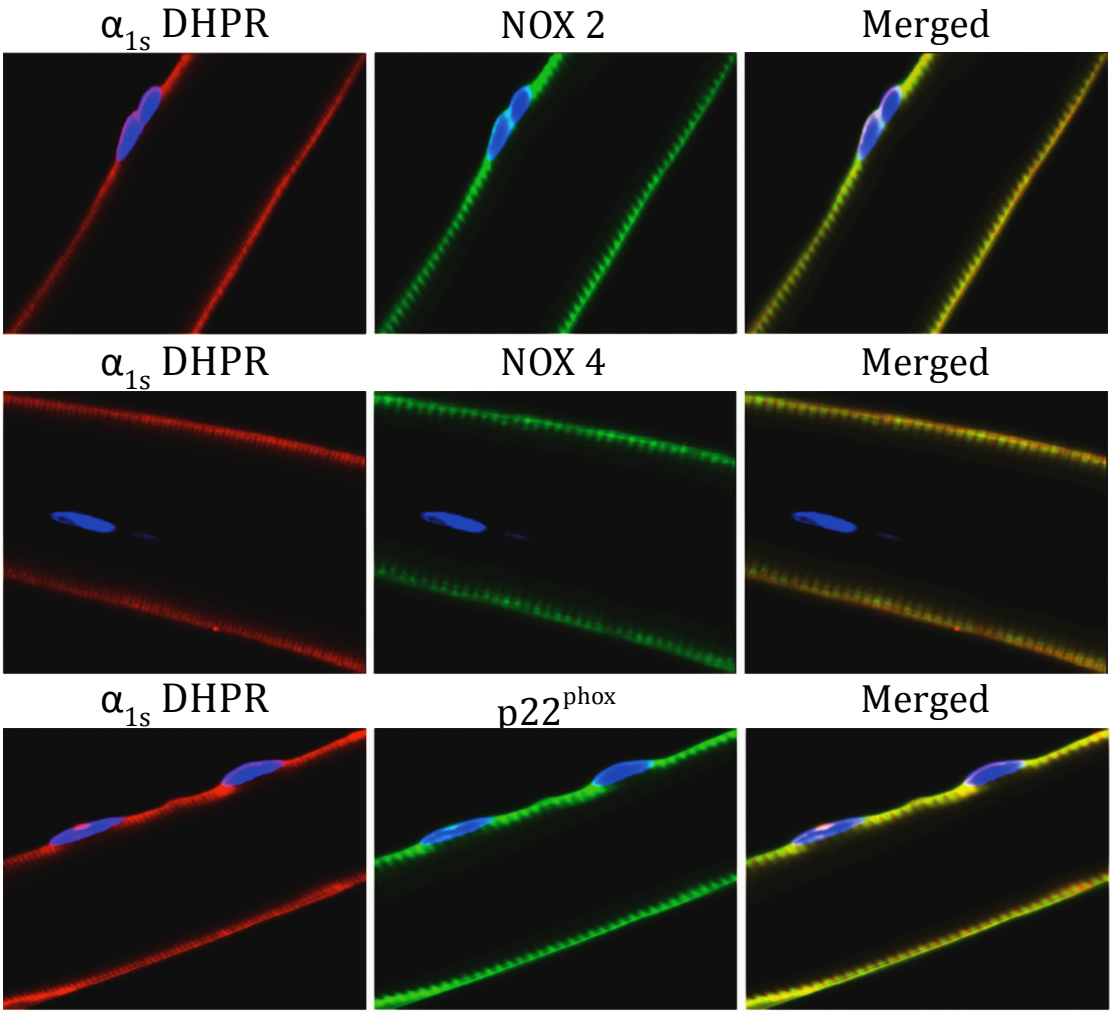

Figure 4.28 Fibres were immunostained using antibodies against NOX2, NOX4 and $p22^{phox}$ and co-immunostained with an antibody to α_{1s} DHPR (red staining) to demonstrate T-Tubular co-localisation (yellow staining).

4.4.3.10 *The effect of contractions on $p40^{phox}$ and $p67^{phox}$ translocation in single skeletal muscle fibres.*

Activation of the NADPH oxidase complex in phagocytic cells requires translocation of the cytosolic components; $p40^{phox}$, $p47^{phox}$ and $p67^{phox}$ to the cell membrane (Babior, 1995; Dusi et al., 1996; Kuribayashi et al., 2002). The confocal images in Figure 4.26 showed that $p40^{phox}$ and $p67^{phox}$ regulatory subunits were present in the cytosolic compartment of quiescent muscle cells. To determine whether the increase in cytosolic superoxide following contractions was associated with translocation of the regulatory subunits to the plasma membrane of the muscle cells, resting and contracted muscle fibres were immunostained-using antibodies against $p40^{phox}$ and $p67^{phox}$ (Figure 4.29). Confocal images showed no evidence for contraction-induced translocation of the $p67^{phox}$ protein, with resting fibres showing a similar intensity of fluorescence at the membrane and in the cytosol compared with fibres subjected to contractions (Figure 4.29). Fibres probed against $p40^{phox}$ showed a different pattern, with the contracted fibres exhibiting a more intense fluorescence at the sarcolemma compared with resting non-contracted fibres (Figure 4.29).

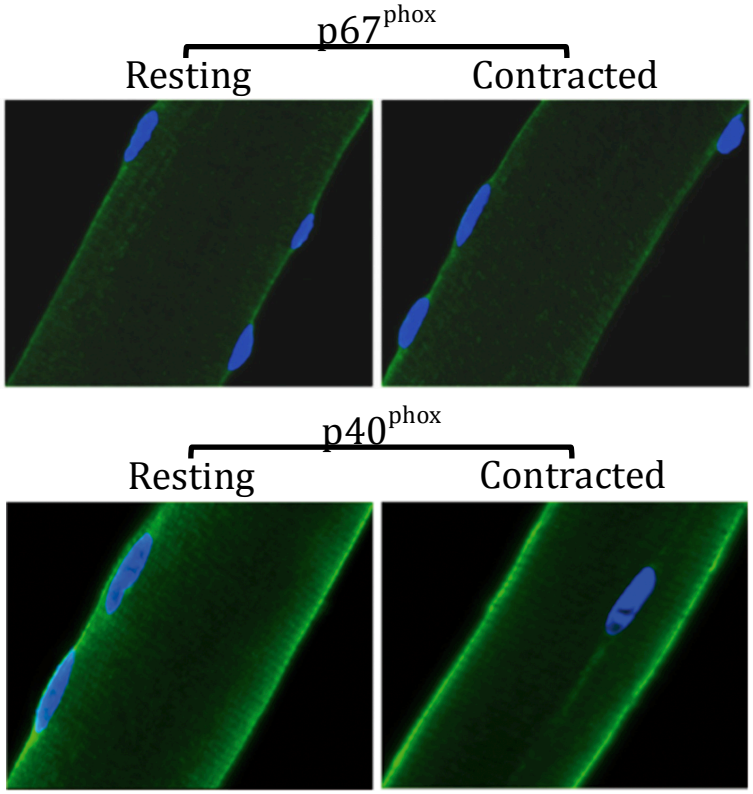

Figure 4.29 Immunocytochemistry of single isolated fibres showing the sub-cellular location of the cytosolic NADPH oxidase subunits; $p40^{phox}$ and $p67^{phox}$, at rest and following a 10 min period of moderate contractions. Nuclei (blue staining) were stained with DAPI.

4.4.3.11 *Fluorescence distribution analysis of $p40^{phox}$ in contracted and resting single skeletal muscle fibres.*

To examine the possible translocation of $p40^{phox}$ following contractions, shown in images of Figure 4.29 quantification of sub-cellular fluorescent distribution analysis for $p40^{phox}$ (Figure 4.30) was undertaken by utilizing the NIH Image J software. Quantification of sub-cellular fluorescent distribution analysis for $p40^{phox}$ (Figure 4.30) showed an increased proportion of the fibre fluorescence at the sarcolemma and a relative reduction in the cytosolic compartment of contracted fibres compared with quiescent fibres, suggesting that NADPH oxidase activation in skeletal muscle fibres during contractions involves translocation of $p40^{phox}$ to the plasma membrane.

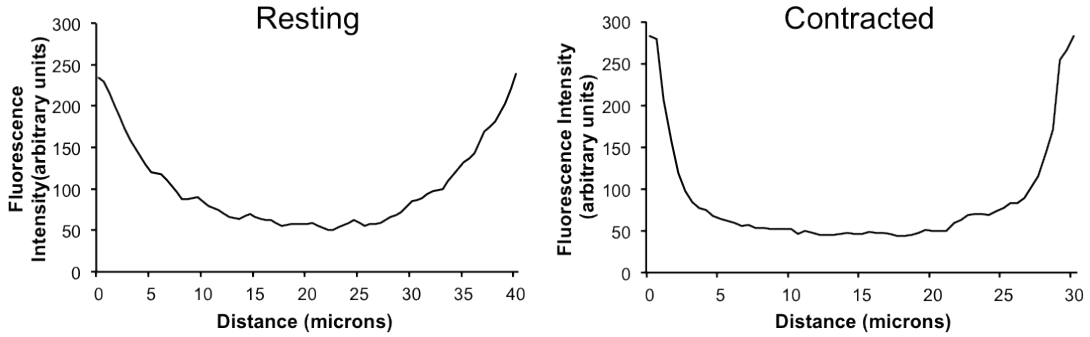

Figure 4.30 Profile of the distribution of fluorescence from immunostaining for $p40^{phox}$ across the single resting and contracted fibres shown in Figure 4.29.

4.5 DISCUSSION

Since the initial observations that skeletal muscle produces free radicals, a great deal of research has been undertaken to identify potential sources that are responsible for the increased generation of RONS during contractions. It is now clear that superoxide and NO are the primary reactive oxygen and nitrogen species generated within skeletal muscle both at rest and during contractile activity and although the production of NO by the nitric oxide synthases has been well described, there is still considerable debate over the prime cytosolic source(s) of superoxide in skeletal muscle. The work described in this chapter has examined potential pathways that are involved in the regulation of cytosolic superoxide content both at rest and during contractile activity in single isolated mature skeletal muscle fibres by monitoring real time changes in DHE and MitoSOX Red oxidation using fluorescence microscopy.

4.5.1 Potential cytosolic sources of superoxide in single skeletal muscle fibres

Many studies have demonstrated an increase in end-point indicators of the reactions of RONS in tissues during and following exercise, and the increase in RONS

appears to be in major part due to generation by contracting skeletal muscle (Jackson, 2005). The main objective of the present study was to determine the major sites that contribute to changes in cytosolic superoxide in skeletal muscle both at rest and following contractile activity.

Previous work from my MPhil thesis (Figure 4.1) showed that the contraction-induced increase in superoxide in response to contractions is proportional to the intensity of the contraction protocol/frequency of contractions. This finding is in agreement with previous studies which demonstrated that intracellular (Silveira et al., 2003) and extracellular ROS (Kolbeck et al., 1997; Reid et al., 1992) generation in myotubes and diaphragm tissue was higher following an intense electrical stimulation protocol than with a moderate stimulation protocol.

4.5.2 Contribution of mitochondria to cytosolic superoxide in single skeletal muscle fibres

It has been well described that the increase in ATP production via oxidative phosphorylation is associated with elevated O_2 consumption that occurs with increased mitochondrial activity and early studies examining the sources of superoxide production reported that 2-5% of the total O_2 consumed by mitochondria may undergo one electron reduction with the generation of superoxide (Boveris and Chance, 1973; Loschen et al., 1974; Halliwell and Gutteridge, 2007). Although recent assessments of the rate of superoxide production by mitochondria indicate that only ~0.15% of the total O_2 consumed is reduced to superoxide (St-Pierre et al., 2002), this might imply that the contraction intensity-dependent increase in cytosolic superoxide assessed via changes in

DHE oxidation (Figure 4.1) might be a result of increased mitochondrial superoxide increase due to a greater demand for ATP production.

However, the rapid increase in superoxide observed following contractions (Figure 4.1) likely originated from non-mitochondrial sources since the change in DHE oxidation reflects reaction with superoxide within the cytosolic compartment of the muscle cells (Johnson-Cadwell et al., 2007). Superoxide is a membrane impermeant anion, but recent evidence has indicated that superoxide can diffuse out of isolated mitochondria through the mitochondrial permeability transition pore (mPTP) (Abou-Sleiman et al., 2006), the inner mitochondrial anion channel (iMAC) (Dai et al., 2011) and through channels located on the outer mitochondrial membrane (OMM) (Budzinska et al., 2009; Han et al., 2003).

Studies have shown that isolation techniques can severely disturb mitochondrial structural integrity, associated with marked impairments of mitochondrial function. Reports indicate that skeletal muscle mitochondria exhibit a markedly diverse architecture (Kirkwood et al., 1986; Kayar et al., 1988) with some mitochondria exhibiting elongated tubular branched structures (Ogata and Yamasaki, 1997) and extensive functional connections (Fang et al., 2011). However, electron microscopy images of isolated mitochondria from healthy tissues show disrupted architecture such as lower electron density of the matrix space, dysmorphic and irregular inner mitochondrial membrane structure and swelling of the inter-membrane (Schwerzmann et al., 1989). Mitochondrial morphology is closely associated to aspects of mitochondrial function and recent evidence has shown that isolation techniques can cause striking adverse effects such as loss of soluble matrix enzymes (Schwerzmann et

al., 1989; Picard et al., 2010), increased mitochondrial permeability transition pore (mPTP) sensitivity to Ca^{2+} (Picard et al., 2011b), altered respiratory responses and increased H_2O_2 production (Picard et al., 2011a; Picard et al., 2011b).

These findings demonstrate that mitochondrial isolation techniques can profoundly impact several aspects of mitochondrial function, which raises concerns regarding the interpretation of results obtained in studies using isolated mitochondria. Hence, the current study examined mitochondrial superoxide release from intact mitochondria within single muscle fibres, thus preserving the mitochondrial morphology, maintaining the functional interactions with other cellular compartments (such as sarcoplasmic reticulum, lipid droplets and cytoskeleton) (Goodman, 2008; Saks et al., 2010) and keeping the organelles in their native intracellular and systemic environment.

In order to induce an increase in superoxide generation by mitochondria and examine the potential release of superoxide to the cytosol, two approaches were used. Fibres were either treated with Ant A which is reported to increase superoxide generation at complex III leading to release to both the matrix and MIS (Muller et al., 2004), or fibres were treated with Rot which is reported to increase superoxide generation at complex I leading to release to the matrix only (Muller et al., 2004). Both of these treatments were found to increase the oxidation of matrix-localised MitoSOX Red, but only Ant A caused an increase in cytosolic DHE oxidation supporting the possibility that only superoxide within the intermembrane space can contribute to cytosolic superoxide.

The lack of any role for matrix superoxide in oxidation of DHE in the cytoplasm was supported by the lack of effect of the SS-31 peptide on DHE oxidation. The mitochondrial targeted SS-31 peptide accumulates on the IMM and recent reports have shown that it can directly scavenge superoxide produced within the mitochondrial matrix (Dai et al., 2011; Maack and Bohm, 2011). The lack of effect observed in this study provides evidence that superoxide generated by complex III and released into the matrix, does not escape from intact mitochondria in muscle fibres. These findings are consistent with previous reports that failed to show any extramitochondrial superoxide release from mitochondria in response to the addition of rotenone (Muller et al., 2004; Gao and Wolin, 2008), indicating that complex I-dependent superoxide is exclusively released into the matrix. Inhibitors of iMAC or mPTP were also ineffective in reducing cytosolic DHE oxidation in Ant A-treated fibres, which argues against a role for these channels in release of superoxide from the mitochondrial matrix to the cytosol of muscle fibres.

A role for OMM channels in release of superoxide from the MIS to the cytoplasm was supported by the effects of VDAC and Bax inhibitors. The three VDAC isoforms (VDAC1, VDAC2 and VDAC3) and the Bax channel were detected in mitochondrial fractions and lysates from single muscle fibres. Both VDAC and Bax channel inhibitors (DS and Bax CB) attenuated the anticipated increase in DHE oxidation following treatment with Ant A indicating that VDAC and Bax can potentially act as superoxide channels. This observation is consistent with early studies (Lynch and Fridovich, 1978) and with recent reports examining superoxide release from isolated cardiac mitochondria which confirmed VDAC can mediate the release of superoxide from the MIS across the OMM (Han et al., 2003). Inhibition of VDAC

reduced DHE oxidation to a greater extent than Bax inhibition, potentially since VDACs are the major channels of the OMM responsible for the passage of proteins and solutes between the OMM and cytosplasm (Mannella, 1998). Neither DS nor Bax CB fully inhibited the extramitochondrial superoxide release suggesting that either the inhibitors failed to completely close the respective channels or other channels, such the peptide-sensitive channel (Juin et al., 1995) or the translocase of outer membrane (Budzinska et al., 2009) may also mediate the release of superoxide across the OMM.

Single muscle fibres were also incubated in the presence of VDAC and/or Bax channel inhibitors to attempt to inhibit the increase in DHE oxidation following a 10 min period of contractile activity, but no significant effects were seen. These data strongly suggest that the increase in cytosolic superoxide during contractions does not derive from mitochondrial sources. Interestingly, DHE oxidation following contractions increased by 20% whereas, the relative change in fluorescence in response to Ant A increased by 90%. Thus, the observed increase in superoxide following addition of Ant A may be considered "non physiological" compared with that following a period of contractile activity. Hence, it is argued that intact mitochondria do not release superoxide to the cytosplasm of skeletal muscle fibres at rest or in response to a physiological stimulus such as contractile activity, but can release superoxide under pathological conditions, where mitochondrial superoxide production is grossly excessive.

4.5.3 Contribution of $iPLA_2$ enzymes to cytosolic superoxide in skeletal muscle fibres

Recent work by Reid and colleagues demonstrated that $iPLA_2$ enzymes can modulate the cytosolic oxidant activity in skeletal muscle cells as indicated by a reduction in 2', 7'- dichlorodihydrofluorescin (DCFH) oxidation following inhibition of $iPLA_2$ (Gong et al., 2006). DCFH oxidation is considered to be a general indicator of ROS activities (Palomero et al., 2008). Western blots for $iPLA_2$ confirmed the presence of this enzyme in the cytosolic compartment of skeletal muscles and lysates from single fibres, but no effect of the $iPLA_2$ inhibitors on DHE oxidation was seen. In the study by Reid and colleagues (Gong et al., 2006), the $iPLA_2$ selective inhibitor BEL was used at concentration of 10 μM, a concentration that exceeds the IC_{50} by more than three fold (Hazen et al., 1991), whereas in the present study, single muscle cells were incubated with 0.6 μM since in preliminary studies higher concentrations were found to affect the viability of muscle fibres. Concentrations as low as 0.6 μM have previously shown to inhibit $iPLA_2$ activity by 100% (Ackermann et al., 1995). Overall, our data imply that that the cytosolic superoxide levels either at rest or during contractions in single skeletal muscle fibres are not modulated by the activity of the $iPLA_2$ enzymes. In relation to this, work from Zuo and colleagues showed that the PLA_2 enzymes do not specifically produce superoxide but can release arachidonic acid, which is a substrate for superoxide generating enzyme systems such as the lipoxygenases (Zuo et al., 2004).

4.5.4 Expression of NADPH oxidase and its contribution to cytosolic superoxide in skeletal muscle fibres

Skeletal muscles have previously been shown to express NADPH oxidase(s) (Espinosa et al., 2006; Hidalgo et al., 2006; Mofarrahi et al., 2008; Whitehead et al.,

2010), but little information has been published regarding the role and regulation of this complex in generation of superoxide in muscles. Our initial results show mRNA and protein expression of NADPH oxidase subunits in single isolated fibres from the *FDB* muscle. Others have identified various NADPH oxidase subunits in mouse and rabbit skeletal muscles (Whitehead et al., 2010; Hidalgo et al., 2006), but this appears to be the first report to demonstrate the expression of all NADPH oxidase components in a pure muscle fibre preparation devoid of all non-myogenic cells.

Inhibitor studies support a role for NADPH oxidase in contributing to cytosolic superoxide production. Resting fibres treated with APO and gp91ds-tat inhibitors showed a decrease in DHE oxidation compared with control fibres, suggesting that the complex is active and modulates superoxide generation under resting conditions. Similarly, fibres subjected to contractile activity showed a significantly lower increase in DHE oxidation following treatment with APO whereas gp91ds-tat treatment abolished the increase in response to contractions. Scrambled-tat pretreated fibres also showed a decrease in fluorescence following contractions, but some previous studies have also observed this (Rey et al., 2001). Gp91ds-tat appeared to be more effective than APO, which can be attributed to the different inhibitory properties of the compounds.

Recent evidence suggests that APO might require activation by peroxidases (Wind et al., 2010) and can additionally act as an antioxidant scavenger for ROS, excluding superoxide, in cellular systems that lack myeloperoxidase, or produce low amounts of ROS (Heumuller et al., 2008). The proposed inhibitory mechanism of action of APO on NADPH oxidase is to prevent the translocation of $p47^{phox}$ and $p67^{phox}$ to the

membrane-located catalytic subunits (Muijsers et al., 2000) whereas gp91ds-tat peptide, the most potent inhibitor (IC_{50}: 3 μM) selectively inhibits NOX2-oxidase (Csanyi et al., 2011), although early studies suggested the possibility that the peptide may additionally inhibit NOX1 and NOX4 homologues (Brandes, 2003; Rey et al., 2001) by preventing their interaction with $p47^{phox}$ (Rey et al., 2001). The inhibitory effects of both APO and gp91ds-tat imply that $p47^{phox}$ is a critical component of the NADPH oxidase complex and can regulate the activity of the enzyme in skeletal muscle.

Treatment of resting fibres with the non-specific inhibitor DPI showed a paradoxical increase in DHE oxidation. Lack of specificity of DPI in inhibiting flavoenzymes besides NADPH oxidase, such as nitric oxide synthase, xanthine oxidase and NADPH-cytochrome P450 reductase (Balcerczyk et al., 2005; Longpre and Loo, 2008; Park et al., 2007) imply that this compound can affect multiple cellular processes unrelated to NADPH oxidase. Data on the regulation of intracellular ROS by DPI are controversial, with both inhibitory and stimulatory actions of DPI being reported. Studies have shown that DPI can induce the production of reactive oxygen (Li et al., 2003; Riganti et al., 2004) and nitrogen species (Balcerczyk et al., 2005), thus affecting the cellular redox status as indicated by increased levels of lipid peroxidation (Riganti et al., 2004) and DNA damage (Longpre and Loo, 2008; Park et al., 2007), an increase in glutathione disulfide (Riganti et al., 2004) and apoptosis (Balcerczyk et al., 2005; Longpre and Loo, 2008; Park et al., 2007), as well as increased nitration of tyrosine residues of cellular proteins (Balcerczyk et al., 2005). Previous studies have also reported an increased oxidation of ROS-sensitive probes including dHR 123 (Park et al., 2007) and H_2DCF-DA (Balcerczyk et al., 2005; Park et al., 2007) following addition of DPI. Potential mechanisms through which DPI can stimulate RONS production have

been reported including mitochondrial superoxide production via inhibition of complex I (Li et al., 2003; Li and Trush, 1998), but also due to the inhibitory mechanism of DPI which incudes formation of phenyl radicals (O'Donnell et al., 1993; Longpre and Loo, 2008). However, the data presented in this chapter argue that the increase in DHE oxidation following addition of DPI is not related to complex I mitochondrial superoxide production since other experiments indicate that complex I-dependent superoxide production within the mitochondrial matrix (Figure 3.10) does not diffuse to the cytoplasmic compartment of the muscle fibres (Figure 4.5).

The data presented imply that NOX2 is likely to be the predominant oxidase system contributing to cytosolic superoxide generation in muscle fibres since most recent data indicate that the gp91ds-tat peptide selectively inhibits the assembly of NOX2 oxidase (Csanyi et al., 2011). Immunocytochemistry of single isolated fibres from the *FDB* muscle revealed that NOX isoforms and subunits were localized on, or in close proximity to the plasma membrane of muscle fibres although $p40^{phox}$ and $p67^{phox}$ were also present in the cytosolic compartment of quiescent muscle fibres. Further experiments supported previous findings (Espinosa et al., 2006; Hidalgo et al., 2006) of apparent localization of these subunits to the T-Tubules. In addition, NOX4 was found to be present in skeletal muscle mitochondria. Recent reports have shown NOX4 localized to cardiac (Ago et al., 2010; Dai et al., 2011; Kuroda et al., 2010) and liver (Block et al., 2009) mitochondria. NOX4 has been predicted to localize on the inner mitochondrial membrane (Block et al., 2009) and produce hydrogen peroxide (von Lohneysen et al., 2008) but recent reports have shown that it can also regulate changes in superoxide within the mitochondrial matrix (Ago et al., 2010; Block et al., 2009; Dai et al., 2011; Kuroda et al., 2010). These findings however, have not been examined in

skeletal muscle, thus future studies are warranted to examine the role of NOX4 in skeletal muscle mitochondria. Updated schematic figures that show the cytosolic and mitochondrial RONS sources in skeletal muscle were produced to highlight these findings (Figures 4.31 and 4.32).

In phagocytic cells, NADPH oxidase activation requires the translocation of the cytosolic-regulatory subunits to cytochrome b_{558}, the catalytic core of the enzyme (Dusi et al., 1996; Kuribayashi et al., 2002). Fluorescent distribution analysis showed no evidence for translocation of the $p67^{phox}$ protein following contractions but $p40^{phox}$ immunostained fibres showed an increased proportion of fluorescence at the membrane and a reduction in the cytoplasmic compartment following contractions, which suggests that NADPH oxidase activation in single skeletal muscle fibres from young mice in response to contractions may involve translocation of the $p40^{phox}$ regulatory subunit to the plasma membrane. Although the role of $p40^{phox}$ has been controversial, studies in phagocytes indicate that on stimulation, $p40^{phox}$ translocates to cytochrome b_{558} (Dusi et al., 1996) and functions as a positive regulator of the superoxide–producing phagocyte oxidase by enhancing recruitment of $p67^{phox}$ and $p47^{phox}$ to the membrane (Kuribayashi et al., 2002). In addition, lack of $p40^{phox}$ in homozygotic knockout mice has been reported to reduce superoxide production in both *in vivo* and *in vitro* models (Ellson et al., 2006) and decrease the expression of $p67^{phox}$ (Ellson et al., 2006; Tian et al., 2008).

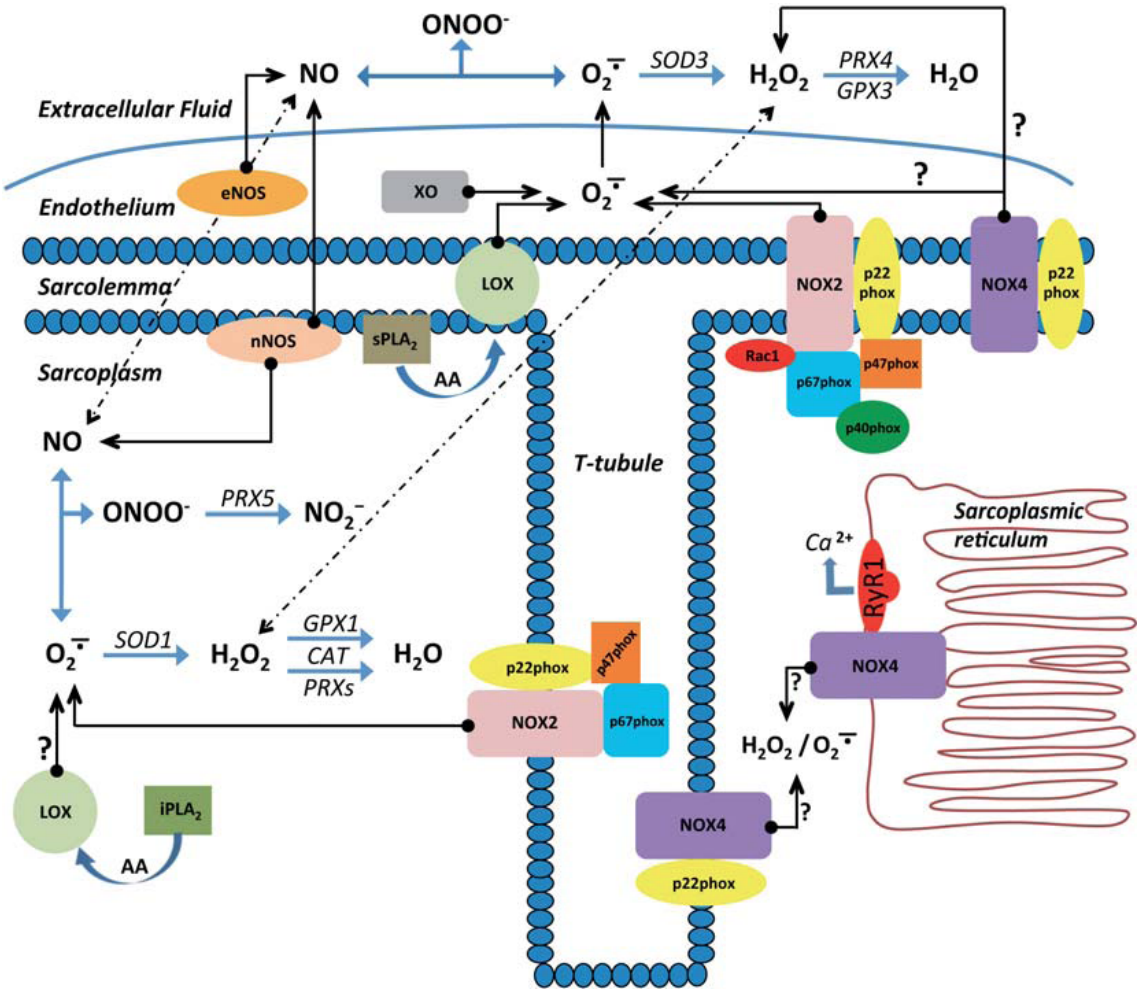

Figure 4.31 Schematic representation of the non-mitochondrial sites for superoxide and nitric oxide production in skeletal muscle. Superoxide (O_2-) is produced by multicomponent NAD(P)H oxidase 2 (*NOX2*), xanthine oxidase (*XO*) and the lipoxygenases (*LOX*) which activity is regulated by the phospholipase A_2 enzymes. Arachidonic acid (*AA*) release by the membrane bound calcium-dependent phospholipase A_2 enzymes ($sPLA_2$) facilitates extracellular O_2- release by the membrane bound LOX. It is uncertain whether the cytosolic LOX enzymes contribute to intracellular O_2- changes which substrate availability might be regulated by the cytosolic calcium-independent phospholipase A_2 enzymes ($iPLA_2$). NAD(P)H oxidase 4 (*NOX4*) also contributes to ROS changes, though the primary ROS product, O_2- or hydrogen peroxide (H_2O_2) of NOX4 is uncertain. Cytosolic and extracellular O_2- is dismuted into H_2O_2 by superoxide dismutase (*SOD*), SOD1 and SOD3 respectively, or reacts rapidly with membrane permeant nitric oxide (*NO*) produced by the endothelial and neuronal nitric oxide synthase (*eNOs and nNOS*) to form peroxynitrite ($ONOO^-$). H_2O_2 formed within the extracellular space is reduced into H_2O by the action of

glutathione peroxidase 3 (*GPX3*) or peroxiredoxin IV (*PRX4*), while cytosolic H_2O_2 is reduced into H_2O by glutathione peroxidase 1 (*GPX1*), catalase (*CAT*) or peroxiredoxins (*PRXs*). $ONOO^-$ can be reduced predominantly into nitrite ($NO2^-$) by peroxiredoxin V (*PRX5*), (Sakellariou et al., 2013b)

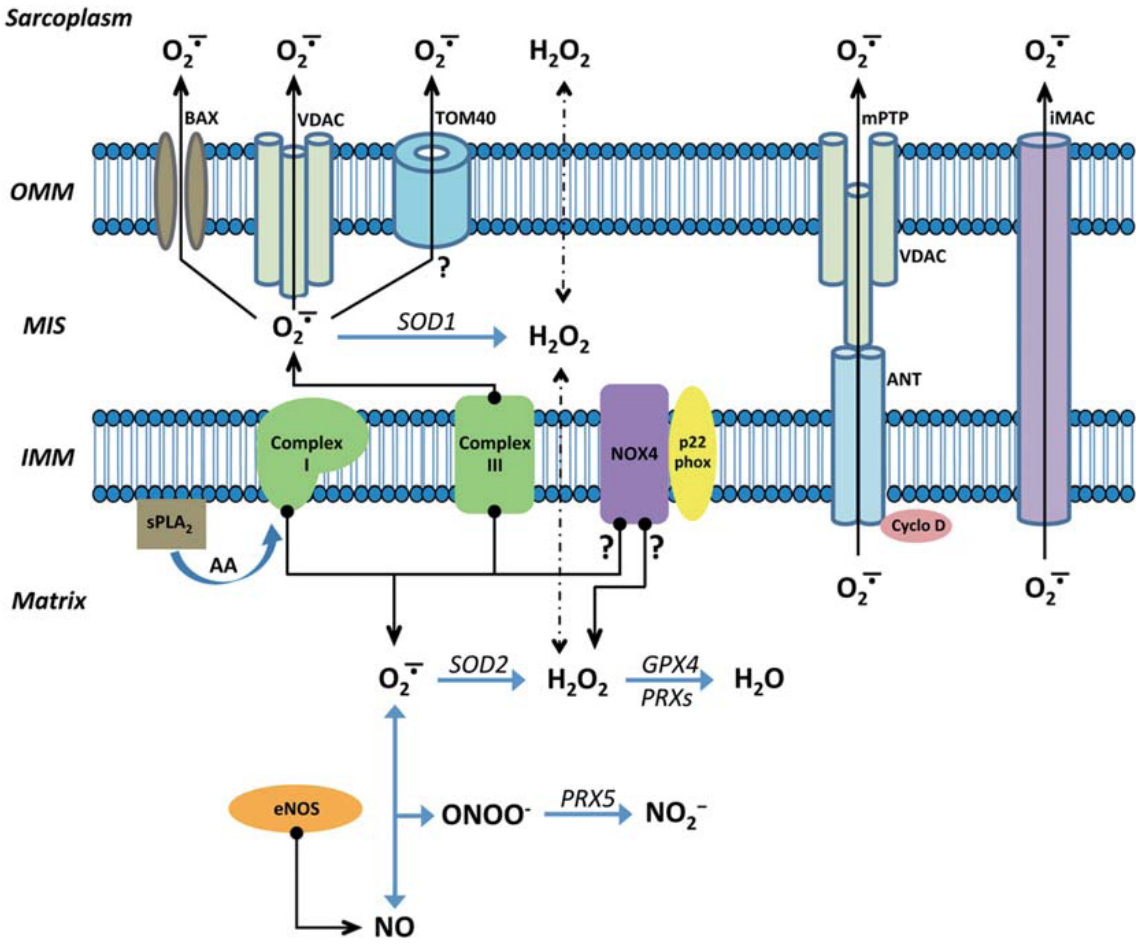

Figure 4.32 Schematic representation of the mitochondrial sites for superoxide production and the channels that mediate the release to the cytosolic compartment in skeletal muscle. Superoxide (O_2-) is produced by complex I and complex III of the mitochondrial ETC of the inner mitochondrial membrane (*IMM*) and released into the matrix and the mitochondrial intermembrane space (*MIS*). NAD(P)H oxidase 4 (*NOX4*) also contributes to ROS changes, though the primary ROS product, O_2- or hydrogen peroxide (H_2O_2) of NOX4 is uncertain. Arachidonic acid (*AA*) release by the calcium-dependent phospholipase A_2 enzymes ($sPLA_2$) interacts with complex I and enhances superoxide generation by this complex. O_2- released into the matrix and MIS is

dismuted into H_2O_2 by superoxide dismutase (*SOD*), SOD2 and SOD1 respectively, or reacts rapidly with nitric oxide (*NO*) produced by the endothelial nitric oxide synthase (*eNOS*) to form peroxynitrite ($ONOO^-$). H_2O_2 is reduced into H_2O by the action of glutathione peroxidase 4 (*GPX4*) or peroxiredoxins (*PRXs)*, $ONOO^-$ can be reduced predominantly into nitrite ($NO2^-$) by peroxiredoxin V (*PRX5*). O_2- is essentially membrane impermeable while H_2O_2 is readily diffusible. Matrix O_2- can diffuse to the cytosol through the inner membrane anion channel (*iMAC*) that spans the IMM and the outer mitochondrial membrane (*OMM*) or via the mitochondrial permeability transition pore (*mPTP*) comprised of the voltage dependent anion channels (*VDAC*) on the OMM, the adenine-nucleotide translocator (*ANT*) located on the IMM and cyclophilin D (*Cyclo D*) located in the matrix. Channels of the OMM including VDAC, BAX and possibly the translocase of outer membrane 40 (*TOM40*) can also mediate the release of O_2- from the MIS to the cytosol, (Sakellariou et al., 2013b)

4.5.5 Physiological implications

Previous studies indicated that myotube depolarisation induced superoxide generation through activation of NADPH oxidase (Espinosa et al., 2006) and data presented here support this proposal. The electrical field stimulation used to induce contractile activity results in membrane depolarisation and the generation of action potentials which are transmitted to the interior of the muscle fibres along the T-tubules (Mougios, 2006). The presence of T-Tubule-localised NADPH oxidase expression reported by Hidalgo *et al* (Hidalgo et al., 2006) and observed in the present study in conjunction with the effect of increasing frequency of contractions on superoxide content presented in Figure 4.1, imply that repeated membrane depolarisation may regulate the activity of skeletal muscle NADPH oxidase. Data from the present study showed that NADPH oxidase-dependent superoxide production was directly related to the frequency of contractions of the fibre, with the greatest intensity of contractions causing the highest cytosolic DHE oxidation. A possible physiological role was proposed by Hidalgo and colleagues who suggested that superoxide generated by

NADPH oxidase can stimulate calcium release from the sarcoplasmic reticulum through oxidative modification of the ryanodine receptor (Hidalgo et al., 2006).

There is also emerging evidence of interplay between ROS generated by NADPH oxidases and that by mitochondria. Studies in vascular tissue have shown that NOX derived cytosolic superoxide can trigger mitochondrial ROS formation (Brandes, 2005) by opening the mitochondrial ATP-sensitive potassium channels, leading to changes in the mitochondrial membrane potential (Doughan et al., 2008). Conversely, increased mitochondrial H_2O_2 release has been reported to activate NADPH oxidase via a protein kinase C dependent pathway, resulting in increased cytosolic superoxide production (Doughan et al., 2008; Daiber, 2010), supporting the concept that NADPH oxidase can trigger mitochondrial ROS formation and vise-verse. In relation to this, pharmacological studies which induced mild mitochondrial dysfunction (Wosniak et al., 2009) but also transgenic approaches including thioredoxin 2 overexpressing mice (Widder et al., 2009) have shown that both experimental models attenuated angiotensin-II mediated increase in mRNA (Wosniak et al., 2009) and protein (Widder et al., 2009) NADPH oxidase expression implying that mitochondrial ROS can regulate the expression of the NADPH oxidase components. Although, the cross-talk between mitochondrial and Nox-derived ROS in skeletal muscle remains unclear, the presence of NOX4 in skeletal muscle mitochondria observed in the present study further supports the concept of interplay between the NADPH oxidases and mitochondrial ROS sources. However, further research is warranted to examine the relationship between cytosolic and mitochondria ROS sources in skeletal muscle at rest and during contractile activity.

4.6 CONCLUSION

In conclusion, this is the first study to report the relative contribution of potential mitochondrial and cytosolic sources to superoxide production within the cytosolic compartment of single muscle fibres both at rest and during contractile activity. Data indicated that contractile activity increased superoxide content in an intensity dependent manner. Experiments with intact mitochondria in isolated mature skeletal muscle fibres support the conclusion that mitochondrial sources do not contribute to cytosolic superoxide increase either at rest or following a physiological stimulus such as contractile activity. In contrast, under pathological conditions when mitochondrial superoxide production is grossly excessive, channels of the outer mitochondrial membrane such as VDAC and Bax appear to be able to release superoxide from the MIS to the cytosol of skeletal muscle fibres. Cytosolic superoxide levels were not modulated by the activity of the $iPLA_2$ enzymes in single skeletal muscle fibres, but inhibition of NADPH oxidase activity induced a significant decrease in DHE oxidation at rest and following contractions. Our data suggest that NADPH oxidase is the major contributor to superoxide production both at rest and during contractile activity in skeletal muscle.

CHAPTER 5

IDENTIFYING THE REACTIVE SPECIES INVOLVED IN THE ACCELERATED AGE-RELATED LOSS OF MUSCLE MASS IN MICE LACKING CU, ZN SUPEROXIDE DISMUTASE AND TO EXAMINE THE CHANGES IN REDOX STATUS AND ADAPTIVE RESPONSES THAT OCCUR IN SKELETAL MUSCLES FROM THESE MICE

5.1 INTRODUCTION

Ageing skeletal muscle is characterized by a progressive loss of mass and contractile force and has a profound impact on the quality of life of older people. The loss of muscle mass and strength that occurs during ageing contributes to frailty and loss of independence (Marcell, 2003) and by the age of 70, the cross-sectional area of skeletal muscle is reduced by 25-30%, inducing a subsequent decrease in muscle strength and power by 30-40% (Porter et al., 1995). As mentioned in the introduction (Section 1.5), oxidative damage has been claimed to be involved in the loss of tissue function that occurs during ageing and it is well recognised that skeletal muscle of aged rodents contains increased amounts of the products of oxidative damage to biomolecules such as lipids, DNA and proteins in comparison with young or adult rodents (Sastre et al., 2003; Broome et al., 2006; Vasilaki et al., 2007; Kaneko et al., 1996).

The mechanisms by which the age-related loss of muscle mass and function occur are poorly understood and the hypothesis that an increased generation of oxidants *in vivo* plays a key role in age-related tissue dysfunction has been examined in a number of transgenic studies with inconsistent results (Huang et al., 2000; Schriner et al., 2005; Muller et al., 2006; Vasilaki et al., 2010; Elchuri et al., 2005). Studies from this group have examined skeletal muscle of mice lacking various key regulatory enzyme systems involved in the detoxification of ROS to determine whether specific defects in antioxidant protection and the resultant changes in ROS influence the onset and/or rate of age-related muscle dysfunction (Broome et al., 2006; McArdle et al., 2004; Vasilaki et al., 2007; Vasilaki et al., 2010). In collaboration with colleagues from the Universities of Texas and Michigan, USA it has been identified that a lack of

CuZnSOD (SOD1) in homozygotic SOD1 knockout (SOD1KO) mice induced a rapid acceleration of the age-related loss of skeletal mass which resembles an acceleration of normal age-related sarcopenia and potentially provides a useful model to study the role of chronic oxidative stress in loss of skeletal muscle (Muller et al., 2006; Vasilaki et al., 2010; Jang et al., 2010).

As mentioned in the introduction (chapter 1, Section 1.2.2), superoxide and nitric oxide (NO) are the primary radical species generated by skeletal muscle and increased during periods of contractile activity (Balon and Nadler, 1994; Close et al., 2005; Jackson, 2011; Jackson et al., 2007; Kobzik et al., 1994; Reid et al., 1992). The production of NO has been well described by the nitric oxide synthases (NOS) including the neuronal (nNOS), endothelium (eNOS) and inducible (iNOS) isoforms (Stamler and Meissner, 2001) whereas the sources of intracellular superoxide generation that occur in skeletal muscles include the mitochondrial respiratory chain (Muller et al., 2004) and, as presented in chapter 3 and by others (Mofarrahi et al., 2008; Whitehead et al., 2010; Espinosa et al., 2006; Xia et al., 2003), the nicotinamide adenine dinucleotide phosphate (NADPH) oxidase enzymes.

Superoxide and NO are the precursors for the generation of a number of secondary species and muscle and other tissues have developed sophisticated enzymatic systems that control the cellular activities of these species. Intracellular superoxide is regulated by the activities of the superoxide dismutases (SODs); SOD1 (Cu, Zn SOD, located in the cytosol and mitochondrial inter-membrane space), SOD2 (MnSOD, located in the mitochondrial matrix) and SOD3 (ecSOD, which is present in the extracellular space) (Powers and Jackson, 2008), for a detailed description of the SOD

enzymes see chapter 1, Section 1.3. When superoxide and NO are both present, their chemical reaction to form peroxynitrite is likely and competes with the dismutation of superoxide to hydrogen peroxide (H_2O_2) by SODs (Beckman and Koppenol, 1996), but there is little direct evidence for formation of peroxynitrite in skeletal muscle.

In mice lacking SOD1, the general assumption has been that the toxicity and tissue damage that contributes to the accelerated muscle ageing phenotype may be associated with excess superoxide within the sarcoplasm of the muscle cells, but it is possible that alternative species play important roles in the initiation of degeneration. Thus peroxynitrite, or a reduction in NO bioavailability due to reaction with excess superoxide might both affect tissue function. In recent studies from this group, it was demonstrated that resting muscle fibres from *FDB* muscle of SOD1KO mice show a higher rate of increase in oxidation of the non-specific intracellular ROS probe, 5- (and 6-) chloromethyl-2', 7'-dichlorodihydrofluorescin diacetate (CM-DCFH DA), compared with fibres from WT mice (Vasilaki et al., 2010), but surprisingly show no further increase in oxidation following contractile activity whereas in fibres from WT mice, the increase was evident (Vasilaki et al., 2010). DCFH is reported to be relatively insensitive to oxidation by superoxide, but to be oxidised by H_2O_2, hydroxyl radicals, peroxynitrite and NO (Murrant and Reid, 2001; Palomero et al., 2008).

Monitoring of the amounts of specific ROS in cells is inherently difficult due to the labile and reactive nature of these species. Techniques for examination of intracellular NO in single muscle fibres have been published (Pye et al., 2007) but no reliable technique for monitoring of peroxynitrite formation in muscle cells is available and evidence for peroxynitrite formation is usually implied from the presence of 3-

nitrotyrosine (3-NT) groups in proteins and from changes in superoxide and/or NO (Beckman and Koppenol, 1996; Close et al., 2005; Pattwell et al., 2004; Vasilaki et al., 2006b). A validated technique for assessment of real-time cytosolic superoxide changes in skeletal muscle fibres both at rest and following contractions was developed as part of the current work (Chapter 3) and is based on monitoring changes in dihydroethidium (DHE) oxidation.

5.2 AIMS

The current study was therefore designed to: (i) characterise the changes in redox status that occur in skeletal muscles from SOD1KO mice by assessing changes in the amounts of the products of oxidative damage to biomolecules, (ii) assess the potential changes in the protein expression of the regulatory enzymes for the primary radical species (SODs and NOS), (iii) determine whether a lack of SOD1 in muscle was associated with an increase in superoxide, a change in NO availability or an increase in peroxynitrite formation and (iv) determine whether the experimental manipulation of intracellular NO availability (through transgenic overexpression of nNOS) would induce changes in peroxynitrite formation and modify the expression of the main regulatory enzymes (SODs and NOS). It was hypothesised that when enzymatic dismutation of superoxide in muscle was reduced due to a lack of SOD1, the muscle would have increased cytosolic superoxide, decreased intracellular NO content and increased formation of 3-NT groups on muscle proteins due to increased formation of peroxynitrite.

5.3 EXPERIMENTAL PROCEDURES

5.3.1 Mice

5.3.1.1 *Generation of SOD1KO mice*

These studies used male adult (5–11 months) mice lacking SOD1 (C57Bl⁄6 SOD1KO) and their control (C57Bl⁄6 WT) mice. SOD1KO mice used in this study were generated by Dr. Charles Epstein's laboratory at the University of California San Francisco and obtained from Dr Harlan Richardson (University of Texas Health Science Center, San Antonio, Texas, USA). Details of the generation and characterization of the knockout mouse model have been reported previously (Elchuri et al., 2005; Muller et al., 2006; Huang et al., 1997). Using homologous recombination in embryonic stem cells the entire coding sequence of the mouse SOD1 gene was removed. The mutant embryonic cells were in turn used to create the homozygous SOD1KO mice. To confirm the targeted disruption of the SOD1 gene, muscles and tissues were dissected and assayed for SOD1 protein (Figure 5.1). Mice were supplied by Dr Holly Van Remmen (University of Texas Health Science Center, San Antonio, Texas, USA).

5.3.1.2 *Generation of nNOS transgenic mice*

These studies used male adult (5–11 months) muscle specific transgenic mice overexpressing nNOS (C57Bl⁄6 nNOSTg) and their control (C57Bl⁄6 WT) mice. Details of the generation and characterization of the transgenic mouse model have been reported previously (Nguyen and Tidball, 2003). Rat brain nNOS in pCMV5 was cloned downstream of the 2.2-kb human skeletal actin promoter and the vp1 intron. The NOS cDNA was followed by the SV-40 large T poly-A site. The Clal-Dral–digested DNA was injected to the pronucleus of F2 hybrid zygotes of C57 Bl6 C3H parents. To

confirm the overexpression of nNOS in skeletal muscle, muscles were dissected and assayed for nNOS protein (see results Section, Figure 5.28). Mice were supplied by Dr Holly Van Remmen (University of Texas Health Science Center, San Antonio, Texas, USA).

All experiments were performed in accordance with the UK Home Office guidelines and under the UK Animals (Scientific Procedures) Act 1986. Mice were killed by cervical dislocation and the *flexor digitorum brevis* (*FDB*) muscles were rapidly removed for isolation of single muscle fibres, other muscles and tissues were harvested and stored at -70^{o}C until analysis.

5.3.2 Chemicals and Reagents

Unless stated otherwise, all chemicals used in this study were obtained from Sigma Chemical Company, Dorset, UK.

5.3.3 Haematoxylin and eosin (H&E) staining

For details see Section 2.12. Briefly, transverse sections from *AT* and *GTN* muscles were taken onto glass cover slips using a cryostat (Bright Instrument Co., Huntingdon, UK) and were placed in Harris' Haematoxylin reagent for 3-5 min. Sections were rinsed in distilled H_2O and counterstained in eosin for 30 sec. Sections were then dehydrated in 3x Absolute alcohol and cleaned in xylene. Cover slips were mounted onto microscope slides using DPX mountant and sections were analysed with the use of an inverted miscroscope (Zeiss Axiovert 200M microscope).

5.3.4 Isolation of single mature skeletal muscle fibres

Single muscle fibres were isolated from the *FDB* muscles of mice as previously described in Section 2.2. Briefly, *FDB* muscles were dissected and incubated for 1.5 h in collagenase to digest the connective tissue. Muscles were agitated every 30 min during the digestion period and single myofibres were released by gentle trituration with a wide-bore pipette. Fibres were washed three times in MEM containing 10% FBS and were plated onto precooled culture dishes precoated with Matrigel (BD Biosciences) and were allowed to attach for 45 min before adding 1 mL MEM containing 10% FBS. Analyses were only performed on fibres that displayed good morphology and prominent cross-striations.

5.3.5 Use of dihydroethidium (DHE) and 4-Amino-5-Methylamino-2', 7'-Difluorofluorescein Diacetate (DAF-FM DA) to monitor superoxide and NO changes in isolated fibres

A detailed description of the ROS sensitive dyes used in this study is presented in Section 2.3. Briefly, single isolated mature fibres were loaded by incubation in 2mL Dulbecco's phosphate-buffered saline (D-PBS) containing 5μM dihydroethidium (DHE) or 10μM 4-amino-5-methylamino-2′,7′-difluorofluorescein diacetate (DAF-FM DA) for 30 min at 37^{o}C. Cells were then washed twice with D-PBS and the fibres were maintained in MEM without Phenol Red during the experimental protocol.

5.3.6 Microscopy and fluorescent imaging

For details see Section 2.4. Briefly, the image capture system consisted of a Zeiss Axiovert 200M microscope equipped with 500/20 nm excitation, 535/30 nm emission filter set for DAF-FM fluorescence and a 510–560 nm excitation/590 nm

emission filter set for the detection of ethidium (E^+) fluorescence. Using a X20 objective, fluorescence images were captured with a computer-controlled Zeiss MRm charged-coupled device (CCD) camera (Carl Zeiss GmbH) and analysed with Axiovision 4.0 image capture and analysis software (Carl Zeiss Vision GmbH).

5.3.7 Contractile activity induced be electrical stimulation

Contractions in single isolated muscle fibres were induced by electrical field stimulation using established techniques (Palomero et al., 2008; Pye et al., 2007). For details see Section 2.5. Briefly, fibres were electrically stimulated with trains of bipolar square wave pulses of 2ms in duration for 0.5 of a sec every 5 sec at 50 Hz and 30 V/well. A schematic illustration of the standard contractile activity protocol is shown in Figure 2.1.

5.3.8 Western blotting of muscle proteins

For details see Section 2.8. Briefly, 30-100μg of total protein was applied to a 8-15% polyacrylamide gel with a 4% stacking gel. Proteins were separated by electrophoresis and were transferred to a nitrocellulose membrane by a Multiphore continuous blotting system (Pharmacia, Uppsala, Sweden). Membranes were blocked for 2h in a 3% milk solution at room temperature and probed overnight using antibodies shown in Table 5.1. Glyceraldehyde 3-phosphate dehydrogenase (GAPDH) protein content was also determined and served the control-loading sample. Horseradish peroxidase conjugated anti-mouse IgG, or anti-rabbit IgG (Cell Signaling, Hitchin, UK), were used as the secondary antibody. Peroxidase activity was detected using an ECL kit (Amersham International Cardiff, UK), and band intensities were analysed using Quantity One Software (Biorad, US). The specificity of the bands were identified in

comparison with a sample that had not been exposed to the primary antibody and the molecular weight was determined by using rainbow coloured protein markers (Amersham International).

Antibody	Company	Catalogue No	Species	Dilution
GAPDH	Abcam	Ab8245	Mouse	1:5000
SOD1	Enzo Life Sciences	ADI-SOD-100-F	Rabbit	1:1000
SOD2	Enzo Life Sciences	ADI-SOD-111-F	Rabbit	1:1000
SOD3	Enzo Life Sciences	SOD-105	Rabbit	1:500
nNOS	Abcam	Ab76067	Rabbit	1:500
eNOS	Abcam	Ab76198	Mouse	1:500
iNOS	Abcam	Ab49999	Mouse	1:500
PRX1	Abcam	Ab15571	Rabbit	1:1000
PRX2	Abcam	Ab59539	Rabbit	1:1000
PRX3	Abcam	Ab16751	Mouse	1:1000
PRX4	Abcam	Ab16943	Mouse	1:1000
PRX5	Abcam	Ab16944	Mouse	1:1000
PRX6	Abcam	Ab59543	Rabbit	1:1000
4-HNE	Abcam	Ab46545	Rabbit	1:1000
MDA	Cell Biolabs	STA-331	Rabbit	1:1000
3-NT	Cayman	189542	Rabbit	1:1000
Prot. Carbonyls	Cell Biolabs	STA-308	Rabbit	1:1000
GPX1	Abcam	Ab22604	Rabbit	1:500
Catalase	Sigma	C 0979	Mouse	1:1000

Table 5.1 Antibodies used for western blotting.

5.3.9 Analyses of the 3-nitrotyrosine (3-NT) content of muscle carbonic anhydrase III (CAIII).

Changes in the 3-nitrotyrosine (3-NT) content of the major muscle protein, carbonic anhydrase III (CAIII) were assessed as described in Section 2.11. Briefly, 50μg of total protein was separated on 1D SDS-PAGE followed by western blotting as described in Section 2.8. The content of 3-NT was analyzed by using a mouse monoclonal antibody (Cayman Chemical Co., Ann Arbor, Michigan, USA), and the bands were visualized using a Biorad Chemi-Doc System (Biorad Laboratories Ltd, Hemel Hempstead, UK). Densitometric quantification of the CAIII band was undertaken, and the protein content was normalized to the GAPDH content of the same sample. Comparisons were made between samples on the same gel/western blot.

5.3.10 Determination of protein oxidation and lipid peroxidation.

Changes in protein oxidation and lipid peroxidation were assessed as described in Section 2.8. Following the electroblotting step, proteins were derivatized and membranes were blocked and probed for 2h using an Anti-DNP antibody (Cell Biolabs, San Diego, CA, USA). Secondary HRP conjugated antibody was applied as described in Section 2.8.

Lipid peroxidation was assessed via changes in 4-hydroxynonenal (4-HNE) protein conjugates and malondialdehyde (MDA) - protein adducts. Both markers were assessed using the same protocol as for 3-NT (Section 5.3.9). Rabbit Anti-MDA primary antibodies (Cell Biolabs, San Diego, CA, USA) and rabbit anti 4-HNE (Abcam, Cambridge, UK) were used.

5.4 RESULTS

AIM I:IDENTIFYING THE INTRACELLULAR CHANGES IN RONS AND ADAPTIVE RESPONSES IN SKELETAL MUSCLE FROM HOMOZYGOTIC SOD1 KNOCKOUT (SOD1KO) MICE.

5.4.1 SOD1 in muscles/tissues from SOD1KO mice

To confirm the lack of SOD1 in the SOD1KO mice, mice were culled by cervical dislocation and a variety of tissues including: anterior tibialis (AT), gastrocnemius (GTN), soleus (SOL) and extensor digitorum longus (EDL), kidneys, heart, liver, spleen, lungs, brain and also nerves were dissected and their protein content of SOD1 was examined. A representative western blot of the SOD1 protein content is shown in Figure 5.1. SOD1 was not detectable in any of the tissues from the SOD1KO mice (Figure 5.1)

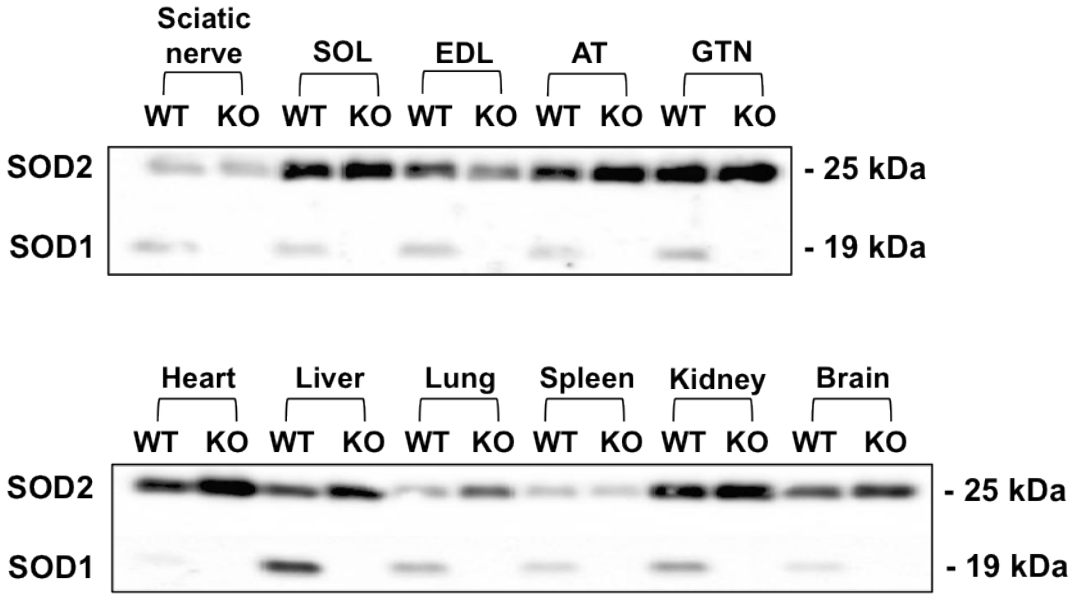

Figure 5.1 Representative western blots of superoxide dismutase 1 and 2 (SOD1 and SOD2) proteins from gastrocnemius *(GTN),* anterior tibialis (*AT),* extensor digitorum longus (*EDL),* soleus (*SOL), sciatic nerve, brain, kidney, spleen, lung, liver* and *heart* of WT and SOD1KO mice.

5.4.2 Comparison of muscle/tissue weights in WT and SOD1KO mice

Previous studies have shown that SOD1KO mice show an age dependent loss in muscle mass (Muller et al., 2006; Jang et al., 2010) and Figure 5.2 shows the gross morphology of skinned hindlimb muscles of a 20-month-old SOD1KO and WT mouse. In the present study, to further assess whether the loss in muscle mass in the SOD1KO mice was specific to skeletal muscle, the absolute mass of other tissues/organs was studied (Table 5.2). The age-related decrease in mass was observed in specific skeletal muscle tissues (*AT* and *GTN* muscles), as the mass of the *EDL*, *SOL*, heart, liver, kidney, spleen, lung, and brain was similar to tissues of the age-matched WT littermates (Table 5.2).

Figure 5.2 Gross morphology of skinned hindlimb muscles of 20-month-old SOD1KO and WT mice. (Image from Jang *et al.* 2010)

Tissue (gr)	WT mice (n=8)	SOD1KO mice (n=8)	P value
Body weight	32.03 ± 1.17	30.73 ± 1.40	0.493
AT	0.110 ± 0.02	0.042 ± 0.00	**0.013**
EDL	0.013 ± 0.00	0.012 ± 0.00	0.243
GTN	0.230 ± 0.02	0.121 ± 0.01	**0.000**
SOL	0.011 ± 0.00	0.011 ± 0.00	0.756
Heart	0.178 ± 0.01	0.191 ± 0.03	0.705
Liver	1.769 ± 0.09	1.850 ± 0.24	0.766
Kidneys	0.238 ± 0.03	0.276 ± 0.04	0.444
Spleen	0.119 ± 0.02	0.173 ± 0.03	0.166
Lungs	0.180 ± 0.03	0.215 ± 0.04	0.441
Brain	0.440 ± 0.03	0.445 ± 0.04	0.920

Table 5.2 Comparison of tissue weights from WT and SOD1KO mice (10±1 months of age). Values are presented as the mean ± SEM. Bold values represent statistically significant differences among groups, $P < 0.05$.

5.4.3 Changes in muscle structure in muscles from SOD1KO mice

To assess whether the accelerated muscle ageing phenotypic changes observed in the *AT* and *GTN* muscles of the SOD1KO mice was associated with changes in muscle structure, transverse sections of the *GTN* muscles from WT and SOD1KO mice were stained with Haematoxylin and Eosin (Figure 5.3). Muscles from the SOD1KO mice showed minor changes in structure, such as greater variability in fibre size and the presence of occasional central nuclei compared with muscles from WT mice, implying that the loss of mass observed in the muscles of the SOD1KO mouse model is likely primarily due to a complete loss of muscle fibres.

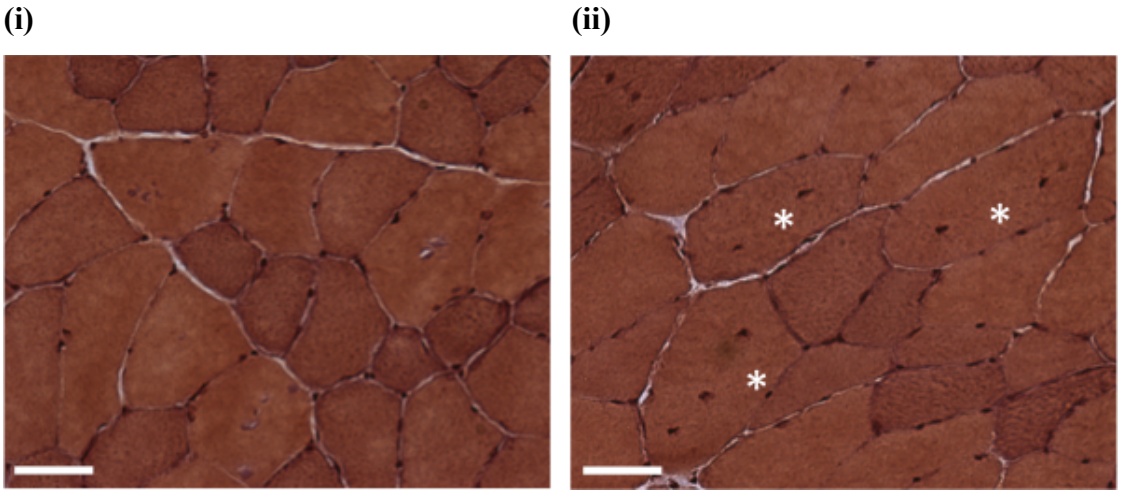

Figure 5.3 Example Haematoxylin and Eosin stained 8-micron transverse sections of the *GTN* muscle from WT (i) and SOD1KO (ii) mice. Asterisks (*) represent fibres with centrally located nuclei, (bar = 200 μm).

5.4.4 Changes in oxidative damage in muscles from SOD1KO mice

5.4.4.1 *Changes in protein oxidation*

Several assays were carried out to determine changes in muscle redox status by assessing the level of oxidative damage in muscles of SOD1KO mice. The overall level of oxidative modification of proteins in *GTN* muscles of SOD1KO mice was assessed with Western blot analyses and the protein carbonyl immunoblot kit (Figure 5.4). A consistent increase in protein oxidation was detected in *GTN* homogenates from the knockout group, suggesting that protein oxidation is a prominent feature in SOD1KO mice (Figure 5.4).

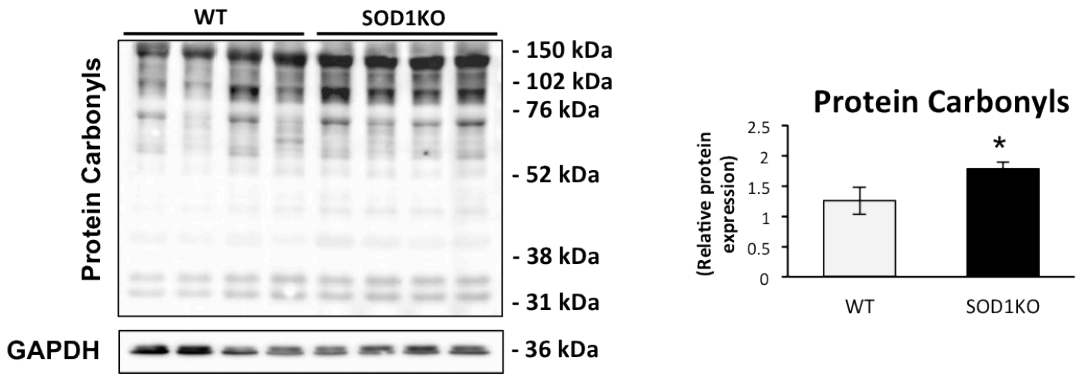

Figure 5.4 Oxidative modification of proteins. Oxyblot analysis of the protein carbonyl level in *GTN* muscles from WT and SOD1KO mice, along with densitometric quantification of the blot, *P < 0.05 compared to values for muscles from WT mice.

5.4.4.2 *Changes in lipid peroxidation*

To determine the extent of lipid peroxidation, 4-hydroxynonenal (4-HNE) protein conjugates and malondialdehyde (MDA) protein adducts were measured in *GTN* muscles from SOD1KO and age-matched controls (Figures 5.5 and 5.6). Both compounds increased in skeletal muscles from the knockout group suggesting that the lack of SOD1 leads to an increase in oxidative modifications of lipids (Figures 5.5 and 5.6).

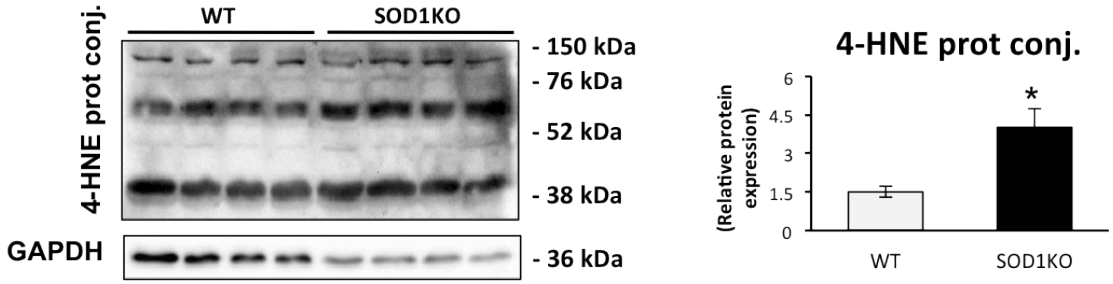

Figure 5.5 Oxidative modification of lipids. Representative Western blots of 4-hydroxynonenal (4-HNE) protein conjugates in *GTN* muscles from WT and SOD1KO mice and densitometric quantification of the blots for 4-HNE, *P < 0.05 compared to values for muscles from WT mice.

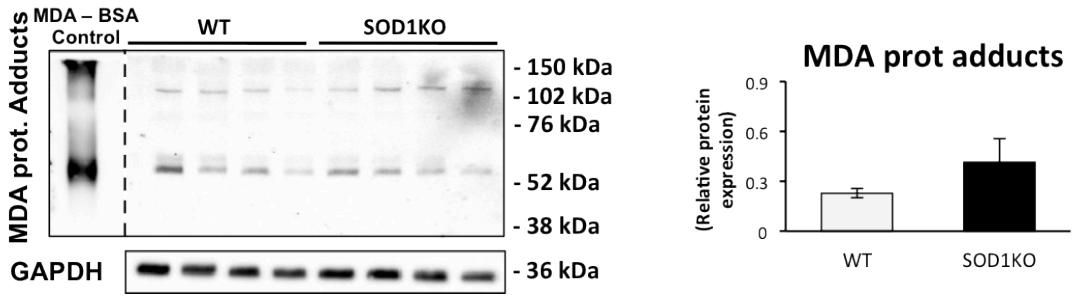

Figure 5.6 Oxidative modification of lipids. Representative Western blots of Malondialdehyde (MDA) protein adducts in *GTN* muscles from WT and SOD1KO mice and densitometric quantification of the blots for MDA protein adducts.

5.4.4.3 *Changes in DNA damage*

To determine if there was an increase in DNA damage, the protein expression of the oxidative DNA repair enzyme; 8-Oxoguanine glycosylase (OGG1) was studied. Reports have shown that OGG1 is a base excision repair protein which activity increases following exposure to oxidative stress (Mirbahai et al., 2010). Lack of SOD1 in *GTN* muscles from SOD1KO mice significantly increased the expression of OGG1 indicating a potential increase in DNA damage (Figure 5.7).

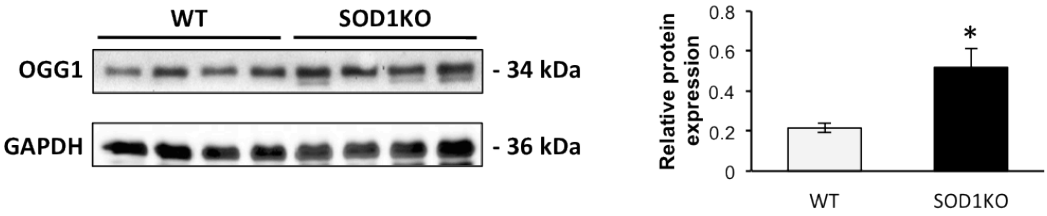

Figure 5.7 Representative western blots of 8-Oxoguanine glycosylase (OGG1) protein in *GTN* muscles of WT and SOD1KO mice and densitometric quantification of the blots for OGG1, *P < 0.05 compared with values for muscles from WT mice.

5.4.5 Changes in superoxide in single isolated muscle fibres from SOD1KO mice

To identify the reactive species that are responsible for the increased oxidative damage in muscles from the SOD1KO mice, fluorescent microscopic techniques were applied. To examine ROS changes in muscle fibres in the absence of non-myogenic cells, single fibres from the flexor digitorum brevis (FDB) muscle were isolated as previously described (Section 2.2). Changes in superoxide were assessed by monitoring dihydroethidium (DHE) oxidation, a technique that was developed and optimised in chapter 3.

Images of a single isolated fibre from an adult WT mouse loaded with DHE and 4',6-diamidino-2-phenylindole dihydrochloride (DAPI) to visualize nuclei are shown in Figure 5.8. As shown in chapter 3 (Figure 3.1), the predominant ethidium (E^+) fluorescence from the DHE-loaded fibre was from nuclei indicated by the co-localization of DAPI with E^+ fluorescence (Figure 5.8) and measurements from nuclei were therefore used for all further studies, because fluorescence values were much higher from this site, and hence, the sensitivity of the method might be optimized.

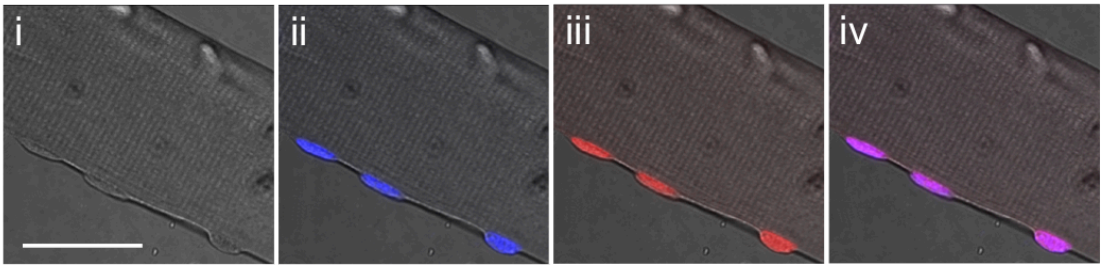

Figure 5.8 Images of a single isolated fibre from the *FDB* muscle after 24 hours in culture photographed under bright field (i), fluorescent image following loading with DAPI (ii), fluorescent image showing ethidium (E^+) fluorescence following loading with DHE (iii) and a merged image of ii and iii (iv), (bar = 30 μm).

Single muscle fibres from the *FDB* muscle from WT and SOD1KO mice were loaded with DHE and changes in E^+ fluorescence were monitored in resting fibres (Figure 5.9) and fibres subjected to a period of contractions (Figure 5.10). Surprisingly, data showed that E^+ fluorescence from fibres of the two groups did not differ at rest although the mean values from fibres of the SOD1KO mice tended to be higher, indicating that the content of superoxide did not vary significantly between fibres of the two groups (Figure 5.9). The effect of 10 min period of contractions on DHE oxidation from *FDB* fibres of WT and SOD1KO mice is shown in Figure 5.10. Following contractile activity, a significant increase in fluorescence was seen from muscle fibres of both the WT and SOD1KO mice (Figure 5.10). However, the overall increase following contractions was much smaller and significantly less in fibres from the knockout group than that seen from fibres of WT mice indicating a lower rate of increase in superoxide with contractions (Figure 5.10).

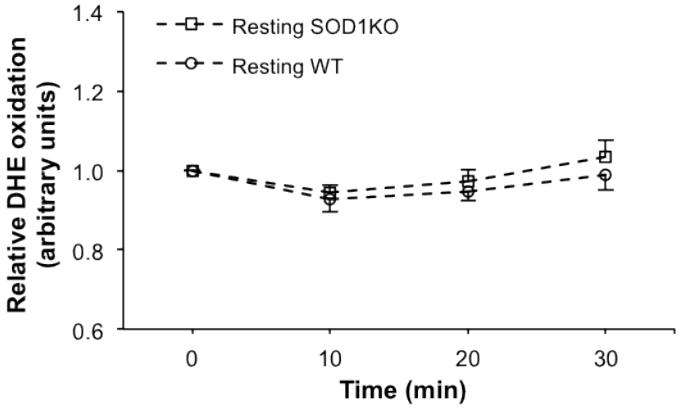

Figure 5.9 Relative change in DHE oxidation from resting DHE-loaded *FDB* fibres of WT and SOD1KO over 30 minutes at rest, (n = 9–10 fibres in each group).

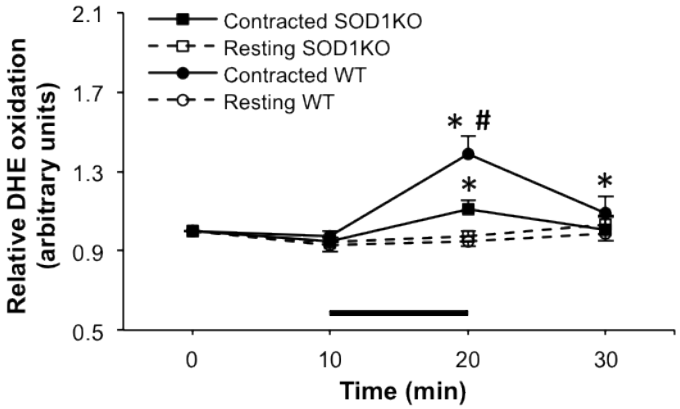

Figure 5.10 Relative change in DHE oxidation from DHE-loaded *FDB* fibres of WT and SOD1KO mice at rest and following 10 minutes of contractions between 10 and 20 minutes of the experimental period. *P<0.05 compared with values for fibres from the same group at the previous time point; #P<0.05 compared with contacted fibres from SOD1KO mice at the same time point, (n = 10–11 fibres in each group).

5.4.6 Changes in NO in single isolated muscle fibres from SOD1KO mice

To monitor changes in NO, single muscle fibres from WT and SOD1KO mice were loaded with 4-amino-5-methylamino-2′,7′-difluorofluorescein diacetate (DAF-FM DA), a method developed and described in detail by Pye *et al*. (Pye et al., 2007). Images of DAF-FM fluorescence from a resting fibre from an adult WT mouse appeared to be homogeneous across the cell, indicating a lack of any sub-cellular localisation of this fluorescent probe (Figure 5.11 ii & iii).

The DAF-FM fluorescence from quiescent fibres of WT and SOD1KO mice is shown in Figure 5.12. Fibres from WT mice showed a significant increase in DAF-FM fluorescence over time at rest, but this rate of increase was significantly lower in fibres from SOD1KO mice (Figure 5.12). Following contractions, a small increase in DAF-

FM fluorescence was observed in both groups (Figure 5.13). However, the increase did not reach statistical significance for either group (Figure 5.13).

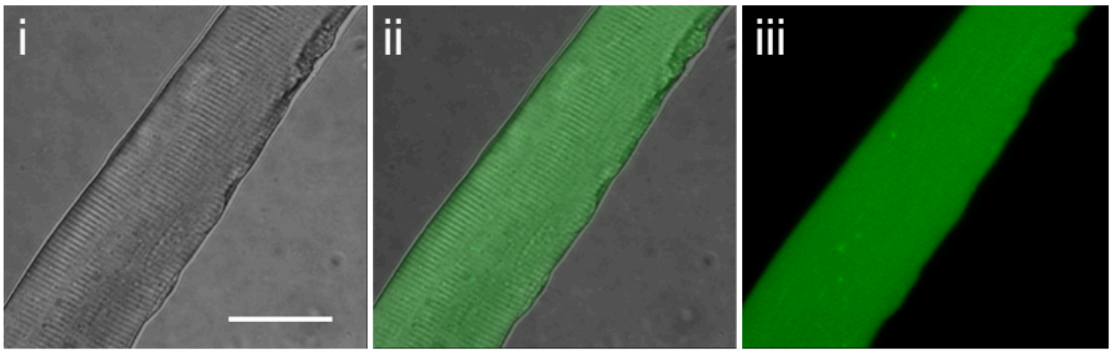

Figure 5.11 Image of a single isolated fibre from the *FDB* muscle after 24 h in culture under bright field (i), fluorescent image following loading with 4-amino-5-methylamino-2',7'-difluorofluorescein diacetate (DAF-FM DA) (ii) and merge image of i and ii (iii), (bar = 30 μm).

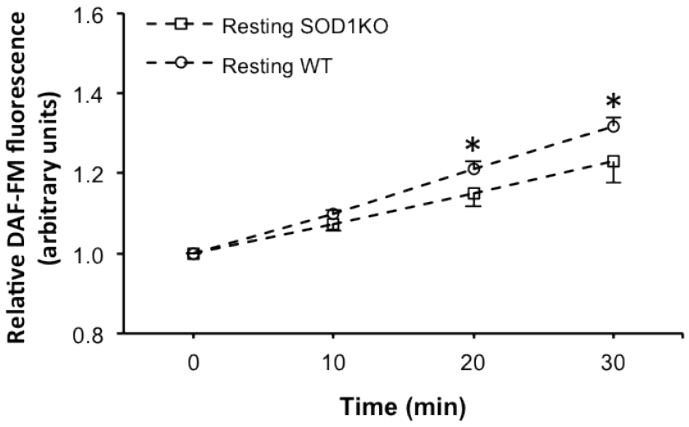

Figure 5.12 Relative change in DAF-FM fluorescence from DAF-FM DA loaded *FDB* fibres of WT and SOD1KO mice over 30 min at rest. *P < 0.05 compared with values for fibres from SOD1KO mice at the same time point, (n = 8–9 fibres in each group).

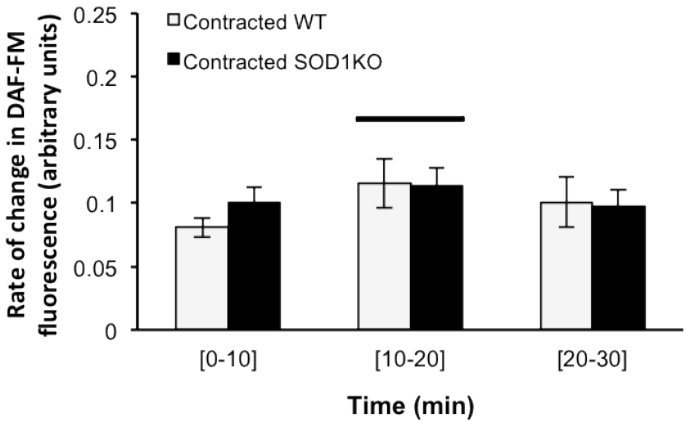

Figure 5.13 Rate of change in DAF-FM fluorescence from *FDB* muscle fibres of WT and SOD1KO mice over 30 min with 10 min of electrically stimulated contractions between 10 and 20 min of the experimental period, (n = 7–8 fibres in each group).

5.4.7 Changes in peroxynitrite in single isolated muscle fibres from SOD1KO mice

Specific fluorescent dyes for the detection of peroxynitrite are not available, thus changes in peroxynitrite were assessed via changes in nitration (3-NT) of the major muscle protein, carbonic anhydrase III (CAIII). Previous studies have shown that 3-NT of CAIII, is a relatively sensitive marker of muscle oxidative stress (Vasilaki et al., 2007), and details on the analysis of 3-NT are described in "Experimental methods" (chapter 2, Section 2.11.1). An example western blot of the 3-NT content of CAIII, in muscles from the WT and SOD1KO mice is shown in Figure 5.14. Quantification of the 3-NT blots showed a significant increase in the 3-NT content of CAIII in comparison with muscles from WT mice.

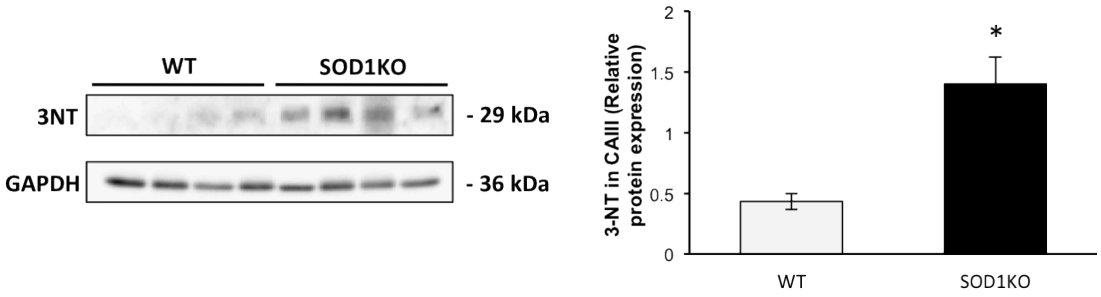

Figure 5.14 Representative western blots of the 3-nitrotyrosine (3-NT) content of carbonic anhydrase III (CAIII) in *GTN* muscles of WT and SOD1KO mice and densitometric quantification of the blots, *P < 0.05 compared with values for muscles from WT mice.

In light of the increase in 3-NT content of muscle CAIII observed in SOD1KO mice, western blots were also probed for peroxiredoxin V (PRXV) as this protein is a peroxynitrite reductase and known to be increased in conditions where peroxynitrite is increased (Dubuisson et al., 2004; Trujillo et al., 2008). A typical western blot together with quantification of the PRXV bands is shown in Figure 5.15. These indicate a significant increase in the PRXV content of muscles from SOD1KO mice compared with WT mice implying that a lack of SOD1 induces an increase in peroxynitrite formation.

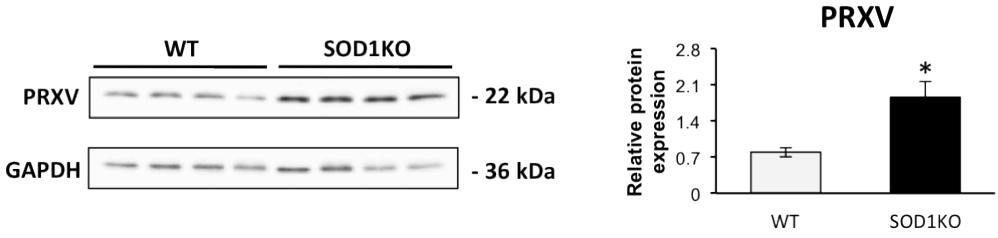

Figure 5.15 Representative western blots of peroxiredoxin V (PRX V) protein in *GTN* muscles of WT and SOD1KO mice and densitometric quantification of the blots,s *P < 0.05 compared with values for muscles from WT mice.

5.4.8 Changes in RONS regulatory enzymes in muscles from SOD1KO mice

5.4.8.1 *Changes in SOD protein expression*

The effect of a lack of SOD1 on the expression of the main regulatory enzymes for superoxide was also studied. All of the three superoxide dismutase (SOD) isoforms (SOD1, SOD2, and SOD3) were detected in skeletal muscles from WT mice. Figures 5.16 and 5.17 show representative western blots from the muscles of WT and SOD1KO mice together with quantification of these blots by densitometry. As anticipated, SOD1 was absent from the muscles of SOD1KO mice, but there was a small but significant increase in the content of SOD2 (Figure 5.16). The contents of extracellular SOD (SOD3) were unchanged in muscles of SOD1KO mice compared with WT mice (Figure 5.17).

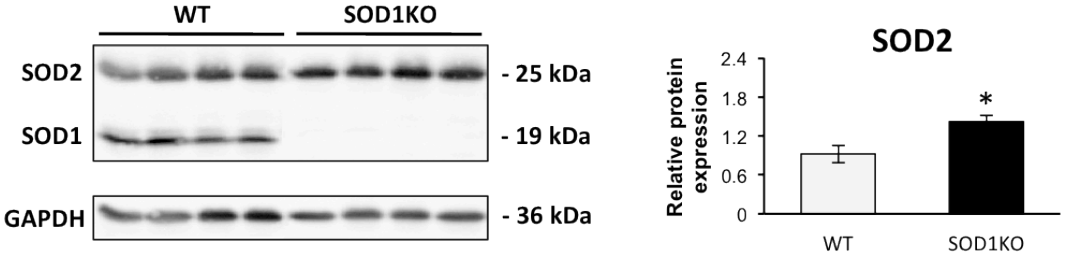

Figure 5.16 Representative western blots of SOD1 and SOD2 proteins in *GTN* muscles of WT and SOD1KO mice and densitometric quantification of the blots for SOD2, *P < 0.05 compared to values for muscles from WT mice.

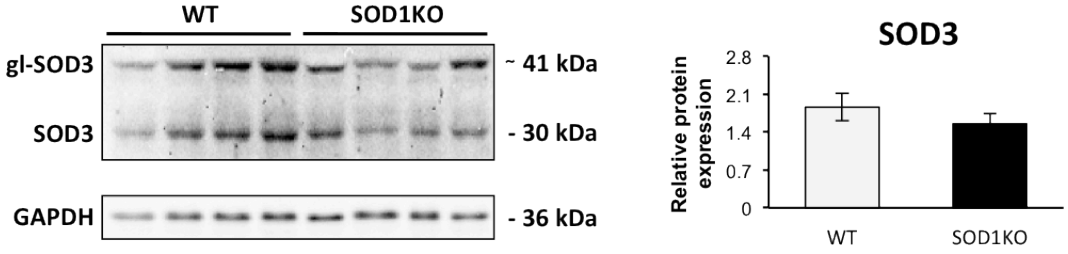

Figure 5.17 Representative western blots of superoxide dismutase 3 (SOD3) protein in *GTN* muscles of WT and SOD1KO mice and densitometric quantification of the SOD3 band (see text for explanation of the presence of two bands).

5.4.8.2 *Changes in NOS protein expression*

The possibility that the lack of SOD1 might have induced adaptations in the content of NOS enzymes and thus influence NO availability was examined by western blot analysis. All of the three NOS isoforms (nNOS, eNOS, and iNOS) were detected in muscles from WT and SOD1KO mice, but no significant differences in contents were seen (Figures 5.18, 5.19 and 5.20).

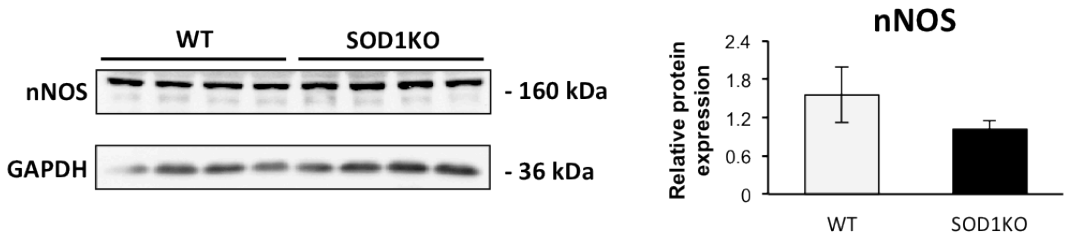

Figure 5.18 Representative western blots of neuronal nitric oxide synthase (nNOS) protein in *GTN* muscles of WT and SOD1KO mice and densitometric quantification of the blots for nNOS.

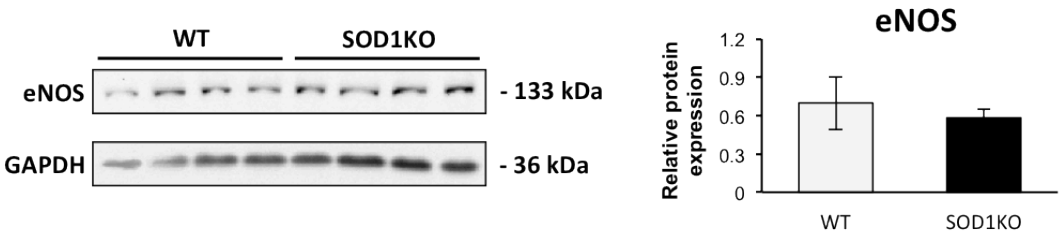

Figure 5.19 Representative western blots of endothelium nitric oxide synthase (eNOS) protein in *GTN* muscles of WT and SOD1KO mice and densitometric quantification of the blots for eNOS.

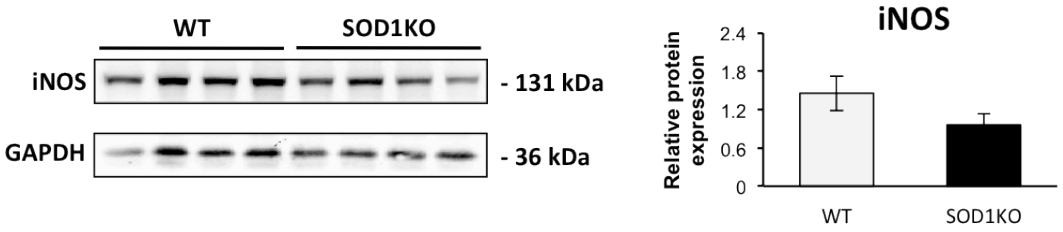

Figure 5.20 Representative western blots of the inducible nitric oxide synthase (iNOS) protein in *GTN* muscles of WT and SOD1KO mice and densitometric quantification of the blots for iNOS.

5.4.8.3 *Changes in PRX protein expression*

PRXV was unregulated in muscles from SOD1KO mice (Figure 5.15). The possibility that the lack of SOD1 might have led to adaptive changes in the contents of the other PRX enzymes was further examined. All of the six PRX isoforms including PRXI, PRXII, PRXIII, PRXIV, PRXV (see Figure 5.15) and PRXVI were detected in muscles from WT and SOD1KO mice. Figures 5.21, 5.22, 5.23, 5.24, and 5.25 show representative western blots of PRX isoforms from the muscles of WT and SOD1KO

mice together with quantification of these blots by densitometry. Muscles from SOD1KO mice showed an upregulation in the protein expression of all PRX protective enzymes apart from PRXI, a cytosolic isoform of the PRX family (Jarvis et al., 2012).

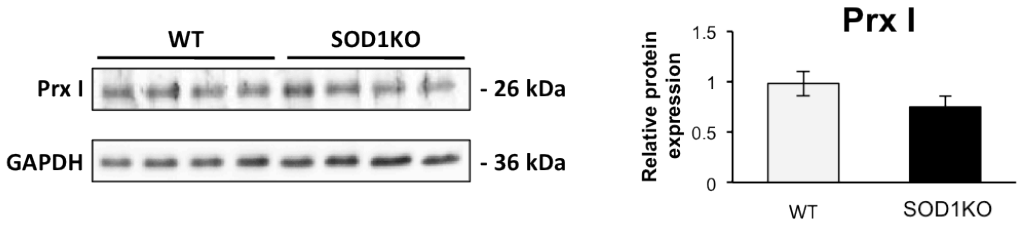

Figure 5.21 Representative western blots of peroxiredoxin I (PRX I) protein in *GTN* muscles of WT and SOD1KO mice and densitometric quantification of the blots for PRX I.

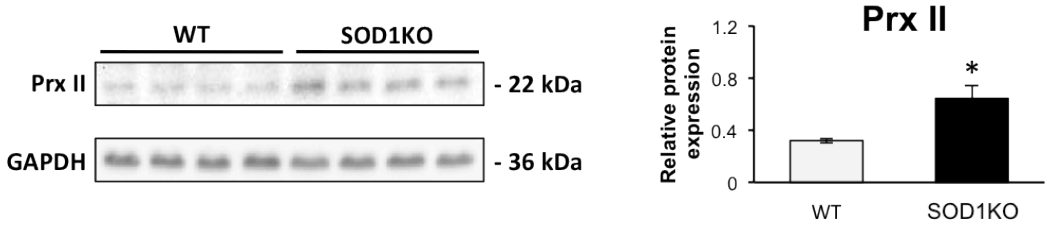

Figure 5.22 Representative western blots of peroxiredoxin II (PRX II) protein in *GTN* muscles of WT and SOD1KO mice and densitometric quantification of the blots for PRX II, *P < 0.05 compared to values for muscles from WT mice.

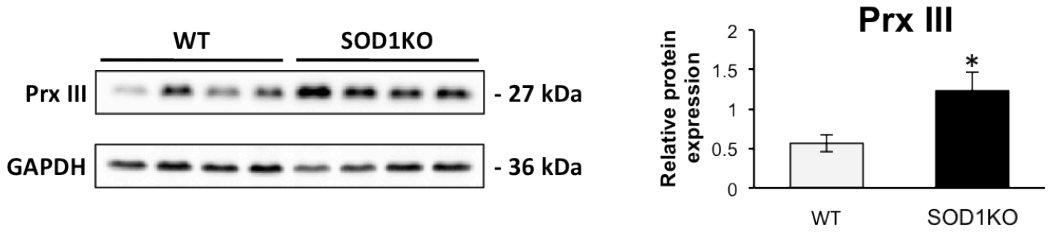

Figure 5.23 Representative western blots of peroxiredoxin III (PRX III) protein in *GTN* muscles of WT and SOD1KO mice and densitometric quantification of the blots for PRX III, *P < 0.05 compared to values for muscles from WT mice.

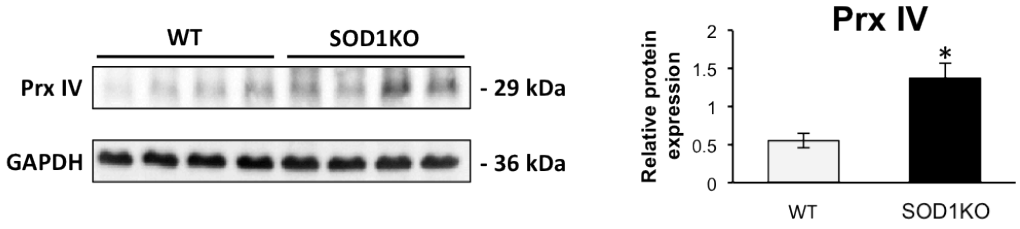

Figure 5.24 Representative western blots of peroxiredoxin IV (PRX IV) protein in *GTN* muscles of WT and SOD1KO mice and densitometric quantification of the blots for PRX IV, *P < 0.05 compared to values for muscles from WT mice.

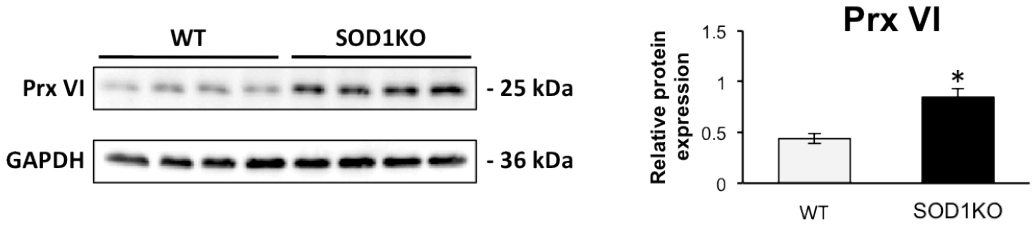

Figure 5.25 Representative western blots of peroxiredoxin VI (PRX VI) protein in *GTN* muscles of WT and SOD1KO mice and densitometric quantification of the blots for PRX VI, *P < 0.05 compared to values for muscles from WT mice.

5.4.8.4 *Changes in protein expression of the main H_2O_2 reducing enzymes*

In light of the increase in PRXII, PRXIII, PRXIV & PRXVI content observed in muscles from SOD1KO mice (see Figures 5.22, 5.23, 5.24 and 5.25), western blots were also probed for catalase (CAT) and glutathione peroxidase I (GPX1) as these proteins are the main H_2O_2 reducing systems (the activity and regulation of CAT and GPX1 have been described in detail in Section 1.3). Both CAT and GPX1 protein levels were significantly upregulated in muscles from the SOD1KO mice compared to WT mice (Figures 5.26 and 5.27, respectively). The increase in protein expression of CAT and GPX1 along with the increase in PRXII, PRXIII, PRXIV & PRXVI indicate the

adaptations that occur in skeletal muscles from the SOD1KO mice due to the higher content of H_2O_2 in comparison to muscles from the WT group.

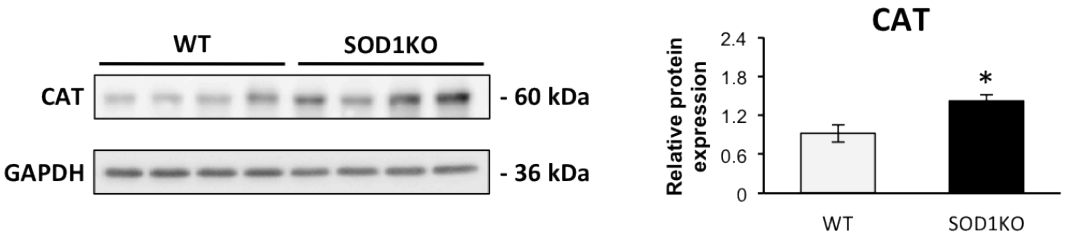

Figure 5.26 Representative western blots of catalase (CAT) protein in *GTN* muscles of WT and SOD1KO mice and densitometric quantification of the blots for CAT, *P < 0.05 compared to values for muscles from WT mice.

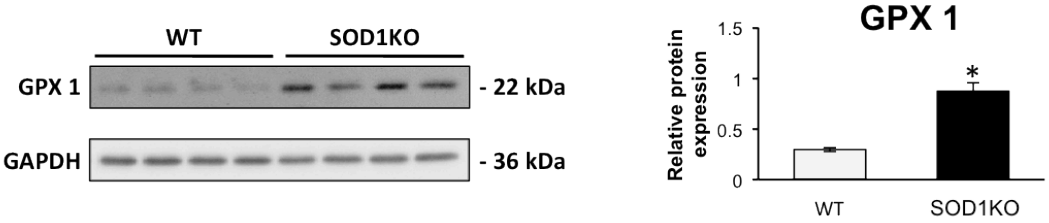

Figure 5.27 Representative western blots of glutathione peroxidase 1 (GPX 1) protein in *GTN* muscles of WT and SOD1KO mice and densitometric quantification of the blots for GPX 1, *P < 0.05 compared to values for muscles from WT mice.

AIM II:IDENTIFYING THE ADAPTIVE RESPONSES IN SKELETAL MUSCLES OF NEURONAL NITRIC OXIDE OVEREXPRESSOR MICE.

The first aim of this study was to determine the reactive species that are modulated in skeletal muscles from SOD1KO mice and data obtained from Figures 5.10, 5.12, 5.14 and 5.15 indicate that the potential increased superoxide content due to the lack of SOD1 rapidly reacted with NO to generate peroxynitrite as shown by the reduction in NO availability (Figure 5.12), the increase in CAIII nitration (Figure 5.14) and the upregulation of PRXV protein (Figure 5.15). Superoxide and NO are the main

radical species generated by skeletal muscle and the second aim of this study was to examine whether manipulation of NO (through transgenic overexpression of nNOS) would have an effect on peroxynitrite formation in muscle specific nNOS transgenic (nNOSTg) mice.

5.4.9 Expression of nNOS in muscles from nNOSTg mice

To confirm the overerexpression of nNOS in the nNOSTg mice, mice were culled by cervical dislocation, *GTN* skeletal muscles were dissected and the protein content of nNOS was examined. A representative western blot of the protein content of nNOS is shown in Figure 5.28. Muscles from the nNOSTg mice showed a > 100-fold increase in nNOS content with the western blot showing the two nNOS bands (full-length nNOS and a nNOS fragment) described by Nguyen & Tidball (Nguyen and Tidball, 2003).

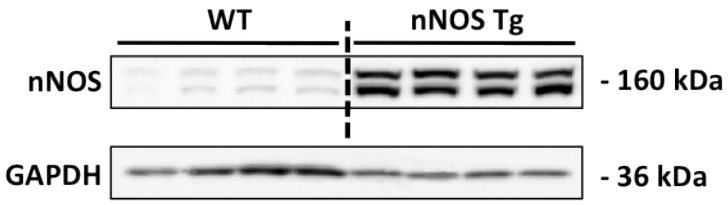

Figure 5.28 Representative western blots of nNOS protein in *GTN* muscles of WT and nNOSTg mice. nNOS content was increase >100 fold in the nNOSTg group. The immunoblot for *GTN* muscles of the nNOSTg mice was exposed for 10 seconds whereas for muscles of the WT group, the immunoblot was exposed for 10 minutes.

5.4.10 Effect of nNOS overexpression in peroxynitrite formation

Previous experiments in single muscle fibres from the *FDB* muscles of nNOSTg mice (work presented in my MPhil thesis), (Sakellariou., 2009) showed that overexpression of nNOS is associated with increased intracellular NO content (see Figure 5.29) and a reduction in superoxide (see Figure 5.30) as indicated by the increase in DAF-FM fluorescence and the reduction in DHE oxidation. The reduction in superoxide in muscles from the nNOSTg mice implied the possibility of a peroxynitrite formation.

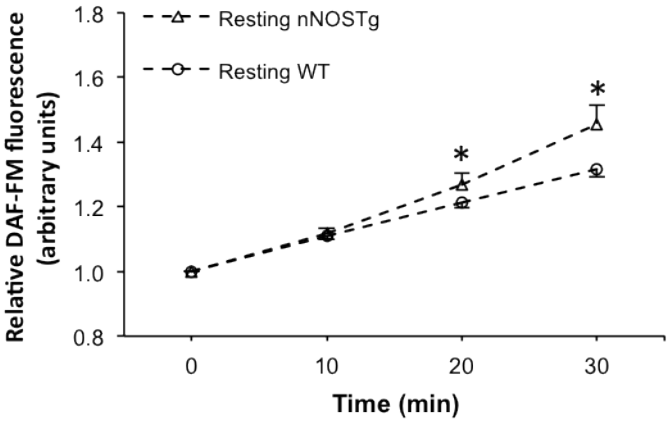

Figure 5.29 Relative change in DAF-FM fluorescence from resting fibres of WT and nNOSTg mice over 30 min. *P < 0.05 compared with fibres from WT mice at the same time point, (n = 7–8 fibres in each group).

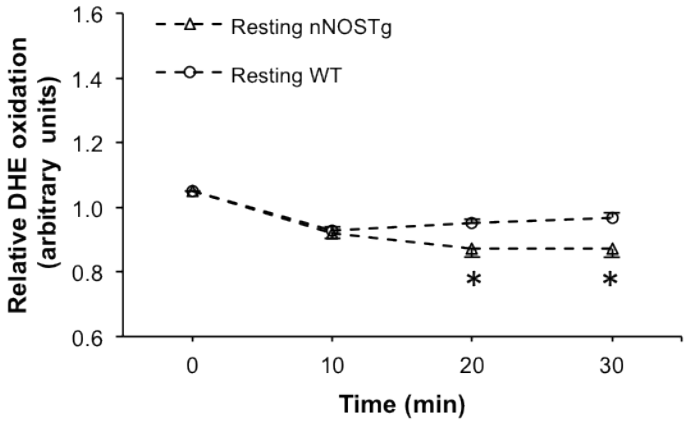

Figure 5.30 Relative change in E^+ fluorescence from DHE loaded fibres of WT and nNOSTg mice over 30 min. *P < 0.05 compared with fibres from WT mice at the corresponding time point, (n = 7–8 fibres in each group).

To assess changes in peroxynitrite formation, the 3-NT content of CAIII in the *GTN* muscles of WT and nNOSTg mice was examined. An example western blot of the 3-NT content of CAIII in muscles from the WT and nNOSTg mice is shown in Figure 5.31. Quantification of the 3-NT blots showed a significant increase in the 3-NT content of CAIII in the transgenic group in comparison with muscles from WT mice (Figure 5.31). However, no significant changes in PrxV were observed (Figure 5.32) with muscles from the nNOSTg group showing a similar PRXV expression compared to *GTN* muscles from the WT mice.

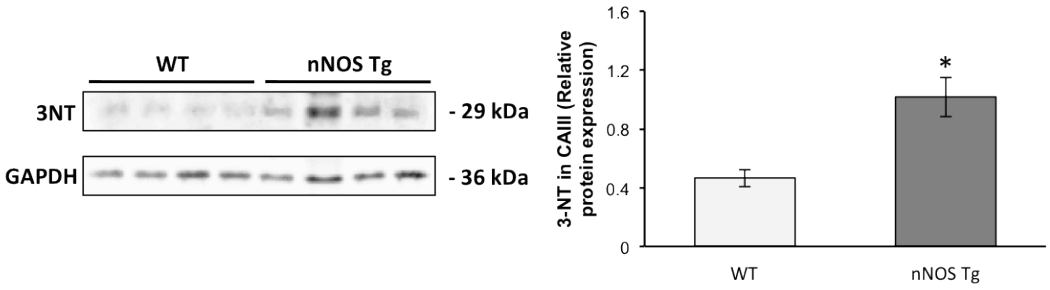

Figure 5.31 Representative western blots of the 3-NT content of CAIII in *GTN* muscles of WT and nNOSTg mice and densitometric quantification of the blots, *P < 0.05 compared with values for muscles from WT mice.

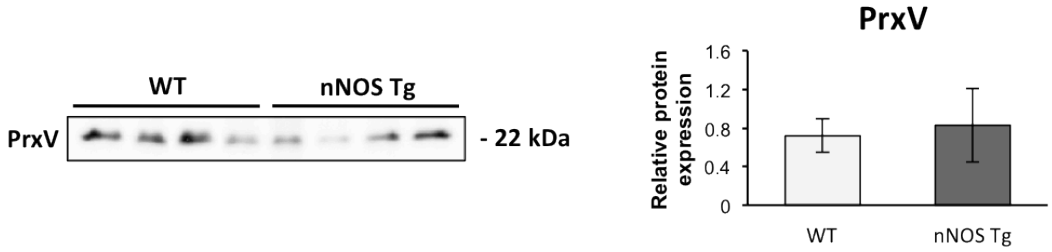

Figure 5.32 Representative western blots of PRX V protein in *GTN* muscles of WT and nNOSTg mice and densitometric quantification of the blots.

5.4.11 Changes in the protein expression of the mail regulatory enzymes for superoxide and NO in muscles from nNOSTg mice

5.4.11.1 *Changes in NOS protein expression*

The effect of nNOS overexpression on the muscle content of the other two NOS isoenzymes (eNOS & iNOS) in comparison with WT mice was also studied. Figures 5.33 and 5.34 show representative western blots of eNOS and iNOS isoforms from the muscles of WT and nNOSTg mice together with quantification of these blots by

densitometry. Muscles from the transgenic mice showed a significant increase in iNOS content compared with WT mice (Figure 5.34) but no significant changes in the content of eNOS were seen (Figure 5.33).

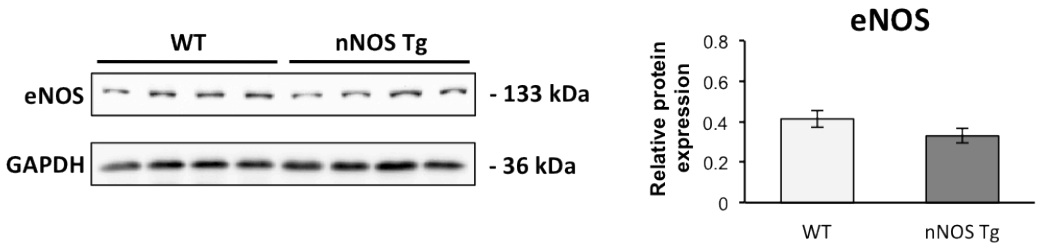

Figure 5.33 Representative western blots of eNOS protein in *GTN* muscles of WT and nNOSTg mice and densitometric quantification of the blots for eNOS.

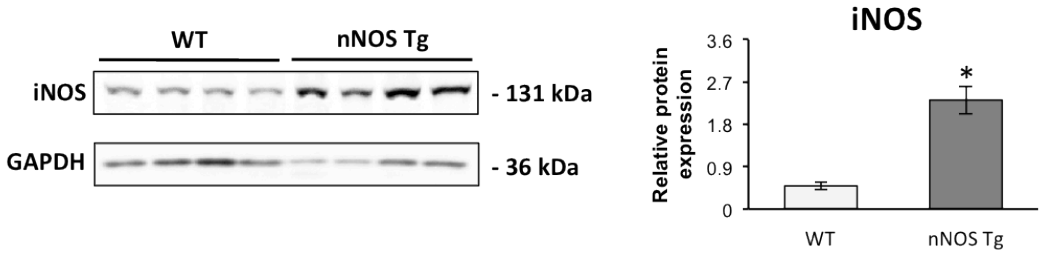

Figure 5.34 Representative western blots of iNOS protein in *GTN* muscles of WT and nNOSTg mice and densitometric quantification of the blots for iNOS, *P < 0.05 compared to values for muscles from WT mice.

5.4.11.2 *Changes in SOD protein expression*

The possibility that nNOS overexpression might have induced adaptations in the content of SOD enzymes and thus influence superoxide availability was further examined by comparing the protein expression of the three SOD enzymes (SOD1, SOD2, and SOD3) in *GTN* muscles of nNOSTg mice in comparison with muscles from

WT mice (Figures 5.35 and 5.36). Muscles of nNOSTg mice showed a significant increase in all three SOD isoforms compared with muscles from the WT mice.

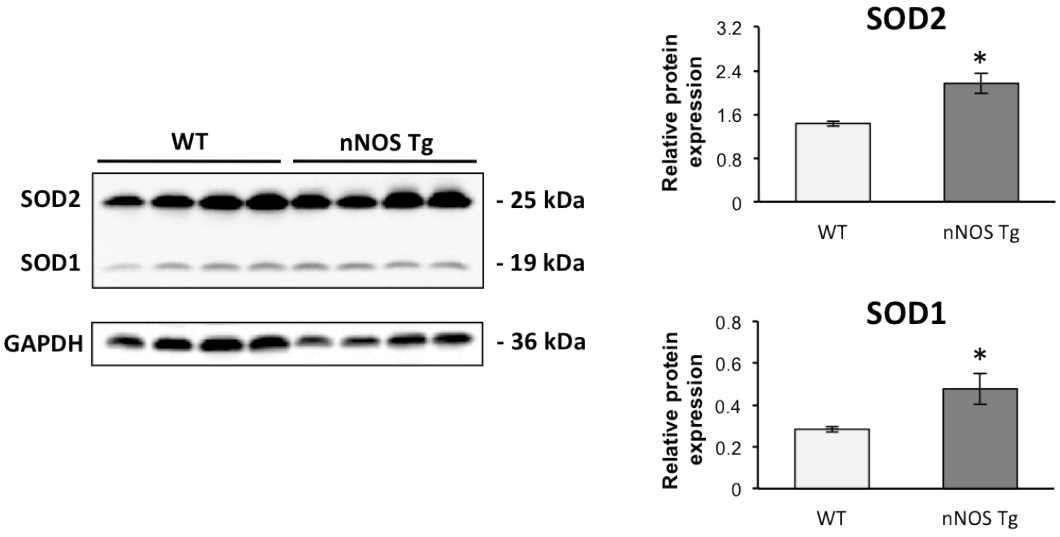

Figure 5.35 Representative western blots of SOD1 and SOD2 proteins in *GTN* muscles of WT and nNOSTg mice and densitometric quantification of the blots for SOD1 and SOD2, *P < 0.05 compared to values for muscles from WT mice.

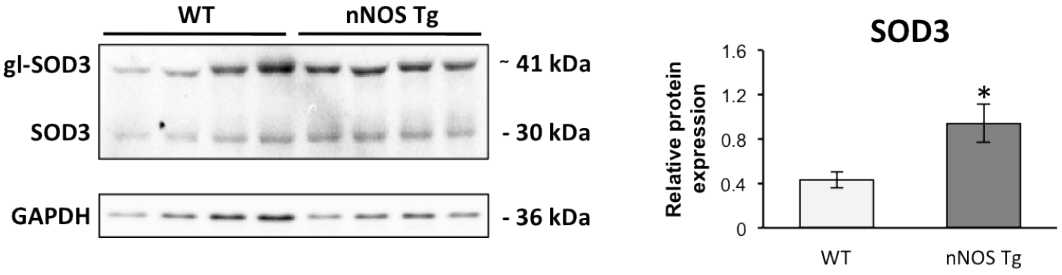

Figure 5.36 Representative western blots of SOD3 protein in *GTN* muscles of WT and nNOSTg mice and densitometric quantification of the SOD3 band (see text for explanation of the presence of two bands), *P < 0.05 compared to values for muscles from WT mice.

5.5 DISCUSSION

Superoxide and NO are the primary reactive oxygen and nitrogen species generated within skeletal muscle both at rest and during contractile activity. While further reaction of both species is well described with the generation of secondary ROS such as H_2O_2 and hydroxyl radicals from superoxide (Jackson, 2008) and interaction of NO with targets such as guanylate cyclase (Halliwell and Gutteridge, 2007), the reaction of superoxide with NO has been described in simple chemical and some biological systems (Beckman and Koppenol, 1996), but the functional effects of this interaction in skeletal muscle have not been defined.

In nonstimulated cells, NO is present in the cytoplasm at 10^{-9} to 10^{-8} M, whereas superoxide is reported to be present at 10^{-12} to 10^{-13} M (Chance et al., 1979; Halliwell and Gutteridge, 2007). The chemical reaction of superoxide with NO to generate peroxynitrite has a reaction rate of ~7 x 10^9 M^{-1} s^{-1} which is approximately threefold higher than the superoxide dismutase catalyzed conversion of superoxide to H_2O_2 of ~2 x 10^9 M^{-1} s^{-1} (Beckman and Koppenol, 1996). Thus, theoretically, an increase in superoxide generation will lead to peroxynitrite formation in preference to formation of H_2O_2 in muscle and other cells. NO is usually present in cells to at least 100-fold excess, but the relatively large quantity of superoxide dismutase present in cytoplasm (SOD1) or mitochondria (SOD2) of cells appears to ensure that H_2O_2 is a major product under normal physiological conditions. Where superoxide generation or flux is increased, it is unclear what proportion of the extra superoxide might generate peroxynitrite in the presence of excess NO. Such a situation may be present in ageing where increased generation of superoxide has been implicated in the loss of muscle mass and function that occurs (Melov et al., 2000; Sastre et al., 2003). Data from Muller

et al. (Muller et al., 2006) indicated that mice lacking Cu,Zn SOD (SOD1) showed an accelerated skeletal muscle ageing phenotype that is characterized by loss of muscle fibres and degeneration of the innervating motor neurons (Kostrominova et al., 2007). In addition, adult mice lacking SOD1 also mimic other aspects of the normal ageing phenotype such as an inability to activate adaptive responses to contractions (Vasilaki et al., 2010). Collectively, these data support the theory that reactive species play a key role in skeletal muscle ageing and it is therefore essential to establish the changes in RONS that occur in SOD1KO mice because this may provide evidence about the species that are involved in the degeneration of skeletal muscle in this animal mouse model and also inform further mechanistic studies during normal ageing.

Larger limb muscles of the SO1KO mice, such as the *GTN*, have been shown to have a decreased number of fibres (Muller et al., 2006) compared with WT mice. In the present study, it was further shown that muscles from SOD1KO mice show only minor changes in structure compared with WT mice. An increase in the variability of fibre sizes and numbers of fibres having central nuclei is apparent which appear to reflect previous cycles of degeneration and regeneration and provide further evidence that the observed loss of muscle mass is due to a complete loss of muscle fibres. In addition, recent work has also shown that the lack of SOD1 in SOD1KO mice is associated with the selective loss of white/fast glycolytic (Type IIb), or the conversion to either fast oxidative (Type IIa) or slow fibres (Type I) (Jang et al., 2010).

5.5.1 DHE oxidation by single muscle fibres from SOD1KO mice

The single isolated mature skeletal muscle fibre preparation from the mouse *FDB* muscle has been previously used with ROS-sensitive fluorescent probes (Palomero

et al., 2008; Pye et al., 2007; Vasilaki et al., 2010) and was applied here. Changes in superoxide were assessed by monitoring the rate of change in dihydroethidium (DHE) oxidation and application of this technique to the study of superoxide changes in single isolated mature skeletal muscle fibres has been reported in detail in chapter 3.

Resting fibres from SOD1KO mice showed no increase in DHE oxidation compared with those from WT mice with no statistical differences between the groups over the experimental period (Figure 5.9). In fibres from WT mice, contractile activity induced a substantial increase in DHE oxidation, indicating an increase in superoxide in response to contractions, but in muscle fibres from SOD1KO mice, the contraction induced increase in E^+ fluorescence was much smaller (Figure 5.10). Thus, these data indicate that any rise in superoxide in fibres from the SOD1KO mice at rest was much less than that which occurs during physiological contractions of skeletal muscle and that the SOD1KO mice generated much less superoxide in muscle than WT mice following contractions. A similar pattern of ROS changes following contractions was observed in previous work from this group in which single *FDB* muscle fibres from the SOD1KO mice failed to increase CM-DCF fluorescence following contactions (Vasilaki et al., 2010).

Failure of skeletal muscle fibres to generate superoxide to the same extent as fibres from the WT mice following contractions implies that that a lack of SOD1 appears to lead to a partial lack of activation of the systems that generate superoxide during contractions. The experimental data obtained in chapter 4 suggest that the NADPH oxidase system is the major cytosolic source of superoxide both at rest and following contractions in skeletal muscle. This implies that the small increase in

superoxide observed following contractile activity in skeletal muscles from SOD1KO mice (Figure 5.10) might be due to a partial lack of activation of the NADPH oxidase system. In relation to this, work by Harraz *et al.* showed that SOD1 is not just a catabolic enzyme, catalyzing the dismutation of superoxide into O_2 and H_2O_2, but it can also directly regulate the NADPH oxidase dependent superoxide production by binding Rac1 (a regulatory component of the NADPH oxidase complex) and inhibiting its GTPase activity (Harraz et al., 2008). Hence, the potential lack of activation of the NADPH oxidase system may be the mechanism that accounts for the smaller increase in superoxide observed in skeletal muscles from the SOD1KO mice in response to contractions.

5.5.2 NO and peroxynitrite in muscles from SOD1KO mice

DAF-FM fluorescence from fibres of SOD1KO mice at rest was decreased to a small but significant extent throughout the period of study compared with that from fibres of WT mice (Figure 5.12). These data are compatible with a reduced NO availability in fibres from the SOD1KO mice. The 3-NT content of CAIII in muscles was also increased in muscles from SOD1KO mice compared with those from WT mice (Figure 5.14). These data are therefore entirely compatible with an increased generation of peroxynitrite in the muscle fibres of SOD1KO mice. Previous studies from this laboratory have indicated that measurements of the 3-NT content of the major cytosolic protein CAIII is a more sensitive marker of oxidative modifications to muscle than measurements of total muscle 3-NT content (Vasilaki et al., 2007). The western blotting approach used to assess the 3-NT content of muscle proteins in the current study is not sufficiently sensitive to demonstrate any potential changes in the 3-NT content of relatively low abundance proteins in the cytosol or mitochondrial intermembrane space

of muscle (Vasilaki et al., 2006a) although such analyses might provide information on important sites for peroxynitrite action in the SOD1KO mice.

All of the six mammalian PRX proteins act to degrade H_2O_2 (Wood et al., 2003), but PRXV also has the highest reported peroxynitrite reductase activity (Dubuisson et al., 2004; Trujillo et al., 2008). This function appears important *in vivo* because previous studies have shown that changes in PRXV expression modulated peroxynitrite toxicity and the cellular content of the enzyme was found to be upregulated in conditions associated with increased peroxynitrite formation (Trujillo et al., 2008). The muscle content of PRXV was found to be increased in SOD1KO mice compared with WT mice (Figure 5.15), which provides further support for a substantial increase in peroxynitrite generation in this model.

5.5.3 Muscles from SOD1KO mice show increased oxidative damage

The increase in peroxynitrite formation observed in muscles from SOD1KO mice was associated with increased oxidative damage (Figures 5.4, 5.5, 5.6 & 5.7). Protein, lipid and DNA damage was increased in muscles lacking SOD1 as indicated by the higher content in protein carbonyls, 4-HNE protein conjugates, MDA protein adducts, and increased OGG1 protein expression. These data further suggest that an increase in peroxynitrite formation can oxidative modify lipids, proteins and DNA in skeletal muscle tissue from SOD1KO mice.

5.5.4 Adaptive responses in muscles from SOD1KO mice

To identify if the increased oxidative damage observed in muscles from SOD1KO mice induced changes in protective systems, the protein expression of the

main enzymes that regulate changes in reactive species was also assessed. Mice lacking SOD1 showed a small but significant increase on muscle SOD2 content (Figure 5.16) that may reflect the increased number of mitochondria reported to be present in muscles of these mice (Kostrominova et al., 2007). No significant changes in the muscle contents of SOD3 (Figure 5.17) or of the three NOS isoforms were seen (Figures 5.18 5.19 & 5.20). The lack of SOD1 in SOD1KO mice was also associated with increased protein expression of H_2O_2 reducing enzymes such as PRXII, PRXIII, PRXIV, PRXVI, CAT, and GPX1 (Figures 5.22, 5.23, 5.24, 5.25, 5.26 & 5.27. These data imply that skeletal muscles from SOD1KO mice show increased H_2O_2 levels in comparison to WT mice and this finding is in agreement with previous findings from this group which showed that resting muscle fibres from the knockout mice showed a higher increase in CM-DCF fluorescence (Vasilaki et al., 2010).

5.5.5 Can modification of NO availability affect changes in peroxynitrite in muscles from nNOSTg mice?

To determine whether a substantial increase in NO formation might modify peroxynitrite, the effect of overexpression of nNOS in muscle was also examined. Initial studies demonstrated the substantial increase in nNOS content that occurred in the muscle of nNOSTg mice (Figure 5.28) and also that this was associated with an increase in iNOS content (Figure 5.34). All three of the SOD isoforms were found to be elevated in the muscle of the nNOSTg mice compared with WT (Figures 5.35 & 5.36). These data indicate a substantial adaptive response to the overexpression of nNOS in muscle and further demonstrate the close link between NO and superoxide metabolism in this tissue.

The experimental data presented in my MPhil thesis showed that, resting muscle fibres from nNOSTg mice showed a significant increase in DAF-FM fluorescence (Figure 5.29) in comparison with those from WT mice, indicating that nNOS plays a significant role on NO generation on muscle at rest as previously reported (Nguyen and Tidball, 2003). The nNOS overexpression appeared to reduce superoxide availability in resting fibres from the transgenic group as shown by the reduction in DHE oxidation in comparison to fibres from the WT mice (Figure 5.30). The possibility that this was because of increased reaction of NO with superoxide to generate peroxynitrite is supported by the increase in the 3-NT content of CAIII in the muscle of nNOSTg mice compared with WT mice that was seen (Figure 5.31), although the adaptive changes in SOD contents seen in muscles of the nNOSTg mice may also have played a role to reduce superoxide availability and hence DHE oxidation.

The overall increase in peroxynitrite in muscles of the nNOSTg mice appeared to be lower than that seen in the muscles of SOD1KO mice because the 3-NT content of CAIII was not increased to the same extent (Figure 5.14 compared with Figure 5.31). In addition, no upregulation of PRXV was seen in the nNOSTg mice (Figure 5.32), whereas the content of PRXV was increased significantly in muscles of the SOD1KO mice (Figure 5.15). It is also likely that the predominant sub-cellular sites for increased peroxynitrite generation differed in the muscles of SOD1KO mice compared with nNOSTg mice because SOD1 is found in the cytoplasm and mitochondrial intermembrane space, whereas endogenous nNOS is localized to the inside of the muscle plasma membrane (Crosbie et al., 1998). PRXV is localized predominantly to mitochondria (Wood et al., 2003), and hence, the increase in expression seen in muscle of SOD1KO mice supports a substantial increase in peroxynitrite in that compartment.

The western blots for SOD3 (extracellular SOD) in Figures 5.17 and 5.36 show two predominant bands. There is considerable discrepancy in the published literature concerning the pattern and molecular weight of SOD3 seen in mouse tissues. Published data show either a single band (Wiggers et al., 2008), a doublet (Kliment et al., 2009) or the two major bands reported here (Lavina et al., 2009). This pattern appears in part related to the nature of the antibody that was used, and detailed examination of the ~30 kDa band shown in Figure 5.17 indicates that it is a doublet. The two bands in the doublet are thought to represent the 'full length' and 'proteolyzed' forms of the protein in which the heparin-binding portion of the protein is removed. The higher molecular weight band in Figures 5.17 and 5.36 has been described as a highly glycosylated form of the protein (Lavina et al., 2009).

5.6 CONCLUSION

In conclusion, these data indicate that removal of SOD-catalyzed conversion of cytosolic superoxide to H_2O_2 in SOD1KO mice caused no significant increase in the apparent superoxide availability in muscle fibres at rest, although a substantial increase in superoxide availability was observed following contractile activity in muscle fibres of WT mice. The lack of SOD1 caused a substantial increase in peroxynitrite formation, which is likely to be due to the excess NO concentration that is present in the muscle fibres. Furthermore, the lack of SOD1 appeared to prevent the increase in generation of superoxide that occurs in muscle fibres during contractile activity in WT mice. The increase in basal peroxynitrite formation and decreased NO in muscles of SOD1KO mice was also associated with an accelerated age-related loss of muscle mass and function. An increase in superoxide has been implicated in the loss of skeletal muscle mass and function that accompanies ageing, and several studies have attempted to

modify superoxide in skeletal muscle through interventions to increase superoxide scavenging capacity without clear success (Martin et al., 2009; Melov, 2002; Melov et al., 2000). It is feasible that these studies may have been ineffective because of the inability of the additional superoxide scavengers to compete with NO for reaction with superoxide, and the data presented here indicate that alternative approaches based on scavenging of peroxynitrite may be more effective. Peroxynitrite has been shown to inactivate aconitase (Castro et al., 1994; Hausladen and Fridovich, 1994) and is hypothesized to decompose to generate the hydroxyl radical which can oxidize proteins, lipid, and DNA and hence is a potential initiator of degradative processes in muscle (Beckman and Koppenol, 1996). In comparison to superoxide or hydroxyl radical, peroxynitrite is relatively stable, and therefore, there is the opportunity to scavenge this molecule prior to its decomposition although efficient approaches to this have not yet been described (Beckman and Koppenol, 1996; Guven et al., 2008; Jiao et al., 2009).

CHAPTER 6

GENERAL DISCUSSION AND FUTURE DIRECTIONS

6.1 GENERAL DISCUSSION

The current study was designed to determine the intracellular sites that regulate changes in superoxide in skeletal muscle both at rest and during contractile activity (AIM2), to identify the reactive species that are involved in the accelerated loss of muscle mass observed in homozygotic SOD1 knockout mouse model and to characterize the changes in redox status and adaptive responses that occur in muscles from the SOD1 knockout mice (AIM3). For the purposes of this study, a reliable technique to assess specific changes in superoxide was required and the findings of this study are based on techniques, that were optimized and developed in the present work (AIM 1), which enabled real-time detection of superoxide within the mitochondrial and cytosolic compartment of skeletal muscle.

To examine superoxide changes in a pure skeletal muscle preparation, avoiding any contribution to ROS generation from non-myogenic cells, an *ex vivo* experimental model, which involved the isolation of single mature skeletal muscle fibres from the flexor digitorum brevis muscle was utilised. This approach has significant advantages over current techniques, since the measurements were made from mature skeletal muscle fibres that had been isolated from adult muscle and hence are likely to reflect the situation in muscle *in vivo*.

6.2 SUMMARY OF MAJOR FINDINGS

The current study identified that:

1. The techniques based on use of single mature skeletal muscle fibres loaded with dihydroethidium and MitoSOX Red appear capable of detecting cellular changes in superoxide within the cytosolic and mitochondrial compartments that occur in

response to a pharmacological stimulant or in response to a physiological stimulus such as contractile activity. The specificity of this method was evaluated with the use of superoxide inducers but also scavengers and the experimental evidence showed that menadione, a redox cycling agent, which is known to stimulate superoxide production,(Rosen and Freeman, 1984) caused a significant increase in DHE oxidation (Figure 3.2). To further assess the sensitivity of DHE oxidation in response to a physiological stimulus, single muscle fibres were subjected to a 10 min period of contractile activity, fibres showed a significant increase in DHE oxidation following contractions as assessed via changes in E^+ fluorescence (Figure 3.3). The specificity of DHE oxidation towards superoxide was assessed with the use of superoxide scavengers (Tiron and Tempol) which blocked completely the anticipated increase in DHE oxidation following contractions suggesting that DHE oxidation reflects an increase in superoxide (Figure 3.3). Similarly, the electron transport chain inhibitors Antimycin A (Figure 3.9) and Rotenone (Figure 3.10) increased MitoSOX Red fluorescence indicating that the superoxide sensitive fluorescent probe MitoSOX Red is sensitive to changes in superoxide. The selective accumulatation of MitoSOX Red in the mitochondrial matrix was shown by the co-localization of MitoTracker Green FM with MitoSOX Red fluoresncence (Figure 3.8). Finally, the specificity of DHE and MitoSOX Red towards superoxide was examined by treatment of fibres with exogenous H_2O_2 and NO. Positive control experiments using 5- (and 6-) chloromethyl-2',7'-dichlorodihydrofluorescein diacetate (CM-DCFH DA) and 4-amino-5-methylamino-2',7'-difluorofluorescein diacetate (DAF-FM DA) loaded fibres showed a marked increase in DCF fluorescence following addition of H_2O_2 or

DAF-FM fluorescence following NOC-7 indicating an intracellular increase in H_2O_2 and NO (Figures 3.6 and 3.7, respectively). However, DHE and MitoSOX Red loaded fibres showed no changes in fluorescence in response to exogenous H_2O_2 and NO (Figures 3.4, 3.5, 3.12 and 3.13) implying that the superoxide sensitive fluorescent dies DHE and MitoSOX Red are selective towards superoxide and are capable of detecting changes in superoxide at rest but also in response to a physiological stimulus such as contractile activity..

2. Contractile activity increased cytosolic superoxide, an increase that appeared to be related to the number of contractions to which the fibres were subjected. Fibres subjected to the High, Moderate and Low contraction protocols showed a 5.8, 4.1 and 2.8 fold increase in DHE oxidation following contractions compared with resting fibres (Figure 4.1) implying that contractile activity increased the cytosolic superoxide content of single muscle fibres in an intensity dependent manner since DHE oxidation reflects changes in superoxide within the cytoplasmic compartment of the muscle fibres. This finding further imply that the activity of the sources that regulate cytosolic superoxide content in skeletal muscle is dependent on the number of contractions to which the fibres are subjected.
3. Intact mitochondria in isolated mature skeletal muscle fibres produce superoxide from complex I and complex III of the mitochondrial electron transport chain as shown by the effect of Rotenone and Antimycin A, respectively (Figures 3.9 and 3.10). Superoxide generated by complex I was exclusively released in the mitochondrial matrix as shown by the increase in MitoSOX Red fluorescence (Figure 3.9). No effect was seen on DHE oxidation indicating that complex I-

dependent superoxide release into the mitochondrial matrix and does not diffuse to the cytoplasm from intact mitochondria (Figure 4.5).

4. Superoxide generation by complex III was released to both sides of the inner mitochondrial membrane, the matrix and the intermembrane space. Treatment of fibres with Antimycin A induced a dose dependent increase in DHE oxidation compared with control untreated fibres, indicating extramitochondrial superoxide release (Figure 4.2). Reports have shown that superoxide can diffuse out of isolated mitochondria through the mitochondrial permeability transition pore (mPTP) (Abou-Sleiman et al., 2006), the inner mitochondrial anion channel (iMAC) (Dai et al., 2011) and through channels located on the outer mitochondrial membrane (OMM) (Budzinska et al., 2009; Han et al., 2003). The potential role of the mPTP and iMAC in release of superoxide following Antimycin A was examined in this study using the mPTP - cyclosporin A (CsA) and iMAC - 4 chlorodiazepam (4Cl-DZP) inhibitors (Figure 4.4). Neither CsA or 4CL-DZP were found to affect DHE oxidation in Antimycin A-treated fibres (Figure 4.4) providing evidence that superoxide formed within the mitochondrial matrix does not diffuse to the cytosplasm of single muscle fibres. These data further suggested that the diffusion of superoxide from the mitochondria to the cytosol of single muscle fibres following treatment with Antimycin A likely derived from the mitochondrial intermembrane space. To identify the channels that might play a role in the diffusion of superoxide from the mitochondrial intermembrane space to the cytosol in single muscle fibres, mitochondrial and cytosolic fractions from GTN muscles were prepared and were assessed for the protein expression of the voltage dependent anion channels (VDACs), the major outer membrane proteins known also as mitochondrial porin, which can

facilitate the diffusion of superoxide from the mitochondrial intermembrane space in isolated cardiac mitochondria (Han et al., 2003). All three isoforms of VDACs (VDAC1, VDAC2 & VDAC3) were highly expressed in the skeletal muscle mitochondrial fractions (Figure 4.7) and their contribution to the extramitochondrial superoxide release following in response to Antimycin A was confirmed in inhibition studies. Specifically, treatment of single muscle fibres with dextran sulfate, a VDAC inhibitor partially inhibited the anticipated increase in DHE oxidation following treatment with Antimycin A (Figure 4.8) implying that VDACs play a key role in mitochondrial superoxide release. In addition, further experiments showed that the Bax channel, an additional channel located on the outer mitochondrial membrane (Martinou, 1999), played a synergistic role in mediating the diffusion of superoxide from the MIS across the outer mitochondrial membrane, shown by the effect of the Bax channel blocker which partially inhibited DHE oxidation in response to Antimycin A (Figure 4.11).

5. Intact mitochondria in isolated mature skeletal muscle fibres did not contribute to cytosolic superoxide increase either at rest or following a physiological stimulus such as contractile activity. Single isolated fibres incubated in the presence of dextran sulfate, a VDAC inhibitor, showed no effect on baseline DHE oxidation (Figure 4.9) implying that intact skeletal muscle mitochondria do not release superoxide to the cytosol of resting muscle fibres. Similarly, no differences in the rate of change in DHE oxidation were observed between untreated fibres and fibres treated with VDAC and/or Bax inhibitors following contractions (Figure 4.12) indicating that the increase in superoxide in response to contractions was unlikely to derive from the mitochondrial intermembrane

space and likely originated from non-mitochondrial sources. However under "pathological" conditions when mitochondrial superoxide production was grossly excessive (i.e following addition of Antimycin A), channels of the outer mitochondrial membrane such as VDAC and Bax appear to release superoxide from the mitochondrial intermembrane space to the cytosol of skeletal muscle fibres (Figure 4.11).

6. Cytosolic superoxide levels were not modulated by the activity of the $iPLA_2$ enzymes in single skeletal muscle fibres. Expression of $iPLA_2$ was confirmed in cytosolic fractions from *GTN* muscle and in lysate from single muscle fibres (Figure 4.13). Selective $iPLA_2$ inhibition with the use of bromoenol lactone failed to alter DHE oxidation in both quiescent and contracted fibres (Figures 4.14 and 4.15, respectively) indicating that $iPLA_2$ enzymes did not contribute to changes in superoxide either at rest or during contractile activity.
7. mRNA and protein expression of various NADPH oxidase subunits including NOX2, NOX4, Rac1, $p67^{phox}$, $p47^{phox}$, $p22^{phox}$ and $p40^{phox}$ was identified in pure skeletal muscle preparations (Figures 4.16 and 4.17). Additional experiments were undertaken to identify if either NOX2 or NOX4 oxidases are present in skeletal muscle mitochondria and demonstrated the presence of NOX4 but not NOX2 in this fraction (Figure 4.18).
8. The role of NADPH oxidase complexes in producing superoxide under resting and contracting conditions was assessed by use of specific and non-specific inhibitors. Inhibition of NADPH oxidase activity with the use of the non-specific inhibitor, diphenyleneiodonium chloride (DPI) induced an unexpected increase in DHE oxidation compared with control non-treated fibres (Figure 4.19). The mechanism by which DPI induced increased DHE oxidation in the

current study is unclear, but DPI has been reported to inhibit flavoenzymes in addition to NADPH oxidases, such as NOS, xanthine oxidase, and NADPH-cytochrome P450 reductase (Balcerczyk et al., 2005; Longpre and Loo, 2008; Park et al., 2007), and hence it can affect cellular processes unrelated to NADPH oxidase. In addition, studies have indicated that DPI can stimulate the production of ROS (Li et al., 2003; Riganti et al., 2004) and reactive nitrogen species (Balcerczyk et al., 2005), affecting cellular redox status indicated by increased levels of lipid peroxidation (Riganti et al., 2004) and DNA damage (Longpre and Loo, 2008; Park et al., 2007), an increase in glutathione disulfide (Riganti et al., 2004) and apopoptosis (Balcerczyk et al., 2005; Longpre and Loo, 2008; Park et al., 2007), as well as increased nitration of tyrosine residues of cellular proteins (Balcerczyk et al., 2005)

9. NADPH oxidase contributes to changes in superoxide at rest and during contractile activity in skeletal muscle. Single muscle fibres incubated in the presence of apocynin (Figures 4.20, 4.21 and 4.22), and gp91ds-tat (Figures 4.24 and 4.25) NADPH oxidase inhibitors, showed a significant reduction in fluorescence at rest and following contractions. The contraction–induced increase in fluorescence was reduced by a mean of 70% in apocynin-treated fibres compared with untreated fibres (Figure 4.21). Treatment of fibres with gp91ds-tat abolished the increase in DHE oxidation in response to contractions (Figure 4.25) indicating that NADPH oxidase is a major contributor to superoxide production both at rest and during contractile activity in skeletal muscle.
10. The inhibitory effects of the NADPH oxidase inhibitors apocynin and gp91ds-tat imply that $p47^{phox}$ is a critical component of the NADPH oxidase complex and

can regulate the activity of the enzyme in skeletal muscle. The proposed inhibitory mechanism of action of apocynin on NADPH oxidase is to prevent the translocation of $p47^{phox}$ and $p67^{phox}$ to the membrane-located catalytic subunits (Muijsers et al., 2000) whereas gp91ds-tat peptide selectively inhibits NOX2-oxidase (Csanyi et al., 2011), although early studies suggested the possibility that the peptide may additionally inhibit NOX1 and NOX4 homologues (Brandes, 2003; Rey et al., 2001) by preventing their interaction with $p47^{phox}$. These finding suggests that NOX2 isoform is likely to be the major cytosolic regulator of superoxide in skeletal muscle in response to contractile activity.

11. Immmunocolocalisation techniques showed that the regulatory subunits ($p40^{phox}$, $p47^{phox}$, $p67^{phox}$ and Rac1) of the NADPH oxidase complex were found to be localized on, or in close proximity to the sarcolemma, but immunofluorescence from $p40^{phox}$ and $p67^{phox}$ was also observed in the cytosolic compartment of the muscle fibres (Figure 4.26). The catalytic subunits (NOX2 and NOX4) and the small membrane-bound integral subunit ($p22^{phox}$) were found to be localised on the plasma membrane of the muscle fibres, as indicated by co-localisation with caveolin-3, the muscle-specific caveolin isoform, present in sarcolemmal caveolae (Whitehead et al., 2010), (Figure 4.27). In addition, NOX2, NOX4 and $p22^{phox}$ proteins were also expressed on T-tubules as indicated by co-localisation with the α_{1s} subunit of the dihydropyridine receptor (α_{1s} DHPR), that is located on the T-tubule membrane (Hidalgo et al., 2006) (Figure 4.28). Updated schematic figures that show the cytosolic and mitochondrial RONS sources in skeletal muscle were produced to highlight these findings (Figures 4.31 and 4.32).

12. Increased NADPH oxidase activity in response to contractions requires translocation of the $p40^{phox}$ cytosolic component to the muscle plasma membrane (Figure 4.29). Activation of the NADPH oxidase complex in phagocytic cells requires translocation of the $p40^{phox}$, $p47^{phox}$ and $p67^{phox}$ components to the cell membrane and work from this study revealed that $p40^{phox}$ immunostained fibres exhibited a more intense fluorescence at the sarcolemma compared with resting non-contracted fibres following contractions (Figures 4.29 and 4.30). No evidence for contraction-induced translocation of the $p67^{phox}$ protein was observed, with resting fibres showing a similar intensity of fluorescence at the membrane and in the cytosol compared with fibres subjected to contractions (Figure 4.29).
13. Removal of SOD1 in homozygotic SOD1 knockout mice induced overt phenotypic changes of accelerated ageing in the anterior tibialis and gastrocnemius muscles of SOD1 knockout mice (Table 5.2). Other tissues/organs including the heart, liver, kidneys, spleen, brain and lungs were unaffected indicating that removal of SOD1 induces specific effects in skeletal muscle (Table 5.2). Muscles from SOD1 knockout mice showed minor changes in structure, such as greater variability in fibre size and the presence of occasional central nuclei compared with muscles from WT mice (Figure 5.3), implying that the loss of mass observed in the muscles of the SOD1 knockout mouse model is likely primarily due to a complete loss of muscle fibres.
14. Skeletal muscle ageing phenotypic changes were associated with increased oxidative damage as shown by the increase in protein oxidation (Figure 5.4), lipid peroxidation (Figures 5.5 and 5.6) and DNA damage (Figure 5.7) in muscles form the SOD1 knockout mice.

15. Removal of SOD-catalyzed conversion of cytosolic superoxide to H_2O_2 in SOD1 knockout mice caused no significant increase in the apparent superoxide availability in muscle fibres, as indicated by changes in DHE oxidation (Figure 5.9) but decreased nitric oxide availability shown by the reduction in DAF-FM fluorescence (Figure 5.12). The possibility that a lack of SOD1 lead to the formation of peroxynitrite was supported by the higher level of nitration of tyrosine residues of the major muscle protein carbonic anhydrase III (Figure 5.14) as well as by the higher protein expression of peroxiredoxin V, a peroxynitrite reductase, in muscles from the SOD1 knockout mice (Figure 5.15). carbonic anhydrase III.
16. Lack of SOD1 induced a compensatory up-regulation of RONS protective enzymes in skeletal muscles from the SOD1 knockout mice including an increase in SOD2, peroxiredoxin II, peroxiredoxin III, peroxiredoxin IV, peroxiredoxin VI, catalase and glutathione peroxidase I (Figures 5.16, 5.22, 5.23, 5.24, 5.25, 5.26 and 5.27) which indicate the adaptations that occur in skeletal muscles from the SOD1 knockout mice due to higher RONS content in comparison to muscles from the WT group. The possibility that the lack of SOD1 might have induced adaptations in the content of nitric oxide synthase (NOS) enzymes was also examined, no significant differences in the contents of all the three NOS isoforms (nNOS, eNOS, and iNOS) were seen (Figures 5.18, 5.19 and 5.20).
17. Muscle specific nNOS transgenic mice showed a > 100-fold increase in nNOS protein content in comparison to WT mice (Figure 5.28). nNOS overexpression augmented the formation of peroxynitrite as shown by the higher 3-nitrotyrosine content of the carbonic anhydrase III in the transgenic group in comparison with

muscles from WT mice (Figure 5.31). However, no significant changes in peroxiredoxin V were observed with muscles from the transgenic group showing a similar peroxiredoxin V protein expression compared to muscles from the WT mice (Figure 5.32). nNOS overexpression induced adaptations in the content of SOD enzymes, the protein expression of the three SOD enzymes (SOD1, SOD2, and SOD3) was significantly upregulates in muscles of the transgenic mice in comparison with muscles from WT mice (Figures 5.35 and 5.36). In addition, the effect of nNOS overexpression on the muscle content of the other two NOS isoenzymes (eNOS & iNOS) was also examined, iNOS content was significantly upregulated in the transgenic mice compared with WT mice (Figure 5.34) but no significant changes in the content of eNOS were seen (Figure 5.33).

6.3 LIMITATIONS

6.3.1 Use of ethidium (E^+) fluorescence to monitor changes in superoxide.

The work described in this thesis has examined the use of dihydroethidium (DHE) and MitoSOX Red superoxide sensitive florescent dyes to determine changes in superoxide within the cytosolic and mitochondrial compartment of mature single muscle fibres. Oxidation of DHE and MitoSOX Red fluorescence has been used as a means of monitoring cytosolic and mitochondrial changes in superoxide by following ethidium (E^+) and 2-hydroxyethidium (2-OH-E^+) formation (Zielonka and Kalyanaraman, 2010) and the experimental findings in this current work are based on monitoring changes in E^+ fluorescence from single muscle fibres. Though the experiments undertaken in chapter 3 indicate that the techniques based on monitoring E^+ fluorescence from single muscle cells appear capable of detecting changes in superoxide at rest but also in response to contractile activity, assessment of E^+ fluorescence as a

measure of superoxide anion radical in cellular compartments has been criticised and recent studies have identified 2-hydroxyethidium (2-OH-E^+) as a specific product of the reaction of DHE and MitoSOX Red with superoxide (Zielonka and Kalyanaraman, 2010). Hence, , future studies are required to assess whether 2-OH-E^+ changes in skeletal muscle is a more reliable way of monitoring real-time changes in superoxide in skeletal muscle fibres.

6.3.2 Oxygen tension under which single muscle fibre experiments were conducted.

Molecular oxygen is one of the most abundant elements in the atmosphere (nearly 21% by volume), and its ability to accept electrons makes it vital for a variety of physiological processes. Resting and contracting skeletal muscles require energy and in biological systems, the energy is accumulated as ATP and released by its hydrolysis (Marieb and Hoehn, 2010; Martini, 2005). Skeletal muscle mitochondria are implicated in the processes of ATP production via mitochondrial oxidative phosphorylation, which results in the production of ATP by reducing oxygen to water (Scheffler, 1999). Although oxidative phosphorylation is a vital part of metabolism, it also produces reactive oxygen intermediates. Single isolated muscle fibres used in this study were exposed to environmental oxygen though the tension of oxygen in skeletal muscle *in vivo* varies between 2-7 %. Recent studies from Vasilaki *et al*. (unpublished data) have shown that different oxygen concentrations can modify ROS generation in skeletal muscle cells. Specifically, skeletal muscle myoblasts and myotubes grown in 6% oxygen showed a lower rate of increase in DHE oxidation as assessed via changes in 2-OH-E^+ in comparison to cells grown in 20% oxygen. These data imply that the RONS changes observed in the current study might be higher than the actual changes that

occur in skeletal muscle *in vivo*. Hence, future studies are required to assess RONS changes in single skeletal muscle cells in the presence of 2-7% oxygen environments.

6.3.3 Genders of mice used in this study.

Male and female mice were used in this study. Specifically, results in chapter 3 and 4 report findings in female WT mice whereas in chapter 5, male SOD1 knockout and male nNOS transgenic mice were used. The selection of gender of mice for each study was based entirely on the available mice at that time. Studies have shown that on average, the skeletal muscle of women typically has 60–80% of the strength, muscle fibre cross sectional area and whole muscle anatomical cross-sectional area of men (Folland and Williams, 2007). There is no evidence in the literature to suggest that skeletal muscles from female mice show a different pattern in RONS activation in comparison to skeletal muscles from male mice. However, studies that have assessed and compared the neurological and morphological adaptations in skeletal muscle following resistance exercise between men and women have shown that the relative improvements both in hypertrophy and strength adaptations are similar and that relative to the amount of muscle mass, men and women experience similar gains of strength (Folland and Williams, 2007). In relation to this, studies from this group have also shown that the loss of muscle mass that occurs in SOD1 knockout mice is similar between male and female mice. Though this evidence might indicate that the changes in RONS in skeletal muscle might not differ between male and female mice, future studies are required to assess directly whether there are any major differences in the subcellular sites that regulate RONS, but also examine the adaptations that occur in response to a stimulus such as contractile activity.

6.4 FUTURE DIRECTIONS

6.4.1 Use of dihydroethidium and MitoSOX Red superoxide-sensitive dyes.

The development of techniques to examine real-time changes in cytosolic and mitochondrial superoxide in skeletal muscle may have biologically and potentially clinically relevant implications for the understanding of diverse scientific areas. The production of reactive oxygen and nitrogen species by skeletal muscle is important as it underlies oxidative damage in many degenerative muscle diseases and plays multiple regulatory roles by fulfilling important cellular functions. Hence application of these techniques may provide useful information with regards to the responses of muscle to exercise training, age-related loss of muscle mass and function, as well as inflammatory or degenerative muscle diseases, such as the muscular dystrophies that are associated with increased levels of oxidative damage and muscle weakness.

6.4.2 NAD(P)H oxidase expression in skeletal muscle.

The experimental data from the current work indicated that NAD(P)H oxidases and particularly NOX2 is likely to be a major cytosolic regulator of superoxide in skeletal muscle in response to contractile activity. However, several aspects of NOX regulation remain uncertain. DUOX1 and DUOX2 have shown to be expressed in skeletal muscle and generate H_2O_2 although the precise location of these enzymes remains unidentified. The uncertainty regarding the primary ROS product released by NOX4 requires clarification and further research is required to assess the potential cross-talk between the mitochondrial NOX4 isoform and the superoxide generating sites of the mitochondrial electron transport chain in skeletal muscle. Finally, the recent finding that mitochondrial NOX4 can enhance H_2O_2 production and induce mitochondrial dysfunction in a cultured endothelial cell aging-induced senescence

model (Koziel et al., 2013; Wolin, 2013) raises the possibility that mitochondrial NOX4 might be implicated in the processes of skeletal muscle ageing and future studies are required to examine the role of NAD(P)H oxidases in the loss of muscle mass that occurs with ageing.

6.4.3 Formation of peroxynitrite in skeletal muscles from SOD1 knockout mice.

The present finding that peroxynitrite is implicated in the processes of skeletal muscle ageing in SOD1 knockout mice highlights the role that this oxidant might play in skeletal muscle degeneration. Preliminary, unpublished data from this group have also shown that skeletal muscles from aged mice show an increase in the level of nitration of tyrosine residues of proteins in muscle implying that skeletal muscles from aged mice exhibit an increase in peroxynitrite formation. Peroxynitrite is a relatively stable RNS, in comparison to superoxide or hydroxyl radical and therefore, there is the opportunity to scavenge this molecule prior to its decomposition. Hence, future studies are required to assess whether direct reduction of peroxynitrite in skeletal muscle would induce changes in muscle mass or prevent the accelerated muscle atrophy observed in the SOD1 knockout mouse model.

Finally, it should be noted that the lack of SOD1 within the mitochondrial intermembrane space might also play a major role in the skeletal muscle ageing phenotype observed in SOD1 knockout mice. Experimental evidence has shown that muscle atrophy in SOD1 knockout mice is associated with mitochondrial dysfunction including an increased elevation of mitochondrial ROS production, a progressive decline in mitochondrial bioenergetic function and an elevated apopoptotic potential (Jang et al., 2010). These data suggest that SOD1 is critically important to maintain

mitochondrial function in skeletal muscle. It is also widely accepted that mitochondria from aged skeletal muscle tissues generate higher amounts of ROS in comparison to young tissues and that mitochondrial dysfunction is implicated in the processes of ageing. In the present study we identified that skeletal muscles from SOD1 knockout mice show an increase in peroxynitrite formation within the cytosolic compartment as assessed via changes in the level of nitration of tyrosine residues of carbonic anhydrase III. The potential increase in peroxynitrite formation within the mitochondrial intermembrane space was not assessed and further studies are required to assess the potential increase in peroxynitrite in the intermembrane space and its potential effect on skeletal muscle ageing. In support of this, the functional significance of SOD1 in the mitochondrial intermembrane space has recently been examined in transgenic studies in which SOD1 was exclusively expressed in the mitochondrial intermembrane space from SOD1 knockout mice (Fischer et al., 2011). Mitochondrial SOD1 expression was sufficient to prevent the biochemical and morphological defects and to rescue the motor axon degeneration phenotype in the SOD1 knockout mouse model (Fischer et al., 2011), implying that SOD1 in the mitochondrial intermembrane space is fundamental for motor axon maintenance.

6.4.4 Which is the primary initiating factor for the accelerated muscle ageing phenotype observed in SOD1 knockout mice; Failure of redox homeostasis in motor neurons or in muscle?

Elucidation of the primary mechanisms underlying sarcopenia has proved difficult, in part because of difficulty in unraveling the interplay between the loss of muscle mass and loss of functional motor units, both of which occur with ageing (Larsson and Wahlstrom, 1998). Skeletal muscle atrophy in SOD1 knockout mice is

associated with neuromuscular junction alterations including moton axon degeneration and postsynaptic endplate fragmentation (Fischer et al., 2011; Jang et al., 2010). These data suggest that neuromuscular junction degeneration is a critical part of the muscle atrophy phenotype exhibited in the SOD1 knockout mouse model. To unravel whether changes in redox homeostasis in motor nerves or in muscle initiates the observed muscle atrophy, mouse models of conditional deletion of specific RONS regulatory enzymes provide a valuable tool to determine whether site specific changes in redox homeostasis alter the processes of skeletal muscle ageing. Recent work from this laboratory has examined whether specific SOD1 gene deletion targeted to skeletal muscle leads to muscle atrophy and showed that lack of SOD1 protein expression within the muscle tissue alone was not sufficient to cause muscle atrophy (Zhang et al., 2013). To further dissect the relative roles of skeletal muscle and motor neurons in the process of skeletal muscle ageing, current experiments are undertaken to generate a nerve transgenic SOD1 knockout mouse model to determine whether nerve-specific SOD1 expression is sufficient to prevent muscle atrophy in SOD1 knockout mice. This study will provide evidence as to whether a failure in redox homeostasis in motor neurons is the primary initiating factor for the loss of muscle mass that occurs in the SOD1 knockout mouse model.

REFERENCES

ABOU-SLEIMAN, P. M., MUQIT, M. M. & WOOD, N. W. 2006. Expanding insights of mitochondrial dysfunction in parkinson's disease. Nature Reviews Neuroscience, 7, 207-19.
ABRAMSON, J. J. & SALAMA, G. 1989. Critical sulfhydryls regulate calcium release from sarcoplasmic reticulum. Journal of Bioenergetics and Biomembranes, 21, 283-94.
ACKERMANN, E. J., CONDE-FRIEBOES, K. & DENNIS, E. A. 1995. Inhibition of macrophage Ca^{2+}-independent phospholipase A_2 by bromoenol lactone and trifluoromethyl ketones. The Journal of Biological Chemistry, 270, 445-50.
ADHIHETTY, P. J., LJUBICIC, V., MENZIES, K. J. & HOOD, D. A. 2005. Differential susceptibility of subsarcolemmal and intermyofibrillar mitochondria to apoptotic stimuli. American Journal of Physiology Cell Physiology, 289, C994-C1001.
AGHDASI, B., ZHANG, J. Z., WU, Y., REID, M. B. & HAMILTON, S. L. 1997. Multiple classes of sulfhydryls modulate the skeletal muscle Ca^{2+} release channel. The Journal of Biological Chemistry, 272, 3739-48.
AGO, T., KURODA, J., PAIN, J., FU, C., LI, H. & SADOSHIMA, J. 2010. Upregulation of Nox4 by hypertrophic stimuli promotes apoptosis and mitochondrial dysfunction in cardiac myocytes. Circulation Research, 106, 1253-64.
ANDERSON, E. J. & NEUFER, P. D. 2006. Type II skeletal myofibers possess unique properties that potentiate mitochondrial H_2O_2 generation. American Journal of Physiology. Cell Physiology, 290, C844-51.
ANDRADE, F. H., REID, M. B., ALLEN, D. G. & WESTERBLAD, H. 1998. Effect of hydrogen peroxide and dithiothreitol on contractile function of single skeletal muscle fibres from the mouse. The Journal of Physiology, 509 (Pt 2), 565-75.
ANZUETO, A., ANDRADE, F. H., MAXWELL, L. C., LEVINE, S. M., LAWRENCE, R. A. & JENKINSON, S. G. 1993. Diaphragmatic function after resistive breathing in vitamin E-deficient rats. Journal of Applied Physiology, 74, 267-71.
ARNER, E. S. & HOLMGREN, A. 2000. Physiological functions of thioredoxin and thioredoxin reductase. European Journal of Biochemistry / FEBS, 267, 6102-9.
AYDIN, J., ANDERSSON, D. C., HANNINEN, S. L., WREDENBERG, A., TAVI, P., PARK, C. B., LARSSON, N. G., BRUTON, J. D. & WESTERBLAD, H. 2009. Increased mitochondrial Ca^{2+} and decreased sarcoplasmic reticulum Ca^{2+} in mitochondrial myopathy. Human Molecular Genetics, 18, 278-88.
BABIOR, B. M. 1978. Oxygen-dependent microbial killing by phagocytes (first of two parts). The New England Journal of Medicine, 298, 659-68.
BABIOR, B. M. 1995. The respiratory burst oxidase. Current Opinion in Hematology, 2, 55-60.
BALCERCZYK, A., SOSZYNSKI, M., RYBACZEK, D., PRZYGODZKI, T., KAROWICZ-BILINSKA, A., MASZEWSKI, J. & BARTOSZ, G. 2005. Induction of apoptosis and modulation of production of reactive oxygen species in human endothelial cells by diphenyleneiodonium. Biochemical Pharmacology, 69, 1263-73.
BALON, T. W. & NADLER, J. L. 1994. Nitric oxide release is present from incubated skeletal muscle preparations. Journal of Applied Physiology, 77, 2519-21.
BARANANO, D. E., RAO, M., FERRIS, C. D. & SNYDER, S. H. 2002. Biliverdin reductase: a major physiologic cytoprotectant. Proceedings of the National Academy of Sciences of the United States of America, 99, 16093-8.
BARJA, G. 1999. Mitochondrial oxygen radical generation and leak: sites of production in states 4 and 3, organ specificity, and relation to aging and longevity. Journal of Bioenergetics and Biomembranes, 31, 347-66.

BAUM, H., RIESKE, J. S., SILMAN, H. I. & LIPTON, S. H. 1967. On the mechanism of electron transfer in complex iii of the electron transfer chain. Proceedings of the National Academy of Sciences of the United States of America, 57, 798-805.
BECKMAN, J. S. & KOPPENOL, W. H. 1996. Nitric oxide, superoxide, and peroxynitrite: the good, the bad, and ugly. The American Journal of Physiology, 271, C1424-37.
BEDARD, K. & KRAUSE, K. H. 2007. The NOX family of ROS-generating NADPH oxidases: physiology and pathophysiology. Physiological Reviews, 87, 245-313.
BERNDT, C., LILLIG, C. H. & HOLMGREN, A. 2007. Thiol-based mechanisms of the thioredoxin and glutaredoxin systems: implications for diseases in the cardiovascular system. American Journal of Physiology Heart and Circulatory Physiology, 292, H1227-36.
BEYER, R. E. 1994. The role of ascorbate in antioxidant protection of biomembranes: interaction with vitamin E and coenzyme Q. Journal of Bioenergetics and Biomembranes, 26, 349-58.
BINDOKAS, V. P., JORDAN, J., LEE, C. C. & MILLER, R. J. 1996. Superoxide production in rat hippocampal neurons: selective imaging with hydroethidine. The Journal of Neuroscience: the Official Journal of the Society for Neuroscience, 16, 1324-36.
BJORNSTEDT, M., XUE, J., HUANG, W., AKESSON, B. & HOLMGREN, A. 1994. The thioredoxin and glutaredoxin systems are efficient electron donors to human plasma glutathione peroxidase. The Journal of Biological Chemistry, 269, 29382-4.
BLOCK, K., GORIN, Y. & ABBOUD, H. E. 2009. Subcellular localization of Nox4 and regulation in diabetes. Proceedings of the National Academy of Sciences of the United States of America, 106, 14385-90.
BOVERIS, A. & CHANCE, B. 1973. The mitochondrial generation of hydrogen peroxide. General properties and effect of hyperbaric oxygen. Biochemical Journal, 134, 707-16.
BRANDES, R. P. 2003. A radical adventure: the quest for specific functions and inhibitors of vascular NAPDH oxidases. Circulation Research, 92, 583-5.
BRANDES, R. P. 2005. Triggering mitochondrial radical release: a new function for NADPH oxidases. Hypertension, 45, 847-8.
BRENMAN, J. E., CHAO, D. S., GEE, S. H., MCGEE, A. W., CRAVEN, S. E., SANTILLANO, D. R., WU, Z., HUANG, F., XIA, H., PETERS, M. F., FROEHNER, S. C. & BREDT, D. S. 1996. Interaction of nitric oxide synthase with the postsynaptic density protein PSD-95 and alpha1-syntrophin mediated by PDZ domains. Cell, 84, 757-67.
BRENMAN, J. E., CHAO, D. S., XIA, H., ALDAPE, K. & BREDT, D. S. 1995. Nitric oxide synthase complexed with dystrophin and absent from skeletal muscle sarcolemma in Duchenne muscular dystrophy. Cell, 82, 743-52.
BREWER, A. C., MURRAY, T. V., ARNO, M., ZHANG, M., ANILKUMAR, N. P., MANN, G. E. & SHAH, A. M. 2011. Nox4 regulates Nrf2 and glutathione redox in cardiomyocytes in vivo. Free Radical Biology & Medicine, 51, 205-15.
BRIGELIUS-FLOHE, R. 1999. Tissue-specific functions of individual glutathione peroxidases. Free Radical Biology & Medicine, 27, 951-65.
BRODIE, A. E. & REED, D. J. 1987. Reversible oxidation of glyceraldehyde 3-phosphate dehydrogenase thiols in human lung carcinoma cells by hydrogen peroxide. Biochemical and Biophysical Research Communications, 148, 120-5.
BROOME, C. S., KAYANI, A. C., PALOMERO, J., DILLMANN, W. H., MESTRIL, R., JACKSON, M. J. & MCARDLE, A. 2006. Effect of lifelong overexpression of

HSP70 in skeletal muscle on age-related oxidative stress and adaptation after nondamaging contractile activity. The Journal of the Federation of American Societies for Experimental Biology, 20, 1549-51.
BROWNSON, C., ISENBERG, H., BROWN, W., SALMONS, S. & EDWARDS, Y. 1988. Changes in skeletal muscle gene transcription induced by chronic stimulation. Muscle & Nerve, 11, 1183-9.
BUDZINSKA, M., GALGANSKA, H., KARACHITOS, A., WOJTKOWSKA, M. & KMITA, H. 2009. The TOM complex is involved in the release of superoxide anion from mitochondria. Journal of Bioenergetics and Biomembranes, 41, 361-7.
CADENAS, E., BOVERIS, A., RAGAN, C. I. & STOPPANI, A. O. 1977. Production of superoxide radicals and hydrogen peroxide by NADH-ubiquinone reductase and ubiquinol-cytochrome c reductase from beef-heart mitochondria. Archives of Biochemistry and Biophysics, 180, 248-57.
CARLSSON, L. M., JONSSON, J., EDLUND, T. & MARKLUND, S. L. 1995. Mice lacking extracellular superoxide dismutase are more sensitive to hyperoxia. Proceedings of the National Academy of Sciences of the United States of America, 92, 6264-8.
CARR, A. & FREI, B. 1999. Does vitamin C act as a pro-oxidant under physiological conditions? The Journal of the Federation of American Societies for Experimental Biology, 13, 1007-24.
CASTRO, L., RODRIGUEZ, M. & RADI, R. 1994. Aconitase is readily inactivated by peroxynitrite, but not by its precursor, nitric oxide. The Journal of Biological Chemistry, 269, 29409-15.
CHAE, H. Z., KIM, I. H., KIM, K. & RHEE, S. G. 1993. Cloning, sequencing, and mutation of thiol-specific antioxidant gene of Saccharomyces cerevisiae. The Journal of Biological Chemistry, 268, 16815-21.
CHANCE, B., SIES, H. & BOVERIS, A. 1979. Hydroperoxide metabolism in mammalian organs. Physiological Reviews, 59, 527-605.
CHEREDNICHENKO, G., ZIMA, A. V., FENG, W., SCHAEFER, S., BLATTER, L. A. & PESSAH, I. N. 2004. NADH oxidase activity of rat cardiac sarcoplasmic reticulum regulates calcium-induced calcium release. Circulation Research, 94, 478-86.
CHIUEH, C. C. 1999. Neuroprotective properties of nitric oxide. Annals of the New York Academy of Science, 890, 301-11.
CLOSE, G. L., ASHTON, T., MCARDLE, A. & JACKSON, M. J. 2005. Microdialysis studies of extracellular reactive oxygen species in skeletal muscle: factors influencing the reduction of cytochrome c and hydroxylation of salicylate. Free Radical Biology & Medicine, 39, 1460-7.
CLOSE, G. L., ASHTON, T., MCARDLE, A. & MACLAREN, D. P. 2005. The emerging role of free radicals in delayed onset muscle soreness and contraction-induced muscle injury. Comparative Biochemistry and Physiology Part A: Molecular & Integrative Physiology, 142, 257-66.
CLOSE, G. L., KAYANI, A. C., ASHTON, T., MCARDLE, A. & JACKSON, M. J. 2007. Release of superoxide from skeletal muscle of adult and old mice: an experimental test of the reductive hotspot hypothesis. Aging Cell, 6, 189-95.
COIRAULT, C., GUELLICH, A., BARBRY, T., SAMUEL, J. L., RIOU, B. & LECARPENTIER, Y. 2007. Oxidative stress of myosin contributes to skeletal muscle dysfunction in rats with chronic heart failure. American Journal of Physiology Heart and Circulatory Physiology, 292, H1009-17.
CONRAD, M., JAKUPOGLU, C., MORENO, S. G., LIPPL, S., BANJAC, A., SCHNEIDER, M., BECK, H., HATZOPOULOS, A. K., JUST, U., SINOWATZ, F., SCHMAHL, W., CHIEN, K. R., WURST, W., BORNKAMM, G. W. &

BRIELMEIER, M. 2004. Essential role for mitochondrial thioredoxin reductase in hematopoiesis, heart development, and heart function. Molecular and Cellular Biology, 24, 9414-23.
COTTO, J. J. & MORIMOTO, R. I. 1999. Stress-induced activation of the heat-shock response: cell and molecular biology of heat-shock factors. Biochemical Society Symposia, 64, 105-18.
CROSBIE, R. H., STRAUB, V., YUN, H. Y., LEE, J. C., RAFAEL, J. A., CHAMBERLAIN, J. S., DAWSON, V. L., DAWSON, T. M. & CAMPBELL, K. P. 1998. mdx muscle pathology is independent of nNOS perturbation. Human Molecular Genetics, 7, 823-9.
CROSS, A. R. & JONES, O. T. 1991. Enzymic mechanisms of superoxide production. Biochimica et Biophysica Acta, 1057, 281-98.
CSANYI, G., CIFUENTES-PAGANO, E., AL GHOULEH, I., RANAYHOSSAINI, D. J., EGANA, L., LOPES, L. R., JACKSON, H. M., KELLEY, E. E. & PAGANO, P. J. 2011. Nox2 B-loop peptide, Nox2ds, specifically inhibits the NADPH oxidase Nox2. Free Radical Biology & Medicine, 51, 1116-25.
CULOTTA, V. C., YANG, M. & O'HALLORAN, T. V. 2006. Activation of superoxide dismutases: putting the metal to the pedal. Biochimica et Biophysica Acta, 1763, 747-58.
CUTLER, R. G. 1991. Human longevity and aging: possible role of reactive oxygen species. Annals of the New York Academy of Sciences, 621, 1-28.
DAI, D. F., CHEN, T., SZETO, H., NIEVES-CINTRON, M., KUTYAVIN, V., SANTANA, L. F. & RABINOVITCH, P. S. 2011. Mitochondrial targeted antioxidant peptide ameliorates hypertensive cardiomyopathy. Journal of the American College of Cardiology, 58, 73-82.
DAIBER, A. 2010. Redox signaling (cross-talk) from and to mitochondria involves mitochondrial pores and reactive oxygen species. Biochimica et Biophysica Acta, 1797, 897-906.
DAVIDSON, S. M. & DUCHEN, M. R. 2006. Effects of NO on mitochondrial function in cardiomyocytes: Pathophysiological relevance. Cardiovascular Research, 71, 10-21.
DAVIES, K. J., MAGUIRE, J. J., BROOKS, G. A., DALLMAN, P. R. & PACKER, L. 1982a. Muscle mitochondrial bioenergetics, oxygen supply, and work capacity during dietary iron deficiency and repletion. American Journal of Physiology, 242, E418-27.
DAVIES, K. J., QUINTANILHA, A. T., BROOKS, G. A. & PACKER, L. 1982b. Free radicals and tissue damage produced by exercise. Biochemical and Biophysical Research Communications, 107, 1198-205.
DAVIES, K. J., SEVANIAN, A., MUAKKASSAH-KELLY, S. F. & HOCHSTEIN, P. 1986. Uric acid-iron ion complexes. A new aspect of the antioxidant functions of uric acid. Biochemical Journal, 235, 747-54.
DE LA ASUNCION, J. G., MILLAN, A., PLA, R., BRUSEGHINI, L., ESTERAS, A., PALLARDO, F. V., SASTRE, J. & VINA, J. 1996. Mitochondrial glutathione oxidation correlates with age-associated oxidative damage to mitochondrial DNA. The Journal of the Federation of American Societies for Experimental Biology, 10, 333-8.
DEMIREL, H. A., HAMILTON, K. L., SHANELY, R. A., TUMER, N., KOROLY, M. J. & POWERS, S. K. 2003. Age and attenuation of exercise-induced myocardial HSP72 accumulation. American journal of physiology. Heart and Circulatory Physiology, 285, H1609-15.
DI MEO, S. & VENDITTI, P. 2001. Mitochondria in exercise-induced oxidative stress. Biological Signals and Receptors, 10, 125-40.

DIAZ, P. T., SHE, Z. W., DAVIS, W. B. & CLANTON, T. L. 1993. Hydroxylation of salicylate by the in vitro diaphragm: evidence for hydroxyl radical production during fatigue. Journal of Applied Physiology, 75, 540-5.
DILLARD, C. J., LITOV, R. E., SAVIN, W. M., DUMELIN, E. E. & TAPPEL, A. L. 1978. Effects of exercise, vitamin E, and ozone on pulmonary function and lipid peroxidation. Journal of Applied Physiology, 45, 927-32.
DIMAURO, I., PEARSON, T., CAPOROSSI, D. & JACKSON, M. J. 2012. A simple protocol for the subcellular fractionation of skeletal muscle cells and tissue. BMC Research Notes, 5, 513.
DIMAURO, I., PEARSON, T., CAPOROSSI, D. & JACKSON, M. J. 2012. In vitro susceptibility of thioredoxins and glutathione to redox modification and aging-related changes in skeletal muscle. Free Radical Biology & Medicine, 53, 2017-27.
DOUGHAN, A. K., HARRISON, D. G. & DIKALOV, S. I. 2008. Molecular mechanisms of angiotensin II-mediated mitochondrial dysfunction: linking mitochondrial oxidative damage and vascular endothelial dysfunction. Circulation Research, 102, 488-96.
DROGE, W. 2002. Free radicals in the physiological control of cell function. Physiological Reviews, 82, 47-95.
DU, J., WANG, X., MIERELES, C., BAILEY, J. L., DEBIGARE, R., ZHENG, B., PRICE, S. R. & MITCH, W. E. 2004. Activation of caspase-3 is an initial step triggering accelerated muscle proteolysis in catabolic conditions. The Journal of Clinical Investigation, 113, 115-23.
DUBUISSON, M., VANDER STRICHT, D., CLIPPE, A., ETIENNE, F., NAUSER, T., KISSNER, R., KOPPENOL, W. H., REES, J. F. & KNOOPS, B. 2004. Human peroxiredoxin 5 is a peroxynitrite reductase. Federation of European Biochemical Societies Letters, 571, 161-5.
DUSI, S., DONINI, M. & ROSSI, F. 1996. Mechanisms of NADPH oxidase activation: translocation of p40phox, Rac1 and Rac2 from the cytosol to the membranes in human neutrophils lacking p47phox or p67phox. The Biochemical Journal, 314 (Pt 2), 409-12.
DWEIK, R. A., LASKOWSKI, D., ABU-SOUD, H. M., KANEKO, F., HUTTE, R., STUEHR, D. J. & ERZURUM, S. C. 1998. Nitric oxide synthesis in the lung. Regulation by oxygen through a kinetic mechanism. The Journal of Clinical Investigation, 101, 660-6.
ELCHURI, S., OBERLEY, T. D., QI, W., EISENSTEIN, R. S., JACKSON ROBERTS, L., VAN REMMEN, H., EPSTEIN, C. J. & HUANG, T. T. 2005. CuZnSOD deficiency leads to persistent and widespread oxidative damage and hepatocarcinogenesis later in life. Oncogene, 24, 367-80.
ELLSON, C. D., DAVIDSON, K., FERGUSON, G. J., O'CONNOR, R., STEPHENS, L. R. & HAWKINS, P. T. 2006. Neutrophils from p40phox-/- mice exhibit severe defects in NADPH oxidase regulation and oxidant-dependent bacterial killing. The Journal of Experimental Medicine, 203, 1927-37.
ENOKSSON, M., FERNANDES, A. P., PRAST, S., LILLIG, C. H., HOLMGREN, A. & ORRENIUS, S. 2005. Overexpression of glutaredoxin 2 attenuates apoptosis by preventing cytochrome c release. Biochemical and Biophysical Research Communications, 327, 774-9.
ESPINOSA, A., LEIVA, A., PENA, M., MULLER, M., DEBANDI, A., HIDALGO, C., CARRASCO, M. A. & JAIMOVICH, E. 2006. Myotube depolarization generates reactive oxygen species through NAD(P)H oxidase; ROS-elicited Ca^{2+} stimulates ERK, CREB, early genes. Journal of Cellular Physiology, 209, 379-88.

FANG, H., CHEN, M., DING, Y., SHANG, W., XU, J., ZHANG, X., ZHANG, W., LI, K., XIAO, Y., GAO, F., SHANG, S., LI, J. C., TIAN, X. L., WANG, S. Q., ZHOU, J., WEISLEDER, N., MA, J., OUYANG, K., CHEN, J., WANG, X., ZHENG, M., WANG, W. & CHENG, H. 2011. Imaging superoxide flash and metabolism-coupled mitochondrial permeability transition in living animals. Cell Research, 21, 1295-304.
FENN, W. O., GERSCHMAN, R., GILBERT, D. L., TERWILLIGER, D. E. & COTHRAN, F. V. 1957. Mutagenic effects of high oxygen tensions on escherichia coli. Proceedings of the National Academy of Sciences of the United States of America, 43, 1027-32.
FISCHER, L. R., IGOUDJIL, A., MAGRANE, J., LI, Y., HANSEN, J. M., MANFREDI, G. & GLASS, J. D. 2011. SOD1 targeted to the mitochondrial intermembrane space prevents motor neuropathy in the Sod1 knockout mouse. Brain : a Journal of Neurology, 134, 196-209.
FOLLAND, J. P. & WILLIAMS, A. G. 2007. The adaptations to strength training : morphological and neurological contributions to increased strength. Sports Medicine, 37, 145-68.
FREY, R. S., USHIO-FUKAI, M. & MALIK, A. B. 2009. NADPH oxidase-dependent signaling in endothelial cells: role in physiology and pathophysiology. Antioxidants & Redox Signaling, 11, 791-810.
FRIDOVICH, I. 1986. Biological effects of the superoxide radical. Archives of Biochemistry and Biophysics, 247, 1-11.
FRIDOVICH, I. 1995. Superoxide radical and superoxide dismutases. Annual Review of Biochemistry, 64, 97-112.
FRIEDL, H. P., SMITH, D. J., TILL, G. O., THOMSON, P. D., LOUIS, D. S. & WARD, P. A. 1990. Ischemia-reperfusion in humans. Appearance of xanthine oxidase activity. The American Journal of Pathology, 136, 491-5.
GAO, Q. & WOLIN, M. S. 2008. Effects of hypoxia on relationships between cytosolic and mitochondrial NAD(P)H redox and superoxide generation in coronary arterial smooth muscle. American Journal of Physiology Heart and Circulatory Physiology, 295, H978-H989.
GARCIA-CARDENA, G., FAN, R., SHAH, V., SORRENTINO, R., CIRINO, G., PAPAPETROPOULOS, A. & SESSA, W. C. 1998. Dynamic activation of endothelial nitric oxide synthase by Hsp90. Nature, 392, 821-4.
GARDNER, P. R., RAINERI, I., EPSTEIN, L. B. & WHITE, C. W. 1995. Superoxide radical and iron modulate aconitase activity in mammalian cells. The Journal of Biological Chemistry, 270, 13399-405.
GATH, I., CLOSS, E. I., GODTEL-ARMBRUST, U., SCHMITT, S., NAKANE, M., WESSLER, I. & FORSTERMANN, U. 1996. Inducible NO synthase II and neuronal NO synthase I are constitutively expressed in different structures of guinea pig skeletal muscle: implications for contractile function. The Journal of the Federation of American Societies for Experimental Biology, 10, 1614-20.
GERSCHMAN, R., GILBERT, D. L., NYE, S. W., DWYER, P. & FENN, W. O. 1954. Oxygen poisoning and x-irradiation: a mechanism in common. Science, 119, 623-6.
GILDA, J. E. & GOMES, A. V. 2013. Stain-Free total protein staining is a superior loading control to beta-actin for western blots. Analytical Biochemistry, 440, 186-8.
GO, Y. M. & JONES, D. P. 2010. Redox control systems in the nucleus: mechanisms and functions. Antioxidants & Redox Signaling, 13, 489-509.
GOHIL, K., ROTHFUSS, L., LANG, J. & PACKER, L. 1987. Effect of exercise training on tissue vitamin E and ubiquinone content. Journal of Applied Physiology, 63, 1638-41.

GOMEZ-CABRERA, M. C., CLOSE, G. L., KAYANI, A., MCARDLE, A., VINA, J. & JACKSON, M. J. 2010. Effect of xanthine oxidase-generated extracellular superoxide on skeletal muscle force generation. American Journal of Physiology-Regulatory, Integrative and Comparative Physiology, 298, R2-8.
GOMEZ-CABRERA, M. C., PALLARDO, F. V., SASTRE, J., VINA, J. & GARCIA-DEL-MORAL, L. 2003. Allopurinol and markers of muscle damage among participants in the Tour de France. The Journal of the American Medical Association, 289, 2503-4.
GONG, M. C., ARBOGAST, S., GUO, Z., MATHENIA, J., SU, W. & REID, M. B. 2006. Calcium-independent phospholipase A_2 modulates cytosolic oxidant activity and contractile function in murine skeletal muscle cells. Journal of Applied Physiology, 100, 399-405.
GOODMAN, J. M. 2008. The gregarious lipid droplet. The Journal of Biological Chemistry, 283, 28005-9.
GORECKI, M., BECK, Y., HARTMAN, J. R., FISCHER, M., WEISS, L., TOCHNER, Z., SLAVIN, S. & NIMROD, A. 1991. Recombinant human superoxide dismutases: production and potential therapeutical uses. Free Radical Research Communications, 12-13 Pt 1, 401-10.
GOTO, S., YOSHIKAWA, M., YAMADA, K. & USHIO, Y. 1995. Survival of neurons containing the enzyme nicotinamide adenine dinucleotide phosphate (NADPH) diaphorase in static slice cultures of adult rat striatum. Neuroscience Letters, 195, 129-32.
GREENBERG, J. T., MONACH, P., CHOU, J. H., JOSEPHY, P. D. & DEMPLE, B. 1990. Positive control of a global antioxidant defense regulon activated by superoxide-generating agents in escherichia coli. Proceedings of the National Academy of Sciences of the United States of America, 87, 6181-5.
GROEMPING, Y. & RITTINGER, K. 2005. Activation and assembly of the NADPH oxidase: a structural perspective. The Biochemical Journal, 386, 401-16.
GUVEN, A., UYSAL, B., AKGUL, O., CERMIK, H., GUNDOGDU, G., SURER, I., OZTURK, H. & KORKMAZ, A. 2008. Scavenging of peroxynitrite reduces renal ischemia/reperfusion injury. Renal Failure, 30, 747-54.
HALL, D. M., XU, L., DRAKE, V. J., OBERLEY, L. W., OBERLEY, T. D., MOSELEY, P. L. & KREGEL, K. C. 2000. Aging reduces adaptive capacity and stress protein expression in the liver after heat stress. Journal of Applied Physiology, 89, 749-59.
HALLIWELL, B. & GUTTERIDGE, J. 2007. Free Radicals in Biology and Medicine. Oxford: Oxford University Press. ed.
HAN, D., ANTUNES, F., CANALI, R., RETTORI, D. & CADENAS, E. 2003. Voltage-dependent anion channels control the release of the superoxide anion from mitochondria to cytosol. The Journal of Biological Chemistry, 278, 5557-63.
HARMAN, D. 1956. Aging: a theory based on free radical and radiation chemistry. Journal of Gerontology, 11, 298-300.
HARMAN, D. 1972. The biologic clock: the mitochondria? Journal of the American Geriatrics Society, 20, 145-7.
HARRAZ, M. M., MARDEN, J. J., ZHOU, W., ZHANG, Y., WILLIAMS, A., SHAROV, V. S., NELSON, K., LUO, M., PAULSON, H., SCHONEICH, C. & ENGELHARDT, J. F. 2008. SOD1 mutations disrupt redox-sensitive Rac regulation of NADPH oxidase in a familial ALS model. The Journal of Clinical Investigation, 118, 659-70.
HARRINGTON, W. F. & RODGERS, M. E. 1984. Myosin. Annual Review of Biochemistry, 53, 35-73.

HAUSLADEN, A. & FRIDOVICH, I. 1994. Superoxide and peroxynitrite inactivate aconitases, but nitric oxide does not. The Journal of biological Chemistry, 269, 29405-8.
HAZEN, S. L., ZUPAN, L. A., WEISS, R. H., GETMAN, D. P. & GROSS, R. W. 1991. Suicide inhibition of canine myocardial cytosolic calcium-independent phospholipase A_2. Mechanism-based discrimination between calcium-dependent and -independent phospholipases A_2. The Journal of Biological Chemistry, 266, 7227-32.
HERRERO, A. & BARJA, G. 1997. ADP-regulation of mitochondrial free radical production is different with complex I- or complex II-linked substrates: implications for the exercise paradox and brain hypermetabolism. Journal of Bioenergetics and Biomembranes, 29, 241-9.
HEUMULLER, S., WIND, S., BARBOSA-SICARD, E., SCHMIDT, H. H., BUSSE, R., SCHRODER, K. & BRANDES, R. P. 2008. Apocynin is not an inhibitor of vascular NADPH oxidases but an antioxidant. Hypertension, 51, 211-7.
HEUNKS, L. M., MACHIELS, H. A., DE ABREU, R., ZHU, X. P., VAN DER HEIJDEN, H. F. & DEKHUIJZEN, P. N. 2001. Free radicals in hypoxic rat diaphragm contractility: no role for xanthine oxidase. American Journal of Physiology Lung Cellular and Molecular Physiology, 281, L1402-12.
HICKNER, R. C., FISHER, J. S., EHSANI, A. A. & KOHRT, W. M. 1997. Role of nitric oxide in skeletal muscle blood flow at rest and during dynamic exercise in humans. The American Journal of Physiology, 273, H405-10.
HIDALGO, C., SANCHEZ, G., BARRIENTOS, G. & ARACENA-PARKS, P. 2006. A transverse tubule NADPH oxidase activity stimulates calcium release from isolated triads via ryanodine receptor type 1 S -glutathionylation. The Journal of Biological Chemistry, 281, 26473-82.
HIRSCHFIELD, W., MOODY, M. R., O'BRIEN, W. E., GREGG, A. R., BRYAN, R. M., JR. & REID, M. B. 2000. Nitric oxide release and contractile properties of skeletal muscles from mice deficient in type III NOS. American Journal of Physiology-Regulatory, Integrative Comparative Physiology, 278, R95-R100.
HOLMGREN, A. 1985. Thioredoxin. Annual Review of Biochemistry, 54, 237-71.
HOLMGREN, A., JOHANSSON, C., BERNDT, C., LONN, M. E., HUDEMANN, C. & LILLIG, C. H. 2005. Thiol redox control via thioredoxin and glutaredoxin systems. Biochemical Society Transactions, 33, 1375-7.
HUANG, T. T., CARLSON, E. J., GILLESPIE, A. M., SHI, Y. & EPSTEIN, C. J. 2000. Ubiquitous overexpression of CuZn superoxide dismutase does not extend life span in mice. The Journals of Gerontology: Series A: Biological Sciences and Medical Sciences, 55, B5-9.
HUANG, T. T., YASUNAMI, M., CARLSON, E. J., GILLESPIE, A. M., REAUME, A. G., HOFFMAN, E. K., CHAN, P. H., SCOTT, R. W. & EPSTEIN, C. J. 1997. Superoxide-mediated cytotoxicity in superoxide dismutase-deficient fetal fibroblasts. Archives of Biochemistry and Biophysics, 344, 424-32.
HUNTER, T. 1995. Protein kinases and phosphatases: the yin and yang of protein phosphorylation and signaling. Cell, 80, 225-36.
HUXLEY, A. F. & NIEDERGERKE, R. 1954. Structural changes in muscle during contraction; interference microscopy of living muscle fibres. Nature, 173, 971-3.
HWANG, C., SINSKEY, A. J. & LODISH, H. F. 1992. Oxidized redox state of glutathione in the endoplasmic reticulum. Science, 257, 1496-502.
ISCHIROPOULOS, H., ZHU, L., CHEN, J., TSAI, M., MARTIN, J. C., SMITH, C. D. & BECKMAN, J. S. 1992. Peroxynitrite-mediated tyrosine nitration catalyzed by superoxide dismutase. Archives of Biochemistry and Biophysics, 298, 431-7.

JACKSON, M. J. & MCARDLE, A. 2011. Age-related changes in skeletal muscle reactive oxygen species generation and adaptive responses to reactive oxygen species. The Journal of Physiology, 589, 2139-45.
JACKSON, M. J. 2005. Reactive oxygen species and redox-regulation of skeletal muscle adaptations to exercise. Philosophical Transactions of the Royal Society B: Biological Sciences, 360, 2285-91.
JACKSON, M. J. 2008. Free radicals generated by contracting muscle: by-products of metabolism or key regulators of muscle function? Free Radical Biology & Medicine, 44, 132-41.
JACKSON, M. J. 2009. Redox regulation of adaptive responses in skeletal muscle to contractile activity. Free Radical Biology & Medicine, 47, 1267-75.
JACKSON, M. J. 2011. Control of reactive oxygen species production in contracting skeletal muscle. Antioxidants & Redox Signaling, 15, 2477-86.
JACKSON, M. J., EDWARDS, R. H. & SYMONS, M. C. 1985. Electron spin resonance studies of intact mammalian skeletal muscle. Biochimica et Biophysica Acta, 847, 185-90.
JACKSON, M. J., JONES, D. A. & EDWARDS, R. H. 1983. Vitamin E and skeletal muscle. Ciba Foundation Symposium, 101, 224-39.
JACKSON, M. J., KHASSAF, M., VASILAKI, A., MCARDLE, F. & MCARDLE, A. 2004. Vitamin E and the oxidative stress of exercise. Annals of the New York Academy of Sciences, 1031, 158-68.
JACKSON, M. J., PAPA, S., BOLANOS, J., BRUCKDORFER, R., CARLSEN, H., ELLIOTT, R. M., FLIER, J., GRIFFITHS, H. R., HEALES, S., HOLST, B., LORUSSO, M., LUND, E., OIVIND MOSKAUG, J., MOSER, U., DI PAOLA, M., POLIDORI, M. C., SIGNORILE, A., STAHL, W., VINA-RIBES, J. & ASTLEY, S. B. 2002. Antioxidants, reactive oxygen and nitrogen species, gene induction and mitochondrial function. Molecular Aspects of Medicine, 23, 209-85.
JACKSON, M. J., PYE, D. & PALOMERO, J. 2007. The production of reactive oxygen and nitrogen species by skeletal muscle. Journal of Applied Physiology, 102, 1664-70.
JAKUPOGLU, C., PRZEMECK, G. K., SCHNEIDER, M., MORENO, S. G., MAYR, N., HATZOPOULOS, A. K., DE ANGELIS, M. H., WURST, W., BORNKAMM, G. W., BRIELMEIER, M. & CONRAD, M. 2005. Cytoplasmic thioredoxin reductase is essential for embryogenesis but dispensable for cardiac development. Molecular and Cellular Biology, 25, 1980-8.
JANG, Y. C., LUSTGARTEN, M. S., LIU, Y., MULLER, F. L., BHATTACHARYA, A., LIANG, H., SALMON, A. B., BROOKS, S. V., LARKIN, L., HAYWORTH, C. R., RICHARDSON, A. & VAN REMMEN, H. 2010. Increased superoxide in vivo accelerates age-associated muscle atrophy through mitochondrial dysfunction and neuromuscular junction degeneration. The Journal of the Federation of American Societies for Experimental Biology, 24, 1376-90.
JARVIS, R. M., HUGHES, S. M. & LEDGERWOOD, E. C. 2012. Peroxiredoxin 1 functions as a signal peroxidase to receive, transduce, and transmit peroxide signals in mammalian cells. Free Radical Biology & Medicine, 53, 1522-30.
JAVESGHANI, D., MAGDER, S. A., BARREIRO, E., QUINN, M. T. & HUSSAIN, S. N. 2002. Molecular characterization of a superoxide-generating NAD(P)H oxidase in the ventilatory muscles. American Journal of Respiratory and Critical Care Medicine, 165, 412-8.
JI, L. L. 1995. Exercise and oxidative stress: role of the cellular antioxidant systems. Exercise and Sport Sciences Reviews, 23, 135-66.

JI, L. L., STRATMAN, F. W. & LARDY, H. A. 1988. Antioxidant enzyme systems in rat liver and skeletal muscle. Influences of selenium deficiency, chronic training, and acute exercise. Archives of Biochemistry and Biophysics, 263, 150-60.
JIAO, X. Y., GAO, E., YUAN, Y., WANG, Y., LAU, W. B., KOCH, W., MA, X. L. & TAO, L. 2009. INO-4885 [5,10,15,20-tetra[N-(benzyl-4'-carboxylate)-2-pyridinium]-21H,23H-porphine iron(III) chloride], a peroxynitrite decomposition catalyst, protects the heart against reperfusion injury in mice. The Journal of Pharmacology and Experimental Therapeutics, 328, 777-84.
JOHNSON-CADWELL, L. I., JEKABSONS, M. B., WANG, A., POLSTER, B. M. & NICHOLLS, D. G. 2007. 'Mild Uncoupling' does not decrease mitochondrial superoxide levels in cultured cerebellar granule neurons but decreases spare respiratory capacity and increases toxicity to glutamate and oxidative stress. Journal of Neurochemistry, 101, 1619-31.
JUIN, P., PELLESCHI, M., SAGNE, C., HENRY, J. P., THIEFFRY, M. & VALLETTE, F. M. 1995. Involvement of the peptide sensitive channel in the translocation of basic peptides into mitochondria. Biochemical and Biophysical Research Communications, 211, 92-9.
KANEKO, M., SUZUKI, H., MASUDA, H., YUAN, G., HAYASHI, H., KOBAYASHI, A. & YAMAZAKI, N. 1992. [Effects of oxygen free radicals on Ca^{2+} binding to cardiac troponin]. Japanese Circulation Journal, 56 Suppl 5, 1288-90.
KANEKO, T., TAHARA, S. & MATSUO, M. 1996. Non-linear accumulation of 8-hydroxy-2'-deoxyguanosine, a marker of oxidized DNA damage, during aging. Mutation Research, 316, 277-85.
KANTER, M. M. 1994. Free radicals, exercise, and antioxidant supplementation. Journal of the International Society of Sports Nutrition, 4, 205-20.
KAYAR, S. R., HOPPELER, H., MERMOD, L. & WEIBEL, E. R. 1988. Mitochondrial size and shape in equine skeletal muscle: a three-dimensional reconstruction study. The Anatomical Record, 222, 333-9.
KEMP, G. J. 2004. Mitochondrial dysfunction in chronic ischemia and peripheral vascular disease. Mitochondrion, 4, 629-40.
KHASSAF, M., MCARDLE, A., ESANU, C., VASILAKI, A., MCARDLE, F., GRIFFITHS, R. D., BRODIE, D. A. & JACKSON, M. J. 2003. Effect of vitamin C supplements on antioxidant defence and stress proteins in human lymphocytes and skeletal muscle. The Journal of Physiology, 549, 645-52.
KIM, K., KIM, I. H., LEE, K. Y., RHEE, S. G. & STADTMAN, E. R. 1988. The isolation and purification of a specific "protector" protein which inhibits enzyme inactivation by a thiol/Fe(III)/O_2 mixed-function oxidation system. The Journal of Biological Chemistry, 263, 4704-11.
KIM, H. J. & VAZIRI, N. D. 2010. Contribution of impaired Nrf2-Keap1 pathway to oxidative stress and inflammation in chronic renal failure. American Journal of Physiology. Renal Physiology, 298, F662-71.
KIM, K., RHEE, S. G. & STADTMAN, E. R. 1985. Nonenzymatic cleavage of proteins by reactive oxygen species generated by dithiothreitol and iron. The Journal of Biological Chemistry, 260, 15394-7.
KIRKWOOD, S. P., MUNN, E. A. & BROOKS, G. A. 1986. Mitochondrial reticulum in limb skeletal muscle. The American Journal of Physiology, 251, C395-402.
KLIMENT, C. R., SULIMAN, H. B., TOBOLEWSKI, J. M., REYNOLDS, C. M., DAY, B. J., ZHU, X., MCTIERNAN, C. F., MCGAFFIN, K. R., PIANTADOSI, C. A. & OURY, T. D. 2009. Extracellular superoxide dismutase regulates cardiac function and fibrosis. Journal of Molecular and Cellular Cardiology, 47, 730-42.

KOBZIK, L., REID, M. B., BREDT, D. S. & STAMLER, J. S. 1994. Nitric oxide in skeletal muscle. Nature, 372, 546-8.
KOJIMA, H., URANO, Y., KIKUCHI, K., HIGUCHI, T., HIRATA, Y. & NAGANO, T. 1999. Fluorescent Indicators for Imaging Nitric Oxide Production. Angewandte Chemie, 38, 3209-3212.
KOLBECK, R. C., SHE, Z. W., CALLAHAN, L. A. & NOSEK, T. M. 1997. Increased superoxide production during fatigue in the perfused rat diaphragm. American Journal of Respiratory and Critical Care Medicine, 156, 140-5.
KONDO, H., MIURA, M. & ITOKAWA, Y. 1991. Oxidative stress in skeletal muscle atrophied by immobilization. Acta Physiologica Scandinavica, 142, 527-8.
KONDO, H., MIURA, M., NAKAGAKI, I., SASAKI, S. & ITOKAWA, Y. 1992. Trace element movement and oxidative stress in skeletal muscle atrophied by immobilization. The American Journal of Physiology, 262, E583-90.
KONDO, H., NAKAGAKI, I., SASAKI, S., HORI, S. & ITOKAWA, Y. 1993. Mechanism of oxidative stress in skeletal muscle atrophied by immobilization. The American Journal of Physiology, 265, E839-44.
KOREN, A., SAUBER, C., SENTJURC, M. & SCHARA, M. 1983. Free radicals in tetanic activity of isolated skeletal muscle. Comparative biochemistry and physiology. B, Comparative Biochemistry, 74, 633-5.
KOSTROMINOVA, T. Y., PASYK, K. A., VAN REMMEN, H., RICHARDSON, A. G. & FAULKNER, J. A. 2007. Adaptive changes in structure of skeletal muscles from adult Sod1 homozygous knockout mice. Cell and Tissue Research, 327, 595-605.
KOZIEL, R., PIRCHER, H., KRATOCHWIL, M., LENER, B., HERMANN, M., DENCHER, N. A. & JANSEN-DURR, P. 2013. Mitochondrial respiratory chain complex I is inactivated by NADPH oxidase Nox4. The Biochemical Journal, 452, 231-9.
KOZLOV, A. V., SZALAY, L., UMAR, F., KROPIK, K., STANIEK, K., NIEDERMULLER, H., BAHRAMI, S. & NOHL, H. 2005. Skeletal muscles, heart, and lung are the main sources of oxygen radicals in old rats. Biochimica et Biophysica Acta, 1740, 382-9.
KRAUSE, K. M., MOODY, M. R., ANDRADE, F. H., TAYLOR, A. A., MILLER, C. C., 3RD, KOBZIK, L. & REID, M. B. 1998. Peritonitis causes diaphragm weakness in rats. American Journal of Respiratory and Critical Care Medicine, 157, 1277-82.
KREJSA, C. M., FRANKLIN, C. C., WHITE, C. C., LEDBETTER, J. A., SCHIEVEN, G. L. & KAVANAGH, T. J. 2010. Rapid activation of glutamate cysteine ligase following oxidative stress. The Journal of Biological Chemistry, 285, 16116-24.
KRETZSCHMAR, M., PFEIFER, U., MACHNIK, G. & KLINGER, W. 1992. Glutathione homeostasis and turnover in the totally hepatectomized rat: evidence for a high glutathione export capacity of extrahepatic tissues. Experimental and Toxicologic Pathology: official journal of the Gesellschaft fur Toxikologische Pathologie, 44, 273-81.
KRINSKY, N. I. 1998. The antioxidant and biological properties of the carotenoids. Annals of the New York Academy of Science, 854, 443-7.
KURIBAYASHI, F., NUNOI, H., WAKAMATSU, K., TSUNAWAKI, S., SATO, K., ITO, T. & SUMIMOTO, H. 2002. The adaptor protein p40(phox) as a positive regulator of the superoxide-producing phagocyte oxidase. The EMBO Journal, 21, 6312-20.
KURODA, J., AGO, T., MATSUSHIMA, S., ZHAI, P., SCHNEIDER, M. D. & SADOSHIMA, J. 2010. NADPH oxidase 4 (Nox4) is a major source of oxidative stress in the failing heart. Proceedings of the National Academy of Sciences of the United States of America, 107, 15565-70.

KUSSMAUL, L. & HIRST, J. 2006. The mechanism of superoxide production by NADH:ubiquinone oxidoreductase (complex I) from bovine heart mitochondria. Proceedings of the National Academy of Sciences of the United States of America, 103, 7607-12.
LAMBETH, J. D. 2004. NOX enzymes and the biology of reactive oxygen. Nature reviews. Immunology, 4, 181-9.
LAMBETH, J. D., KAWAHARA, T. & DIEBOLD, B. 2007. Regulation of Nox and Duox enzymatic activity and expression. Free Radical Biology & medicine, 43, 319-31.
LANDIS, G. N. & TOWER, J. 2005. Superoxide dismutase evolution and life span regulation. Mechanisms of Ageing and Development, 126, 365-79.
LARKIN, L. M., DAVIS, C. S., SIMS-ROBINSON, C., KOSTROMINOVA, T. Y., REMMEN, H. V., RICHARDSON, A., FELDMAN, E. L. & BROOKS, S. V. 2011. Skeletal muscle weakness due to deficiency of CuZn-superoxide dismutase is associated with loss of functional innervation. American Journal of Physiology Regulatory, Integrative and Comparative Physiology, 301, R1400-7.
LARSSON, J. E. & WAHLSTROM, G. 1998. The influence of age and administration rate on the brain sensitivity to propofol in rats. Acta Anaesthesiol Scandinavica, 42, 987-94.
LASSEGUE, B. 2007. How does the chloride/proton antiporter ClC-3 control NADPH oxidase? Circulation Research, 101, 648-50.
LAUGHLIN, M. H., SIMPSON, T., SEXTON, W. L., BROWN, O. R., SMITH, J. K. & KORTHUIS, R. J. 1990. Skeletal muscle oxidative capacity, antioxidant enzymes, and exercise training. Journal of Applied Physiology, 68, 2337-43.
LAVINA, B., GRACIA-SANCHO, J., RODRIGUEZ-VILARRUPLA, A., CHU, Y., HEISTAD, D. D., BOSCH, J. & GARCIA-PAGAN, J. C. 2009. Superoxide dismutase gene transfer reduces portal pressure in CCl4 cirrhotic rats with portal hypertension. Gut, 58, 118-25.
LEE, T. H., KIM, S. U., YU, S. L., KIM, S. H., PARK, D. S., MOON, H. B., DHO, S. H., KWON, K. S., KWON, H. J., HAN, Y. H., JEONG, S., KANG, S. W., SHIN, H. S., LEE, K. K., RHEE, S. G. & YU, D. Y. 2003. Peroxiredoxin II is essential for sustaining life span of erythrocytes in mice. Blood, 101, 5033-8.
LEEUWENBURGH, C., FIEBIG, R., CHANDWANEY, R. & JI, L. L. 1994. Aging and exercise training in skeletal muscle: responses of glutathione and antioxidant enzyme systems. The American Journal of Physiology, 267, R439-45.
LEEUWENBURGH, C., HOLLANDER, J., LEICHTWEIS, S., GRIFFITHS, M., GORE, M. & JI, L. L. 1997. Adaptations of glutathione antioxidant system to endurance training are tissue and muscle fiber specific. The American Journal of Physiology, 272, R363-9.
LI, N., RAGHEB, K., LAWLER, G., STURGIS, J., RAJWA, B., MELENDEZ, J. A. & ROBINSON, J. P. 2003. DPI induces mitochondrial superoxide-mediated apoptosis. Free Radical Biology & Medicine, 34, 465-77.
LI, Y. & TRUSH, M. A. 1998. Diphenyleneiodonium, an NAD(P)H oxidase inhibitor, also potently inhibits mitochondrial reactive oxygen species production. Biochemical and Biophysical Research Communications, 253, 295-9.
LI, Y., HUANG, T. T., CARLSON, E. J., MELOV, S., URSELL, P. C., OLSON, J. L., NOBLE, L. J., YOSHIMURA, M. P., BERGER, C., CHAN, P. H., WALLACE, D. C. & EPSTEIN, C. J. 1995. Dilated cardiomyopathy and neonatal lethality in mutant mice lacking manganese superoxide dismutase. Nature Genetics, 11, 376-81.

LIU, Y., LIU, J., TETZLAFF, W., PATY, D. W. & CYNADER, M. S. 2006. Biliverdin reductase, a major physiologic cytoprotectant, suppresses experimental autoimmune encephalomyelitis. Free Radical Biology & Medicine, 40, 960-7.
LONGPRE, J. M. & LOO, G. 2008. Paradoxical effect of diphenyleneiodonium in inducing DNA damage and apoptosis. Free Radical Research, 42, 533-43.
LOSCHEN, G., AZZI, A., RICHTER, C. & FLOHE, L. 1974. Superoxide radicals as precursors of mitochondrial hydrogen peroxide. FEBS Letters, 42, 68-72.
LU, S. C., GE, J. L., KUHLENKAMP, J. & KAPLOWITZ, N. 1992. Insulin and glucocorticoid dependence of hepatic gamma-glutamylcysteine synthetase and glutathione synthesis in the rat. Studies in cultured hepatocytes and in vivo. The Journal of Clinical Investigation, 90, 524-32.
LUCAS, K. A., PITARI, G. M., KAZEROUNIAN, S., RUIZ-STEWART, I., PARK, J., SCHULZ, S., CHEPENIK, K. P. & WALDMAN, S. A. 2000. Guanylyl cyclases and signaling by cyclic GMP. Pharmacological Reviews, 52, 375-414.
LYNCH, R. E. & FRIDOVICH, I. 1978. Effects of superoxide on the erythrocyte membrane. The Journal of Biological Chemistry, 253, 1838-45.
MAACK, C. & BOHM, M. 2011. Targeting mitochondrial oxidative stress in heart failure. Journal of the American College of Cardiology, 58, 83-6.
MANN, G. E., NIEHUESER-SARAN, J., WATSON, A., GAO, L., ISHII, T., DE WINTER, P. & SIOW, R. C. 2007a. Nrf2/ARE regulated antioxidant gene expression in endothelial and smooth muscle cells in oxidative stress: implications for atherosclerosis and preeclampsia. Sheng Li Xue Bao: [Acta physiologica Sinica], 59, 117-27.
MANN, G. E., ROWLANDS, D. J., LI, F. Y., DE WINTER, P. & SIOW, R. C. 2007b. Activation of endothelial nitric oxide synthase by dietary isoflavones: role of NO in Nrf2-mediated antioxidant gene expression. Cardiovascular Research, 75, 261-74.
MANNELLA, C. A. 1998. Conformational changes in the mitochondrial channel protein, VDAC, and their functional implications. Journal of Structural Biology, 121, 207-18.
MARCELL, T. J. 2003. Sarcopenia: causes, consequences, and preventions. The Journals of Gerontology: Series A, Biological Sciences and Medical Sciences, 58, M911-6.
MARIEB, E. N. & HOEHN, K. 2010. Human anatomy and physiology. Benjamin-Cummings Publishing Company, Subs of Addison Wesley Longman, Inc. 8th edition .
MARTIN, I., JONES, M. A. & GROTEWIEL, M. 2009. Manipulation of Sod1 expression ubiquitously, but not in the nervous system or muscle, impacts age-related parameters in Drosophila. FEBS Letters, 583, 2308-14.
MARTINI, F. H. 2005. Fundamentals of anatomy and physiology. Benjamin-Cummings Publishing Company, Subs of Addison Wesley Longman, Inc.
MARTINOU, J. C. 1999. Apoptosis. Key to the mitochondrial gate. Nature, 399, 411-2.
MATE, S. E., VAN DER MEULEN, J. H., ARYA, P., BHATTACHARYYA, S., BAND, H. & HOFFMAN, E. P. 2012. Eps homology domain endosomal transport proteins differentially localize to the neuromuscular junction. Skeletal Muscle, 2, 19.
MATES, J. M. & SANCHEZ-JIMENEZ, F. 1999. Antioxidant enzymes and their implications in pathophysiologic processes. Frontiers in Bioscience: a Journal and Virtual Library, 4, D339-45.
MATSUI, M., OSHIMA, M., OSHIMA, H., TAKAKU, K., MARUYAMA, T., YODOI, J. & TAKETO, M. M. 1996. Early embryonic lethality caused by targeted disruption of the mouse thioredoxin gene. Developmental Biology, 178, 179-85.
MAXWELL, S. R., THOMASON, H., SANDLER, D., LEGUEN, C., BAXTER, M. A., THORPE, G. H., JONES, A. F. & BARNETT, A. H. 1997. Antioxidant status in

patients with uncomplicated insulin-dependent and non-insulin-dependent diabetes mellitus. European Journal of Clinical Investigation, 27, 484-90.
MAYNARD SMITH, J. 1962. Review lectures on senescence. I. The causes of ageing. The Royal Society.
MCARDLE, A. & JACKSON, M. J. 2000. Exercise, oxidative stress and ageing. Journal of Anatomy, 197 Pt 4, 539-41.
MCARDLE, A., DILLMANN, W. H., MESTRIL, R., FAULKNER, J. A. & JACKSON, M. J. 2004. Overexpression of HSP70 in mouse skeletal muscle protects against muscle damage and age-related muscle dysfunction. The Journal of the Federation of American Societies for Experimental Biology, 18, 355-7.
MCARDLE, A., PATTWELL, D., VASILAKI, A., GRIFFITHS, R. D. & JACKSON, M. J. 2001. Contractile activity-induced oxidative stress: cellular origin and adaptive responses. American Journal of Physiology-Cell Physiology, 280, C621-7.
MCARDLE, A., VAN DER MEULEN, J. H., CATAPANO, M., SYMONS, M. C., FAULKNER, J. A. & JACKSON, M. J. 1999. Free radical activity following contraction-induced injury to the extensor digitorum longus muscles of rats. Free Radical Biology & Medicine, 26, 1085-91.
MCARDLE, F., PATTWELL, D. M., VASILAKI, A., MCARDLE, A. & JACKSON, M. J. 2005. Intracellular generation of reactive oxygen species by contracting skeletal muscle cells. Free Radical Biology & Medicine, 39, 651-7.
MCCLUNG, J. M., KAVAZIS, A. N., DERUISSEAU, K. C., FALK, D. J., DEERING, M. A., LEE, Y., SUGIURA, T. & POWERS, S. K. 2007. Caspase-3 regulation of diaphragm myonuclear domain during mechanical ventilation-induced atrophy. American Journal of Respiratory and Critical Care Medicine, 175, 150-9.
MCCORD, J. M. & FRIDOVICH, I. 1969. The utility of superoxide dismutase in studying free radical reactions. I. Radicals generated by the interaction of sulfite, dimethyl sulfoxide, and oxygen. The Journal of Biological Chemistry, 244, 6056-63.
MECOCCI, P., FANO, G., FULLE, S., MACGARVEY, U., SHINOBU, L., POLIDORI, M. C., CHERUBINI, A., VECCHIET, J., SENIN, U. & BEAL, M. F. 1999. Age-dependent increases in oxidative damage to DNA, lipids, and proteins in human skeletal muscle. Free Radical Biology & Medicine, 26, 303-8.
MEISTER, A. & ANDERSON, M. E. 1983. Glutathione. Annual Review of Biochemistry, 52, 711-60.
MELLO FILHO, A. C., HOFFMANN, M. E. & MENEGHINI, R. 1984. Cell killing and DNA damage by hydrogen peroxide are mediated by intracellular iron. The Biochemical Journal, 218, 273-5.
MELOV, S. 2002. Therapeutics against mitochondrial oxidative stress in animal models of aging. Annals of the New York Academy of Sciences, 959, 330-40.
MELOV, S., RAVENSCROFT, J., MALIK, S., GILL, M. S., WALKER, D. W., CLAYTON, P. E., WALLACE, D. C., MALFROY, B., DOCTROW, S. R. & LITHGOW, G. J. 2000. Extension of life-span with superoxide dismutase/catalase mimetics. Science, 289, 1567-9.
MICHAELSON, L. P., SHI, G., WARD, C. W. & RODNEY, G. G. 2010. Mitochondrial redox potential during contraction in single intact muscle fibers. Muscle Nerve, 42, 522-9.
MIQUEL, J., RAMIREZ-BOSCA, A., SOLER, A., DIEZ, A., CARRION-GUTIERREZ, M. A., DIAZ-ALPERI, J., QUINTANILLA-RIPOLL, E., BERND, A. & QUINTANILLA-ALMAGRO, E. 1998. Increase with age of serum lipid peroxides: implications for the prevention of atherosclerosis. Mechanisms of Ageing and Development, 100, 17-24.

MIRBAHAI, L., KERSHAW, R. M., GREEN, R. M., HAYDEN, R. E., MELDRUM, R. A. & HODGES, N. J. 2010. Use of a molecular beacon to track the activity of base excision repair protein OGG1 in live cells. DNA Repair, 9, 144-52.
MIRO, O., CASADEMONT, J., CASALS, E., PEREA, M., URBANO-MARQUEZ, A., RUSTIN, P. & CARDELLACH, F. 2000. Aging is associated with increased lipid peroxidation in human hearts, but not with mitochondrial respiratory chain enzyme defects. Cardiovascular Research, 47, 624-31.
MOFARRAHI, M., BRANDES, R. P., GORLACH, A., HANZE, J., TERADA, L. S., QUINN, M. T., MAYAKI, D., PETROF, B. & HUSSAIN, S. N. 2008. Regulation of proliferation of skeletal muscle precursor cells by NADPH oxidase. Antioxidants & Redox Signaling, 10, 559-74.
MONCADA, S., PALMER, R. M. & HIGGS, E. A. 1991. Nitric oxide: physiology, pathophysiology, and pharmacology. Pharmacological Reviews, 43, 109-42.
MOSCOW, J. A., MORROW, C. S., HE, R., MULLENBACH, G. T. & COWAN, K. H. 1992. Structure and function of the 5'-flanking sequence of the human cytosolic selenium-dependent glutathione peroxidase gene (hgpx1). The Journal of Biological Chemistry, 267, 5949-58.
MOUGIOS, V. 2006. Exercise Biochemistry. Human Kinetics.
MUIJSERS, R. B., VAN DEN WORM, E., FOLKERTS, G., BEUKELMAN, C. J., KOSTER, A. S., POSTMA, D. S. & NIJKAMP, F. P. 2000. Apocynin inhibits peroxynitrite formation by murine macrophages. British Journal of Pharmacology, 130, 932-6.
MULLER, F. L., LIU, Y. & VAN REMMEN, H. 2004. Complex III releases superoxide to both sides of the inner mitochondrial membrane. Journal of Biological Chemistry, 279, 49064-49073.
MULLER, F. L., LUSTGARTEN, M. S., JANG, Y., RICHARDSON, A. & VAN REMMEN, H. 2007. Trends in oxidative aging theories. Free Radical Biology & Medicine, 43, 477-503.
MULLER, F. L., SONG, W., LIU, Y., CHAUDHURI, A., PIEKE-DAHL, S., STRONG, R., HUANG, T. T., EPSTEIN, C. J., ROBERTS, L. J., 2ND, CSETE, M., FAULKNER, J. A. & VAN REMMEN, H. 2006. Absence of CuZn superoxide dismutase leads to elevated oxidative stress and acceleration of age-dependent skeletal muscle atrophy. Free Radical Biology & Medicine, 40, 1993-2004.
MUMBENGEGWI, D. R., LI, Q., LI, C., BEAR, C. E. & ENGELHARDT, J. F. 2008. Evidence for a superoxide permeability pathway in endosomal membranes. Molecular and Cellular Biology, 28, 3700-12.
MURALIKRISHNA ADIBHATLA, R. & HATCHER, J. F. 2006. Phospholipase A_2, reactive oxygen species, and lipid peroxidation in cerebral ischemia. Free Radical Biology & Medicine, 40, 376-87.
MURPHY, M. P. 2009. How mitochondria produce reactive oxygen species. Biochemical Journal, 417, 1-13.
MURRANT, C. L. & REID, M. B. 2001. Detection of reactive oxygen and reactive nitrogen species in skeletal muscle. Microscopy Research and Technique, 55, 236-48.
NAQUI, A., CHANCE, B. & CADENAS, E. 1986. Reactive oxygen intermediates in biochemistry. Annual Review of Biochemistry, 55, 137-66.
NETHERY, D., STOFAN, D., CALLAHAN, L., DIMARCO, A. & SUPINSKI, G. 1999. Formation of reactive oxygen species by the contracting diaphragm is PLA_2 dependent. Journal of Applied Physiology, 87, 792-800.
NEUMANN, C. A., KRAUSE, D. S., CARMAN, C. V., DAS, S., DUBEY, D. P., ABRAHAM, J. L., BRONSON, R. T., FUJIWARA, Y., ORKIN, S. H. & VAN

ETTEN, R. A. 2003. Essential role for the peroxiredoxin Prdx1 in erythrocyte antioxidant defence and tumour suppression. Nature, 424, 561-5.
NGUYEN, H. X. & TIDBALL, J. G. 2003. Expression of a muscle-specific, nitric oxide synthase transgene prevents muscle membrane injury and reduces muscle inflammation during modified muscle use in mice. The Journal of Physiology, 550, 347-56.
NONN, L., WILLIAMS, R. R., ERICKSON, R. P. & POWIS, G. 2003. The absence of mitochondrial thioredoxin 2 causes massive apoptosis, exencephaly, and early embryonic lethality in homozygous mice. Molecular and Cellular Biology, 23, 916-22.
OAKLEY, F. D., ABBOTT, D., LI, Q. & ENGELHARDT, J. F. 2009. Signaling components of redox active endosomes: the redoxosomes. Antioxidants & Redox Signaling, 11, 1313-33.
O'DONNELL, B. V., TEW, D. G., JONES, O. T. & ENGLAND, P. J. 1993. Studies on the inhibitory mechanism of iodonium compounds with special reference to neutrophil NADPH oxidase. The Biochemical Journal, 290 (Pt 1), 41-9.
OGATA, T. & YAMASAKI, Y. 1997. Ultra-high-resolution scanning electron microscopy of mitochondria and sarcoplasmic reticulum arrangement in human red, white, and intermediate muscle fibers. The Anatomical Record, 248, 214-23.
OH-ISHI, S., KIZAKI, T., NAGASAWA, J., IZAWA, T., KOMABAYASHI, T., NAGATA, N., SUZUKI, K., TANIGUCHI, N. & OHNO, H. 1997. Effects of endurance training on superoxide dismutase activity, content and mRNA expression in rat muscle. Clinical and Experimental Pharmacology & Physiology, 24, 326-32.
PACKER, J. E., SLATER, T. F. & WILLSON, R. L. 1979. Direct observation of a free radical interaction between vitamin E and vitamin C. Nature, 278, 737-8.
PALOMERO, J. & JACKSON, M. J. 2010. Redox regulation in skeletal muscle during contractile activity and aging. Journal of Animal Science, 88, 1307-13.
PALOMERO, J., PYE, D., KABAYO, T., SPILLER, D. G. & JACKSON, M. J. 2008. In situ detection and measurement of intracellular reactive oxygen species in single isolated mature skeletal muscle fibers by real time fluorescence microscopy. Antioxid Redox Signal, 10, 1463-74.
PAMPLONA, R. & COSTANTINI, D. 2011. Molecular and structural antioxidant defenses against oxidative stress in animals. American Journal of Physiology. Regulatory, Integrative and Comparative Physiology, 301, R843-63.
PARK, S. E., SONG, J. D., KIM, K. M., PARK, Y. M., KIM, N. D., YOO, Y. H. & PARK, Y. C. 2007. Diphenyleneiodonium induces ROS-independent p53 expression and apoptosis in human RPE cells. FEBS Letters, 581, 180-6.
PATTWELL, D. M., MCARDLE, A., MORGAN, J. E., PATRIDGE, T. A. & JACKSON, M. J. 2004. Release of reactive oxygen and nitrogen species from contracting skeletal muscle cells. Free Radical Biology & Medicine, 37, 1064-72.
PATTWELL, D., ASHTON, T., MCARDLE, A., GRIFFITHS, R. D. & JACKSON, M. J. 2003. Ischemia and reperfusion of skeletal muscle lead to the appearance of a stable lipid free radical in the circulation. American Journal of Physiology-Heart and Circulatory Physiology, 284, H2400-4.
PEREZ, V. I., BOKOV, A., VAN REMMEN, H., MELE, J., RAN, Q., IKENO, Y. & RICHARDSON, A. 2009a. Is the oxidative stress theory of aging dead? Biochimica et Biophysica Acta, 1790, 1005-14.
PEREZ, V. I., VAN REMMEN, H., BOKOV, A., EPSTEIN, C. J., VIJG, J. & RICHARDSON, A. 2009b. The overexpression of major antioxidant enzymes does not extend the lifespan of mice. Aging Cell, 8, 73-5.

PHUNG, C. D., EZIEME, J. A. & TURRENS, J. F. 1994. Hydrogen peroxide metabolism in skeletal muscle mitochondria. Archives of Biochemistry and Biophysics, 315, 479-82.
PICARD, M., CSUKLY, K., ROBILLARD, M. E., GODIN, R., ASCAH, A., BOURCIER-LUCAS, C. & BURELLE, Y. 2008. Resistance to Ca^{2+}-induced opening of the permeability transition pore differs in mitochondria from glycolytic and oxidative muscles. American Journal of Physiology. Regulatory, Integrative and Comparative Physiology, 295, R659-68
PICARD, M., HEPPLE, R. T. & BURELLE, Y. 2012. Mitochondrial functional specialization in glycolytic and oxidative muscle fibers: tailoring the organelle for optimal function. American Journal of Physiology. Cell Physiology, 302, C629-41.
PICARD, M., RITCHIE, D., WRIGHT, K. J., ROMESTAING, C., THOMAS, M. M., ROWAN, S. L., TAIVASSALO, T. & HEPPLE, R. T. 2010. Mitochondrial functional impairment with aging is exaggerated in isolated mitochondria compared to permeabilized myofibers. Aging Cell, 9, 1032-46.
PICARD, M., TAIVASSALO, T., GOUSPILLOU, G. & HEPPLE, R. T. 2011a. Mitochondria: isolation, structure and function. The Journal of Physiology, 589, 4413-21.
PICARD, M., TAIVASSALO, T., RITCHIE, D., WRIGHT, K. J., THOMAS, M. M., ROMESTAING, C. & HEPPLE, R. T. 2011b. Mitochondrial structure and function are disrupted by standard isolation methods. PLOS One, 6, e18317.
PILLAY, C. S., HOFMEYR, J. H., OLIVIER, B. G., SNOEP, J. L. & ROHWER, J. M. 2009. Enzymes or redox couples? The kinetics of thioredoxin and glutaredoxin reactions in a systems biology context. The Biochemical Journal, 417, 269-75.
PLANT, D. R., LYNCH, G. S. & WILLIAMS, D. A. 2000. Hydrogen peroxide modulates Ca^{2+}-activation of single permeabilized fibres from fast- and slow-twitch skeletal muscles of rats. Journal of Muscle Research and Cell Motility, 21, 747-52.
PORTER, M. M., VANDERVOORT, A. A. & LEXELL, J. 1995. Aging of human muscle: structure, function and adaptability. Scandinavian Journal of Medicine & Science in Sports, 5, 129-42.
POUVREAU, S. 2010. Superoxide flashes in mouse skeletal muscle are produced by discrete arrays of active mitochondria operating coherently. PLOS One, 5.
POWERS, S. K. & JACKSON, M. J. 2008. Exercise-induced oxidative stress: cellular mechanisms and impact on muscle force production. Physiological Reviews, 88, 1243-76.
POWERS, S. K., CRISWELL, D., LAWLER, J., JI, L. L., MARTIN, D., HERB, R. A. & DUDLEY, G. 1994. Influence of exercise and fiber type on antioxidant enzyme activity in rat skeletal muscle. The American Journal of Physiology, 266, R375-80.
POWERS, S. K., KAVAZIS, A. N. & MCCLUNG, J. M. 2007. Oxidative stress and disuse muscle atrophy. Journal of Applied Physiology, 102, 2389-97.
POWIS, G. & MONTFORT, W. R. 2001. Properties and biological activities of thioredoxins. Annual Review of Biophysics and Biomolecular Structure, 30, 421-55.
PULLIAM, D. A., BHATTACHARYA, A. & VAN REMMEN, H. 2012. Mitochondrial dysfunction in aging and longevity: A causal or protective role? Antioxidants & Redox Signaling.
PYE, D., PALOMERO, J., KABAYO, T. & JACKSON, M. J. 2007. Real-time measurement of nitric oxide in single mature mouse skeletal muscle fibres during contractions. The Journal of Physiology, 581, 309-18.
RADAK, Z. 2000. Free radicals in exercise and aging. Human Kinetics.

RADI, R., BECKMAN, J. S., BUSH, K. M. & FREEMAN, B. A. 1991. Peroxynitrite oxidation of sulfhydryls. The cytotoxic potential of superoxide and nitric oxide. The Journal of Biological Chemistry, 266, 4244-50.
RAN, Q., LIANG, H., IKENO, Y., QI, W., PROLLA, T. A., ROBERTS, L. J., 2ND, WOLF, N., VAN REMMEN, H. & RICHARDSON, A. 2007. Reduction in glutathione peroxidase 4 increases life span through increased sensitivity to apoptosis. The Journals of Gerontology: Series A: Biological Sciences and Medical Sciences, 62, 932-42.
RECKELHOFF, J. F., KANJI, V., RACUSEN, L. C., SCHMIDT, A. M., YAN, S. D., MARROW, J., ROBERTS, L. J., 2ND & SALAHUDEEN, A. K. 1998. Vitamin E ameliorates enhanced renal lipid peroxidation and accumulation of F_2-isoprostanes in aging kidneys. The American Journal of Physiology, 274, R767-74.
REID, M. B. & MOODY, M. R. 1994. Dimethyl sulfoxide depresses skeletal muscle contractility. Journal of Applied Physiology, 76, 2186-90.
REID, M. B., HAACK, K. E., FRANCHEK, K. M., VALBERG, P. A., KOBZIK, L. & WEST, M. S. 1992. Reactive oxygen in skeletal muscle. I. Intracellular oxidant kinetics and fatigue in vitro. Journal of Applied Physiology, 73, 1797-804.
REID, M. B., KHAWLI, F. A. & MOODY, M. R. 1993. Reactive oxygen in skeletal muscle. III. Contractility of unfatigued muscle. Journal of Applied Physiology, 75, 1081-7.
REID, M. B., SHOJI, T., MOODY, M. R. & ENTMAN, M. L. 1992. Reactive oxygen in skeletal muscle. II. Extracellular release of free radicals. Journal of Applied Physiology, 73, 1805-9.
REY, F. E., CIFUENTES, M. E., KIARASH, A., QUINN, M. T. & PAGANO, P. J. 2001. Novel competitive inhibitor of NAD(P)H oxidase assembly attenuates vascular O_2^- and systolic blood pressure in mice. Circulation Research, 89, 408-14.
RHEE, S. G., CHAE, H. Z. & KIM, K. 2005a. Peroxiredoxins: a historical overview and speculative preview of novel mechanisms and emerging concepts in cell signaling. Free Radical Biology & Medicine, 38, 1543-52.
RHEE, S. G., KANG, S. W., JEONG, W., CHANG, T. S., YANG, K. S. & WOO, H. A. 2005b. Intracellular messenger function of hydrogen peroxide and its regulation by peroxiredoxins. Current Opinion in Cell Biology, 17, 183-9.
RHEE, S. G., YANG, K. S., KANG, S. W., WOO, H. A. & CHANG, T. S. 2005c. Controlled elimination of intracellular H_2O_2: regulation of peroxiredoxin, catalase, and glutathione peroxidase via post-translational modification. Antioxidants & Redox Signaling, 7, 619-26.
RIGANTI, C., GAZZANO, E., POLIMENI, M., COSTAMAGNA, C., BOSIA, A. & GHIGO, D. 2004. Diphenyleneiodonium inhibits the cell redox metabolism and induces oxidative stress. The Journal of Biological Chemistry, 279, 47726-31.
ROBINSON, J. M. 2008. Reactive oxygen species in phagocytic leukocytes. Histochemistry and Cell Biology, 130, 281-97.
ROBINSON, J. M. 2009. Phagocytic leukocytes and reactive oxygen species. Histochemistry and Cell Biology, 131, 465-9.
ROBINSON, K. M., JANES, M. S., PEHAR, M., MONETTE, J. S., ROSS, M. F., HAGEN, T. M., MURPHY, M. P. & BECKMAN, J. S. 2006. Selective fluorescent imaging of superoxide in vivo using ethidium-based probes. Proceedings of the National Academy of Sciences of the United States of America, 103, 15038-43.
ROSEN, G. M. & FREEMAN, B. A. 1984. Detection of superoxide generated by endothelial cells. Proceedings of the National Academy of Sciences of the United States of America, 81, 7269-73.

RUFF, R. L. 2011. Endplate contributions to the safety factor for neuromuscular transmission. Muscle & Nerve, 44, 854-61.
SAFDAR, A., DEBEER, J. & TARNOPOLSKY, M. A. 2010. Dysfunctional Nrf2-Keap1 redox signaling in skeletal muscle of the sedentary old. Free Radical Biology & Medicine, 49, 1487-93.
SAKELLARIOU, G. K., PYE, D., VASILAKI, A., ZIBRIK, L., PALOMERO, J., KABAYO, T., MCARDLE, F., VAN REMMEN, H., RICHARDSON, A., TIDBALL, J. G., MCARDLE, A. & JACKSON, M. J. 2011. Role of superoxide-nitric oxide interactions in the accelerated age-related loss of muscle mass in mice lacking Cu,Zn superoxide dismutase. Aging Cell, 10, 749-60.
SAKELLARIOU, G. K., JACKSON, M. J. & VASILAKI, A. 2013b. Redefining the major contributors to superoxide production in contracting skeletal muscle. The role of NAD(P)H oxidases. Free Radical Research.
SAKELLARIOU, G. K., VASILAKI, A., PALOMERO, J., KAYANI, A., ZIBRIK, L., MCARDLE, A. & JACKSON, M. J. 2013a. Studies of mitochondrial and nonmitochondrial sources implicate nicotinamide adenine dinucleotide phosphate oxidase(s) in the increased skeletal muscle superoxide generation that occurs during contractile activity. Antioxidants & Redox Signaling, 18, 603-21.
SAKELLARIOU, G. K. 2009. Factors influencing the intracellular generation of ROS by skeletal muscle fibres. MPhil Thesis. University of Liverpool.
SAKS, V., GUZUN, R., TIMOHHINA, N., TEPP, K., VARIKMAA, M., MONGE, C., BERAUD, N., KAAMBRE, T., KUZNETSOV, A., KADAJA, L., EIMRE, M. & SEPPET, E. 2010. Structure-function relationships in feedback regulation of energy fluxes in vivo in health and disease: mitochondrial interactosome. Biochimica et Biophysica Acta, 1797, 678-97.
SAMRA, Z. Q., OGURO, T., FONTAINE, R. & ASHRAF, M. 1991. Immunocytochemical localization of xanthine oxidase in rat myocardium. Journal of Submicroscopic Cytology and Pathology, 23, 379-90.
SASTRE, J., PALLARDO, F. V. & VINA, J. 2003. The role of mitochondrial oxidative stress in aging. Free Radical Biology & Medicine, 35, 1-8.
SCHEFFLER, I. E. 1999. Mitochondria. Wiley-Liss, New York.
SCHMIDT, H. H., LOHMANN, S. M. & WALTER, U. 1993. The nitric oxide and cGMP signal transduction system: regulation and mechanism of action. Biochimica et Biophysica Acta, 1178, 153-75.
SCHRINER, S. E., LINFORD, N. J., MARTIN, G. M., TREUTING, P., OGBURN, C. E., EMOND, M., COSKUN, P. E., LADIGES, W., WOLF, N., VAN REMMEN, H., WALLACE, D. C. & RABINOVITCH, P. S. 2005. Extension of murine life span by overexpression of catalase targeted to mitochondria. Science, 308, 1909-11.
SCHWERZMANN, K., HOPPELER, H., KAYAR, S. R. & WEIBEL, E. R. 1989. Oxidative capacity of muscle and mitochondria: correlation of physiological, biochemical, and morphometric characteristics. Proceedings of the National Academy of Sciences of the United States of America, 86, 1583-7.
SEN, C. K., MARIN, E., KRETZSCHMAR, M. & HANNINEN, O. 1992. Skeletal muscle and liver glutathione homeostasis in response to training, exercise, and immobilization. Journal of Applied Physiology, 73, 1265-72.
SENA, C. M., NUNES, E., GOMES, A., SANTOS, M. S., PROENCA, T., MARTINS, M. I. & SEICA, R. M. 2008. Supplementation of coenzyme Q10 and alpha-tocopherol lowers glycated hemoglobin level and lipid peroxidation in pancreas of diabetic rats. Nutrition Research, 28, 113-21.

SENTMAN, M. L., GRANSTROM, M., JAKOBSON, H., REAUME, A., BASU, S. & MARKLUND, S. L. 2006. Phenotypes of mice lacking extracellular superoxide dismutase and copper- and zinc-containing superoxide dismutase. The Journal of Biological Chemistry, 281, 6904-9.
SEVANIAN, A., DAVIES, K. J. & HOCHSTEIN, P. 1985. Conservation of vitamin C by uric acid in blood. Free Radical Biology & Medicine, 1, 117-24.
SHEFER, G. & YABLONKA-REUVENI, Z. 2005. Isolation and culture of skeletal muscle myofibers as a means to analyze satellite cells. Methods in Molecular Biology, 290, 281-304.
SIES, H. & GRAF, P. 1985. Hepatic thiol and glutathione efflux under the influence of vasopressin, phenylephrine and adrenaline. The Biochemical Journal, 226, 545-9.
SILVAGNO, F., XIA, H. & BREDT, D. S. 1996. Neuronal nitric-oxide synthase-mu, an alternatively spliced isoform expressed in differentiated skeletal muscle. The Journal of Biological Chemistry, 271, 11204-8.
SILVEIRA, L. R., PEREIRA-DA-SILVA, L., JUEL, C. & HELLSTEN, Y. 2003. Formation of hydrogen peroxide and nitric oxide in rat skeletal muscle cells during contractions. Free Radical Biology & Medicine, 35, 455-64.
SIMIC, M. G. 1992. The rate of DNA damage and aging. Birkauser Verlag, Basel, Switzerland.
SMITH, M. A. & REID, M. B. 2006. Redox modulation of contractile function in respiratory and limb skeletal muscle. Respiratory Physiology & Neurobiology, 151, 229-41.
SOHAL, R. S. & ORR, W. C. 2012. The redox stress hypothesis of aging. Free Radical Biology & Medicine, 52, 539-55.
SOHAL, R. S. & WEINDRUCH, R. 1996. Oxidative stress, caloric restriction, and aging. Science, 273, 59-63.
SPICKETT, C. M., JERLICH, A., PANASENKO, O. M., ARNHOLD, J., PITT, A. R., STELMASZYNSKA, T. & SCHAUR, R. J. 2000. The reactions of hypochlorous acid, the reactive oxygen species produced by myeloperoxidase, with lipids. Acta biochimica Polonica, 47, 889-99.
SPYROU, G., ENMARK, E., MIRANDA-VIZUETE, A. & GUSTAFSSON, J. 1997. Cloning and expression of a novel mammalian thioredoxin. The Journal of Biological Chemistry, 272, 2936-41.
ST-PIERRE, J., BUCKINGHAM, J. A., ROEBUCK, S. J. & BRAND, M. D. 2002. Topology of superoxide production from different sites in the mitochondrial electron transport chain. The Journal of Biological Chemistry, 277, 44784-90.
STAMLER, J. S. & MEISSNER, G. 2001. Physiology of nitric oxide in skeletal muscle. Physiological Reviews, 81, 209-237.
STEINBAUGH, M. J., SUN, L. Y., BARTKE, A. & MILLER, R. A. 2012. Activation of genes involved in xenobiotic metabolism is a shared signature of mouse models with extended lifespan. American journal of physiology. Endocrinology and Metabolism, 303, E488-95.
STEPKOWSKI, T. M. & KRUSZEWSKI, M. K. 2011. Molecular cross-talk between the NRF2/KEAP1 signaling pathway, autophagy, and apoptosis. Free Radical Biology & Medicine, 50, 1186-95.
STOCKER, R., GLAZER, A. N. & AMES, B. N. 1987a. Antioxidant activity of albumin-bound bilirubin. Proceedings of the National Academy of Sciences of the United States of America, 84, 5918-22.

STOCKER, R., YAMAMOTO, Y., MCDONAGH, A. F., GLAZER, A. N. & AMES, B. N. 1987b. Bilirubin is an antioxidant of possible physiological importance. Science, 235, 1043-6.
SUN, Q. A., HESS, D. T., NOGUEIRA, L., YONG, S., BOWLES, D. E., EU, J., LAURITA, K. R., MEISSNER, G. & STAMLER, J. S. 2011. Oxygen-coupled redox regulation of the skeletal muscle ryanodine receptor-Ca^{2+} release channel by NADPH oxidase 4. Proceedings of the National Academy of Sciences of the United States of America, 108, 16098-103.
SZABO, C., ISCHIROPOULOS, H. & RADI, R. 2007. Peroxynitrite: biochemistry, pathophysiology and development of therapeutics. Nature Reviews Drug Discovery, 6, 662-80.
SZETO, H. H. 2006a. Cell-permeable, mitochondrial-targeted, peptide antioxidants. The American Journal of the Association of Pharmaceutical Scientists, 8, E277-83.
SZETO, H. H. 2006b. Mitochondria-targeted peptide antioxidants: novel neuroprotective agents. The American Journal of the Association of Pharmaceutical Scientists, 8, E521-31.
TAKEYA, R. & SUMIMOTO, H. 2003. Molecular mechanism for activation of superoxide-producing NADPH oxidases. Molecules and Cells, 16, 271-7.
THOMAS, G. D. & VICTOR, R. G. 1998. Nitric oxide mediates contraction-induced attenuation of sympathetic vasoconstriction in rat skeletal muscle. The Journal of Physiology, 506 (Pt 3), 817-26.
THOMPSON, M., BECKER, L., BRYANT, D., WILLIAMS, G., LEVIN, D., MARGRAF, L. & GIROIR, B. P. 1996. Expression of the inducible nitric oxide synthase gene in diaphragm and skeletal muscle. Journal of Applied Physiology, 81, 2415-20.
TIAN, W., LI, X. J., STULL, N. D., MING, W., SUH, C. I., BISSONNETTE, S. A., YAFFE, M. B., GRINSTEIN, S., ATKINSON, S. J. & DINAUER, M. C. 2008. Fc gamma R-stimulated activation of the NADPH oxidase: phosphoinositide-binding protein p40phox regulates NADPH oxidase activity after enzyme assembly on the phagosome. Blood, 112, 3867-77.
TREBERG, J. R., QUINLAN, C. L. & BRAND, M. D. 2010. Hydrogen peroxide efflux from muscle mitochondria underestimates matrix superoxide production--a correction using glutathione depletion. The Journal of the Federation of European Biochemical Societies, 277, 2766-78.
TRUJILLO, M., FERRER-SUETA, G. & RADI, R. 2008. Peroxynitrite detoxification and its biologic implications. Antioxidants & Redox Signaling, 10, 1607-20.
TURRENS, J. F., ALEXANDRE, A. & LEHNINGER, A. L. 1985. Ubisemiquinone is the electron donor for superoxide formation by complex III of heart mitochondria. Archives of Biochemistry and Biophysics, 237, 408-14.
URSO, M. L. & CLARKSON, P. M. 2003. Oxidative stress, exercise, and antioxidant supplementation. Toxicology, 189, 41-54.
VALKO, M., LEIBFRITZ, D., MONCOL, J., CRONIN, M. T., MAZUR, M. & TELSER, J. 2007. Free radicals and antioxidants in normal physiological functions and human disease. The International Journal of Biochemistry & Cell Biology, 39, 44-84.
VALKO, M., RHODES, C. J., MONCOL, J., IZAKOVIC, M. & MAZUR, M. 2006. Free radicals, metals and antioxidants in oxidative stress-induced cancer. Chemico-Biological Interactions, 160, 1-40.
VASILAKI, A., MANSOURI, A., REMMEN, H., VAN DER MEULEN, J. H., LARKIN, L., RICHARDSON, A. G., MCARDLE, A., FAULKNER, J. A. &

JACKSON, M. J. 2006a. Free radical generation by skeletal muscle of adult and old mice: effect of contractile activity. Aging Cell, 5, 109-17.
VASILAKI, A., MCARDLE, F., IWANEJKO, L. M. & MCARDLE, A. 2006b. Adaptive responses of mouse skeletal muscle to contractile activity: The effect of age. Mechanisms of Ageing and Development, 127, 830-9.
VASILAKI, A., SIMPSON, D., MCARDLE, F., MCLEAN, L., BEYNON, R. J., VAN REMMEN, H., RICHARDSON, A. G., MCARDLE, A., FAULKNER, J. A. & JACKSON, M. J. 2007. Formation of 3-nitrotyrosines in carbonic anhydrase III is a sensitive marker of oxidative stress in skeletal muscle. Proteomics-Clinical Applications, 1, 362-72.
VASILAKI, A., VAN DER MEULEN, J. H., LARKIN, L., HARRISON, D. C., PEARSON, T., VAN REMMEN, H., RICHARDSON, A., BROOKS, S. V., JACKSON, M. J. & MCARDLE, A. 2010. The age-related failure of adaptive responses to contractile activity in skeletal muscle is mimicked in young mice by deletion of Cu,Zn superoxide dismutase. Aging Cell, 9, 979-90.
VAZQUEZ-TORRES, A., JONES-CARSON, J., MASTROENI, P., ISCHIROPOULOS, H. & FANG, F. C. 2000. Antimicrobial actions of the NADPH phagocyte oxidase and inducible nitric oxide synthase in experimental salmonellosis. I. Effects on microbial killing by activated peritoneal macrophages in vitro. The Journal of Experimental Medicine, 192, 227-36.
VETRANO, A. M., HECK, D. E., MARIANO, T. M., MISHIN, V., LASKIN, D. L. & LASKIN, J. D. 2005. Characterization of the oxidase activity in mammalian catalase. The Journal of Biological Chemistry, 280, 35372-81.
VON LOHNEYSEN, K., NOACK, D., JESAITIS, A. J., DINAUER, M. C. & KNAUS, U. G. 2008. Mutational analysis reveals distinct features of the Nox4-p22 phox complex. The Journal of Biological Chemistry, 283, 35273-82.
WALLACE, G. Q. & MCNALLY, E. M. 2009. Mechanisms of muscle degeneration, regeneration, and repair in the muscular dystrophies. Annual Review of Physiology, 71, 37-57.
WANG, A. L., LUKAS, T. J., YUAN, M. & NEUFELD, A. H. 2010. Age-related increase in mitochondrial DNA damage and loss of DNA repair capacity in the neural retina. Neurobiology of Aging, 31, 2002-10.
WEI, S. J., BOTERO, A., HIROTA, K., BRADBURY, C. M., MARKOVINA, S., LASZLO, A., SPITZ, D. R., GOSWAMI, P. C., YODOI, J. & GIUS, D. 2000. Thioredoxin nuclear translocation and interaction with redox factor-1 activates the activator protein-1 transcription factor in response to ionizing radiation. Cancer Research, 60, 6688-95.
WHITEHEAD, N. P., YEUNG, E. W., FROEHNER, S. C. & ALLEN, D. G. 2010. Skeletal muscle NADPH oxidase is increased and triggers stretch-induced damage in the mdx mouse. PLOS One, 5, e15354.
WIDDER, J. D., FRACCAROLLO, D., GALUPPO, P., HANSEN, J. M., JONES, D. P., ERTL, G. & BAUERSACHS, J. 2009. Attenuation of angiotensin II-induced vascular dysfunction and hypertension by overexpression of Thioredoxin 2. Hypertension, 54, 338-44.
WIGGERS, G. A., PECANHA, F. M., BRIONES, A. M., PEREZ-GIRON, J. V., MIGUEL, M., VASSALLO, D. V., CACHOFEIRO, V., ALONSO, M. J. & SALAICES, M. 2008. Low mercury concentrations cause oxidative stress and endothelial dysfunction in conductance and resistance arteries. American Journal of Physiology Heart and Circulatory Physiology, 295, H1033-H1043.

WIND, S., BEUERLEIN, K., EUCKER, T., MULLER, H., SCHEURER, P., ARMITAGE, M. E., HO, H., SCHMIDT, H. H. & WINGLER, K. 2010. Comparative pharmacology of chemically distinct NADPH oxidase inhibitors. British Journal of Pharmacology, 161, 885-98.
WINK, D. A., GRISHAM, M. B., MITCHELL, J. B. & FORD, P. C. 1996. Direct and indirect effects of nitric oxide in chemical reactions relevant to biology. Methods in Enzymology, 268, 12-31.
WOLIN, M. S. 2013. Evidence for novel aspects of Nox4 oxidase regulation of mitochondrial function and peroxide generation in an endothelial cell model of senescence. The Biochemical Journal, 452, e1-2.
WONG, M. & MARTIN, L. J. 2010. Skeletal muscle-restricted expression of human SOD1 causes motor neuron degeneration in transgenic mice. Human Molecular Genetics, 19, 2284-302.
WOOD, Z. A., SCHRODER, E., ROBIN HARRIS, J. & POOLE, L. B. 2003. Structure, mechanism and regulation of peroxiredoxins. Trends in Biochemical Sciences, 28, 32-40.
WOSNIAK, J., JR., SANTOS, C. X., KOWALTOWSKI, A. J. & LAURINDO, F. R. 2009. Cross-talk between mitochondria and NADPH oxidase: effects of mild mitochondrial dysfunction on angiotensin II-mediated increase in Nox isoform expression and activity in vascular smooth muscle cells. Antioxidants & Redox Signaling, 11, 1265-78.
XIA, R., WEBB, J. A., GNALL, L. L., CUTLER, K. & ABRAMSON, J. J. 2003. Skeletal muscle sarcoplasmic reticulum contains a NADH-dependent oxidase that generates superoxide. American Journal of Physiology Cell Physiology, 285, C215-21.
YAMADA, T., MISHIMA, T., SAKAMOTO, M., SUGIYAMA, M., MATSUNAGA, S. & WADA, M. 2006. Oxidation of myosin heavy chain and reduction in force production in hyperthyroid rat soleus. Journal of Applied Physiology, 100, 1520-6.
YU, B. P. 1994. Cellular defenses against damage from reactive oxygen species. Physiological Reviews, 74, 139-62.
YU, B. P., KANG, C. M., HAN, J. S. & KIM, D. S. 1998. Can antioxidant supplementation slow the aging process? BioFactors, 7, 93-101.
ZAMOCKY, M. & KOLLER, F. 1999. Understanding the structure and function of catalases: clues from molecular evolution and in vitro mutagenesis. Progress in Biophysics and Molecular Biology, 72, 19-66.
ZELKO, I. N., MARIANI, T. J. & FOLZ, R. J. 2002. Superoxide dismutase multigene family: a comparison of the CuZn-SOD (SOD1), Mn-SOD (SOD2), and EC-SOD (SOD3) gene structures, evolution, and expression. Free Radical Biology & Medicine, 33, 337-49.
ZHANG, Y., DAVIS, C., SAKELLARIOU, G. K., SHI, Y., KAYANI, A. C., PULLIAM, D., BHATTACHARYA, A., RICHARDSON, A., JACKSON, M. J., MCARDLE, A., BROOKS, S. V. & VAN REMMEN, H. 2013. CuZnSOD gene deletion targeted to skeletal muscle leads to loss of contractile force but does not cause muscle atrophy in adult mice. The Journal of the Federation of American Societies for Experimental Biology.
ZHAO, X., BEY, E. A., WIENTJES, F. B. & CATHCART, M. K. 2002. Cytosolic phospholipase A_2 ($cPLA_2$) regulation of human monocyte NADPH oxidase activity. $cPLA_2$ affects translocation but not phosphorylation of p67phox and p47phox. The Journal of Biological Chemistry, 277, 25385-92.
ZIEGLER, D. M. 1985. Role of reversible oxidation-reduction of enzyme thiols-disulfides in metabolic regulation. Annual Review of Biochemistry, 54, 305-29.

ZIELONKA, J. & KALYANARAMAN, B. 2010. Hydroethidine- and MitoSOX-derived red fluorescence is not a reliable indicator of intracellular superoxide formation: another inconvenient truth. Free Radical Biology & Medicine, 48, 983-1001.
ZUO, L. & CLANTON, T. L. 2002. Detection of reactive oxygen and nitrogen species in tissues using redox-sensitive fluorescent probes. Methods Enzymol, 352, 307-25.
ZUO, L., CHRISTOFI, F. L., WRIGHT, V. P., BAO, S. & CLANTON, T. L. 2004. Lipoxygenase-dependent superoxide release in skeletal muscle. Journal of Applied Physiology, 97, 661-8.
ZUO, L., CHRISTOFI, F. L., WRIGHT, V. P., LIU, C. Y., MEROLA, A. J., BERLINER, L. J. & CLANTON, T. L. 2000. Intra- and extracellular measurement of reactive oxygen species produced during heat stress in diaphragm muscle. American Journal of Physiology Cell Physiology, 279, C1058-66.